GCA CORPORATION

Bedford, Massachusetts

GCA-TR-68-12-G

GCA CORPORATION
GCA TECHNOLOGY DIVISION
Bedford, Massachusetts

September 1968

Prepared for

JET PROPULSION LABORATORY
Pasadena, California

# AEROMETRY INSTRUMENTATION STUDY

H. Geary P. Lilienfeld
G. Ohring W. Shenk

FINAL REPORT

Contract No. 951954

## ABSTRACT

Possible observational techniques and instrument types for the measurement of meteorological parameters in the atmospheres of Mars and Venus are described. The meteorological parameters considered are atmospheric temperature, pressure, density, wind velocity, water vapor content, and particulate suspensions. A wide range of techniques and instruments are included since the purpose of the study was not to select instrumentation for a particular mission but rather to provide information on all conceivable instrumentation for such measurements. The emphasis is on in-situ observing instruments although information is also provided on remote sensing (from orbiters or flybys) techniques. The information provided includes a discussion of the scientific basis of each measurement technique, a description of the instrument and its operation, procedures for the interpretation of the measurement, and details concerning instrument characteristics, instrument output, payload integration parameters, and the state of development of the instrument. The report is essentially a compendium of information, with references, on possible meteorological observing techniques and instruments for planetary exploration applications.



This work was performed for the Jet Propulsion Laboratory, California Institute of Technology, sponsored by the National Aeronautics and Space Administration under Contract NAS7-100.

TABLE OF CONTENTS

## LIST OF ILLUSTRATIONS

# 1. INTRODUCTION

This final report presents the results of a six-month study of possible observational techniques and instrument types that could be adapted for the measurement of meteorological parameters in the atmospheres of Mars and Venus. The meteorological parameters considered are atmospheric temperature, pressure, density, wind velocity, water vapor content, and particulate suspensions (including liquid and solid aerosols and condensation products). The objective of the study was to provide information on the physical principles of possible measurement techniques and on the characteristics of the associated instrumentation. No attempt was made to evaluate the relative merits of the possible techniques and instruments for a planetary mission. However, the considerable information provided on conceivable techniques and instruments should aid space agency planners in the task of instrument evaluation and selection for specific planetary missions.

Although the scope of the study included in-situ (using atmospheric capsules, landers, etc.) observations as well as remote sensing (from orbiters, flybys, etc.) observations of both planets, the emphasis was on in-situ observations, and, in particular, measurements of the near surface meteorological environment on Mars for a landed vehicle. This relative emphasis is reflected in the discussions of possible techniques and instruments.

For each meteorological parameter, there are a number of different possible measurement techniques. For each measurement technique, there may be one or more instrument types. In the study, those instruments associated with a particular measurement technique were grouped together. The results of the study are presented in the following manner. For each measurement technique, a discussion of the scientific basis of the technique is presented. For each instrument type, information is presented on a description of the instrument and its operation, procedures for interpretation of the measurement, instrument characteristics, instrument output, payload integration parameters, and the state of development of the instrument. To maintain uniform discussions, it was decided to present the information on each technique and instrument type with the use of a common outline. The adopted outline is shown below.

1. TECHNIQUE OR PHYSICAL PRINCIPLE

   A discussion of the scientific basis of the measurement.

   1.1 INSTRUMENT

      1.1.1 NARRATIVE DESCRIPTION OF THE INSTRUMENT

      1.1.2 INTERPRETATION OF MEASUREMENT

         Additional information needed to interpret measurement.
         Method for analysis and interpretation of data.

1.1.3 INSTRUMENT CHARACTERISTICS

Total and dynamic ranges
Accuracy
Signal to noise
Frequency response
Environmental effects

1.1.4 INSTRUMENT OUTPUT

Output signal
Bits per observation

1.1.5 PAYLOAD INTEGRATION

Weight
Volume
Power
Radio frequency interference
Magnetic moment
Erection, orientation, or booms
Compatibility with sterilization at 145°C
Special requirements - mounting, viewing, etc.

1.1.6 STATE OF DEVELOPMENT

REFERENCES
(Including commercial sources and literature)

Since most of the techniques and instruments discussed in this report have found application in the measurement of meteorological parameters of the Earth's atmosphere, they were not designed principally for measurement from a space probe on another planet. Therefore, in many cases, information on some of the payload integration parameters, instrument output parameters, and instrument characteristics are presently unknown so that where possible estimates have been made of these parameters. Thus, this information should be considered as a guide rather than as detailed specifications.

The following six sections — one for each meteorological parameter — of this report contain the detailed discussions of possible in-situ measurement techniques and instrument types. Each is prefaced by a short summary of available information on the magnitude and variations of the particular parameter in the atmospheres of Mars and Venus. Section 8 contains a discussion of possible techniques for remote (orbiter or flyby) observations of these meteorological parameters. A summary list of all techniques and instrument types considered may be found in Section 9. References of a particular technique or instrument type may be found immediately after the discussion of the technique or instrument. References concerning our present knowledge of meteorological parameters on Mars and Venus are included at the end of the report. As part of the study, a survey of recent developments and references to meteorological instrumentation for the Earth's atmosphere was performed. The results of this survey are contained in the Appendix. In addition, a loose-leaf volume of commercial literature on meteorological instruments has been assembled and furnished to the contracting agency, the Jet Propulsion Laboratory.

The results of the present study provide a compendium of information on possible meteorological observing techniques and instruments for planetary exploration applications. A suggested next step would involve the planning of specific planetary missions and the selection and specification of meteorological payloads, based on the information provided in this report, to accomplish the scientific objectives of these missions.

## 2. WATER VAPOR

Spectroscopic observations of Martian water vapor content indicate values of the order of 10μ precipitable water vapor (Kaplan et al., 1964; Schorn et al., 1967); photometric observations (Dollfus, 1963) suggest values an order of magnitude higher. If the water vapor is uniformly mixed throughout the atmosphere (constant mixing ratio), the water vapor pressure near the surface is between $7.5 \times 10^{-4}$ mb and $7.5 \times 10^{-3}$ mb (assumming a value of 0.5 for the ratio of the molecular weight of water vapor to the molecular weight of Mars' atmosphere). The corresponding frost points are 195°K and 210°K. For a constant water vapor mixing ratio, the water vapor pressure would decrease with altitude at the same rate as the pressure.

It is conceivable that the water vapor mixing ratio is not constant with altitude, i.e., the water vapor mixing ratio may decrease with altitude as is the case in the Earth's atmosphere. Or it may vary locally. If this is true, the water vapor content near the surface may be higher than the values given above. To allow for this, we may assume that the maximum likely water vapor pressure near the surface is perhaps an order of magnitude greater than the higher of the two values given above, or $7.5 \times 10^{-2}$ mb, which corresponds to a frost point of 228°K.

Small amounts of water vapor have been detected photometrically (Dollfus, 1963) and spectrometrically (Bottema et al., 1965; Spinrad and Shawl, 1966; Belton and Hunten, 1966) in the Cytherean atmosphere. Because of the unknown scattering properties of the Cytherean atmosphere and clouds, it is difficult to derive an exact estimate of the amount of water vapor detected spectroscopically. However, the order of magnitude of the precipitable water vapor content above the clouds is 100μ. For a cloud pressure of ~ 0.1 atmosphere, the water vapor mixing ratio is then of the order of $10^{-4}$, and the water vapor partial pressure in the vicinity of the cloud is of the order of $10^{-2}$ mb. These estimates, because of uncertainties in the interpretation of the observations and because of uncertainties in the vertical distribution of the observed water vapor, may easily be off by an order of magnitude. A vapor pressure of $10^{-2}$ mb corresponds to a frost point temperature of 213°K.

Preliminary results announced for the Venus IV spacecraft observations indicate that the water vapor mixing ratio is between $10^{-3}$ and $7 \times 10^{-3}$. Assuming a value of $4 \times 10^{-3}$, we obtain a water vapor partial pressure in the vicinity of the cloud of $4 \times 10^{-1}$ mb, which corresponds to a frost point temperature of 243°K. This same water vapor mixing ratio yields a partial pressure of water vapor near the surface of 80 mb (based on surface pressure of ~ 20 atm), which corresponds to a dewpoint temperature of 315°K.

## 2.1 CONDUCTIVITY HYGROMETERS

This moisture measurement technique involves the detection of the changes in electrical conductivity across the sensor. Absorption of moisture by chemical compounds and elements produces different humidity-resistance relationships. There are several mechanisms by which the electrical resistance is affected by humidity changes.

### 2.1.1 PHOSPHOROUS PENTOXIDE

#### 2.1.1.1 NARRATIVE DESCRIPTION OF THE INSTRUMENT

This mixing ratio detecting instrument is a chemical moisture trap and electrolytic cell utilizing a water vapor sensor that absorbs the water vapor from the air passing through a tube and, by an electrolyzing process, allows a current to flow that is exactly proportional to the rate of water vapor absorption (MacCready and Lake, 1965). The measurement of mixing ratio can be made independent of ambient temperature and pressure. Three basic components make up the instrument. These are the moisture cell, the mass flow sensor, and the pump system. The moisture cell is an electrolytic cell, the operation of which is described by MacCready and Lake (1965):

"The trapping agent, $P_2O_5$, maintains a very low water vapor pressure and equilibrates quite rapidly. The electrolytic cell has two platinum electrodes wound as a very tight double helix on the inside of a small glass tube. The electrolyte, the $P_2O_5.xH_2O$, is introduced as a 10 percent solution in acetone. When the acetone has evaporated, a potential is applied across the two electrodes to drive off the moisture which is present in the hydrate. The sensor is then prepared to pick up moisture from the atmosphere, electrolyze it, and pass the current necessary to read."

The mass flow through the cell must be determined in order to ascertain the mixing ratios. It is convenient to servo-control the mass flow rate to be constant. Thus, the flow sensor is always operating at one point. Further, this allows the cell meter to be calibrated directly in terms of mixing ratio. A heated thermistor bead is placed in and is cooled by the flow. When the bead is placed in a Wheatstone bridge arrangement, it gives an output as a function of mass flow. To stabilize the flow sensor, a second thermistor is placed at one of the other legs of the bridge and the bridge is designed so that both thermistors are at about the same temperature. Also, the temperature of the flow sensor housing is controlled to prevent large temperature changes.

The diaphragm type pump system is constantly adjusted by the servo-control to maintain the proper rate of mass flow. A radial whirling rod on a dc motor is used which pulls air in through the center axis due to centrifugal force and aerodynamic effects at the rod tips.

#### 2.1.1.2 INTERPRETATION OF MEASUREMENT

Additional information needed to interpret the measurement — The mass flow through the electrolytic cell must be measured in order to determine the mixing ratio.

Method for analysis and interpretation of data — The output is electric current and varies essentially linearly with mixing ratio.

### 2.1.1.3 INSTRUMENT CHARACTERISTICS

Total and dynamic ranges - The total range of the instrument is mixing ratios between 0.003 g/kg to 30 g/kg. Calibration is difficult to perform below 0.01 g/kg. The current through the cell becomes great enough to heat the instrument above 30 g/kg.

Accuracy - Flight tests (aircraft) have shown that there is good agreement between mixing ratio data for this instrument and radiosonde data up to 650 mb. Also, the instrument gave correct measurements inside clouds and responded rapidly to the strong moisture gradients which are present near cloud edges.

Signal to noise - Not applicable.

Frequency response - The time constant varies from cell to cell. Time constants have been as small as less than a second up to ten seconds. There has been no noticeable variation of the time constant with temperature, at least down to -20°C.

Environmental effects - Sudden temperature changes affect the mass flow sensor system. However, care has been taken in the design to control this problem.

### 2.1.1.4 INSTRUMENT OUTPUT

Output signal - This is an absolute measuring technique with analog output. There is a linear relation between output current and mixing ratio.

Bits per observation - It would require sixteen bits per observation for the two place accuracy of both the mass flow and current measurements.

### 2.1.1.5 PAYLOAD INTEGRATION

The following statistics are for the MRI (Meteorology Research, Inc.) Model 901 unit.

Weight - 16 lbs. A special unit, designed to measure mixing ratios in a descent through the Martian atmosphere, weighs only 11 ounces.

Volume - Less than 1 $ft^3$.

Power - 80 mW for the flow sensor, about 300 mW for 10-20 sec. to warm up the heater, and 100 mW for electronics.

Radio frequency interference - None.

Magnetic moment - Not known.

Erection, orientation or booms - None.

Compatibility with sterilization at 145°C - The pump system is compatible with sterilization.

Special requirements - None.

#### 2.1.1.6 STATE OF DEVELOPMENT

Considerable effort has been expended on this technique by MRI for JPL to develop a suitable instrument to measure the moisture of the Martian atmosphere. The instrument is still considered developmental, but some operational uses have been made for it.

### 2.1.2 ALUMINUM OXIDE

#### 2.1.2.1 NARRATIVE DESCRIPTION OF THE INSTRUMENT

This element can be developed in several configurations. The sensor designed for radiosonde use consists of a base of aluminum, an oxide that is made by anodizing the base material, and an evaporated conductive coating of metal (Stover, 1963). The base metal behaves as one electrode, and the evaporated metal as the other, or outer, electrode.

The surface of the anodized layer is porous (Jason, 1965). This porous nature of the oxide layers presents an enormous area for the absorption of gases and vapors. At low humidities the measured capacitance of the element comes almost entirely from the bulk mixing dielectric which consists of air, aluminum oxide and water. At higher humidities, parallel conduction paths are established through the absorbed water down the pore surface. Thus, the electrical characteristics are largely determined by the magnitude of the combined resistance of these conduction paths and the capacitance between the pore base and the metal.

The theoretical development for this element is done for a circuit representing a single pore. All pores are identical and parallel so that any given area of the layer may be represented by the same equivalent circuit with appropriate values for the parameters. The capacitance between the two outer conducting layers separated by the mixed dielectric of thickness d is $C_o$ and the parallel capacitance for a pore circuit is $C_p$ at frequency f. The measured quantity $C_p - C_o$ is related to parallel resistance $R_p$ by

$$C_p - C_o = \frac{A}{8\pi^2 f^2} \pm \frac{1}{2}\left[\left(\frac{A}{4\pi^2 f^2}\right)^2 - \frac{1}{\pi^2 f^2 R_p^2}\right]^{\frac{1}{2}}$$

where $A = 4\pi^2 f^2 C^2 + 1/R_2^2 C_2$ and $R_2$ is the leakage resistance through the oxide at the pore base, and $C_2$ is the pore base capacitance. In general $R_p$ decreases as $C_p - C_o$ increases. Also relative humidity increases as $C_p - C_o$ increases.

### 2.1.2.2 INTERPRETATION OF MEASUREMENT

Additional information needed to interpret measurement- The temperature must be known if the instrument is to be operated below -15°C where the calibration begins to change with temperature.

Method for analysis and interpretation of data - The measured quantity can be the capacitance difference, $C_p - C_o$, the parallel resistance $R_p$, or the impedance (radiosonde). Roughly a logarithmic relation exists beween $C_p - C_o$ and relative humidity (RH), and between RH and $R_p$. For the specially designed radiosonde circuit, measured impedance of the element usually follows the curve of water vapor pressure. In this latter case, the element gives a measure of absolute humidity.

### 2.1.2.3 INSTRUMENT CHARACTERISTICS

Total and dynamic ranges - The theoretical total range of the sensor is from -90°C to around 600-700°C. However, since sensor development has been primarily oriented towards meeting standard meteorological needs, most of the testing has been below 30°C.

Accuracy - Laboratory tests have shown the accuracy to be about 1 to 2 percent RH except at the extremes of high and low humidities. Hysteresis effects are small provided the instrument does not have prolonged exposure to high humidities.

Signal to noise - The signal to noise data will depend on the circuity and telemetry selected to send and receive the data.

Frequency response - The time constant determined from step changes for the radiosonde designed sensor varies from 0.2 sec at 20°C to 21 sec at -20°C (Chleck, 1966). However, other evidence suggests that the response at the lower temperature is close to that observed at 20°C.

Environmental effects - The element cannot remain exposed to high humidities for a prolonged period.

### 2.1.2.4 INSTRUMENT OUTPUT

Output signal - The calibrated analog output generally has been capacitance ($C_p - C_o$) for laboratory measurements and the RH-capacitance curve is approximately logarithmic. Impedance measurements from the circuit for the designed radiosonde element in analog form are related to the water vapor pressure.

Bits per observation - The number of bits will depend on the form of the output desired. With the accuracies cited above a two-place output seems logical. Therefore, allowing for exponents and for simultaneous measurement of temperature, fourteen bits would be needed per observation.

#### 2.1.2.5 PAYLOAD INTEGRATION

There are many different possible circuits and instrument packages that support and relay the information from the element itself. As a result the specifics of the payload integration data cover a wide range. The element itself is small. There are several varieties. The designed radiosonde element is 5/8 in. x 3/16 in. x < 1/16 in. A rod element is a short 3 mm in diameter aluminum welding rod, while needle elements consist of 1/2-mm diameter aluminum wire attached to a 3-mm diameter rod. Obviously, the weight is small.

#### 2.1.2.6 STATE OF DEVELOPMENT

This sensor is still in the developmental stage. No flight testing has been reported. At the present time, most research has concentrated on solving the problem of calibration drift with storage.

### 2.1.3 BARIUM FLUORIDE

#### 2.1.3.1 NARRATIVE DESCRIPTION OF THE INSTRUMENT

The barium fluoride element consists of a glass substrate, a layer of chromium 0.15μ thick for the electrode, and a film of $BaF_2$ with a thickness of 0.3μ (Jones and Wexler, 1960). This element responds to variations in relative humidity with changes in resistance that depend on calibration temperature. The element, besides having been laboratory tested, has been flown simultaneously with a lithium chloride element on a modified radiosonde balloon (Jones, 1963). Due to a smaller constant at low temperatures than either the lithium chloride or carbon strip elements, the element is useful for radiosonde measurements of tropospheric humidities. However, calibration drift difficulties have been encountered when the sensor is stored. Jones (1967) indicates that the source of the drift has been found and that it can be controlled.

#### 2.1.3.2 INTERPRETATION OF MEASUREMENT

Additional information needed to interpret measurement- The temperature must be known along with the relative humidity to properly interpret the relative humidity-temperature-resistance calibration nomogram.

Method for analysis and interpretation of data - For radiosonde-borne elements, the output is analyzed in the same fashion as the lithium chloride output.

#### 2.1.3.3 INSTRUMENT CHARACTERISTICS

Total and dynamic ranges - There is no theoretical limit to the range of the sensor. In practice the sensor has been used to measure relative humidities between 1.5 and 100 percent for dry bulb temperatures between 33 and -59°C.

Accuracy - No complete evaluation of accuracy over the entire practical range of the instrument has been reported. From the comparison flights between the barium fluoride and lithium chloride sensors, Jones (1963) has indicated the capability of the sensor to properly define cloudy regions (100-percent relative humidity) that were located by radar. Thus, the instrument seems to give satisfactory results at high humidity. At low humidities the accuracy is about 5-percent relative humidity. Various laboratory tests conducted by Jones and Wexler (1960) indicated an accuracy of 2 percent at various discrete values of temperature and moderate relative humidities. The element also functioned properly after a prolonged exposure of 2 months at 97-percent relative humidity.

Signal to noise - Same as lithium chloride.

Frequency response - The average time constant, determined in the laboratory, was 1.0 and 1.9 sec for increasing and decreasing relative humidity respectively at -20°C and about 3 sec for both increasing and decreasing relative humidity at -40°C. These response times are nearly an order of magnitude less than the time constants for the carbon strip at similar temperatures and more than an order of magnitude less than those for the lithium chloride element.

Environmental effects - The instrument is small and rugged. It should experience no adverse environmental effects.

2.1.3.4 INSTRUMENT OUTPUT

Output signal - The calibrated analog voltage output from the radiosonde package is linearly related to resistance which in turn is nonlinearly related to temperature and relative humidity.

Bits per observation - Fourteen bits per observation are needed.

2.1.3.5 PAYLOAD INTEGRATION

Weight - Less than two ounces.

Volume - The slide glass is 4 x 13/16 x 1/32 inches and comprises nearly the entire size of the element.

Power - Approximately 0.1 W for electronics.

Radio frequency interference - None.

Magnetic moment - Not known.

Erection, orientation, or booms - None.

Compatibility with sterilization at 145°C - Compatibility with sterilization cannot be determined.

Special requirements - The element should be well ventilated.

## 2.1.4 LITHIUM CHLORIDE HYGROMETER

### 2.1.4.1 NARRATIVE DESCRIPTION OF THE INSTRUMENT

Mathews (1965) describes the lithium chloride radiosonde hygrometer as "a polystyrene blank with conducting tin edges that is dipped in a formula of lithium chloride, polyvinyl alcohol, water and a nonionic surface active agent. Its resistance varies with relative humidity and temperature, and is read by the radiosonde measuring circuit." Changes in ionic mobility occur with variations in the relative humidity. The radiosonde is the payload on a helium-filled balloon which rises at a rate of about 1000 ft/min to a height of about 30 km where the balloon bursts. Telemetered resistance measurements relating to the relative humidity are acquired by the receiving station along with pressure and temperature information.

### 2.1.4.2 INTERPRETATION OF MEASUREMENT

Additional information needed to interpret measurement- Simultaneous measurement of temperature is needed since the resistance is a function of relative humidity and temperature.

Method for analysis and interpretation of data - The received voltage data are in continuous wave form. Frequency of oscillation is determined by resistance due to relative humidity, temperature, and a reference resistance. A modulated FM signal is received with the frequency associated with each parameter in sequence as determined from a prearranged schedule. Since pressure is always decreasing with height, the switching device is controlled by changes in pressure. Relative humidity is computed from a nomogram, where temperature and resistance are known, the resistance being a function of the received signal.

### 2.1.4.3 INSTRUMENT CHARACTERISTICS

Total and dynamic ranges - The range of the sensor is from surface conditions (as high as 40°C dry-bulb temperature) down to when the dry-bulb temperature reaches -40°C for a relative humidity range of 11-100 percent. Below -40°C, the element becomes too sluggish to be evaluated.

Accuracy - The sensor tends to read too low by about 10 percent when the element is in clouds. Outside of clouds, the electrolytic strip has an accuracy of ±2.5 percent at -10°C, between 15 and 96 percent relative humidity. The manufacturer's specification accuracy is ±5 percent and a selection accuracy of ±3 percent is used. Test points near 35 and 80 percent relative humidities are used.

Signal to noise - A signal to noise ratio of 10 dB is sufficient for clear reception of the signal.

Frequency response - The time constant is dependent on the ventilation rate as well as the characteristics of the sensor. With a

ventilation rate of $2\frac{1}{2}$ m/sec, the time constant varies between 51-74 sec at -20°C and 120-480 sec at -40°C. The time constants are much smaller for temperatures higher than 0°C.

Environmental effects - The instrument is rugged and can withstand a fairly wide range of temperatures over a long period of time without seriously affecting the calibration. Condensation of liquid water sometimes collects on the sensor as it passes through clouds leading to a "washout" effect.

#### 2.1.4.4 INSTRUMENT OUTPUT

Output signal - The calibrated output is in the form of an oscillating continuous wave. It is linearly dependent on both temperature and resistance.

Bits per observation - Both temperature and resistance information are necessary to determine the relative humidity. Two place accuracy of the observation along with an exponent for the output of both quantities would require 14 bits.

#### 2.1.4.5 PAYLOAD INTEGRATION

Weight - The weight of the element is less than 2 ounces.

Volume - The strip of polystyrene is 4 x 11/16 x 1/32 inches. This strip is dipped into the lithium chloride solution.

Power - Approximately 0.1 W for electronics.

Radio frequency interference - None.

Magnetic moment - Not known.

Erection, orientation, or booms - None.

Compatibility with sterilization at 145°C - Compatibility with sterilization cannot be determined.

Special requirements - The sensor must be well ventilated to reduce the time constant.

#### 2.1.4.6 STATE OF DEVELOPMENT

This sensor has been thoroughly tested and has been used operationally with the radiosonde by the U.S. Weather Bureau for 20 years.

### 2.1.5 LITHIUM BROMIDE

The characteristics of this sensor are very similar to lithium chloride. Substitution of this compound for lithium chloride extends the operating range of the sensor down to 5 percent relative humidity.

### 2.1.6 LEAD IODIDE

The lead iodide element is another one of the series that is being tested for possible radiosonde use (Jones, 1965). Nearly all the testing has been in the laboratory at room temperatures of 24°C. One test flight has been reported (Jones, 1963). The lead iodide element has greater storage stability and a significantly smaller temperature coefficient of electrical resistance than the other film elements.

Lead iodide elements are constructed by depositing the compound into glass substrates which are 21-mm wide and vary in length from 8 to 63 mm.

Laboratory tests were conducted with an ac ohm meter circuit. A multivibrator provided 100 c/s excitation to the film specimen. The film was connected into a voltage divider which had four pairs of "front-to-back" silicon diodes, whose voltage current characteristics made the divided voltage proportional to the logarithm of the film resistance. The divided voltage controlled the frequency of a voltage-controlled oscillator. Thus, the frequency from the oscillator was related to film resistance.

Unlike other elements the effect of temperature on resistance might be negligible at temperatures down to -30°C by placing the electrodes over, rather than under, the film. Thus, temperature would not have to be known in order to determine relative humidity. The logarithm of resistance was found to vary linearly with relative humidity between 45 and 92 percent relative humidity according to the relation

$$R = R_c (RH)^{-7.0}$$

where $R$ = surface resistance,
$R_c$ = resistance characteristic of the individual film specimen (depends principally on the length),
$RH$ = relative humidity.

A discontinuity seems to be present in the RH-resistance relationship at 45-percent RH, and a linear relation above 92 percent RH has a different slope. Most of the research effort on studying the characteristics of the element has been concentrated in the 45-92 percent RH range. The standard error in this range was least (1.2-percent RH) for elements with lengths of 8 and 23 mm and greatest for the 63-mm length (3.6-percent RH).

Lack of understanding of the resistance-RH relation has dampened the development of this sensor. Research is being concentrated in this area. At present its development lags that of the others mentioned above.

## 2.1.7 CARBON STRIP

### 2.1.7.1 NARRATIVE DESCRIPTION OF THE MEASUREMENT

The carbon element sensor is gradually replacing the lithium chloride element for relative humidity measurement in the troposphere and lower stratosphere. This replacement has occurred due to the carbon element's faster response with low temperatures, resistivity to washout effects, and narrower hysteresis loop.

The term carbon strip is probably a misnomer since the finely divided carbon contained in the element is comparatively inert to water vapor. "Cellulose electric hygrometer" is probably a more correct description of the sensor since the cellulose ingredients are more sensitive to water vapor changes. The carbon particles are the conductive part of the sensor and are suspended in a matrix (consisting of hydroethylcellulose, sorbital, and gelling agent) which expands and contracts with variations in the relative humidity. Dilation and contraction of the matrix changes the spacing between the carbon particles and thus the conductivity.

The carbon sensor is flown on the radiosonde balloon in the same general configuration as the lithium chloride element.

### 2.1.7.2 INTERPRETATION OF MEASUREMENT

Additional information needed to interpret measurement- Simultaneous temperature measurement is necessary since the relative humidity resistance relationship is a function of temperature.

Method for analysis and interpretation of data - The analysis of the output is essentially the same as that for the lithium chloride element.

### 2.1.7.3 INSTRUMENT CHARACTERISTICS

Total and dynamic ranges - This sensor operates over the dry-bulb temperature range of + 40°C to -40°C between 10 and 100 percent relative humidities (same as lithium chloride sensor).

Accuracy - Factors affecting the accuracy of this sensor include aging, hysteresis, washout and contamination. No polarization problems have been reported. The hysteresis loop is smaller for this sensor than for lithium chloride and the sensor is not affected by condensation or liquid water unless it is immersed for several hours. Aging offers no serious problem if, with proper storage, the sensor is used within two to four years after manufacture. The overall accuracy of this sensor is better than lithium chloride, especially in clouds.

Signal to noise - Same as lithium chloride.

Frequency response - Under laboratory testing conditions, the time constants are 0.5 sec at 25°C, 2 sec at -5°C, and 6 sec at -20°C. All of the above constants were with a 3m/sec ventilation rate (assumed balloon conditions).

Environmental effects - The sensor is rugged and can withstand the temperature variations of the troposphere and lower stratosphere.

2.1.7.4 INSTRUMENT OUTPUT

Output signal - The calibrated analog voltage output has a nonlinear variation with temperature and relative humidity.

Bits per observation - Fourteen bits per observation are needed.

2.1.7.5 PAYLOAD INTEGRATION

Weight - Less than two ounces.

Volume - The cellulose strip used for radiosonde flights is $2\frac{1}{2}$-inches long, 11/16-inch wide, and 0.040-inch thick.

Power - Approximately 0.1 W for electronics.

Radio frequency interference - None.

Magnetic moment - Not known.

Erection, orientation, or booms - None.

Compatibility with sterilization at 145°C - Compatibility with sterilization cannot be determined.

Special requirements - Sufficient ventilation is required for the time constants mentioned above.

2.1.7.6 STATE OF DEVELOPMENT

This is the standard sensor for the Armed Forces radiosonde and is being increasingly used by civilian agencies for the same purpose. The empirical relations governing the resistance-relative humidity curves are well understood, while some of the chemistry of the substance is not.

### 2.1.8 CERAMIC SENSORS

There are a wide number of ceramic elements that can be used to sense relative humidity. Most of the sensors consist of a specially compounded ceramic base impregnated with slightly soluble inorganic salts.

#### KAOLIN BASE WITH LITHIUM FLUORIDE OR LITHIUM CHLORIDE

The body of this element is made of soft fired kaolin treated with boiling dilute solutions of either lithium fluoride or lithium carbonate (Amour and Nelson, 1965). The characteristics of the sensor with either salt are about the same. A very small fraction of the total area of the sensor (a dish about 1/8-inches wide and $1\frac{1}{2}$ inches in diameter) is involved in the humidity-activated conductivity mechanism. The water molecules are probably sorbed only in certain polar positions within the structure. Further, the bulbs of the internal area most likely have little attraction for water. Contamination particles compete with the water vapor for the relatively small number of available positions. As a result, this element has a serious contamination problem.

The element is best used for the range of dry-bulb temperature between -5°C to 70°C. Calibrations have been prepared down to -25°C for the logarithmic relation between resistance and relative humidity (RH). The calibration varies with temperature. For a given RH, the resistance increases as temperature decreases. Also the instrument appears to have a stable calibration curve between 10 and 100 percent RH. There are no hysteresis effects in the ordinary sense. However, secondary changes in resistance do occur. For example, a sensor exposed for several days at 10 percent RH experiences a 2-percent shift in RH. No accuracy estimates have been reported. The time constant is 15 sec at room temperature.

Due to the lack of stability of the calibration due to contamination, development of this sensor has been discontinued.

#### CERIUM TITANATE

This is another type of ceramic sensor that has better calibration stability (Johnson and Duggan, 1965). The sensing element is comprised of a blend of powdered cerium oxide and titanium dioxide. The compound is fired twice to temperatures up to 2200°F and powdered again between firings. The finished humidity sensor can be shaped in many ways, the most reproducible being a green pill approximately 1/4-inch in diameter and 0.075-inches thick. The density of the finished element is important since the electrical characteristics are sensitive to this density. Both the speed of response and intrinsic impedance decrease with increasing density.

The instrument output is current and varies approximately linearly with RH. The impedance is very high; at a temperature of 24°C and RH of 20 percent, the impedance is about 2000 megohms. The reported

range of operation is between 10°C and 38°C. It is possible that the instrument can operate outside of this range. An ac circuit must be used since the electrodes become oxidized with a dc circuit. As a result, the effect of shunt capacity makes measurement of RH below 20 percent difficult. The impedance changes somewhat with variations in temperatures for a give RH.

The time constants are different for increasing and decreasing humidity. For example, at 24°C, the time constants are 5 sec for increasing humidity and 18 sec for decreasing humidity. The element may be subjected to 100-percent RH indefinitely and still not be affected.

This instrument is currently in the developmental stage. Progress has been made to reduce the impedance without affecting the other parameters. However, no method has been discovered to improve the response and calibration accuracy at RH < 20 percent.

## REFERENCES - CONDUCTIVITY HYGROMETERS


Amdur, E.J., D.E. Nelson, and J.C. Foster, 1965: A ceramic relative humidity sensor. In Humidity and Moisture, Vol. 1, Reinhold Pub. Corp., N.Y., 366-371.

Chleck, D.,1966: Aluminum oxide hygrometer: Laboratory performance and flight results. J. Appl. Meteor., 5(6), 878-886.

Chleck, D., and F J Brousaides, 1965: A partial evaluation of the performance of an aluminum oxide humidity element. In Humidity and Moisture, Vol. 1, Reinhold Pub. Corp., N.Y., 405-414.

Czuha, M., Jr., 1965: Adaptation of the electrolytic moisture detector to atmospheric humidity measurement. In Humidity and Moisture, Vol. 1, Reinhold Pub. Corp., N.Y., 522-528.

Jason., A.C., 1965: Some properties and limitations of the aluminum oxide hygrometer. In Humidity and Moisture, Vol. 1, Reinhold Pub. Corp., N.Y., 372-390.

Johnson, C.E., Jr., and S.R. Duggan, 1965: Humidity meter using cerium titanate elements. In Humidity and Moisture,Vol.1, Reinhold Pub. Corp., N.Y., 358-360.

Jones, F.E., 1963: Performance of the BaF hygrometer element on radiosonde flights. J. Geophys. Res., 68(9), 2735-2751.

_____, 1965: A study of the variation of the surface electrical resistance of lead iodide films with relative humidity at room temperature. In Humidity and Moisture, Vol. 1, Reinhold Pub. Corp., N.Y., 361-365.

_____, 1966: A study of the storage stability of the BaF film electric hygrometer element and a report of 3 experiment applications. National Bureau of Standards, NBS Report No. 9095.

_____, 1967: Study of the storage stability of the barium fluoride film electric hygrometer element. J. of Res. of the National Bureau of Standards, C. Engr. and Instru., Vol. 71C, No. 3, 199-207.

MacCready, P.B., Jr., and J.A.K. Lake, 1965: Mixing ratio indicator. In Humidity and Moisture, Vol. 1, Reinhold Pub. Corp., N.Y.,512-521.

Mathews, D.A., 1965: Review of the lithium chloride radiosonde hygrometer. In Humidity and Moisture, Vol. 1, Reinhold Pub. Corp., N.Y.,219-227.

Stine, S.L., 1965: Carbon humidity elements-manufacture, performance, and theory. In Humidity and Moisture, Vol. 1, Reinhold Pub. Corp.,

Stover, C., 1963: Aluminum oxide humidity element for radiosonde weather use. Rev. Sci. Instru., 34(6), 632-635.

## 2.2 DEW/FROST POINT MEASUREMENTS

Small drops of water or ice crystals condense on the surface of a solid body when it is cooled to the dew/frost point. When the temperature of the surface of the body is measured at the inception of the phenomenon, that temperature is the dew/frost point.

In most cases the solid body has a thermostated, mirrored surface. This mirror is cooled until the dew or frost forms. Then, a stable condensate formation is maintained by controlling the mirror temperature by a sensing and central circuit. The condensate is generally detected by an optical system.

There are inherent difficulties with this system that prevent improvement over present accuracies. This is because there are two physical effects that tend to induce the appearance and disappearance of the condensate over a range of temperatures around the actual dewpoint. The first of these effects is the presence of water-soluble material on the surface of the mirror. This leads to incipient dew/frost formation at temperatures above the actual dewpoint (Raoult effect). In the opposite direction, a suppression of dew/frost formation at the dewpoint occurs due to an elevation of vapor pressure of small droplets arising from the internal pressure generated by surface tension (Kelvin effect). The net result of the two effects is dew/frost formation which does not occur at a precisely defined point.

## 2.2.1 PELTIER DEW/FROST POINT HYGROMETER

### 2.2.1.1 NARRATIVE DESCRIPTION OF THE INSTRUMENT

Most dew/frost hygrometers determine the dew or frost point by measuring the temperature of a polished surface upon which dew or frost has just begun to form. A number of methods of observing and controlling the dew or front formation on the surface have been tried. The instrument to be discussed here consists of a thermoelectrically-cooled surface controlled by an optical dew or frost detecting system and two platinum resistance bulb temperature sensors for determining both ambient temperature and the dew point. This unit was developed and is manufactured by Cambridge Systems Incorporated of Newton, Massachusetts.

The instrument consists of a transmitter unit, containing the aspirated temperature and dewpoint transducers, a control unit, containing the transducer amplifier and signal conditioning equipment, and a readout recorder group, which varies considerably depending on requirements. The transmitter unit and control unit are designed for site installation, and are capable of withstanding the full rigors of the elements, whereas the readout hardware is intended for installation in sheltered, indoor environments.

The dewpoint measurements is made with a primary sensor, utilizing a Peltier-cooled mirror automatically held at the dewpoint temperature by means of a photoresistive, condensate-detecting, optical system. With the mirror so controlled, the mirror temperature is determined with an imbedded platinum resistance thermometer, which then represents the true dewpoint temperature. For dew points below 32°F, the system tracks the frost point. The air temperature is determined with a separate matched platinum resistance thermometer, mounted in a thermally shielded and aspirated thermometer well. The resistance changes of both thermometer elements are converted to millivolt outputs by means of zener-regulated bridge circuits located in the control unit. For installations where the data are transmitted only a short distance, the 0-50 mV outputs are transmitted over conventional signal circuits. For longer runs, a 0-5 volt dc signal is furnished. All output characteristics are essentially linear, and follow the Callendar-VanDusen equation for platinum. Temperature sensors used are NBS-traceable, and are furnished with certified calibrations, which include the thermometer coefficients.

The sensors are exposed in a double-walled and thermally shielded aspirator, so as to eliminate errors from solar heating at all radiation angles. The transmitter is finished in a tough white epoxy enamel to further reduce heating effects, and all exposed hardware is of stainless steel so as to minimize corrosion.

### 2.2.1.2 INTERPRETATION OF THE MEASUREMENT

Additional information needed to interpret measurement- The pressure of the atmosphere must be known to determine the specific humidity or water vapor content.

Method for analysis and interpretation of data - The output of the sensor itself is a resistance change with the temperature of surface upon which the dew or frost is forming. This temperature is known as the dew or frost point and is related to water vapor content. The resistance change is measured using a bridge circuit which has an output of from 0 to 5 volts dc for the full range of the instrument as a standard feature.

### 2.2.1.3 INSTRUMENT CHARACTERISTICS

Total and dynamic ranges -

Standard System: Dew/frost points of from -50°C to +50°C
Special Systems: Dew/frost points of from -80°C to +95°C

Accuracy - Dew points ± 0.5°C, frost points ± 1.0°C

Signal to noise ratio - Depends upon electronics.

Frequency response - Typically, 3°C/sec.

Environmental effects - Ambient temperature limits: Sensor -70 to +85°C; control unit 0°F to 140°F.

### 2.2.1.4 INSTRUMENT OUTPUT

Output signal - Linear 0-50 MVDC or 0-5 VDC signals corresponding to span covered.

Bits per observation - For ± 0.55°F resolution, 9 bits are required using the standard instrument.

### 2.2.1.5 PAYLOAD INTEGRATION

Weight - Total system less than ten pounds.

Volume - Approximately one-third cubic ft.

Power - 20 watts.

Radio frequency interference - All circuits adequately RFI suppressed to eliminate noise.

Magnetic moment - Unknown.

Erection, orientation, or booms - None.

Compatibility with sterilization at 145°C - Unknown.

Special requirements - None.

2.2.1.6 STATE OF DEVELOPMENT

Commercially available. In use aboard both Gemini and Apollo.

2.2.2 GASEOUS COOLANT HYGROMETER

2.2.2.1 NARRATIVE DESCRIPTION OF THE INSTRUMENT

This instrument has an optical-electronic-thermal servo loop to continuously control a mirror at the frostpoint temperature. One phototube receives light specularly reflected by a mirror in thermal contact with a freon 13 heat sink, and another phototube receives light scattered by the mirror and directly from a lamp used to illuminate the mirror. The amount and optical characteristics of the condensate on the mirror determines the relative proportion of light which reaches the two phototubes. The phototubes are connected in a bridge arrangement which governs the output of an rf oscillator which feeds an rf heating coil surrounding the mirror. This induction heating balanced against the heat sink of freon 13 controls the size of the condensate spot on the mirror. The temperature of the mirror is measured by a bead thermistor embedded in the mirror surface to give the frostpoint temperature. A conventional radiosonde transmitter is used to telemeter frostpoint temperature, air temperature and an audio reference signal.

2.2.2.2 INTERPRETATION OF THE MEASUREMENT

Additional information needed to interpret measurement - In addition to the mirror temperature, ambient air temperature has to be known. To determine relative humidity, atmospheric pressure is required in addition.

Method for analysis and interpretation of data - The temperature measurement furnished by the embedded bead thermistor is the dew/frost point temperature. Relative, or specific humidities can be derived from this and the ambient temperature pressure determinations.

2.2.2.3 INSTRUMENT CHARACTERISTICS

Total and dynamic ranges - Dew/frost temperature from about +30°C to less than -100°C (information on exact lower limit is not available).

Accuracy - of the order of 1/2 degree.

Signal to noise - Dependent on surface contamination of the mirror.

Frequency response - Not specified, probably of the order of tens of seconds to minutes.

Environmental effects - Dust contamination can seriously impair accuracy of device.

2.2.2.4 INSTRUMENT OUTPUT

Output signal - Analog signal from thermistor dew/frost sensor, calibrated inverse function of dew/frost temperature.

Bits per observation - 8 or 9, depending on range (for a 1/2°C resolution).

2.2.2.5 PAYLOAD INTEGRATION

Weight - Exact value not available, probably less than 10 lbs and more than 2 lbs.

Volume - Approximately one cubic foot.

Power - Unspecified, could be at least 10 watts. Main power consumer is the induction heater.

Radio frequency interference - Probably high due to rf field set up by heating system.

Magnetic moment - Not known.

Erection, orientation, or booms - Free access of ambient air to sensing mirror has to be assured.

Compatibility with sterilization at 145°C - Undetermined.

Special requirements - Supply of freon 13.

2.2.2.6 STATE OF DEVELOPMENT

Balloon-borne stratospheric investigations are being conducted routinely with an essentially operational instrument.

## REFERENCES - DEW/FROST POINT MEASUREMENTS


Beaubien, J.D., and C.C. Francisco, 1962: Design construction of an electronic dew point indicator. AFCRL-62-218.

Masterbrook, H.J., 1964: Frost-point hygrometer measurements in the stratosphere and the problem of moisture contamination. In Humidity and Moisture, Vol. 2, Reinhold Pub., New York, 480-485.

_____, 1966: Water vapor observation of low middle and high latitudes during 1964 and 1965. NRL Report 6447.

Middleton, W.E., and A.F Spilhaus, 1953: Meteorological Instruments. University of Toronto.

Wexler, A., and W.G. Brombacker, 1939: Smithsonian Meteorological Tables. Smithsonian Institute, Washington, D.C.

_____, 1951: Methods of measuring humidity and testing hygrometers. NBS Circular No. 512.

## 2.3 CAPACITIVE HYGROMETER

The capacitive hygrometer is a liquid film instrument developed at the University of Washington (Charlson, 1964; 1965; Charlson and Buettner, 1964; and Charlson, Buettner, and Maykut, 1966). Its operation is based on Raoults law which states that the ideal relation between the equilibrium mole fraction of water in a nonionizing hygroscopic liquid and the ambient relative humidity is expressed by

$$R = \frac{P_w}{P_T} = \frac{n_w}{n_w + n_s}$$

where R is the relative humidity at the temperature of the instrument T, $P_w$ and $P_T$ are the partial pressures of water vapor in the air sample and over water at the instrument temperature, respectively, $n_w$ is the number of moles of water and $n_s$ is the number of moles of solvent. At low relative humidities ($n_w \ll n_s$)

$$R \cong \frac{n_w}{n_s} \quad .$$

At high relative humidity, $n_w$ becomes large. As a result, a large mass of liquid phase will tend to bleed out of the capacitor. The solution is to raise the temperature in the instrument. Thus leakage is prevented and a linear relationship exists between R and $n_w$.

With the assumption that the dielectric constant is directly proportional to $n_w$, then

$$P_w = \frac{B\Delta C\ P_T}{B\Delta C + h_s} = \frac{\alpha\ \Delta C\ P_T}{\alpha\ \Delta C + 1}$$

where B is the proportionality constant in moles per picofarads, $\alpha = B/n_s$ (sensitivity constant in picofarads$^{-1}$), and $\Delta C$ is the change in capacitance above the dry value due to the sorption of $n_w$ moles of water (in picofarads).

At relative humidities less than 10 percent

$$\frac{P_w}{P_T} = \alpha\ \Delta C \quad .$$

Thus, with a controlled temperature of the sensor, a useful linear relation between R and $\Delta C$, when $P_w \ll P_T$, has been established.

### 2.3.1 LIQUID FILM HYGROMETER

#### 2.3.1.1 NARRATIVE DESCRIPTION OF THE INSTRUMENT

The sensor is a porous capacitor. The dielectric material is granulated fluocarbon (Fluoropak 80) covered with a thin (about 0.25μ) coating of polyethylene glycol (Carbonox 400) acting as the solvent. If the surface area to mass ratio of the solid is large, then a significant fraction of the mass of this heterogeneous mixture can be in the liquid phase. The above 0.25μ glycol coating gives a 20 percent by weight mixture for the hygroscopic liquid. Fluoropak 80 has a surface area of 1 square meter per gram.

The air to be sampled is drawn through the capacitor, which consists of the porous material sandwiched between fine mesh or a sintered porous material. Water vapor contained in the sample maintains an equilibrium with moisture sorbed in the solvent. The variations in the amount of water vapor are related linearly to changes in the capacitance ($P_W << P_T$).

#### 2.3.1.2 INTERPRETATION OF MEASUREMENT

Additional information needed to interpret measurement - The temperature of the instrument must either be known or controlled within $0.1^{o}C$. This is necessary in order to know capacitance changes ($\Delta C$) within 0.6 percent. If the ambient relative humidity is to be determined, then the measurement of the ambient temperature is needed.

Method for analysis and interpretation of data - As long as $P_W << P_T$, the $\Delta C$-R relationship is nearly linear. The $P_W << P_T$ condition can be satisfied by operating the instrument at an elevated temperature.

#### 2.3.1.3 INSTRUMENT CHARACTERISTICS

Total and dynamic ranges - The instrument operates most effectively at R < 50 percent. Above this value of R, sensor damage probably occurs. Instrument noise becomes a problem for $P_W \leq 0.01$ mb.

Accuracy - The overall accuracy of the instrument is estimated to be 3 to 5 percent provided that the optimum calibration point can be found. The optimum calibration point is one that will be close to the expected unknown humidities. There is virtually no hysteresis.

Signal to noise - The noise level of the instrument is about $P_W = 0.01$ mb. It is independent of humidity and random.

Frequency response - For a given sensor, the time constant varies with the flow rate of air through the sensor and with temperature. As the temperature of the sensor decreases and the flow rate

decreases, the time constant becomes larger. Response time can also be shortened by decreasing $n_s$ at the cost of a decrease in $\Delta C$ for a given $P_w$. A time constant of about 20 sec is representative of most sensing elements at an instrument temperature of 300°K.

Environmental effects - None.

### 2.3.1.4 INSTRUMENT OUTPUT

Output signal - The analog calibrated output is capacitance. The relative humidity with respect to the instrument temperature is nearly linearly related to the change in capacitance above a reference dry value as long as R is small. The R-$\Delta C$ relationship begins to lose its linear character rapidly at about R = 2.5. Ambient temperature and instrument temperature must be known in order to compute ambient relative humidity.

Bits per observation - For each observation of ambient relative humidity, measurements of ambient temperature and $\Delta C$ are required. It is assumed that instrument temperature, once determined, remains constant. Thus, for 3-place accuracy of temperature and 2-place accuracy of $\Delta C$, 21 bits are required.

### 2.3.1.5 PAYLOAD INTEGRATION

The specifications given below were estimated from diagrams and descriptions of materials.

Weight - Probably less than 10 lbs (this does not include support electronics).

Volume - Probably less than 1 $ft^3$ (this does not include support electronics).

Power - Depends on associated electronics and pump.

Radio frequency interference - None.

Magnetic moment - Not applicable.

Erection, orientation, or booms - None.

Compatibility with sterilization at 145°C - The sterilization compatibility could not be determined although this instrument has operated at temperatures up to 60°C.

Special requirements - Adequate ventilation is important for the sensing element. A rate of 20 liters/minute was used for one experiment. Also, the temperature of the instrument must be kept constant. Therefore, a sensitive heating device and proper insulation are necessary.

### 2.3.1.6 STATE OF DEVELOPMENT

The instrument is in the developmental stage. Efforts are vigorously being made to improve the calibration characteristics and to discover methods to reduce the problem of strictly controlling the instrument temperature. Some flight tests have been conducted.

## REFERENCES - CAPACITIVE HYGROMETER


Charlson, R.J., and K.J.K. Buettner, 1963: The investigation of some techniques for measurement of humidity at high altitudes. Wash. Univ.,Sci. Rpt. No. 1, AF 19(628)-303, 21pp.

_____, 1964: Liquid film hygrometry. Wash. Univ.,Sci. Rpt. No. 2, AF 19(628)-303, 74pp.

Charlson, R. J., K. J. K., Buettner, and B. A. Maykut, 1966: Liquid film hygrometry. Wash. Univ., Final Rpt., AF 19(628)-303, 12pp.

## 2.4 SPECTROSCOPIC HYGROMETRY

Several schemes have been developed for the measurement of the water vapor content in the atmosphere through its absorption of selected wavelengths in the electromagnetic spectrum. Most of the absorption lines due to water vapor are either in the ultraviolet or in the infrared, and hygrometric measurements have been made in both spectral regions. The choice of a particular wavelength is based on many considerations which in general fall into two groups, natural and instrumental. Natural factors are, among others, sensitivity of a particular absorption band to the presence of water vapor, uniqueness with respect to other absorbing gases which may be present in the sample, path length requirements, etc. Instrumental factors are source and detector spectral characteristics as well as path length characteristics.

## 2.4.1 VACUUM ULTRAVIOLET AND LYMAN ALPHA HYGROMETERS

### 2.4.1.1 NARRATIVE DESCRIPTION OF THE INSTRUMENT

Water vapor absorption bands appear at wavelengths shorter than 1900Å and several experimental systems have been built using that part of the spectrum. It presents several disadvantages with respect to infrared spectroscopy mainly because of the lower atmospheric transparency in the region below 2000Å. The best wavelength in the ultraviolet for the measurement of water vapor concentration appears to be the band at 1220Å which contains the strong Lyman-alpha line of atomic hydrogen. That wavelength (1215.67Å) also coincides with an "oxygen window" which is not available at other $H_2O$ ultraviolet absorption bands. A typical Lyman-alpha ultraviolet hygrometer consists of a hydrogen lamp fed by a suitable power supply (2000 V approx.). This lamp generates, among other wavelengths, the Lyman-alpha line of interest. A measuring path, of the order of one centimeter in length, separates this source from the detector, a nitric oxide ion chamber or a photomultiplier, followed by an electrometer and a logarithmic amplifying circuit. Lithium fluoride windows are used both at the source and at the detector.

### 2.4.1.2 INTERPRETATION OF THE MEASUREMENT

In addition to the output of the instrument it is necessary to transmit a reference signal based on the UV emission of the lamp since it can be expected to vary. Furthermore, knowledge about air density and composition are required to introduce output corrections.

The detector current I follows the equation:

$$I = I_o \exp[-k(\rho/\rho_o)x]$$

where:

$I_o$ = current for vacuum conditions in the path,
$k$ = absorption coefficient for water vapor (387 $cm^{-1}$ at Lyman alpha),
$\rho_o$ = water vapor density at STP,
$\rho$ = water vapor density under ambient conditions,
$x$ = path length.

Thus, through the use of a logarithmic amplifier, the output of the device becomes approximately proportional to the inverse of the water vapor concentration.

### 2.4.1.3 INSTRUMENT CHARACTERISTICS

Total and dynamic ranges - The lower limit of detection depends on the refinement of all the elements of the instrument; concentrations of 10 ppm at STP can be achieved without excessive difficulty.

Accuracy - Of the order of five to ten percent.

Signal to noise - Dependent on signal level, usually minimum detectable level is noise limited.

Frequency response - 10 to 100 Hz.

Environmental effects - Traces of gases absorbing at the operating wavelength will affect the validity of the measurement.

2.4.1.4 INSTRUMENT OUTPUT

Output signal - Analog, calibrated, approximately inversely proportional to water vapor concentration.

Bits per observation - Seven.

2.4.1.5 PAYLOAD INTEGRATION

These parameters will be given for a hypothethical device designed for planetary applications on the basis of estimated state-of-the-art.

Weight - 1 lb approximately.

Volume - 30 $in.^3$ approximately.

Power - 2 W approximately.

Radio frequency interference - None.

Magnetic moment - Not known.

Erection, orientation, or booms - Not critical.

Compatibility with sterilization at 145°C - High.

Special requirements - None.

2.4.1.6 STATE OF DEVELOPMENT

Experimental devices have been used for aircraft soundings.

2.4.2 INFRARED ABSORPTION HYGROMETER

2.4.2.1 NARRATIVE DESCRIPTION OF THE INSTRUMENT

Two types have been developed, one, passive, using solar radiation as the source and the other, active, using an artificial source. Several variations of each exist, especially of the second group. Since many of the characteristics of these two groups are similar, only a general description will be given and the important differences will be pointed out.

A typical passive system uses two detectors, one responding to an $H_2O$ absorption band, for example 0.935μm, and the other a wavelength unaffected by water, for example 0.881μm. The signals of the two detectors can be compared continuously by means of a ratio bridge and the resulting signal is then amplified. An alternative solution is the use of one detector with a wavelength selective filter wheel. The system uses an equatorial sun-following mount. The typical active device uses an infrared source, a tungsten lamp, a sensing path of the order of one meter, a two wavelength detecting configuration consisting of a detector (lead sulfide or similar), and an oscillating or rotating filter system with one wavelength at an absorption band and the other at a reference transmission band. Typical wavelength combinations are: 1.3425μm and 1.3375μm, 1.9μm and 2.2μm, 2.6μm and 2.45μm, etc. The peak to peak amplitude of the resulting alternating signal is a function of the $H_2O$ absorption in the sensing path. This signal is averaged and amplified, either linearly or logarithmically depending on the desired range of operation.

### 2.4.2.2 INTERPRETATION OF THE MEASUREMENT

Atmospheric pressure should be known to interpret the output of the instrument. Its effect is especially important at higher water vapor concentrations, under practical conditions. The absorption of water vapor (over limited ranges) follows approximately an equation of the form:

$$A = (P/P_o)^{\frac{1}{2}} (T_o/T)^{\frac{1}{4}} KW^{\frac{1}{2}}$$

where:

A = fractional absorption,
$T_o$, $P_o$ = standard temperature and pressure,
K = constant depending on wavelength,
W = water mass in centimeters,
T, P = ambient temperature and pressure.

The fact that the actual pressure dependence of the output is dependent on water vapor concentration is caused by the nonideal transmission at the reference wavelength.

### 2.4.2.3 INSTRUMENT CHARACTERISTICS

Total and dynamic ranges - Typical ranges cited in the literature are 10 to 2500 ppm by volume for one instrument, and 0.5 to 95 percent relative humidity for another.

Accuracy - Of the order of 5 to 10 percent.

Signal to noise - Dependent on signal, minimum detectable levels are generally noise limited.

Frequency response - Dependent on chopping frequency, detector and amplifier response, usually of the order of 10 to 100 Hz.

Environmental effects - Atmospheric pressure and temperature are factors influencing calibration.

2.4.2.4 INSTRUMENT OUTPUT

Output signal - Analog, calibrated, approximately inversely proportional to water vapor concentration.

Bits per observation - Seven to ten depending on desired resolution.

2.4.2.5 PAYLOAD INTEGRATION

These parameters will be given for a hypothetical device developed for planetary use on the basis of available information.

Weight - ten lbs approximately.

Volume - 100 to 200 $in.^3$ approximately.

Power - 10 to 100 watts (depending on lamp power).

Radio frequency interference - None.

Magnetic moment - Not known.

Erection, orientation, or booms - Sun pointing equatorial mounting and drive for passive system, not critical for active system.

Compatibility with sterilization at 145°C - High, with appropriate design.

Special requirements - See above for passive system.

2.4.2.6 STATE OF DEVELOPMENT

Field instrumentation, would require redesign for planetary applications.

## REFERENCES - SPECTROSCOPIC HYGROMETRY


Bologna, J. M., et al., 1958: An airborne Lyman-alpha humidometer. NRL Report 5180.

Elagince, L.G., 1962: Optical devices for the measurement of turbulent pulsations of humidity. Academy of Science, USSR Geophys. Series Bulletin 8, 704-708.

Garton, W.R. S., et al., 1957: The application of vacuum ultraviolet techniques to the continuous monitoring of trace concentrations of water in several gases. J. Sci. Instru., 34, 496.

Vaughan, H.C., 1963: Development of a Single Beam Infrared Hygrometer. M.S. Thesis, Meteorology, Iowa State University of Science and Technology.

Wexler, A., (ed.), 1965: Humidity and Moisture. Vol. 1, Reinhold Pub. Corp., N.Y., pg. 417 ff.

Wood, R.C., 1958: Improved infrared absorption spectra hygrometer. Rev. of Sci. Instru., 29, 36-42.

_____, 1959: The infrared hygrometer as a potential meteorlogical aid. Bulletin AMS, 40, 280-284.

### 2.4.3 LASER TECHNIQUE

The vertical profile of the molecular number density of water vapor may be determined by a polychromatic light detection and ranging (PLIDAR) from measurements of the height derivative of the ratio of the intensities of light backscattered from two giant pulsed ruby lasers. This can be accomplished provided that the water vapor absorption is known (Harris, Nugent and Cato, 1965). The temperature profile must be known since the molecular number density is a function of temperature and pressure.

To accomplish the measurement, two giant pulsed lasers or one laser, which can provide two simultaneous pulses at different frequencies by Raman shifting, can be used. One of the pulses will operate at a strong water vapor absorption band and the other will be tuned to an adjacent atmospheric "window".

Another technique (Schotland, Chang, and Bradley, 1965), called DASE (differential absorption of scattered energy), records the time history of the spectral distribution of the backscattered energy. This technique employs a ruby pulse laser. This measurement is interpreted in terms of the spatial distribution of water vapor. The DASE technique is based on an inversion of the transfer function

$$\rho_v(z) = - \frac{1}{2K_w(\lambda_i)} \frac{\partial}{\partial z} \ell n\ R(z)$$

where $\rho_v(z)$ is the vapor density as a function of height,

$K_w(\lambda_i)$ is the spectral characteristic of the water vapor line,

$R(z)$ is the ratio of measured intensity of backscattered light received at the ground in the absorbing band to that received in an adjacent spectral region.

Before DASE or other optical probing techniques can be really successful for probing, more must be understood regarding the effect of temperature and pressure variability of the long path absorption coefficient and the shape of the $H_2O$ absorption lines.

REFERENCES - LASER TECHNIQUE

Harris, E.D., L. J. Nugent, and G.A. Cato, 1965: Laser meteorological radar study. Electro-Optical Systems, Inc., Final Report, Rpt. No. 5990, AF 19(628)-4309, AFCRL-65-177, 93pp.

R. M. Schotland, D. Chang, and J. Bardley, Study of Active Probing of Water Vapor Profiles and Results of Experiments, New York Univ., Final Rpt., Pt. 1 on Optical Sounding II for 6 Nov 63-15 July 65, Contract DA-36-039AMC-03411E.

White, G.R., L.J. Nugent, and L.W. Carrier, 1965: Laser atmospheric probe. Inst. Soc. A., Preprint No. 40.1-1-65, 20th Annual ISA Conference and Exhibit, Los Angeles, 11pp.

## 2.5 PSYCHROMETER

The psychrometer consists essentially of two thermometers exposed side by side; one is an ordinary thermometer, perfectly dry, known as the dry thermometer or dry bulb, while the other has its temperature element surrounded by a thin wet material or covered by a film of water or ice, and is known as the wet thermometer or wet bulb. The temperature of the wet bulb is generally lower than that of the dry bulb, due to the evaporation of water from the wet bulb. The drier the air the more intense will be the evaporation, and the greater the difference in temperature between the two; the vapor pressure can be deduced from the two readings. The reduction of the psychrometer reading to vapor pressure is represented by

$$e = e' - 0.00367\ B(T - T')\left(1 + \frac{T - 32}{1571}\right)$$

where e is the vapor pressure, $e'$ is the pressure for saturated aqueous vapors at temperature $T'$, T is the dry bulb temperature, $T'$ is the wet bulb temperature, and B is the barometric pressure.

Any type of bulb thermometer may be used in the psychrometer. The units used should be shielded from radiation and aspirated in some manner. The speed of response and accuracy of the wet bulb depends somewhat on the ventilation rate. The methods of measuring of the actual wet and dry bulb temperatures, if resistance bulb thermometers are used, are the same as those discussed under temperature sensors and the same instrument specifications apply.

For automatic sensing using the psychrometer, some means must be provided to supply the wet bulb element with water to insure a correct wet bulb temperature. Systems using gravity feed for supplying water have been developed for psychrometers on Earth. However, for applications in space and involving space travel, these systems would hardly be adequate. With the exception of the water supply design, the measuring element specifications are identical with resistance bulb thermometers.

## 2.6 THERMAL (ULTRA-DRY BULB) HYGROMETER

This hygrometer operates on the principle of a temperature rise due to release of heat during sorption of water vapor by hygroscopic material. The temperature rise is related almost linearly to absolute humidity.

### 2.6.1 POROUS BED THERMAL HYGROMETER

#### 2.6.1.1 NARRATIVE DESCRIPTION OF THE INSTRUMENT

The instrument consists of a porous bed of silica gel granules contained in a tube with thermocouples mounted in the air close to each end of the tube (Downes and Nordon, 1963). The thermocouples are connected differentially, the net voltage being measured on a potentiometer recorder. Air is pumped through the tube at a controlled rate and the temperature difference is measured.

#### 2.6.1.2 INTERPRETATION OF MEASUREMENT

Additional information needed to interpret measurement- The rate of flow of the air through the tube must be measured.

Method for analysis and interpretation of data- There will be two outputs. The first is the temperature of the gas before the moisture is removed, and the second, the temperature after sorption of the water vapor. The absolute humidity is nearly linearly related to measured temperature difference. Curves of the temperature difference versus time show a peak difference within 2-3 minutes after the experiment has started (for dry bulb temperature of 20C). This peak difference is the quantity that is used to determine the absolute humidity.

#### 2.6.1.3 INSTRUMENT CHARACTERISTICS

Total and dynamic ranges - The instrument has been tested for absolute humidities as high as 13.3 g/kg. No specific mention is made of a specific low point for its range; however, it is mentioned that the instrument retains its sensitivity at very low values of humidity.

Accuracy - The principal factors that determine the accuracy of the instrument are the precise knowledge of the heat of sorption of the silica gel and its dependence on moisture, and the absence of a "plateau" instead of the observed peak for the maximum temperature difference. Downes and Nordon indicate that this latter feature detracts from the usefulness of the method as a practical hygrometer.

Signal to noise - Signal to noise was not determined.

Frequency response - For a dry bulb temperature of 20C and absolute humidities between 6.9 and 13.3 g/kg, the time constant is about 1 1/2 minutes.

Environmental effects - None.

2.6.1.4 INSTRUMENT OUTPUT

Output signal - The output is a two-analog trace of voltage which is easily converted into temperature according to the calibration. As mentioned above, the peak of the temperature difference curve is nearly linearly related to the absolute humidity.

Bits per observation - Twenty-two bits per observation will be required for the two voltage readings (accurate to three places with exponents).

2.6.1.5 PAYLOAD INTERGRATION

Weight - The bed contains 431g of silica gel. The entire apparatus appears to be lightweight.

Volume - The tube that contains the silica gel is about 15 cm in diameter and 18.5 cm long.

Power - The power for the operation of the two thermocouples is not discussed by Downes and Nordon (1963).

Radio frequency interference - None anticipated.

Magnetic moment - Not known.

Erection, orientation, or booms - None

Compatibility with sterilization at 145°C - It cannot be determined if this instrument would be affected by sterilization at 145°C.

Special requirements - None.

2.6.1.6 STATE OF DEVELOPMENT

Some tests over the high humidity portion of the range have been performed on this device. Tests for low humidity conditions have not been reported. Further development seems necessary for this instrument to become operational.

REFERENCES - THERMAL (ULTRA-DRY BULB) HYGROMETER

Downes, J. G., and P. Nordon, 1963: The thermal or ultra-dry hygrometer, J. of Sci. Instruments, 40(12): 596-598.

## 2.7 COOLED VAPOR TRAP

This technique, which has been described by Barclay, et al (1960), attempts to freeze out the water vapor and carbon dioxide directly from the atmosphere by drawing the atmosphere through a vapor trap cooled with liquid nitrogen. The amount of carbon dioxide collected is used to determine the total amount of atmosphere sampled, assuming that the $CO_2$/atmosphere ratio is known and that it remains constant during the sampling period. The technique has been used in the Earth's stratosphere. The present system requires recovery of the payload.

### 2.7.1 BALLOON-BORNE VAPOR TRAP

#### 2.7.1.1. NARRATIVE DESCRIPTION OF THE INSTRUMENT

The apparatus consists of a U-tube vapor trap, a Dewar flask which houses the liquid nitrogen, a centrifugal blower, and a disc-type rotary valve. Air is forced through an intake pipe, then through a valve and the stainless steel vapor trap. The air exits through another port of the valve and past the blower.

After the balloon-borne apparatus has been flown and recovered, the amount of water vapor is determined by converting the water vapor to hydrogen by passing the gaseous contents of the trap over heated zinc. By measuring the pressure and volume of the hydrogen, the amount of water vapor originally present is deduced.

#### 2.7.1.2 INTERPRETATION OF THE MEASUREMENT

Additional information needed to interpret measurement - In order to determine the mixing ratio, the amount of carbon dioxide must also be measured. The volume of air that passed through the trap is determined from this measurement.

Method for analysis and interpretation of data - As it is presently designed, the instrument package must be recovered. The collected samples of carbon dioxide and water vapor are analyzed in the laboratory as described in the previous section. There are no electronics involved in transmitting the output, only in the operation of the moving parts while the apparatus is conducting the experiment at altitude. For application to the planets, automation of the analysis procedure is required.

#### 2.7.1.3 INSTRUMENT CHARACTERISTICS

Total and dynamic ranges - This instrument is designed to measure stratospheric moisture. It is assumed that it traps all the water vapor present in the air. Theoretically, it can measure any mixing ratio. In the flight test of the experiment that was reported, a mixing ratio of 0.037 g/kg was determined. Some contamination does occur on the ground prior to flight. It was estimated that 0.5 mg of water are contributed to the

overall total by leakage and the gas analysis technique. Thus, measurements of very small amounts of water might have a large percentage error associated with them. However, by drawing large amounts of atmosphere through the trap, very small mixing ratios can be measured.

Accuracy - There is some uncertainty in the collection efficiency of the trap as well as in the contamination and gas analysis error discussed above. The uncertainty regarding collection efficiency can be minimized by the selection of a long tube for the trap. No attempt was made to determine the absolute error, but comparison of the observed mixing ratio measured in a flight test were compared with others determined by different experimenters. The vapor trap results compared favorably.

Signal to noise - If the "noise" is considered to be the weight of water that comes from leakage and from gas analysis, then the signal to noise ratio would be the measured weight of water divided by the estimated weight of water from leakage and gas analysis.

Frequency response - There is no time constant in the strict sense. However, enough air must be drawn through the apparatus to get a reasonable amount of water — more than the amount resulting from leakage and gas analysis.

Environmental effects - Leakage must be kept to a minimum. This can partially be accomplished by pre- and post-flight storage in a dry place.

2.7.1.4 INSTRUMENT OUTPUT

Output signal - Not applicable, since automated analysis procedure not yet developed.

Bits per observation - Not applicable, since automated analysis procedure not yet developed.

2.7.1.5 PAYLOAD INTEGRATION

Refers to system used in Earth's stratosphere.

Weight - 90 lbs.

Volume - Not stated, probably less than 4 $ft^3$.

Power - A 24-volt silver-zinc accumulator was used to power the equipment.

Radio frequency interference - None.

Magnetic moment - Not applicable.

Erection, orientation, or booms - None.

Compatibility with sterilization at 145°C - Yes.

Special requirements - Special care should be taken before the flight to minimize leakage error and the gas analysis should be performed as soon as possible following the experiment for the same reason.

2.7.1.6 STATE OF DEVELOPMENT

This instrument is in the experimental stage. Errors have not been precisely determined. Barclay, et al do mention that further design could substantially reduce the size of the instrument. Application to unmanned missions to planets would require development of automated analysis procedure.

REFERENCES - COOLED VAPOR TRAP

Barclay, F.R., M.J.W. Elliot, P. Goldsmith, and J.V. Jelley, 1960: A direct measurement of the humidity in the stratosphere using a cooled vapor trap. Quart. J of Royal Met. Soc.,86 (368), 259-264.

## 2.8 HAIR HYGROMETER

The hair hygrometer measures humidity by means of the change in dimensions experienced by hygroscopic substances when their moisture content varies. When hair is exposed to an atmosphere containing water vapor it absorbs moisture with a resultant rearrangement of the crystals and thus a slight elongation. The reverse process occurs when the hair is dried. Human hair is found to yield one of the best percentage elongations although synthetic materials such as nylon are now being used. For a change in relative humidity of 0 to 100%, the increase in length is about 2.5%. The temperature coefficient of hair is small and negative, causing small errors in the measurement.

A mechanical lever is connected to the hair element and provides mechanical magnification of the elongation to drive an indicator or transducer. A capacitor is used in the Finnish hair hygrometer for radiosonde. The element is attached between a fixed surface and a movable plate of the capacitor. As the hair changes length the capacitance is varied and is a measurement of relative humidity when used with a calibration curve. The hair hygrometer is useful over a very narrow range of temperature of -30 to +150°F and reliability is doubtful below 0°F. Therefore, the hair hygrometer is not recommended for humidity measurements where temperature extremes are likely to be encountered.

## 2.9 MICROWAVE REFRACTOMETER

At frequencies of 10,000MHz and beyond, the atmospheric refractive index is a strong function of water vapor density due to the large dipole moment of the water vapor molecule. Although the water vapor pressure seldom exceeds 3 to 4 percent of the total atmospheric pressure, it can account for as much as 50 percent of the atmospheric refractive index. The refractive index is also a function of temperature and dry air density. The actual computation of water vapor density is described below.

The microwave refractive index of the air is determined by measuring the resonant frequency of a perforated cavity of fixed dimensions containing an air sample. The resonant frequency of the cavity is given by the expression

$$f = \frac{f_o}{n} = \frac{f_o}{1 + (N \times 10^{-6})}$$

where

$f$ = resonant frequency with ambient gas density

$f_o$ = resonant frequency with cavity evacuated

$n$ = refractive index of ambient gas

$N = (n - 1) \times 10^{-6}$

Since n rarely exceeds 1.004, the variable N is more often used for atmospheric applications. In terms of pressure, temperature and humidity (National Bureau of Standards Circular #6744):

$$N = \frac{77.6}{T} \left(P + 4.81 \times 10^3 \frac{e}{T}\right)$$

where

P = total atmospheric pressure in millibars

e = water vapor pressure in millibars

T = temperature in degrees Kelvin

Finally, the relationship between water vapor density and N is given by

$$\rho = \alpha NT - \beta P$$

where

$\rho$ = water vapor density in $g/m^{-3}$

$\alpha = 5,8004 \times 10^{-4}$

$\beta = 4.5011 \times 10^{-2}$

In practice, the cavity is used as the frequency determining component of a microwave oscillator. The difference in frequency between this oscillator and a reference oscillator in a sealed cavity is used to measure the refractive index.

## 2.10 COATED CRYSTALS

The sensing element of this instrument is a radio frequency quartz crystal. The frequency of the oscillation is decreased when the crystal gains weight due to water sorption of a hygroscopic coating. Since frequency changes can be measured accurately and rapidly, this results in an accurate and simple moisture analyzer. Initial experiments indicate the sensor may be used over a wide range covering moisture contents from less than one part per million to a relative humidity of 90%. The quartz crystal is used in a crystal controlled oscillator circuit whose frequency is a measurement of water vapor content of an atmosphere. The instrument has been under development by Esso Research and Engineering Company.

### Reference

King, W. H., Jr., The Piezoelectric Sorption Hygrometer, Esso Research and Engineering Company, Linden, New Jersey.

## 3. WIND VELOCITY

Wind can be expected to be the most variable of meteorological parameters. For Mars, theoretical work (Leovy and Mintz, 1967; Ryan, 1964; and Tang, 1966) and observations of the drifts of yellow clouds (Gifford, 1964) suggest that winds will vary from zero to about 160 m $sec^{-1}$ in the free atmosphere and from zero to at least 100 m $sec^{-1}$ near the surface. One would expect the maximum values to occur only a very small percentage of the time. Average free atmosphere wind speeds are probably low (< 20 m $sec^{-1}$) in the summer hemisphere and high at middle latitudes of the winter hemisphere (~ 50 m $sec^{-1}$). Average surface winds would follow a similar variation, but with generally lower values.

Theoretical and observational indications of winds on Venus are inconsistent with each other. Since Venus rotates very slowly, Coriolis effects can be assumed negligible as a first approximation. The resultant circulation would then consist of a cell with rising motion at the subsolar point, flow toward the antisolar point at upper levels, descending motion at the antisolar point, and flow toward the subsolar point at low levels. Several recent theoretical models of the Cytherean atmospheric circulation reveal this general pattern (Goody and Robinson, 1966; Hess, 1967; Ohring, Tang, and Mariano, 1965). These models indicate generally low wind speeds (< 10 m $sec^{-1}$) for the lower half of the atmosphere. Maximum winds in these models occur at high levels near the antisolar point and can reach values of 40 to 50 m $sec^{-1}$ (Hess, 1967). It should be realized that the theoretical work on Cytherean circulations is of a highly preliminary nature. Observational indications of winds on Venus have been obtained from analysis of UV photographs to derive cloud drifts. Smith (1967) reports drifts of about 100 m $sec^{-1}$ from such analyses. Such values are clearly higher than those predicted by the theoretical circulation work.

## 3.1 THERMAL (HEAT LOSS) ANEMOMETERS

The rate of cooling of a heated element exposed to the free atmosphere depends, among other factors, on the convectional cooling produced by wind currents. This degree of cooling is a function of the mass flow of gas passing the heated element and thus becomes a function of wind speed, in a given environment. This dependence is the basis for the operation of thermal anemometers.

### 3.1.1 HOT WIRE ANEMOMETERS

The cooling of a hot wire in a moving air stream depends principally upon the normal component of the air mass velocity (that is, the component perpendicular to the hot wire) and upon the temperature difference between the hot wire and the air stream. In fact, the normal component of the air mass velocity is sometimes called simply the "cooling" velocity".

A single hot wire may be used to measure the cooling velocity if, for example, the temperature difference between the wire and the air stream is maintained constant by placing the hot wire in some appropriately controlled electrical heating circuit, and the electrical power supplied to the wire is displayed as the deflection of a needle on a panel meter. The meter scale can then be calibrated in "cooling velocity" units directly. When the hot wire is rotated slowly in the plane of the flow, the reading will reach a maximum when the wire is perpendicular to the air stream and it will reach a sharp minimum when the wire is parallel with the air stream. The maximum reading is the true mass velocity, and the direction of the air stream may be measured accurately by observing the orientation at which the minimum reading occurs.

To measure velocity and direction simultaneously in two-dimensional flow, two hot wires in a fixed X-array may be employed. If the X lies in the plane of the flow,then at any instant the mass velocity is given by the vector sum of the two cooling velocity readings and the direction is given by the quotient of the two readings. If a nondirectional measurement of velocity is desired in two-dimensional flow, it is only necessary to hold a single wire perpendicular to the plane of the flow.

In three-dimensional flow, three mutually perpendicular hot wires may be employed. The velocity is then equal to 0.707 times the vector sum of the three readings, and the direction is given by two quotients (using any two pairs of readings).

If a hot wire is held fixed (say perpendicular to the air stream, for the maximum rate of cooling) and the air mass velocity is increased slowly, starting from zero velocity, the rate of heat removal rises steeply at first and tends to level off at high velocity. This nonlinearity is basic to all hot wire measurements and is a central problem in circuit design and data analysis. Electrical linearizing circuits can, in principle, be constructed to provide an output voltage directly proportional to the cooling velocity; but at present such circuits can be used only over small velocity ranges because of electronic stability limitations.

Response times as short as a few microseconds can be attained by using extremely fine hot wires (0.0001-inch diameter or less) and elaborate electronic circuits. Response time of a few milliseconds are

attained with ordinary hot wires (0.0003 inch to 0.001 inch) in simpler circuits.

There are four basic types of hot wire circuits in wide use, the "uncompensated constant current", the "constant resistance ratio," the "constant resistance," and the "compensated constant current." All operate on the principle that the electrical resistance of a hot wire increases with its own absolute temperature, and therefore produces a bridge unbalance which depends on the cooling. Each circuit has exclusive advantages in certain applications.

The mode of operation closest to that suggested in the opening statement is the "constant resistance ratio" circuit in which the ratio of the resistance of the hot wire to an identical, but unheated wire is automatically maintained constant by feedback. The hot wire heating current depends on the cooling velocity in this case, and air temperature effects are minimized. If the wire current in such a circuit is displayed on a panel meter, then the meter may be calibrated in cooling velocity units.

In practice, it is possible to attain better resolution of slow fluctuations with the "uncompensated constant current" circuit and faster responses to rapid velocity fluctuations by using either the "compensated constant current" circuit or the "constant resistance" circuit. But these alternative circuits are rather sensitive to air temperature changes; typically, a 5°F change in air stream temperature may produce a 5-percent error in the velocity reading. Of course, manual controls can be provided that permit readjusting the operating resistance of the wire when the stream temperature shifts from one steady state level to a new one, to compensate for the air temperature change. But when these circuits are used to measure instantaneous velocity in an unsteady flow where the temperature is fluctuating by more than a few degrees Fahrenheit, then either the hot wire must be operated extremely hot or temperature fluctuations must be measured independently (perhaps by using a second unheated wire or a resistance thermometer) in order to determine corrections.

In still air, heat is removed from the hot wire principally by conduction to the surrounding air and to the metal end supports.* Free convection is negligible except in the case of an unusually long wire (length diameter ratio greater than 200) held in a vertical position. Radiation is negligible unless temperature gradients of many hundreds of degrees Fahrenheit exist in the air stream or at the boundary walls.

---

*Conduction of heat to the massive metal end supports (which remain at air temperature) may account for as much as 50 percent of the total heat removal for ordinary hot wires, but this end conduction does not alter the form of the steady state forced-convection equations presented below.

The rate of heat transfer by conduction is proportional to the temperature difference $\Delta T$ between the wire and the air, and to the thermal conductivity. Since the thermal conductivity of air varies approximately as $T^{0.86}$, where T is air temperature, the rate of heat transfer increases with air temperature even if $\Delta T$ is fixed.

In moving air the additional heat transfer due to forced convection depends upon the Reynolds number, defined as $\rho UD/\mu$ where D is wire diameter, $\mu$ is viscosity, and $\rho$ is atmospheric density. Since viscosity varies approximately as $T^{0.71}$, the increase in rate of heat removal for a given hot wire held perpendicular to a moving air stream depends upon the quantity $\rho U/T^{0.71}$. Extensive testing during the past fifty years has shown that the form of the dependence is exactly a square-root function (King's law). The increment in hot wire cooling is thus exactly proportional to the quantity:

$$\sqrt{\rho U/T^{0.71}}$$

Finally, if the hot wire were infinitely long, then only the normal velocity component ($U \sin \beta$) would carry heat away from the wire. But for wires of ordinary length-diameter ratio (say 200 to 1), the velocity component along the wire also removes enough heat to affect the wire cooling measurably. Fortunately, for most practical purposes, the effect of direction upon the cooling can accurately be described by the simple factor $(\sin \beta)^{1/k}$, where k is a constant equal to about 1.1 for ordinary wires.

Putting these facts together results in the equation of the heat balance for a single hot wire of resistance R heated by current I to temperature $T_W$, in an air stream of velocity U, temperature T, specific gravity $\rho$, and direction $\beta$, relative to the wire:

$$I^2R = (T_W - T)(T/T^*)^{0.86}(A)\left[1 + \sqrt{\frac{\rho U(\sin \beta)^{1/k}(T^*/T)^{0.71}}{C_o}}\right]$$

where A, k, and $C_o$ are calibration constants which take into account wire diameter and end conduction effects.

Depending on the point of view of the user, the hot wire may be said to read velocity, mass velocity, or the pressure-velocity product. In the analysis presented here, the position is taken that the quantity most easily measured is in fact the "cooling velocity" C equal to

$$\rho U(\sin \beta)^{1/k}\ (T^*/T)^{0.71}$$

which is of course simply a quantity proportional to the Reynolds number of the hot wire. A general expression relating this cooling velocity C to the electrical properties of the hot wire (I, R, $R_E$) is derived

$$C = C_o \left[ \frac{I^2}{I_{oo}^2} \frac{R}{R_{oo}} \frac{R_{oo} - R_{E_o}}{R - R_E} \left( \frac{R_{E_o} + b}{R_E + b} \right)^{0.86} - 1 \right]^2 .$$

Strictly speaking, the equation should be further modified for the case of unsteady air temperature, to take into account time variations in end conduction due to the thermal inertia of the metal end supports. To avoid this complication, however, we assume that only extremely long wires (length-diameter ratio of 500 or more) will be used in cases where instantaneous velocity is to be measured in an unsteady temperature environment.

### 3.1.1.1 NARRATIVE DESCRIPTION OF THE INSTRUMENT

A constant temperature anemometer instantaneously measures flow parameters by sensing the heat transfer rate between an electrically heated sensor and the flow medium. The basic signal depends on the fluid composition, mass flow, and temperature difference. For many measurements, density is constant and the instrument measures velocity. When temperature varies, compensation is provided to maintain a constant temperature difference.

The sensors themselves are available in a number of types, each offering some advantages. The tungsten wire offers high strength but is limited to operating in environments of under 300°C in temperature, while the platinum wire has relatively low strength but can be operated in environments of up to 800°C. A platinum-iridium wire combines the advantages of both the tungsten and platinum wire but is limited in its sensitivity. Quartz coated thin film offers most of the advantages of hot wires and, in addition, is less susceptible to contamination. However, due to the increased size, quartz coated sensors have a response time much longer than any of the wire type sensors. Wire sensors are generally recommended for almost all air and gas flow measurements. Films and quartz coated sensors are most useful in environments where particles larger than three times the wire diameter are expected or under severe conditions.

The sensor is heated by current from the amplifier. As the flow increases, the sensor tends to cool causing an off-balance of the bridge measuring circuit. This off-balance is immediately sensed by the amplifier which then corrects the current flow into the sensor to bring the system back into balance. In this way, the sensor is controlled

at a specific resistance which is dependent upon the control resistor in the opposite leg of the bridge circuit.

Measurements of temperature are made by plotting a nonlinear calibration curve of flow vs voltage required to supply the heating current or by adding a linearizing circuit and monitoring the heating voltage to yield a more convenient output.

### 3.1.1.2 INTERPRETATION OF THE MEASUREMENT

Additional information needed to interpret the measurement - 1) Ambient temperature of the atmosphere, 2) density of the atmosphere, 3) composition of the atmosphere.

Method for analysis and interpretation of data - The basic output signal is a voltage which is related to flow, approximately as

$$E^2 \approx [A + B(\rho V)^{1/n}] \ (t_s - t_e)$$

where A and B are constants depending upon the medium properties, $\rho$ is the medium density, V is the velocity, n is an exponent that varies with range and medium properties, $t_s$ is the sensor operating temperature and $t_e$ is the medium temperature. The relationship between voltage and velocity is nonlinear and has a residual dc voltage at zero flow.

### 3.1.1.3 INSTRUMENT CHARACTERISTICS

Total and dynamic range - The minimum flow range of heated sensors depends upon the free convection currents generated by the sensor rather than the electronics. Velocities down to 0.2 f/s in air can be measured. The maximum velocity is generally a physical limitation rather than a heat-transfer limitation. For velocities above 1000 ft/s in air, quartz coated films mounted on wedges or cones are used.

Accuracy - ±0.5 percent with individual sensor calibration.

Signal to noise - Depends on electronics.

Frequency response - The system frequency response depends upon the choice of sensor, the medium, and the velocity. Typical time constants for wire-type sensors are approximately 0.001 seconds.

Environmental effects - Susceptible to sensor damage or degradation in presence of aerosols.

### 3.1.1.4 INSTRUMENT OUTPUT

Output signal - Dependent upon the particular bridge circuit and amplifier selected; typical output signals are: 0-1 V full scale, 10 kΩ output impedance, and 1-100 c/s frequency response. Signals generated at the bridge output are nonlinear but are generally conditioned with additional circuits to be linear and proportional to velocity.

Bits per observation - 11 bits per observation are needed to yield an precision of ±0.05 percent.

### 3.1.1.5 PAYLOAD INTEGRATION

Weight - Total system, 35 lbs; probe less than 8 oz.

Volume - Dependent upon system chosen. Probe volume is approximately 0.1 inch cubed.

Power - 150 to 200 watts.

Radio frequency interference - None.

Magnetic moment - Unknown.

Erection, orientation, or booms - Must be erected into the free stream of the atmosphere and oriented into the flow.

Compatibility with sterilization at 145°C - Yes.

Special requirements - None.

### 3.1.1.6 STATE OF DEVELOPMENT

Commercially available for Earth atmosphere, near-surface wind observations.

## REFERENCES - HOT WIRE ANEMOMETERS


Flow Corporation, Technical Bulletins 37, 71, and 65.

Grant, H.L., R.W. Stewart, and A. Moillient, 1962: Turbulence spectra from a tidal channel. J. of Fluid Mech., 12(2).

Grant, H.P., and R.E. Kronaner, 1962: Fundamentals of hot wire anemometry. Symposium on Measurements in Unsteady Flow, May 1962, ASME.

Pankoff, S.G., and R.S. Rosler, 1962: Temperature hot film anemometers as a tool in liquid turbulence measurements. Rev. of Sci. Instr., 33(11).

### 3.1.2 HEATED THERMOCOUPLE ANEMOMETERS

The heated thermocouple anemometer is basically a hot wire anemometer where the output of a thermocouple is used to determine the temperature of the wire rather than measuring the resistance of the wire. The sensor itself consists of three noble metal thermocouples made from thin wires mounted on a framework. Two of the three thermocouples are connected in series and form two measuring legs of an ac bridge and the third thermocouple is connected to the junction between the other two and is in series with the measuring portion of the bridge. The remaining legs of the bridge circuit are formed by a center-tapped ac power source which is used to supply the heating current for the sensing element. Figure 3-1 is an electrical diagram of a basic heated thermocouple anemometer.

Thermocouples A and B are heated by the ac current. A change in flow causes a change in temperature of the thermocouples, resulting in a change in the dc output from the thermocouples. The third thermocouple, C, is in the dc meter circuit. This thermocouple is unheated. A change in ambient temperature develops voltages across all three thermocouples, but the transient effects in heated and unheated elements are equal and opposite, so the unheated unit compensates for ambient temperature changes. The thermocouple instrument is a mass flow meter as long as $\sqrt{KS\rho}$ is constant, where K is the thermal conductivity, S is the specific heat at constant volume, and $\rho$ is the atmospheric density. The relationship between velocity and thermocouple output is dependent upon an individual calibration and varies with the type of thermocouple material used.

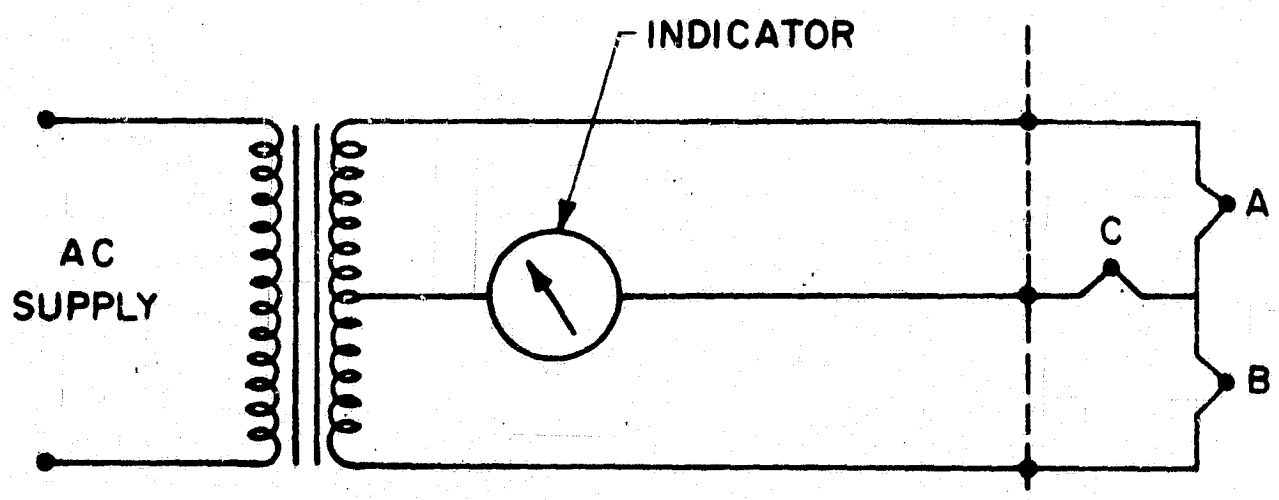


Figure 3-1. Simple heated thermocouple anemometer.

### 3.1.3 WAKE DETECTOR

#### 3.1.3.1 NARRATIVE DESCRIPTION OF THE INSTRUMENT

The wake wind direction indicator is shown in Figure 3-2. It consists of a central coiled wire, which is heated, and sixteen surrounding temperature measuring wires. Each wire comprises one arm of a four element bridge; the other three elements are exposed to the ambient atmosphere and provide temperature compensation. An amplifier-detector is associated with each of the sixteen bridges. The amplifier-detector determines whether or not each wire has detected the warm air flow from the heater. This circuit has a fixed level which the signal must exceed before the temperature is said to be different from ambient. A gating system follows the bridge network, and it allows only one of two adjacent wires to trigger a corresponding output. Finally, the output selects a voltage proportional to the wind direction from a voltage divider network. This technique depends upon the fact that the change in the ambient temperature across the device is smaller than the discrimination level. This requirement will in turn determine the heater power. At the present, this has not been determined but it is felt that a heater power of 0.1 watts or less would produce a temperature change of several degrees,a readily detectable level. The only problem would be the incidence of small scale, large temperature turbulent fluctuations in the atmosphere.

#### 3.1.3.2 INTERPRETATION OF THE MEASUREMENT

Additional information needed to interpret the measurement - None.

Method of analysis and interpretation of the data - The output of the instrument is in the form of a voltage level which is proportional to the wind direction.

#### 3.1.3.3 INSTRUMENT CHARACTERISTICS

Total and dynamic range - Total range 0 to 360°.

Accuracy - 12.5°.

Signal to noise - Unknown but is dependent upon electronics and temperature discrimination ability.

Environmental effects - Contamination of either the heater or sense wires will degrade the data, and large turbulent temperature fluctuations may also affect the output.

#### 3.1.3.4 INSTRUMENT OUTPUT

Output signal - An analog signal whose amplitude is proportional to the wind direction is available as an output.

Bits per observation - A six-bit word is needed to make use of the maximum sensor resolution for each reading.

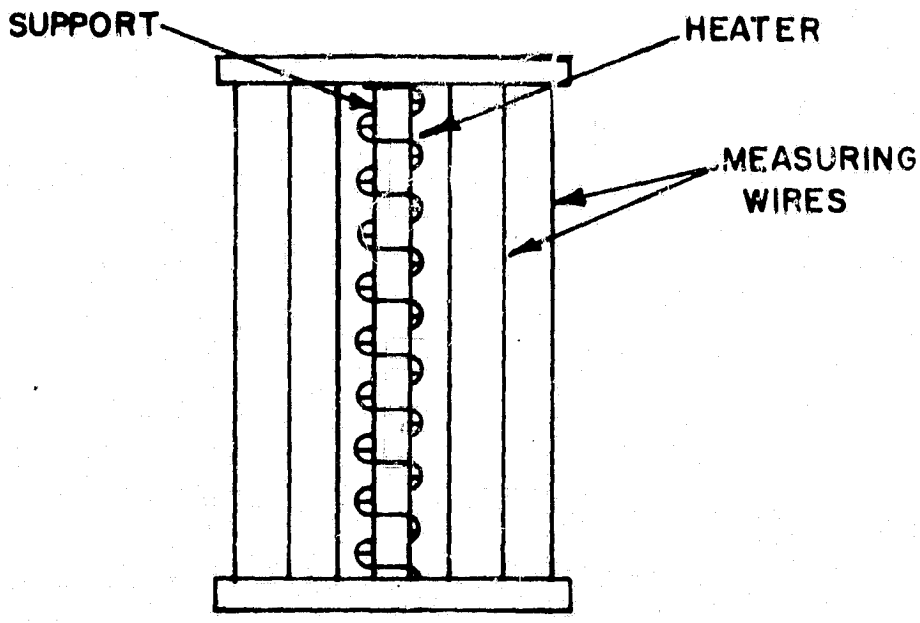


Element Detector and Logic Circuitry




Figure 3-2. "Wake" wind direction indicator.

### 3.1.3.5 PAYLOAD INTEGRATION

Weight - Maximum of 12 oz.

Volume - Maximum of 35 cubic inches.

Power - 0.5 watts during observation.

Radio frequency interference - None.

Magnetic moment - Unknown.

Erection, orientation, or booms - Must be erected in the free-stream wind flow and oriented in a known direction.

Compatibility with sterilization at 145°C - Yes.

Special requirements - None.

### 3.1.3.6 STATE OF DEVELOPMENT

Undeveloped; however, circuitry is straightforward. Major problem is the design of the heat source to obtain maximum temperature at the detectors.

### 3.1.4 KATA THERMOMETER

The Kata thermometer consists of an alcohol thermometer with a large bulb exposed to the air stream. The bulb is heated to a temperature typically 40 or 50°F above ambient; the heat input is then interrupted and its time to cool over a given temperature interval, above ambient is measured. This cooling time is related to the average air velocity during that period of time. The theory of operation is similar to that underlying the hot wire anemometer with the difference that no heat input has to be considered during the cooling period.

This technique has very limited applicability to remote planetary measurements and in addition its long integration time precludes determinations of the structure and variability of winds. Further discussion of this instrument is considered unnecessary.

## 3.2 ACOUSTICAL TECHNIQUES

The measurement of wind velocities using acoustical techniques is based upon the propagation of sound through a gas medium. Sound waves are propagated through gas by virtue of the elastic properties of the gas molecules. Thus, the velocity of the sonic disturbance is superimposed upon the mean gas velocity.

### 3.2.1 SONIC ANEMOMETER

The velocity of sound in a gas at rest is given by

$$C = \left( \gamma \frac{R}{M} T \right)^{\frac{1}{2}}$$

where C = velocity of sound in still gas,
$\gamma$ = ratio of specific heat at a constant pressure to specific heat at a constant volume,
R = universal gas constant,
M = molecular weight of the gas,
T = absolute temperature of the gas.

For any given gas, the velocity of sound is a function of temperature only. Changes in pressureand density at a constant temperature have no effect on the propagation of sound. A measurement of sound velocity in still gas is the basis for the sonic thermometer. However, at a given temperature, the speed of sound is a function of the molecular weight of the gas. In air the most important factor, other than temperature, contributing to variations in the speed of sound is the water vapor concentration. The velocities in $N_2$, $O_2$, and $CO_2$ are similar, but the velocity in $H_2O$ is considerably higher. The velocity of sound given here is based upon ideal gas properties and is satisfactory at low frequencies, while at high frequencies, dispersion takes place.

A point source of sound propagates as a spherical wave in an isotropic medium at rest. Considering a two-dimensional plane through the source, the wave is circular in this plane. The equation for the position of a sonic disturbance in a plane through the point source in a stationary medium is

$$x^2 + y^2 = c^2(t - t_o)^2$$

where x,y = coordinates of a point on the wave front,
c = sonic velocity,
$t_o$ = time the wave leaves the origin,
t = time in question.

If the gas is moving with velocity V at an angle $\theta$ to the abscissa, then this is superimposed upon the above coordinates. Thus,

$$[x - (t - t_o)V \cos \theta]^2 + [y - (t - t_o)V \sin \theta]^2 = c^2(t - t_o)^2.$$

The sonic anemometer measures the gas velocity V by means of the measurements of the sonic transit time along orthogonal axes.

The time required for the sonic disturbance to travel from its origin across a path of length L in the x-direction can be found by solving for $(t-t_o)$ when $x = L$ and $y = 0$

$$(t - t_o)\Big|_{y=0} = \frac{L}{c^2} \frac{c\sqrt{1 - \frac{V^2}{c^2} \sin^2 \theta} - V \cos \theta}{1 - (V/c)^2} .$$

Similarly, the time in the direction of y can be found by solving for $(t - t_o)$ when $y = L$ and $x = 0$

$$(t - t_o)\Big|_{x=0} = \frac{L}{c^2} \frac{c\sqrt{1 - \frac{V^2}{c^2} \cos^2 \theta} - V \sin \theta}{1 - (V/c)^2} .$$

Since c and L are known for a given path and gas temperature, the velocity V can be found from the measurements of the sonic transit time on the orthogonal axes.

Since c is always larger than V, a small percentage change in c can result in a change in $(t - t_o)$ that is larger than the effect of velocity V. This can be eliminated by measuring the time required for a sonic disturbance to travel from $x = 0$ to $x = L$ and subtracting it from the time for another sonic disturbance to travel from $x = L$ to $x = 0$. The expression from this latter time is

$$(t - t_o)\Big|^{*}_{y=0} = \frac{L}{c^2} \frac{c\sqrt{1 - \frac{V^2}{c^2} \sin^2 \theta} + V \cos \theta}{1 - (V/c)^2} .$$

and subtracting from it the first equation results in

$$\Delta t = \frac{2L}{c^2} \frac{V \cos \theta}{\left[1 - (V/c)^2\right]}$$

which is the basic equation for the sonic anemometer.

### 3.2.1.1 NARRATIVE DESCRIPTION OF THE INSTRUMENT

Sonic anemometers have been developed and used in the field by J.C. Kaimal of AFCRL, V.E. Suomi of the University of Wisconsin, R.M. Stewart of Iowa State University, and Cambridge Systems of Newton, Massachusetts. The instrument developed by Kaimal serves both as an anemometer and a sonic thermometer. The instrument discussed here is the Cambridge Systems unit which has been recently developed and marketed commercially.

The Cambridge Systems Sonic Anemometer is available in a one, two, or three axis model. The unit utilizes the pulse technique of alternating the direction of transmission of short bursts of high frequency sonic energy at 230 kHz over a fifteen-inch path. The transducers alternate as transmitters and receivers on a 5-ms basis. Pulses travelling with the wind arrive sooner than those travelling against the wind. The difference between the two transit times in a direct function of the wind velocity along the axis. Since the pulses traverse the same part ac approximately the same time, 5-ms apart, the resulting measurement is free from the first order temperature effects on the propagation of sound. A clock is used to determine the difference between the two transit times. The frequency of the clock has been chosen so that each clock pulse is a representation of a wind velocity of one knot. A temperature dependent network modifies the clock frequency by approximately 0.17 percent/°C in air temperature, removing the second order temperature effects.

The transducers themselves and their associated mounting hardware are the most important components of the whole system, since their performance dictates the overall system specifications. The transducers employed utilize cylindrical piezoelectric ceramic tubes mounted in a hermetically sealed stainless steel case. The diaphragm of the transducer is a thin stainless steel membrane which serves to couple the displacement of the ceramic element to the atmosphere. The transducers are mounted on 3/8-inch heat treated aluminum supports. Relatively light supports can be used with the pulsed technique because the pathlength must remain constant only during the transit time of approximately 1 ms. The entire array is waterproof and rugged, lending itself to field use.

### 3.2.1.2 INTERPRETATION OF THE MEASUREMENT

Additional information needed to interpret measurement- To obtain velocity measurements, the following data must be available for a given medium: molecular weight of the gas and specific heat ratio.

Method for analysis and interpretation of data - The output of the instrument is a digital representation of the wind velocity over a given averaging period or an instantaneous value.

3.2.1.3 INSTRUMENT CHARACTERISTICS

Total and dynamic range - 0 to 150 knots in any axis.

Accuracy - 3 percent of reading.

Signal to noise - Depends on electronics.

Frequency response - Time constant of 5 ms.

Environmental effects - None anticipated.

3.2.1.4 INSTRUMENT OUTPUT

Output signal - Digital signal proportional to the medium velocity.

Bits per observation - Eight.

3.2.1.5 PAYLOAD INTEGRATION

Weight - 1/4 lb (sensor only).

Volume - 20 m by 1/4-inch cylinder.

Power - Unknown.

Radio frequency interference - Produces some rf radiation at 230 kHz.

Magnetic moment - Unknown.

Erection, orientation, or booms - Transducers require mounting in the free stream of the wind flow.

Compatibility with sterilization at 145°C - Yes.

Special requirements - Mounting of transducers in free stream of wind flow.

3.2.1.6 STATE OF DEVELOPMENT

Commercially available.

REFERENCES - SONIC ANEMOMETER

Cambridge Systems, 1967: Technical Specifications and Brochures for Sonic Anemometers.

Kaimal, J.C., and J.A. Businger, 1963: A continuous wave sonic anemometer-thermometer. J. Appl.Meteor.

_____, 1963: Preliminary results from a continuous wave sonic anemometer-thermometer. J. Appl. Meteor.

Suomi, V.E., 1956: Energy budget studies at the Earth's surface and development of the sonic anemometer for power spectrum analysis. AFCRL Tech. Rpt. 56-274.

### 3.2.2 EXPLODING GRENADES AND MICROPHONE ARRAY

#### 3.2.2.1 NARRATIVE DESCRIPTION AND MICROPHONE ARRAY

An accoustical technique for determining wind velocities is employed in the earth's atmosphere for altitudes between 20 km and 100km. This technique employs an array of acoustic detectors at ground level to record sound pulses propagating down from a series of high altitude grenade explosions. The grenades are sequentially ejected from a rocket travelling through the atmosphere. To determine temperature and wind velocity for each height increment between successive grenade bursts, it is necessary to know the exact burst coordinate and burst time of the grenade and the subsequent arrival time at each sound detector of the array whose geographic coordinates are also known to a high degree of accuracy.

The average temperature for the height region between two successive bursts is determined from the calculation of sound speed and the mean molecular weight of the atmospheric height layer. The latter is assumed to be well known in the Earth's atmosphere but would not be in a planetary atmosphere.

The horizontal wind velocity is determined from the magnitude of the spatial difference in a horizontal plane between the projection of the burst point on to the plane of the sound detector array and the virtual point source of the sound pulse that can be determined from the differences in arrival times among the sound detectors in the array. Thus, each sound pulse will have a different virtual point source as determined by the microphone array. This difference between the coordinate position of the virtual source and the actual grenade burst position defines a vector that is associated with the integrated effect of atmospheric wind throughout the entire depth of atmosphere between the burst point and the microphone array.

Grenades used in the atmosphere sounding application are of various sizes. The required weight of explosive charge is determined mainly by the altitude to which sampling is desired. Theoretical calculations indicate that a 1 oz. (28 grams) explosive charge could be detected up to heights of 60 km. Actual experiments have detected the 1 oz. charge to 70 km on all occasions and to 82 km with multiplex acoustical recording; 355 gm grenades have been detected to 107 km. In the altitude region 100-150 km aluminized grenades have an associated glow reaction that is visible and photographable at height. A higher upper limit of 190 km exists for twilight conditions where resonance radiation supplements the chemiluminescent glow reaction that causes the nighttime luminescence.

The wave shape of the sound pulse received at each sound detector in the array is not used to extract information other than to identify weak signals from very high altitude grenade bursts. Even the recording of exact wave shape is not essential in this experimental

technique. The detection of acoustic energy at the ground level is the most sensitive part of the experiment and the principal source of error. In its application to atmospheric sounding of wind and temperature where microphones are separated by distances up to 30 km, extraneous noise is generated by, in addition to atmosperic turbulence, the process of transmission and recording of the sound pulse signal from the microphone array to central processing equipment.

The acoustic detectors that have been evaluated for atmospheric applications are:

(a) the microbarograph,

(b) the capacitor microphone,

(c) the hot wire microphone,

(d) the Solion infrasonic microphone (Collins et al. 1964).

3.2.2.2 INSTRUMENT CHARACTERISTICS

(a) Microbarograph - A microbarograph is normally used at lower frequencies than those in grenade experiments. A control volume in the instrument will change in response to variable atmospheric pressure. The lowest frequency detectable is determined by the variable lead mechanism that allows the control volume to come to ambient pressure. The highest frequency detected is determined by the mechanics of the volume expansion and the method by which it is detected, i.e., whether by mechanical linkage or by an electronic sensing of a variable inductance. The mechanical system is normally more reliable, not being subject to electronic drift.

Frequency range: $10^{-4}$ to 1 c/s

Sensitivities: 1 to 10 dynes/cm$^2$ in the atmosphere (0.1 dynes/cm$^2$ actual).

(b) Capacitor Microphone - A variation of the enclosed volume technique of the microbarograph. It consists of a thin metallic diaphragm mounted against a rigid back plate. Back plate and diaphragm are electrically insulated. When external pressure exceeds that of the enclosed volume, the diaphragm moves changing the electric capacity. Variations in capacity are transformed into an AC voltage changes when a constant charge exists between the electrodes. The charge is maintained by a stabilized DC polarization voltage with a time constant much lower than the period of the sound pressure variation. This type instrument has a wide linear range of response up to 20,000 cycles/sec. The lowest frequency to which it responds is fundamentally limited by the air equalization technique whereby ambient pressure is restored, although normally the low frequency limit is determined by the AC electronics.

(c) Hot Wire Microphone - The hot-wire microphone is basically a Helmholtz resonator in which air oscillates between the enclosed volume and the ambient air. The largest velocities occur in the "neck" or throat that couples the enclosed volume of the oscillator with the atmosphere. A hot wire element woven into the form of a grid is placed in the throat of the oscillator. The element is kept just below red heat by passing a DC current through it and because of its low heat capacity it readily changes temperature when the air in the neck of the resonator is in motion.

A perfect Helmholtz resonator responds to a single tuned frequency. This resonant frequency, $f_r$, is represented by the formula

$$f_r = \frac{c}{2\pi}\sqrt{\frac{\sigma}{V}}$$

where $\sigma$ is the conductance of the neck, V is the enclosed volume, and c is the sound speed. The frequency response of the resonator can be modified and sensitivity increased if the unit is coupled to another cavity, either a pit or internal resonator.

A hot wire microphone, a microbarograph, and a capacitor have been compared in a study by the Schellinger Research Laboratories for NASA (Pruitt, 1964) and it was shown that the hot wire output does not truly reproduce the wave shape of the arriving signals. However, time of arrival, not wave shape, is the important input in computing temperatures and wind profiles from grenade soundings. The advantage of the hot microphone is a better signal to noise ratio for the low frequency return associated with the highest altitude explosions.

### 3.2.2.3 STATE OF DEVELOPMENT POTENTIAL

There are many problems that would accompany any attempt to utilize this technique in planetary exploration.

(a) The problem of establishing an array of microphones with sufficient separation and then determining their coordinates.

(b) Whether the grenades are dropped from an orbiter or carried up from the surface of the planet is an important question; but regardless of the technique used, a more serious problem is to determine the coordinates and time of burst of the grenades.

At this stage of development of planetary exploration, the exploding grenade technique is too complex to be seriously considered.

## REFERENCES


Collins, J. L., Richie, W. C., and English, G. E., 1964: Solion Infrasonic Microphone, J. Acos. Soc. Amen. 36 (7) 1283-1287.

Proconier, R. W., 1966: Measurements of atmospheric structure above 30 km using the grenade method and improved acoustic techniques., Dept. of Physics, University College, London, Sci, Rep. No. 4, Contract AF61 (052)-781, 122p.

Pruitt, J. G., 1964: Report of the conference on atmospheric acoustic propogation, Fort Bliss, Texas, April 22-23

## 3.3 ION TRACER ANEMOMETER

Ion tracer anemometry is based on the measurement of the time interval between the upstream in ection of an ion cloud and its downstream detection at a known distance. Ion injection can be accomplished by ionizing radiation or electrical discharge. This latter approach is generally preferred because it is well suited for well controlled generation of short duration ionizing pulses.

This technique with its inherent independence of air density, temperature and composition makes it particularly useful for remote planetary applications. The basic character of its operating principle makes calibration unnecessary and provides an absolute measure of air velocities without the need for additional measurements. The operation of an electrical discharge ion tracer anemometer improves with decreasing air density down to about $10^{-3}$ or $10^{-4}$ kg $m^{-3}$ (air) because of the combination of lower discharge potentials (Paschen's law) and decreasing ion recombination rates. At even lower densities than the above, increased ion diffusion results in loss of ion cloud definition. Anemometry based on this technique appears especially suited for the Martian surface where the atmospheric density is very nearly at an optimum value for the use of electric discharge ion tracing. Furthermore, the relevant electrical characteristics of $CO_2$ (breakdown potentials and recombination coefficient as a function of density) are very similar to those of air.

### 3.3.1 INSTRUMENT - ION TRACER ANEMOMETER

#### 3.3.1.1 NARRATIVE DESCRIPTION OF THE INSTRUMENT

An operational ion tracer anemometer for the measurement of air flows at stratospheric air densities in ducts has been developed ( Lilienfeld et al., 1967) and successfully field tested on a research balloon flight. It incorporates semiconductor circuitry and an output suitable for direct telemetry. It operates in the closed loop retriggering mode, where the signal generated by the ion cloud at the detector probe triggers the next discharge at the ion discharge probe. This type of operation results in a pulse train whose frequency is directly proportional to the average air velocity between the ion emitter and detector probe. The output frequency is $f = v/L$, where v is the air velocity and L the distance between probes (10 cm. for the operational unit). The above mentioned instrument was designed to operate at altitudes ranging between about 20 and 50 K/m ($10^{-1}$ to $10^{-3}$kg $m^{-3}$)but this technique can be extended to cover densities above sea level values, with increased discharge potentials. The operational apparatus includes a start-keep alive circuit for the pulsed discharge, which is quenched under normal operation.

For meteorological wind application a modified version has been proposed (Lilienfeld, 1967) which would provide directional sensing in addition to the basic velocity measurement. The essential difference of this approach with respect to the above described unidirectional device resides in the design of the detector probe which consists of two coplanar

rings, one inner spiral and an outer circular electrode concentric with respect to the ion discharge source. Both detector elements are common to the input circuitry and the sequential ion detection provides directional information and velocity measurement. Instrument details will be given for the operational unidirectional device, and in parentheses for a proposed omnidirectional version.

3.3.1.2 INTERPRETATION OF MEASUREMENT

Additional information needed to interpret measurement - None

Method of analysis and interpretation of data - Air velocity is a direct function of pulse rate (pulse width indicates azimuth for the omnidirectional instrument).

3.3.1.3 INSTRUMENT CHARACTERISTICS

Total and dynamic range - The available device operates over the range of 5 to 50 m $sec^{-1}$ over a density range of $10^{-1}$ to $10^{-3}$ kg $m^{-3}$ (without change in calibration). Wider ranges can easily be accomplished.

Accuracy - Five per cent of actual measurement (can be improved).

Signal to noise - About 50 db.

Frequency response - >1KHZ for individual pulse duration measurement.

Environmental effects - Unusually large ambient ion concentration fluctuations > $10^8$ ions/$cm^3$ sec could affect accuracy of instrument.

3.3.1.4 INSTRUMENT OUTPUT

Output signal - Pulse train, 10V amplitude, 1 m sec width (variable width for direction sensing version). Absolute; pulse rate linear with respect to air velocity. Rate dependent analog signal is also available.

Bits per observation - Typically up to 10.

3.3.1.5 PAYLOAD INTEGRATION

Weight - 3 lbs. (0.5 to 1 lb.)

Volume - 70 $in^3$ without probes (10 $in^3$ without probes, omnidirectional probe about $10^3$in).

Power - 1.7 watts (<0.5 Watts).

Radio frequency interference - None detected between 0.55 and 108 MHZ; no measurements were performed outside this range.

Magnetic moment - None

Erection, orientation, or booms - Probes should be properly oriented with respect to the local horizontal and away from wind obstructing structures.

Compatibility with sterilization at 145°C - Good if electronic components are adequately chosen.

Special requirements - Positioning has to permit unhindered wind flow from all directions.

3.3.1.6 STATE OF DEVELOPMENT

Unidirectional instrument is operational; omnidirectional version is in the proposed stage.

## REFERENCES


Cooley, W. C. and Stever, H. G., 1952: Rev. Sci. Instr., 23, 151.

Ladenburg, B. L. et al., 1954: Physical Measurements in Gas Dynamics and Combustion, Princeton University Press, Princeton, New Jersey, Vol. IX, p. 139ff.

Lilienfeld, P. et al., 1967: Ion Tracer Anemometer for the Measurement of Low Density Air Flow, Rev. Sci. Instr., 38, 405-409.

Lilienfeld, P., 1967: Ion tracer anemometer for the measurement of wind speed and direction, communication to NASA (notice of intent to submit a proposal for the Voyager 1973 Mars mission), GCA Corp., Bedford, Massachusetts.

Mellen, G. L., 1953: Velocity measuring by use of high energy electrons, U. S. Patent No. 2637208.

Solon, L. R., et al., 1966: A System for Large Volume Aerosol Sampling in the Stratosphere Using Electrostatic Prescription, Final Report of AEC Contract AT(30-1)-2363, Del Electronics Corp., Mt. Vernon, N. Y.

## 3.4 PRESSURE ANEMOMETRY

Bernouilli's equation relating the total pressure $p_t$, at a point on a horizontal streamline of a moving fluid, to the fluid velocity v, at that point is

$$c\ p_t = p_s + \frac{1}{2}\rho\ v^2$$

where $\rho$ is the fluid density, c is a constant dependent on geometry, and $p_s$ is the static pressure. The above equation shows that the total pressure head at a point is equal to the sum of two terms, the static head and the velocity pressure head. The fluid stream velocity can be determined from the measurement of the difference between the total pressure and the static pressure, or by direct measurement of the velocity pressure.

### 3.4.1 PITOT STATIC TUBES

#### 3.4.1.1 NARRATIVE DESCRIPTION OF THE INSTRUMENT

Pitot static tubes are available in a number of configurations depending upon the specific application. In general, the air entering the mouth of the double-walled tube, which is pointed in the exact opposite direction of the flow, is brought to rest so that the pressure inside the mouth is equal to the total head; the static pressure is experienced in the wall of the tube which is opened to the outside through holes drilled in the wall at right angles to the axis of the tube at the point. The difference in pressure between these two spaces is measured by connecting them to opposite limbs of a sensitive manometer. The measurements obtained using this method are dependent upon the medium density in addition to the velocity. The specifications for the measurements of wind velocities with a pitot static tube are generally determined by the pressure transducer used to determine the differential pressure at the pitot tube output. Physically a pitot tube must be mounted heading directly into the wind due to its poor response with varying angles of attack. The density of the medium must also be known to obtain correct velocity.

#### 3.4.1.2 INTERPRETATION OF THE MEASUREMENT

Additional information needed to interpret the measurement - Atmospheric density.

Method for analysis and interpretation of data - The differential pressure, $\Delta P$, is related to wind speed, v, by

$$\Delta P = \frac{1}{2} K \rho v^2$$

where $\rho$ is the density and K is a constant factor determined by the design of the anemometer head.

#### 3.4.1.3 INSTRUMENT CHARACTERISTICS

Total and dynamic range - The total range is almost unlimited depending upon the mechanical design of the instrument while the dynamic range is determined by the type of pressure transducer.

Accuracy - Depending upon transducer and electronics; however, normally 5 percent of reading.

Signal to noise - Dependent upon electronics.

Frequency response - Dependent upon transducer.

Environmental effects - None.

3.4.1.4 INSTRUMENT OUTPUT

Output signal - Dependent upon transducer and electronics.

Bits per observation - Dependent upon electronics.

3.4.1.5 PAYLOAD INTEGRATION

Weight - Less than 2 lbs.

Volume - Approximately 0.5 cubic feet.

Power - Approximately 2 watts.

Radio frequency interference - None.

Magnetic moment - Unknown.

Erection, orientation, or booms - Must be erected into free stream wind flow and be free to turn.

Special requirements - None.

3.4.1.6 STATE OF DEVELOPMENT

For planetary application, integration with an electrical pressure sensor would be required.

### 3.4.2 PRESSURE PLATE ANEMOMETER

#### 3.4.2.1 NARRATIVE DESCRIPTION OF THE INSTRUMENT

If the wind pressure on a flat plate placed normal to the wind direction is balanced by a restoring force brought about by the deflection of the plate, the deflection of the plate is a measurement of wind speed. The force (F) on a plate held normal to the wind is given by

$$F = 1/2C\ A\ \rho\ v^2$$

where C is a constant depending upon the size and shape of the plate, A is the area of the plate, v is the velocity, and $\rho$ is the air density.

The earliest anemometers worked on this pressure plate principle, and consisted of a hanging plate pivoted about a horizontal axis and kept approximately normal to the wind. This type of instrument is not in general use today. However, very light instruments have been used in turbulence studies using photographic means of observing the motions of the plate. It must be realized that resonance is likely to be set up between the gusts and the plate resulting in erroneous readings if the instrument were to be used in the field. The yaw factor, the correction that has to be applied when the wind does not meet at right angles, is not as great as one might expect, being approximately zero over the arc from 0 to 45° angle of incidence.

A reliable commercial version of the swinging plate anemometer is manufactured by Alnor Instrument Company. This instrument has a moving element that consists of a double pivoted spring-controlled aluminum vane mounted in jeweled bearings. The vane transverses a chamber specially shaped so that the deflection of the attached pointer is proportional to the wind speed. Damping is provided through the use of a second vane located in a strong magnetic field. Balance of the system is such that the instrument may be used in any position and only the vane comes in direct contact with the air flowing through the case. Electrical representation of the air flow has been accomplished by Sherlock and Stout by modifying the instrument. The impedance of a coil is altered by attaching its armature to the moving plate and allowing the armature to move in the coil as a function of the wind speed.

#### 3.4.2.2 INTERPRETATION OF THE MEASUREMENT

Additional information needed to interpret the measurement - Gas density.

Method of analysis and interpretation of the data - The measurement of wind velocity is indicated with a mechanical pointer.

Modification of the instrument to provide an electrical signal that is analog to the wind speed, such as that made by Sherlock and Stout, may be acceptable.

3.4.2.3 INSTRUMENT CHARACTERISTICS

Total and dynamic range - The range of this instrument is dependent primarily upon the selection of the input jet design. Input jets are available for ranges between 20 to 2400 feet per minute.

Accuracy - For any given scale, the accuracy of the mechanical pointer is $\pm$ 3% of the full value.

Signal to noise ratio - Unknown

Frequency response - Approximately 2 c/s

Environmental effects - None

3.4.2.4 INSTRUMENT OUTPUT

It is possible to modify the instrument to produce wind speed.

3.4.2.5 PAYLOAD INTEGRATION

Not yet developed for electrical readout or remote sensing. Payload integration parameters, therefore, are unknown.

3.4.2.6 STATE OF DEVELOPMENT

Commercially available without an electrical signal output.

REFERENCES

Her Majesty's Stationary Office, 1961: Handbook of meteorological instrument, Part, London.

Sherlock, R. M., and M. B. Stout, 1931: An anemometer for a study of wind gusts, University of Michigan, Eng. Res. Bull., No. 20, Ann Arbor, Michigan.

Alnor Instrument Company, A Division of Illinois Testing Laboratories, Alnor velometer, Chicago, Illinois.

### 3.4.3 BRIDLED ANEMOMETER

The rotation anemometers turn by virtue of the pressure of the wind on their rotating parts. If these parts are prevented from turning, the force necessary to prevent rotation is a measurement of wind speed. By making use of a set of springs to prevent rotation but allowing a displacement of the cups with changing wind forces, the displacement of the cups is proportional to the square root of the wind force and hence to the speed of the wind. The angular displacement of the cup wheel is measured with a position sensitive transducer whose output is a linear representation of the wind speed. The instrument is not in general use and its accuracy and range are limited. Its calibration is dependent upon the characteristics of the restraining spring and does drift with age and extreme use. A bridled cup anemometer was developed by Bendix Aviation Corporation which consisted of a wheel containing 32 cups. This instrument, however, is no longer being produced.

### 3.4.4 W-PRIME ANEMOMETER

The W-prime meter is based upon the principles of the pressure plate anemometer. A flat plate is mounted in the horizontal plane and mechanically connected to a float resting at equilibrium in a pool of mercury. Forces developed by the vertical component of the wind-flow on the plate are transmitted to the float thereby changing the height at which the balanced condition is reached. Linear movement of the float with increasing vertical wind speed is made possible by the use of a wedge shaped float. The float if positioned on a shaft connecting it to the flat plate with the float's smallest extremity inserted into the pool of mercury. With a properly shaped float, the force necessary to drive it in or out of the pool increases as the square of the distance it is driven. Linear movement of the float is achieved in this manner, as the pressure developed on the plate by the wind-flow also increases as the square of the wind speed. A low torque position transducer is used to determine the level at which the float is riding and by the use of a calibration curve the vertical component of the wind-flow may be found. Many sizes and types of both plates and wedge floats have been experimented with. One instrument was used G. C. Gill to obtain field measurements; however, full development of the technique has not been completed. In any case, the sensor only measures the vertical component of the wind and is primarily designed for turbulence observations.

REFERENCE - W-PRIME METER

Hewson, E. W., 1950: Research on turbulence and diffusion of particulate matter in the lower atmosphere, Progress Reports No. 4,5,6, and 7, under Contract No. AF 28(009)-7, Mass. Inst. of Tech.

### 3.4.5 WIND VANE

Standard wind vanes indicate wind direction by means of a body mounted asymmetrically and free to turn about a vertical axis. The body takes up a position such that the direction of the resultant force on it due to the pressure of the wind passes through the vertical axis, and such that the center of pressure is to the leeward of the axis. A transducer is attached to the body at the vertical axis as a means of obtaining the azimuth information. The desirable properties of wind vanes are:

(1) The turning friction of the pivot should be minimum.
(2) The vane should be balanced to prevent bias when not perfectly oriented.
(3) The vane should be designed to produce maximum torque for changes in wind direction.
(4) Sufficient damping should be provided to prevent oscillation at its resonant frequency.

Wind vanes have been constructed of numerous shapes, sizes and materials; for example, flat plates, splayed vane, air foils and dual mounted vanes. Each of the individual designs exhibits its own characteristics and may be used for particular applications. The vane constructed to be an airfoil section is a somewhat superior type in that it responds to small changes in wind direction more readily than other types. The best modern vanes are airfoil sections with the span being three to four times the cord of the design. These vanes generally will indicate the wind direction with an accuracy of $\pm 1°$ except in very low wind speeds. One of the terms used to define the operating characteristics of wind vanes is the distance constant $D_v$ defined as

$$D_v = T\ V$$

where T is the time required for the vane to reach 63.2 percent of the equilibrium direction after a change, and V is the free stream velocity. Another term is the damping ratio, or the ability of a vane to resist the tendency to overshoot the true wind direction after a change. The damping ratio is defined as

$$h = \frac{1}{\sqrt{1 + \left( \frac{\pi}{\ell n (x_1/x_2)} \right)^2}}$$

where h is the damping ratio and $x_1$ and $x_2$ are the successive amplitudes of overshoot on the decay curve, on the same side, from the final value.

### 3.4.5.1 NARRATIVE DESCRIPTION OF THE INSTRUMENT

The instrument discussed here is a Beckman and Whitley Model 50.2. This vane is a modern airfoil designed for turbulence studies. This wind direction system is supplied with either of two vanes. The first and more sensitive of these is longer and must be orientated with more care than the smaller version. In the Earth's atmosphere these vanes exhibit the following characteristics:

| | Vane 1 | Vane 2 |
|---|---|---|
| Threshold | 0.7 mi/h at 10° | 0.7 mi/h at 10° |
| Distance constant | 5.7 ft | 3.7 ft |
| Damping ratio | 0.6 | 0.6 |

The vanes are coupled to the instrument transducer through low torque bearings. As the wind direction changes, the vane moves, causing an air gap capacitive transducer to phase-shift a 1 kc sinusoidal signal relative to a 1-kHz reference signal by an amount directly proportional to the wind direction azimuth. The output in this form is transmitted to the instrument translator. The translator converts the difference in phase between the reference and signal wave forms to a dc signal that is analog to the wind direction.

### 3.4.5.2 INTERPRETATION OF THE MEASUREMENT

Additional information needed to interpret measurement - A known reference point in the horizontal plane with regard to the system output must be available to correctly identify the wind direction.

Method for analysis and interpretation of data - The output of the system is a dc signal which is linear and analog to the wind direction in a 0 to 360° representation.

### 3.4.5.3 INSTRUMENT CHARACTERISTICS

Total and dynamic ranges - 0 to 360°.

Accuracy - ±2° of azimuth.

Signal to noise - Unknown.

Frequency response - Dependent upon wind speed. Distance constant = 3.7 ft/min.

Environmental effects - Vane material will not stand temperatures above 140°F.

### 3.4.5.4 INSTRUMENT OUTPUT

Output Signal - The output of the sensor is a 1-kHz signal whose phase angle varies directly in a linear fashion with azimuth angle. The translator output is a dc signal which varies in a linear fashion directly with the azimuth angle.

Bits per observation - For an accurate measurement of the wind direction azimuth of ±0.7°, a nine-bit word must be used.

3.4.5.5 PAYLOAD INTEGRATION

Weight - 2 lbs, approx.

Volume - 1/2 $ft^3$, approx.

Power - 12 volts dc at 600 mA, 7.2 W.

Radio frequency interference - Radiation possible at 1 kHz

Magnetic moment - Unknown.

Erection, orientation, or booms - The instrument must be erected into the free stream of the wind flow away from any obstruction. It must also be oriented in such a way that an azimuth reference point with regard to the instruments output can be obtained in order to obtain proper data from the sensor.

Compatibility with sterilization at 145°C - The materials used in the present model of this instrument will not withstand temperatures greater than 140°F. However, an instrument using materials capable of withstanding greater ambient temperatures may be manufactured.

Special requirements - The sensor must be mounted level with respect to the horizontal plane and oriented in a known direction.

3.4.5.6 STATE OF DEVELOPMENT

This instrument has been fully developed for use in the Earth's atmosphere. Development of new designs using different materials must be undertaken in order to make use of this instrument in other planetary atmospheres.

REFERENCES - WIND VANE

Beckman and Whitley, Inc., 1967: Technical Specifications for Series 50. Mountain View, California.

Her Majesty's Stationery Office, 1956: Handbook of Meteorological Instruments. London.

Middelton, W.E., and A.F. Spilhaus, 1953: Meteorological Instruments. University of Toronto Press.

### 3.4.6 SPHERE ANEMOMETER

#### 3.4.6.1 NARRATIVE DESCRIPTION OF THE INSTRUMENT

Sphere anemometers are based upon the pressure or drag forces exerted upon a body when it is placed in a moving fluid or gas. The sphere anemometer is capable of measuring both speed and direction in three dimensions. As the sphere encounters flow, the fluid exerts a drag force over the cross section area of the sphere. A force balance system translates this drag force into force components via strain gauges in each axis.

Determination of the wind velocity through measurement of these forces is a well known technique. To find the force vector acting on the sphere, the output voltage of each strain gage system must be squared and added and the square root of the sum then taken. The vector angle in each plane is simply the arc tangent of the components. The velocity vector lies along the force vector and its length is proportional to the square root of the force vector. Flow Corporation of Cambridge, Massachusetts, has developed and currently markets a sphere anemometer.

#### 3.4.6.2 INTERPRETATION OF THE MEASUREMENT

Additional information needed to interpret the measurement - Atmospheric density.

Method for analysis and interpretation of data - The output of the instrument is in the form of three voltage outputs - one for each plane. Both speed and direction of the wind flow are found from a vector analysis of these outputs.

#### 3.4.6.3 INSTRUMENT CHARACTERISTICS

Total and dynamic range - Total range of 2 to 700 mi/h with dynamic range determined by the individual models, e.g., model 4151-100 has dynamic range of 0 to 100mi/h

Accuracy - 3% of full scale

Signal to noise - Unknown

Frequency response - dc to 6 c/s

Environmental effects - None

#### 3.4.6.5 INSTRUMENT OUTPUT

Instrument output - A calibrated output of 0 to $\pm$.1 volt from each of three axis .

Bits per observation - For a 1% resolution, three eight bit words are needed.

3.4.6.5 PAYLOAD INTEGRATION

Weight - Under 2 pounds

Volume - Approximately 1 cubic foot

Power - 115 Volts ac

Radio frequency interference - None

Magnetic moment - Unknown

Erection, orientation, or booms - Must be erected into free stream wind flow and oriented into a known position.

Compatibility with sterilization at 145°C - Unknown

Special requirements - None

3.4.6.6 STATE OF DEVELOPMENT

Commercially available

REFERENCE

Flow Corporation, Sphere Anemometer Bulletin #42, Cambridge, Massachusetts.

## 3.5 ROTATING ANEMOMETERS

Their operation is based on the continuous or transient transfer of kinetic energy from the air stream to a rotating system. The speed of of rotation of these devices is a function of the average wind speed. Under steady-state conditions, kinetic energy may or may not be transferred from the flow stream, depending on the type of rotor (except for mechanical frictional losses which require a continuous supply of kinetic energy from the flowing air for all types of rotors).

### 3.5.1 WIND MILL

#### 3.5.1.1 NARRATIVE DESCRIPTION OF THE INSTRUMENT

This type of anemometer has a horizontal spindle with radial arms upon which a set of light vanes is mounted. A transducer is attached to the spindle as a means of observing the instrument's performance. The axis of the spindle must be parallel to the wind direction; thus the instrument is generally mounted upon a type of wind vane. If bearing friction could be neglected, the vane speed, u, is related to the wind speed along the spindle axis, v, by

$$u = v \tan \phi$$

where $\phi$ is the angle the vanes are inclined to the wind direction. As $\phi$ is usually in the range of 40 to 50°, u is approximately equal to v, instead of about one-third of v as in the case of cup anemometers. This and the fact that tne radial arms are generally short, means the rate of rotation is very high, and as a consequence, this type of anemometer is unsuitable for measuring high wind speeds. They respond well even to wind speeds below 0.5 mi/h.

In variable winds, as with the cup anemometer, the mean wind speed is over-estimated; the error is, however, less than 1 per cent for a sinusoidal variation of the wind speed of an amplitude of 10 per cent of the mean wind speed. The error increases as the square of the variation amplitude and may be significant in some natural winds.

Systems for using three propeller type anemometers, one in each of three planes, have been developed. By fixing the position of each anemometer and sampling each of the anemometer outputs, resultant wind velocity vector may be found, thus yielding both wind speed and direction. A commercial version of this type of anemometer system is manufactured by R. M. Young of Ann Arbor, Michigan, and the following characteristics apply.

#### 3.5.1.2 INTERPRETATION OF THE MEASUREMENT

Additional information needed to interpret the measurement - Further investigation into the effects of density of the gas are needed.

Methods for analysis and interpretation of data - The propeller of the instrument drives a dc generator whose output represents wind speed in a linear fashion. The relationship between output voltage E and wind speed U is approximately

$$U = 0.5 + 41.6E$$

3.5.1.3 INSTRUMENT CHARACTERISTICS

Total and dynamic range - 0 to 50 mi/h.

Accuracy - Not available

Signal to noise - Not available

Frequency response - Distant constant = 2.4 feet

Environmental effects - Propeller is constructed of foamed polystyrene and cannot withstand temperatures above 140°F. Bearings must be protected against dirt and dust particles in extreme conditions.

3.5.1.4 INSTRUMENT OUTPUT

Output signal - The output of the instrument is an analog dc voltage which represents wind speed in a linear fashion.

Bits per observation - Using the instrument with a 50 mi/h range, a seven bit binary word yields a resolution of 0.78 mi/h.

3.5.1.5 PAYLOAD INTEGRATION

Weight - Approximately 1 lb.

Volume - Approximately 20 cubic inches.

Power - None, except for possible amplification for telemetry.

Radio frequency interference - None

Magnetic moment - Unknown. Magnet is used as field for generator.

Erection, orientation, or booms - Must be mounted and oriented into the free stream of the wind away from obstructions.

Compitability with sterilization at 145°C - Propeller material cannot withstand temperatures above 140°F.

Special requirements - None

3.5.1.6 STATE OF DEVELOPMENT

The instrument is commercially available; however, currently it is not in widespread use.

## REFERENCES

Her Majesty's Stationery Office, London, 1956: Handbook of Meteorological Instruments.

R. M. Young Company, Ann Arbor, Michigan, Propeller Anemometer Specifications.

R. M. Young Company, Ann Arbor, Michigan, VVM Anemometer Production Bulletin.

### 3.5.2 ROTATING CUPS

#### 3.5.2.1 NARRATIVE DESCRIPTION OF THE INSTRUMENT

The cup anemometer normally consists of three or four cups mounted upon a vertical shaft so that the diametral plane of each cup is vertical. As the force on the concave side of any cup, due to wind, is greater than that on the convex side in a similar position, the cup wheel rotates. For any given anemometer, the speed at which the wheel rotates depends, to a good approximation, only upon the wind speed, provided the wind speed is steady and great enough to overcome the friction of the instrument bearings. The rate of rotation does not depend upon wind direction, nor to any appreciable extent on the density of the air. A further investigation into the density effects is needed when considering the use of cup anemometers in atmospheres other than earth's.

The speed of rotation of the wheel at the cup centers with relation to wind speed varies in a complex fashion with the dimensions of the anemometer but, in general, is approximately three. If v is the wind speed and V is the linear speed of the cup centers, it is possible to express the relationship between them for a given anemometer in the form of a power series

$$v = a + bV + cV^2 + \ldots.$$

in which a, b, and c are constants. The best designs are ones in which the constant and the coefficient of $V^2$ and higher powers of V are zero or very small. Many experiments in wind tunnels have been made to determine the best cup anemometer design. In each case, the dimensions, shape and materials have been varied. These experiments have concluded that among other things a three-cup wheel is superior to four-cup systems, a semi-conical shape is better than a hemispherical shape, and beaded edges of the cups reduce errors in turbulent winds. As a result modern cup anemometers are light, small, have large ratios of cup diameter and respond to much lower wind speeds than older designs. A modern cup is described here and is manufactured by Beckman Whitley Inc.

The rotating cup wheel is attached to a shaft which in turn drives a capacitance transducer. The transducer rotates to produce an amplitude-modulated signal which is demodulated to provide a sinusoidal output voltage, the frequency of which is 40 times the shaft rotation. This signal may be either interpreted directly or further reduced to furnish wind speed data.

#### 3.5.2.2 INTERPRETATION OF THE MEASUREMENT

Additional information needed to interpret the measurement - Further investigation into the effects of gas density is needed.

Method of analysis and interpretation of the data - The frequency of the instrument output f, is related to wind speed u, by

$$u = 0.75 + \frac{f}{11.8}$$

3.5.2.3 INSTRUMENT CHARACTERISTICS

Total and dynamic range - Total range - 0 to 90 mi/h

Accuracy - $\pm$ 1 per cent of absolute value

Signal to noise - Unknown

Frequency response - Distance constant is equal to 5 feet of air.

Environmental effects - Bearings must be protected from dirt and dust particles.

3.5.2.4 INSTRUMENT OUTPUT

Output signal - The output is a modulated ac signal where the frequency of the modulation is proportional to wind speed and may be used in a digital system. Some form of time period over which the information is gathered must be used.

Bits per observation - Using a one minute time period approximately 65000 counts must be either accumulated or transmitted.

3.5.2.5 PAYLOAD INTEGRATION

Weight - Approximately 2 lb.

Volume - Approximately 0.5 cubic ft.

Power - Approximately one watt

Radio frequency interference - None

Magnetic moment - Unknown

Erection, orientation, or booms - Must be erected into the free stream wind away from obstructions.

Compatibility with sterilization at 145°C - Yes, with stainless cup wheel.

Special requirements - None

3.5.2.6 STATE OF DEVELOPMENT

The instrument is commercially available and in widespread use on earth.

## 3.6 TRACERS

This wind measurement technique is based upon the tracking of a tracer or characteristic of the atmosphere that responds to atmospheric motions.

### 3.6.1 BALLOONS

In the earth's atmosphere there are four different types of balloons used for wind measurement: ROSE (ascending), ROBIN (descending), radiosonde, and Jimsphere. The ROSE is a superpressured 2-meter diameter aluminized (for easy radar tracking) spherical balloon; the ROBIN is a superpressured 1-meter diameter mylar sphere; the radiosonde is a various-sized neoprene and rubber balloon; and the Jimsphere is a dimpled superpressured ROSE balloon designed to give more detail to recovered wind profiles. The two balloons most widely used from the above listing are the ROBIN (rocket flights) and the radiosonde (routine meteorological soundings). The particulars of the radiosonde balloon will be discussed. Where the ROBIN differs from the radiosonde balloon, this will be noted.

#### 3.6.1.1 RADIOSONDE

The radiosonde balloon is helium filled and is released from the surface. It rises at an assumed rate until it bursts, generally around 30 km. Various radars can be used as tracking equipment to measure azimuth and elevation angles, and slant range.

#### 3.6.1.2 INTERPRETATION OF MEASUREMENT

Additional information needed - None

Method for analysis and interpretation of data - Balloon position is computed from the radar data, and the wind vectors are computed for different intervals based on altitude.

#### 3.6.1.3 INSTRUMENT

Total and dynamic range - Dependent on altitude and integration time.

Accuracy - The accuracy depends on the type of balloon used, the type of radar used for tracking, the height of the balloon, and the elevation angle. Two of these parameters are considered in the following expression

$$\sigma_v = 0.9h \times 10^{-2}/\sin^2 \alpha$$

where $\sigma_v$ is RMS vector error in knots, h is the height of the balloon in thousands of feet and $\alpha$ is the elevation angle. There is general agreement that the error, which increases with height, reaches a maximum of 15 knots at around 30 km.

ROBIN accuracy - RMS error, 4ktsat 60 to 70 km; 2 kts at 50 to 60 km; 1.1 kts at 40 to 50 km.

Signal to noise - Depends upon the type of tracking equipment and the reflection characteristics of the balloons.

Frequency response - The balloon is assumed to be completely responsive to the wind for the time intervals used to compute the individual wind vectors.

Environmental effects - No special environmental effects are encountered.

3.6.1.4 INSTRUMENT OUTPUT

Output signal - Typical radar output.

Bits per observation - For azimuth angle to within 5°, 7 bits; for elevation angle to within 5°, 5 bits; for slant range, 2 bits, for an order of magnitude, 7 bits for 1 per cent accuracy.

3.6.1.5 PAYLOAD INTEGRATION

No balloons of this type has been designed for planetary study. Also, special radar equipment would be required. The balloon itself weighs only a few pounds and can carry payloads up to about 6 pounds. Generally, it is less than 6 feet in diameter fully inflated at the surface.

3.6.1.6 STATE OF DEVELOPMENT

The radiosonde balloon is a throughly tested operational wind measuring device as is the equipment that is used to track it. The ROBIN has been extensively used in the Meteorological Rocket Network.

### 3.6.2 RADAR - REFLECTIVE PARACHUTE

#### 3.6.2.1 NARRATIVE DESCRIPTION OF THE INSTRUMENT

This atmospheric tracer is deployed and tracked in much the same manner as the ROBIN balloon sphere. Two different types of parachutes have been used. The first an 8-ft metalized parachute and the second a 15-ft silvered silk parachute.

#### 3.6.2.2 INTREPRETATION OF MEASUREMENT

Additional information needed - None.

Method for analysis and interpretation of data - The method for analysis of the data is essentially the same as that for the ROBIN balloon sphere. Slant range, azimuth, and elevation angle are the tracking parameters, and from these observed data, the winds can be computed. The winds are averaged over a selected time period for each accepted observation.

#### 3.6.2.3 INSTRUMENT CHARACTERISTICS

Total and dynamic ranges - Dependent on altitude and integration time.

Accuracy - Accuracy estimates have a rather wide range. For the 15-ft parachute the total wind error is about 3 m/sec for 1-minute averaging time (JSAG, 1961). Smith and Vaughan (1961) state that the error in rocketsonde wind speeds is approximately 8 m/sec or 10 per cent of the speed, whichever is greater. Jenkins (1962) found a 30 kt difference in winds measured "simultaneously" by chaff and parachute at 70 km.

Signal to noise - The signal to noise ratio depends primarily on the nature of the tracking equipment.

Frequency response - Once equilibrium is reached with the wind, the parachute is assumed to be completely responsive to atmospheric motion over the time intervals used to compute the individual wind vectors.

Environmental effects - No special environmental effects are encountered.

#### 3.6.2.4 INSTRUMENT OUTPUT

Output signal - Typical radar output

Bits per observation - Total of 21 (see radiosonde balloon).

### 3.6.2.5 PAYLOAD INTEGRATION

The type of tracking equipment will primarily determine the payload integration details. The weight of the 15-ft parachute is 2.14 lbs and the distance from the base of the chute to the base plate slightly above the payload is 18'9".

### 3.6.2.6 STATE OF DEVELOPMENT

The parachute system is one of the major wind measuring instruments used by the Meteorological Rocket Network. Therefore, it is a thoroughly tested system and operational.

### 3.6.3 DIPOLE CHAFF

#### 3.6.3.1 NARRATIVE DESCRIPTION OF THE INSTRUMENT

Lightweight dipole chaff particles are carried aloft by a rocket and ejected into the atmosphere near the apogee of the rocket trajectory. The chaff are generally made of copper, mylar "suchy" metalized material, or aluminum-coated plastic foil. They drift down through the atmosphere and the patch is tracked from the ground. It is assumed that the majority of the particles remain together in a cluster so that tracking data does not become erroneous due to dispersion.

#### 3.6.3.2 INTERPRETATION OF THE MEASUREMENT

Additional information needed to interpret the measurement - None.

Method for analysis and interpretation of data - Like the other tracked objects, the necessary position parameters are obtained and the winds computed from these observed data. The individual wind observations that constitute a wind profile are time averaged.

#### 3.6.3.3 INSTRUMENT CHARACTERISTICS

Total and dynamic range - Dependent on altitude and integration time.

Accuracy - The dispersion problem is one of the chief difficulties with the chaff-measurement technique. The aluminum-coated plastic has a standard error deviation of 23 knots. Errors for the other chaff types cannot be specified accurately.

Signal to noise - The signal to noise ratio depends on the reflection characteristics of the chaff and the nature of the tracking equipment.

Frequency response - After the chaff has been released and approaches the wind velocity, it is assumed that the chaff responds instantaneously to changes in atmospheric motion, at least on the time averaged scale that is used to compute each observed wind vector.

Environmental effects - No special environmental effects are encountered.

#### 3.6.3.4 INSTRUMENT OUTPUT

Output signal - Typical radar output.

Bits per observation - Total of 21 (see radiosonde balloon).

### 3.6.3.5 PAYLOAD INTEGRATION

Payload integration will depend primarily on the type of tracking equipment that will be necessary to perform the experiment.

### 3.6.3.6 STATE OF DEVELOPMENT

Chaff wind measuring techniques are currently employed by some parts of the Meteorological Rocket Network. Thus, the technique is operational and has been thoroughly tested.

### 3.6.4 AEROSOLS

#### 3.6.4.1 DOUBLE-BEAM RADAR

This technique considers two infinitely thin radar beams radiating from a single transmitter, feeding a single receiver, and separated by angle 2δ (Atlas and Wexler, 1965). The wind vector w is assumed constant across the angle 2δ. Echoes from naturally occurring aerosols moving across the first beam produce a small radial Doppler shift $f_1 = +(2/\lambda)w\delta$ while those passing through the second beam produces equal negative shifts $f_2 = -f_1$ where λ is the wavelength of the radar. The resultant echo received at the antenna from both of the above echoes, which arrive simultaneously, fluctuates with the frequency

$$F = f_1 - f_2 = 2f_1 = (2/\lambda)\ (2w\delta)\ .$$

Thus, the dual beam configuration would produce a fluctuation frequency which can be measured by conventional radar which is uniquely related to the transverse component of the wind speed. Since actual beams are not infinitely thin, each beam will observe a spectrum of velocities. Also, the incident radar will observe a spectrum of frequencies. If no contaminating effects were present, the Doppler spectrum observed on each beam would follow a Gaussian function with breadth proportional to the crosswind component. However, with two beams the Doppler spectrum will be an image of the two-lobed pattern of the antenna and the spacing between the peaks will be a unique function of the crosswind component. Each lobe of the spectrum will be broadened by natural atmospheric processes, but as long as the peaks are clearly defined their spacing will not be changed.

For each Doppler spectrum there is a fluctuation spectrum which is given by

$$S(u)du = \int_{-\infty}^{\infty} S(v)\ S(v + u)dv \qquad (1)$$

where $S(u)$ = probability of velocity u,
$S(v)$ = probability of velocity v,
u = relative velocity between particles in the Doppler spectrum,
v = Doppler velocity,

and S(v) for the combined beams can be expressed as

$$S(v) = \exp\left[ - \frac{(v + v_o)^2}{2\sigma^2} \right] + \exp\left[ - \frac{(v - v_o)^2}{2\sigma^2} \right] \qquad (2)$$

where $v_o$ = Doppler component of wind along axis of one beam $v_o = w \sin \delta$,
$\sigma^2$ = total variance of $\sigma_o^2 + \sigma_1^2$ ,
$\sigma_o^2$ = variance due to beam width broadening for a single beam,
$\sigma_1^2$ = variance due to turbulence, wind shear and variable fall speeds of the particles.

Combining (1) and (2) we have

$$S(u) = C\left[2 \exp\left(- \frac{u^2}{4\sigma^2}\right) + \exp -\left(\frac{(u-2v_o)^2}{4\sigma^2}\right) + \exp -\left(\frac{(u-2v_o)^2}{4\sigma^2}\right)\right]$$

where

$$C = \frac{1}{8\sqrt{\pi}\,\sigma} \int_{-\infty}^{\infty} S(u)du = \frac{1}{8\sqrt{\pi}\,\sigma}$$

In some cases it can be more practical to measure the autocorrelation function $\rho(\tau)$ of the intensity I(t) rather than the fluctuation spectrum where $\tau$ is the correlation time. This function is given by

$$\rho(\tau) = \int_{-\infty}^{\infty} S(F) \cos 2\pi F\tau dF$$

where S(F) is the fluctuation spectrum and $F = 2u/\lambda$. The wind speed can be determined by the position of the minimum at $\tau = 1/2F_o$ or the secondary maximum which occurs before $\tau = 1/F_o$.

Practical experience has shown that it is much simpler to measure the variance of the fluctuation spectrum. The variance $s^2$ is expressed by

$$s^2 = 2\sigma^2 + 2\sigma^2 w^2 .$$

The variance for single beam measurements is $2\sigma^2$. Thus the difference in the variance between single beam and dual beam variance is $2\sigma^2 w^2$ which is measured by simple instrumentation. Therefore, $2\sigma^2 w^2$ is a unique measure

of transverse target velocity and is independent of either beam width or spectral broadening by contamination, provided that both variance and wind are constant over the beam spacing.

Detectable scatterers are necessary to measure winds by this technique. While it is uncertain whether or not sufficient reflective material may be present in the Martian atmosphere, the atmosphere of Venus with its clouds offer a greater prospect. This technique can be used for radars with wavelengths between slightly less than 1 cm to 10 cm.

There is no apparent upper boundary to the wind speeds that can be measured. In fact $\delta$ is generally smaller for large wind speeds.

The errors encountered are a function of wind speed and beam separation. For a given wind speed the error decreases with increased beam spacing. For example, wind speed error is $\pm 4$ m/s for 2° beam spacing versus $\pm$ 1 m/s for 8° separation. Naturally, the use of as large a beam spacing as possible is desirable. However, this might cause sizeable differences in both wind and variance from one beam to the other.

### 3.6.4.2 LASER TECHNIQUE

The measurement of wind velocity with laser techniques involves the application of optical Doppler techniques to polychromatic light detection and ranging (PLIDAR) signals from atmospheric aerosols embedded in the wind field. It is assumed that the aerosols are small enough to be completely responsive to the wind at their level.

For the PLIDAR technique to obtain wind velocities, the Doppler-frequency shift must be greater than the output pulse frequency bandwidth. Particle velocities up to 500 m/s can be measured with the Doppler-velocity technique. If higher velocities are to be measured, the laser beam must be subcarrier modulated. White, Nugent, and Carrier (1965) state:

"... it is readily apparent that transmitter characteristics are critical factors in any laser system designed to measure wind velocity by Doppler techniques. Direct optical Doppler will require excessive receiver bandwidth; however, it will allow better range resolution. Subcarrier Doppler, or the other band, while requiring receiver bandwidths of only tens of kilocycles, will require absolute transmitter frequency stability on the order of kilocycles, and range resolution can be seriously degraded."

Aerosols are very responsive to atmospheric motions. This feature gives the aerosol tracer an advantage over other possible tracers.

### 3.6.5 ELECTRO-MAGNETIC ACOUSTIC (EMAC) PROBE

#### 3.6.5.1 NARRATIVE DESCRIPTION OF THE INSTRUMENT

In this wind measuring system (Allen and Weiner, 1963), the Doppler radar tracks an acoustic shock wave which creates a change in the index of refraction. The relation between $P_r$ (received power), $P_i$ (incident power) and n (index of refraction) is

$$\frac{P_r}{P_i} = \left(\frac{\Delta n}{2}\right)^2 .$$

If there is a train of N-shock waves, the reflected power is increased according to

$$\frac{P_r}{P_i} = \left(\frac{\Delta n}{2}\right)^2 N^2 .$$

Wind speeds can be calculated from

$$a_r + V_r = a + V \cos \phi - \frac{V^2}{a} \sin^2 \phi \qquad (1)$$

where $a_r$ = radial component of sound velocity,
$V_r$ = radial component of wind velocity,
$V$ = wind speed,
$a$ = speed of sound,
$\phi$ = angle of radar antenna with horizontal.

The left-hand side of (1) can be determined from the Doppler shift, $f-f_o$ from

$$f - f_o = \frac{2}{c} (a_r + V_r)$$

where f is the frequency of the returned signal, $f_o$ the frequency of the radiated signal and c the speed of light.

The wind direction can be determined from pointing the radar beam in two different directions and measuring the radial velocities. These velocities plus knowledge of the separation angle between the two measurements is enough to define the wind direction.

The most feasible sound source suggested is a burst of sound waves whose wave fronts would steepen to become shock waves within a few hundred feet of the source. These waves would retain their shock character for about two miles. However, under moist conditions, greater attenuation occurs and the shock character would be retained for shorter distances. Thus, it becomes apparent that measurements cannot be made over large areas with this system.

### 3.6.5.2 INTERPRETATION OF THE MEASUREMENT

Additional information needed to interpret measurement- Since the speed of sound varies with the square root of temperature and the ratio of specific heats, simultaneous measurement of the gas composition and the average temperature between the sound source and radar are needed.

Method for analysis and interpretation of data - The Doppler shift in frequency, $f-f_o$, is the measured quantity. Since turbulence is present in the atmosphere, the returned signal has a spread of frequencies. The Doppler shift is measured by comparing the phase difference between transmitted and received signals as a function of time. Then the wind speed is computed from (1). Knowledge of two radial velocities measured in different directions and the separation angle between the measurements defines the wind direction.

### 3.6.5.3 INSTRUMENT CHARACTERISTICS

Total and dynamic ranges - The wind speed range of the sensor has not been indicated precisely. However, it is estimated that winds up to 100 ft/s could be measured. Further, the antenna size and pulse repetition frequency limit the maximum unambiguous radial velocity that can be measured. This velocity is not specified.

Accuracy - From theoretical considerations, it is deduced that the maximum error for wind speed in the direction of search is 10 percent of the measured speed.

Signal to noise - The signal to noise determines the maximum range of the measuring technique. It is computed by equating the received power level to the radiated power level minus a constant power level which depends on the characteristics of the receiver, the strength of the sound source, turbulence scale, turbulent wind speed, temperature and humidity.

Frequency response - The "time constant" is simply the time needed for the radiated signal to leave the radar antenna and the reflected portion to return from the shock front. This time interval is very small. If the shock front is two miles from the radar antenna, the "time constant" is $2 \times 10^{-5}$ s.

Environmental effects - None anticipated.

### 3.6.5.4 INSTRUMENT OUTPUT

Output signal - The output will be in pulse form. A linear relation exists between the Doppler shift and wind speed.

Bits per observation - The number of bits per observation will depend on whether the Doppler shift is measured with or without the presence of turbulence. If turbulence is present, then a spectrum of frequencies is measured and the Doppler shift determined by comparing the phase difference between transmitted and received signals as a function of time. For a temperature measurement (accurate to 3 places), and Doppler shift (accurate to 3 places) 20 bits are needed.

### 3.6.5.5. PAYLOAD INTEGRATION

A standard Doppler radar can be used. Undoubtedly, much further design and development would have to be done before any existing instrument would be suitable for other planetary atmospheric studies.

### 3.6.5.6 STATE OF DEVELOPMENT

This technique has received thorough theoretical treatments, but no testing. No sound system has been developed. Considerable testing is required before the practical accuracy of the system can be assessed.

### 3.6.6 ALKALI METAL CLOUDS

Alkali metal vapor clouds of lithium, sodium, or cesium, when illuminated by solar radiation, emit a characteristic resonance radiation. For sodium this is the "yellow" D line at 5890 Å and 5896 Å. At twilight, when the sun is 6 to 9 degrees below the horizon, a cloud extending upward from 90 km is still illuminated by the sun, while the intensity of the diffuse sky background illumination is reduced sufficiently to allow cloud photography. The wind field is determined from the time transport of the cloud axis that is recorded on successive cloud photographs. Alkali metal clouds can be photographed over a maximum time period of about 15 minutes. There is a lower limit to the height at which this resonance radiation is observed in the Earth's atmosphere and 90 km can be taken as an effective lower bound.

Note that alkali metal clouds require solar illumination and can only be used effectively with ground-based photography at twilight conditions of reduced sky background illumination. Photography of a vapor cloud from an orbiting platform is another variation on the use of such clouds as tracers of atmospheric wind motion. In this case accurate tracking of the cloud axis is complicated by the motion of the platform and under certain conditions the absence of stars as fixed reference points against which the cloud motion can be determined. The actual reduction of wind data from a series of cloud photographs is done either numerically using star positions and spherical geometry or by an analogue technique in which the images of the cloud from several camera sites are projected against the surface of a hemispherical dome. The projected image from two or more camera sites of the same point on a cloud will intersect and determine the x, y, and z position in (analogue) space of that particular point. The spatial position of the "same" cloud point a minute or so later will give the average cloud transport from which velocity components can be obtained. Normally the assumption is made that there is only a very small vertical motion at these heights so that no attempt is made to "track" individual elements within the cloud. The spatial changes in the cloud for two different times and for the same height level are assumed to be representative of the same "cloud particle."

In an application of the vapor trails technique to sounding a planetary atmosphere, the first question that must be answered is whether the chemistry of another planetary atmosphere is such that these vapors would be chemically altered after their release and therefore would no longer emit the characteristic D-line radiation. The second question involves an estimate of the lowest altitude level at which this resonance radiation could occur. The final question involves how to form a cloud in a planetary atmosphere and whether it is reasonable to expect the same accuracy of vertical wind profiles as is obtained in the Earth's atmosphere.

Alkali metal vapor clouds are normally formed by means of a thermal vaporization process. Solid sodium pellets are embedded in an aluminum-thermiate mixture which is ignited by a starter explosive charge. A mass of 400 grams of metallic sodium would contain about $10^{25}$ atoms if completely vaporized. With a vaporization process efficiency of 5 percent and a constant deposition rate over 50 km of atmosphere, an initial line density of $10^{17}$ atoms/cm could be expected. Concentrations of $10^{11}$ atoms/$cm^2$ or greater represent an optically thick cloud so that even a charge of 100 grams should be adequate.

The accuracy of wind measurement achieved with this technique in the Earth's atmosphere should not be obtainable in planetary exploration with present technology and financial resources. For a qualitative measure of wind and, in particular, vertical wind shear, the formation of a twilight sodium (or cesium) vapor trail could be valuable.

The question of how the cloud is formed and how it is photographed, i.e. from the planet's surface or from an orbiting vehicle, must be answered before vapor trails can be given serious consideration at this stage of planetary exploration.

## REFERENCES - TRACERS


Allen, C.H., and S.W. Weiner, 1963: Study directed toward optimization of operating parameters of the EMAC probe for the remote measurement of atmospheric parameters. Bolt, Beranek, and Newman, Inc., Final Report, AF 19(628)-2774, 106pp.

Atlas, D., and R. Wexler, 1965: Wind measurement by conventional radar with a dual beam pattern. J. of Appl. Meteor., 4(5), 598-606.

Ballard, H.N., 1965: Rocketsonde technique for the measurement of temperature and wind in the stratosphere. Army Electronics Research and Development Activity, White Sands Missile Range, New Mexico, 106pp.

Belmont, A., R. Peterson, and W. Shen, 1964: Evaluation of meteorological rocket data. General Mills, Inc., NASA-CR-138, NASW-588, 96pp.

Bollermann, B., and R.L. Walker, 1966: New low cost meteorological rocket system for temperature and wind measurement in the 75,000 to 200,000 feet altitude region. AMS/AIAA Paper No. 66-386 presented at Conf. on Aerospace Met., Los Angeles, Mon. 28-31, 23pp.

Booker, D.R., and L.W. Cooper, 1965: Superpressure balloons for weather research. J of Appl. Meteor., 4(1), 122-129.

Brockman, W.E., 1965: Small scale wind shears from ROSE balloon tracked by AN/FPS 16 radar. Dayton Univ., Research Inst., Final Report, AF 19(604)-7450, AFCRL 65-99, 100pp.

Eckstrom, C.V., 1966: Wind sensing capabilities and rise-rate characteristics of some ground launched rigid balloon systems. AMS/AIAA Paper 66-298 presented at Conf. on Aerospace Met., Los Angeles, Mon. 28-31, 7pp.

Engler, N A., 1965: Development of methods to determine winds, density, pressure, and temperature from the ROBIN falling balloon. Final Report, Univ. of Dayton, Rpt. No. udri TR 77-101, 159pp.

Graham, J.J., Jr., Development of BALLUTE for retardation of Arcas rocketsondes. Goodyear Aerospace Corp., Final Report, AF 19(628)-4194, 129pp.

Harris, E.D., L.J. Nugent, and G.A. Cato, 1965: Laser meteorological radar study. Electro-Optical Systems, Inc., Final Report, Rpt. No. 5990, AF 19(628)-4309, AFCRL-65-177, 93pp.

Laby, J.E., and J.G. Sparrow, 1965: Wind studies using level balloons. J. of Appl. Meteor., 4(5), 585-589.

Leviton, R., 1962: Detailed wind profile sounding techniques. Air Force Survey in Geophysics No. 140, 1, 187-195.

Jenkins, K.R., 1962: Empirical comparisons of meteorological rockets wind sensors, J. of Appl. Meteor., 1(2), p. 196-202.

Joint Scientific Advisory Group to the Meteorological Rocket Network, The Meteorological Rocket Network, 1961: An Analysis of the First Year in Operation, 66(9), J. Geophys. Res., 21 p.

MacCready, P.B., Jr., 1965: Comparison of some balloon techniques. J. of Appl. Meteor., 4(4), 504-508.

McVehil, G.E., R.J. Pilié, and G.A. Zigrossi, 1965: Some measurements of balloon motions with Doppler radar. J. of Appl. Meteor., 4(1), 146-148.

Murrow, H.N., and C.V. Eckstrom, 1966: Description of a new parachute designed for use with meteorological rockets and a consideration of improvements in meteorological measurements. AMS/AIAA Paper 66-399 presented at Conf. on Aerospace Met., Los Angeles, Mon. 28-31, 9pp.

Murrow, H.N., and R.M. Henry, 1965: Self-induced balloon motions. J. of Appl. Meteor., 4(1), 131-138.

Rogers, R.R., and H.G. Camnitz, 1966: An additional note on erratic balloon motions. J. of Appl. Meteor., 5(3), 370-373.

Scoggins, J.R., 1963: An evaluation of detail wind data as measured by the FPS 11 radar/spherical balloon technique. NASA-TN-D-1572, 30pp.

_____, 1964: Aerodynamics of spherical balloon wind sensors. J. Geophys. Res., 69(4), 591-598.

_____, 1965: Spherical balloon wind sensor behavior. J. Appl. Meteor., 4(1), 139-145.

Smith, J. W., and W. W. Vaughan, 1961: Monthly and Annual Wind Distribution as a Function of Altitude for Patrick Air Force Base, Cape Canaveral, Florida, U.S. National Aeronautics and Space Administration, Technical Note, D-610, 118pp.

White, G.R., L.J. Nugent, and L.W. Carrier, 1965: Laser atmospheric probes. Inst. Soc. A., Preprint No. 40.1-1-65, 20th Annual ISA Conference and Exhibit, Los Angeles, 11pp.

## 3.7 ACTIVE FALLING OBJECT

In the active falling object technique, radar tracking establishes the wind direction only. The falling object contains one of two possible measuring devices that combined with the attitude of the object gives sufficient information to determine the speed (Morrissey, 1965). Thus far, instrumentation is in the rough design stage. It has been designed for use as a dropsonde from aircraft.

### 3.7.1 GYROSCOPIC SENSOR

The determination of wind direction is the same for both types of falling objects and is computed from the following equation

$$\text{WIND DIRECTION} = \text{AIRCRAFT HEADING} + \psi + \gamma + \theta$$

The precise aircraft heading is assumed to be known. The angle $\psi$ is the angle between the radiating source and a fixed axis which is on a line along the main axis of the aircraft. However, with a fast-falling sonde instrument, $\psi$ will remain small and is assumed to be zero. The measurement of $\gamma$ (the angle between the sonde axis and the line connecting the aircraft to the position of the sonde) can be accomplished by the sonde having a directional antenna pattern and then rotating the pattern. The received signal strength will be amplitude modulated. If a marker is placed on the transmitted signal where the axis of the antenna pattern is aligned with the axis of the sonde $\gamma$ can be determined by the relative position of the marker in the received radiation pattern. The angle is given by

$$\gamma = 360 \frac{T_\gamma}{T_R}$$

where $T_R$ is the distance between peaks in the signal and $T_\gamma$ is the distance between a peak and the marker. The angle ($\theta$) between the wind direction and the sonde axis depends on the sensor. With a system whose physical orientation was determined by the wind speed, $\theta$ would have to be measured and telemetered. However, with a rotating sensor, the sensitive axis can be aligned and rotate together. Thus, locating the antenna axis, which is accomplished by determining maximum received signal strength, is the same as locating the sensing axis. The sum of $\gamma + \theta$ is accomplished by comparing the phase difference between the telemetered wind speed information and the received signal strength.

To determine the wind speed, gyroscopic action is used to rigidly orient the sonde in the vertical direction and sense angle of attack. The bottom portion of the sonde, containing sensors and antenna, would be rotated at one revolution per second. The sensor would be a differential pressure transducer that would detect the difference in pressure on the opposite sides of the rotating sonde nose. Wind speed is related to the amplitude of the signal and the amplitude is related to the angle of attack ($\alpha$). The relation between wind speed and $\alpha$ is given by

$$\tan \alpha = \frac{V_w}{V_f}$$

where $V_w$ is wind speed and $V_f$ is the fall velocity of the instrument package. With this system, the sonde should be designed for large inertia to give the maximum gyroscopic moment.

### 3.7.2 ANGLE OF ATTACK SENSOR

This is a simpler system than the gyroscopic sensor. The wind direction is measured with the same technique described for the gyroscopic device.

In this technique the wind speed is sensed by having the vechicle aerodynamically designed to seek a zero angle of attack. Then the inclination of the aerodynamic axis to the vertical would be an indicator of the wind speed. The sensor itself would be a rotating accelerometer whose sensitive "plane" would be perpendicular to the aerodynamic axis of the sonde. Assuming no centripetal acceleration, the accelerometer would measure the degree to which the sensitive axis was dipped into the gravitational field of the Earth due to inclination of the sensitive plane with the horizontal. The sensed acceleration as a function of time, a(t), is given by

$$a(t) = \left(g - \frac{dV_F}{dt}\right) \sin \beta \sin \omega t$$

where g is the Earth's gravitational acceleration, $\beta$ is the angle of inclination of the sensitive plane to the horizontal, $\omega t$ defines the position of the sensitive axis in the sensitive plane, and $dV_F/dt$ is acceleration of the sonde. In practice, $dV_F/dt$ is less than 1 ft/sec$^2$; thus the term can be assumed to be zero with less than 3 percent error. The final expression then becomes

$$a(t) = g \sin \beta \sin \omega t.$$

The instrument has been designed for wind measurement from the Earth's surface to 10 km.

REFERENCES - ACTIVE FALLING OBJECT GYROSCOPIC SENSOR & ANGLE OF ATTACK SENSOR

Morrissey, James F., 1965: A System for the Determination of the Vertical Wind Profile from an Aircraft, (Air Force Cambridge Research Laboratories, L. G. Hanscom Field Bedford, Mass.), AFCRL-65-704, Instrumentation Papers, No. 79, 9p.

## 4. DENSITY

Atmospheric densities near the surface of Mars can be expected to lie within $1 \times 10^{-5}$ g cm$^{-3}$ and $3.5 \times 10^{-5}$ g cm$^{-3}$ (House, et al., 1967). The average density scale height is about 17 km near the surface and decreases to about 8 km above 30 km altitude.

Analysis of the Venus IV data suggests that atmospheric densities near the surface of Venus are about 15 times terrestrial values, or of the order of $1.5 \times 10^{-2}$ g cm$^{-3}$. The density scale heights are approximately the same as the pressure scale heights: about 12 km near the surface, decreasing to about 6 km at a height of 30 km. The scale height of the upper neutral atmosphere according to the preliminary results of the S-band occultation experiment on Mariner V, is about 5 km.

## 4.1 DECELERATION OF FALLING BODIES

There are currently several types of balloons and spheres in use or in the planning stages for the determination of the density profiles above the Earth's troposphere. They can be basically broken down into two categories; measurements of atmospheric drag from radar-tracked spheres, where the amount of drag is related to density, and falling bodies with accelerometer measurements. The radar tracking of the sphere requires a large amount of cumbersome ground equipment and is not currently suited for study of the atmospheres of other planets where equipment must be kept to a minimum. This leaves the accelerometer placed inside a falling body — an entry vehicle or a sphere — as the better of the two techniques for planetary observations.

The classical drag equation for a falling sphere is given by the following expression

$$F_D = m\, a_D = 1/2\, \rho\, V^2\, C_D\, A$$

where $F_D$ = drag force,

$m$ = sphere mass,

$A$ = sphere cross-sectional area,

$a_D$ = drag acceleration,

$V$ = sphere velocity,

$C_D$ = coefficient of drag,

$\rho$ = atmospheric density.

If the mass of the body is known and the acceleration measured, the drag force is determined. Then, with the knowledge of the other parameters in the equation, the density can be determined. For a planetary atmosphere, the velocity would be determined by an integration with respect to time of the accelerometer data, where the accelerometer is contained within an uncontrolled freely falling sphere. Further, the altitude h would be calculated from

$$h = h_E - \int_o^t V \sin\theta\, dt$$

where $h_E$ = height of the entry of the body into the atmosphere,

$\theta$ = flight-path angle measured relative to local horizontal,

$t$ = time.

Thus, the height would be calculated starting with t=0 at the time of impact of the body with the surface. Therefore, from the above discussion, it can be seen that the density profile can be calculated even though the entry vehicle is not tracked by radar.

Seiff (1963) discusses the determination of the pressure profile from the recorded density data. One method requires the assumption of an isothermal atmosphere while the other method does not have this limitation. With the second method pressure can be calculated from the following expression

$$p = \int_0^t (g \rho V \sin \theta) dt$$

where $p$ = static pressure,
$t$ = time,
$\rho$ = gas density,
$V$ = velocity of the entry vehicle,
$\theta$ = flight-path angle measured relative to horizontal.

Static pressure thus is calculated by summing up the weight of gas above the given altitude. In fact, pressure can probably be obtained more accurately than density since $\rho V$ is known more precisely than $\rho$. If gas composition is known, then it is possible to calculate the temperature profile from the determined density and pressure data.

### 4.1.1 SPHERICAL ENTRY VEHICLE

#### 4.1.1.1 NARRATIVE DESCRIPTION OF THE INSTRUMENT

This is an instrument system which is currently being proposed for planetary observations. The proposed system is a spherical vehicle with a triaxis accelerometer. The spherical vehicle enters the planetary atmosphere with a known entry angle and speed. As the speed of the vehicle is retarded by the planet's atmosphere the accelerometer continually records data until impact. Then, the data are related to the density profile in the manner discussed earlier.

#### 4.1.1.2 INTERPRETATION OF THE MEASUREMENT

Additional information needed to interpret measurement- The entry angle and speed are required to properly determine the density profile.

Method for analysis and interpretation of data - The output from this instrument package will probably be in the form of a radio signal which will be proportional to the measured acceleration. Then, the density profile will be computed from the mathematical consideration presented above.

### 4.1.1.3 INSTRUMENT CHARACTERISTICS

Total and dynamic ranges - The total range of the instrument will probably be between 0 and 1000 $g_o$ where $g_o$ is the sea level gravity of the celestial body. This range is based on a theoretical study for Mars where the total range was between 0 and 450 $g_o$. The dynamic range would depend on the radio signal used for the experiment. In practice, the range of the instrument will depend on the celestial body to be studied.

Accuracy - There are three primary sources of errors. First, there are the errors in measured acceleration. The error in density will be directly proportional to any error in resultant acceleration. Second, density error is inversely proportional to the square of the error in calculated vehicle speed. This speed error is cumulative with time and is a direct result of integrating an erroneous acceleration measurement. The third source of error comes from having to relate altitude to time to produce the density profile with height . This error results from integrating the time history of speed. The impact of the probe defines the time at which altitude is zero and the integration proceeds above the surface. Therefore, the error in altitude is a maximum at time of entry.

Theoretical estimates of the accuracy have been made by Peterson (1965). Accelerometer accuracy causes the largest amount of uncertainty in the density measurement. Density errors are generally about one to two orders of magnitude when an accelerometer with an accuracy of 0.1 percent encounters a minimum atmosphere when a maximum atmosphere was expected. If the accelerometer accuracy could be improved to 0.01 percent, then the maximum density error would be 1/2 order of magnitude (at low levels). This improvement is not currently within the state of the art. A way to improve the accuracy, at least at the higher levels, is to terminate the experiment at an entry vehicle speed of 750 ft/s (supersonic). Under these circumstances with an accelerometer accurate to 0.3 percent, the density error is about 1/3 to 1/2 of an order of magnitude.

The variations in calculated density produced by errors in entry speed, determination of final altitude, and entry angle are not as great as the variations caused by accelerometer errors. Generally, they are a factor of 2 or 3 for reasonable errors in the above 3 parameters.

With the addition of on-board pressure and temperature transducers, it is also possible to determine densities in the lower part of the planetary atmosphere (subsonic portion) using a technique described by Sommer and Boissevain (1967). Basically, the ambient pressure, temperature, and molecular weight of the atmosphere are obtained as a function of height from measurements of the acceleration history of the vehicle and the local pressure and temperature measurements. Density is then determined from the ideal gas law.

### 4.1.1.4 and 4.1.1.5 INSTRUMENT OUTPUT and PAYLOAD INTEGRATION

No information is currently available on instrument output or anticipated payload integration for an accelerometer that would be expected to perform the technique outlined above. The nature of the expected output from any accelerometer would be in some form that could be related to length/time$^2$.

### 4.1.1.6 STATE OF DEVELOPMENT

There is at present no instrumentation of this type available that is specifically designed to make planetary measurements of atmospheric density. The accelerometers used for this purpose on Earth could perhaps serve the purpose with proper telemetry and accelerometers suited to the expected conditions for a given planet. It is possible that some provision for determining altitude directly might be included in any conducted planetary experiment. An experiment similar to that proposed by Sommer and Boissevain has been tested in the Earth's atmosphere (Sommer and Boissevain, 1967).

## REFERENCES - DECELERATION OF FALLING BODIES


Carten, A.S.,Jr., 1966: Meteorological measurement accuracies for use in the design and operation of aerospace vehicles. AMS/AIAA Paper 66-349 presented at Conference on Aerospace Met., Los Angeles, March 28-31, 1966.

Champion,K.S.W., 1963: Atmospheric structure and its variations in the lower thermosphere. AFCRL-63-873, 20pp.

Engler, N.A., 1966: Development of methods to determine winds, density, pressure, and temperature from the ROBIN falling balloon. University of Dayton, Final Report, Rpt. No. udri-TR-66-101, AF 19(604)-7450, 159pp.

Faucher, G.A., J.F. Morrissey, and C.N. Stark, 1967: Falling sphere density measurements. J. of Geophys. Res., 72(1), 299-305.

Faucher, G.A., R.W. Procunier, and F.S. Sherman, 1963: Upper-atmosphere density obtained from falling sphere drag measurements. AFCRL-63-1156, 27pp.

Peterson, J.W., and H. Hansen, K. McWatters, and F. Bonfanti, 1965:Falling sphere measurements over Kwajalein. J. of Geophys. Res., 70(18), 4477-4489.

Peterson, J.W., K. McWatters, The measurement of upper-air density and temperature by two radar-tracked falling spheres. Michigan University, NASA-CR-29, NASw-138, 41pp.

Peterson, V.L., 1965: A technique for determining planetary atmosphere structure from measured accelerations of an entry vehicle. NASA-TN-D-2669, 20pp.

Peterson, V.L., 1965: Analysis of the errors associated with the determination of planetary atmosphere structure from measured accelerations of an entry vehicle. NASA-TR-R-225, 21pp.

Seiff, A., 1963: Some possibilities for determining the characteristics of the atmospheres of Mars and Venus from gas - dynamic behavior of a probe vehicle. NASA-TN-D-1770, 35pp.

Seiff, A., and D.E Reese, Jr., 1965: Defining Mars' atmosphere - A goal for the early missions. Astronautics and Aeronautics, 3(2), 16-21.

Seiff, A., and D.E. Reese, Jr., 1965: Use of entry vehicle responses to define the properties of the Mars' atmosphere. In Morgenthaler, G.W., and R.G. Morra (eds.), Unmanned Exploration of the Solar System, 19, Advances in the Astronautical Sciences, Periodicals Co., 419-444.

REFERENCES - DECELERATION OF FALLING BODIES (Cont.)

Smalley, J.H., and L.R. Flink, Modification of the ROBIN meteorological balloon - Vol. 1 - Design and test. Litton Systems, Inc., Final Report, No. 2873, AF 19(628)-2945, 52pp.

Sommer, S., and A. Boissevain, 1967: Astronautics and Aeronautics, Feb., 50-54.

Welinski, B.R., Research and development of ROBIN meteorological balloons. 1, Schjeldahl (G.T.) Co., AF 19(604)-8034.

## 4.2 LOW DENSITY IONIZATION GAUGES

This group covers instruments designed for the measurement of vacuum or low density environments of the order of $10^{-5}$ kg $m^{-3}$ or less (10 $\mu$mHg pressure at room temperature). Ionization type instruments operating at higher densities are discussed in separate sections. An exception to this low density criterion is the radioactive type ionization gauge, which, however, will be included in this group. Low density ionization gauges (LDIG for brevity) operate on the basis of gas molecule ionization, and measurement of the resulting ion current, which is a function of the number of gas molecules available for ionization. The means to generate this ionization is the common criterion for the classification of these gauges. The three main methods of ionization used are: (a) ionization by thermionically generated electrons accelerated in an electric field, (b) ionization by self sustained high voltage glow discharge, and (c) ionization by means of radiation (alpha, beta, and gamma).

### 4.2.1 INSTRUMENT

#### 4.2.1.1 NARRATIVE DESCRIPTION OF THE INSTRUMENT

The three categories mentioned above are represented by an equal number of instrument groups with some variation within each. The discussion of these instrument groups will be separated only insofar as their differences are concerned.

Based on their method of generation of ionization, instruments of this type fall into the following groups: (a) thermionic ionization gauge (commonly known as ionization gauge), (b) cold cathode gauge (commonly known as Philips or Penning gauge), and (c) radioactive ionization gauge (Alphatron, typ.).

(a) The thermionic ionization gauge consists of a hot filament emitting electrons which are accelerated by a positive grid (100-300V) and the resulting positive ions are collected by a negative electrode whose current is a measure of air density. Several variations of this instrument exist, one of which, the Bayard-Alpert gauge is designed for vacuum measurement at pressure of the order of $10^{-10}$ torr. Lower pressure measurements have recently been achieved by the use of magnetic fields ($10^{-13}$ torr).

(b) The Philips-Penning gauges consist of a glow discharge electrode pair where the small number of ions generated by the application of a high potential is significantly increased by the use of a magnetic field which increases the electron path causing a corresponding increase in the number of ionizing collisions. Again, the magnitude of the ion current measured is proportional to the gas density.

(c) The Alphatron is a typical representation of a group of instruments that use ionizing radiation to impart charge to the gas molecules. The alphatron consists of an electrode pair, across which a potential of about 30 or 40 V is applied, and an alpha radiation source that ionizes the gas between the electrodes. This source is generally a gold-radium alloy containing typically 0.2 mg of radium. Beta and gamma sources have also been used.

#### 4.2.1.2 INTERPRETATION OF MEASUREMENT

Additional information needed to interpret measurement - The essential parameter required for all the above instruments is the gas composition. The calibration is always performed for a given gas.

Method of analysis and interpretation of data - In all the above instruments the ion current is proportional to gas density, thus the measurement is interpreted on the basis of a prior calibration.

#### 4.2.1.3 INSTRUMENT CHARACTERISTICS

Total and dynamic range - (a) $10^{-2}$ to $10^{-7}$ torr ($\sim 10^{-5}$ kg m$^{-3}$) for the "common ionization gauge." Low end extended to $10^{-13}$ torr ($10^{-16}$ kg m$^{-3}$) for especially designed Bayard-Alpert gauges.

(b) $10^{-2}$ to $10^{-10}$ torr ($\sim 10^{-5}$ to $10^{-13}$ kg m$^{-3}$), down to $10^{-14}$ torr with special designs recently developed.

(c) 10 to $10^{-3}$ torr ($\sim 10^{-2}$ to $10^{-6}$ kg m$^{-3}$).

Accuracy - Ten percent of full scale for each range (all types).

Signal to noise - Dependent on actual density, about 20 dB at low end of useful range.

Frequency response - Time constants of the order of 0.1 to 1 s.

Environmental effects - High ambient gas ionization would affect operation (actual limits dependent on density). External magnetic fields of the order of 100 gauss or more may affect the operation of the instrument.

#### 4.2.1.4 INSTRUMENT OUTPUT

Output signal - Analog, calibrated, essentially linear. Typical sensitivities are:

(a) 12 $\mu$A/$\mu$mHg/mA, for nitrogen (output current at 1 micron pressure for an electron current of 1 mA).

(b) 1 mA at $10^{-3}$ torr and 2000 V applied.

(c) $2.5 \times 10^{-4}$ $\mu$A/torr (air).

Bits per observation - Dependent on desired resolution and range of interest. In general, total bits = 7 + number of decade ranges.

#### 4.2.1.5 PAYLOAD INTEGRATION

Both the cold cathode or Penning type glow discharge and the thermionic (Bayard-Alpert) gauges have recently been developed for space applications. Payload integration parameters will be given for the former since they are similar to those of the thermionic gauges, and because of their inherent superiority over the latter in terms of sensitivity, ruggedness, lower power consumption, etc.

Weight - 2 lb. approximately

Volume - 30 $in^3$, approximately

Power - 1 W, approximately

Radio frequency interference - None

Magnetic moment - The gauge operates with a permanent magnet with a 1000 gauss field.

Erection, orientation, or booms - Free access of ambient air should be provided.

Compatibility with sterilization at 145°C - High

Special requirements - None

4.2.1.5 STATE OF DEVELOPMENT

Semi-operational for planetary surface operation, various types have been used for Earth orbital and deep space measurements. Because of low density ranges covered, more useful for upper atmosphere density observations.

## REFERENCES


Condon, E, V, and Odishaw, H., 1958: Handbook of Physics, McGraw-Hill Book Co., Inc., New York.

Instrument and Spacecraft, October 1957 to March 1965, NASA SP-3028.

Kreisman, W., 1964: Measurement of the Lowest Pressures in Space and the Laboratory., GCA Report No. 64-8-N.

Kreisman, W.. 1964: Development of Cold Cathode Ionization Gauges for Space Vehicles, GCA Report No. 64-17-N.

Leck, J. H., et al., 1957: Pressure measurement in vacuum systems, The Institute of Physics, London.

McGraw-Hill Encyclopedia of Science and Technology, 1960: 7, pg. 253.

Newton et al., 1964: Response of Modified Redhead Magneton and Bayard-Alpert Vacuum Gauges Aboard Explorer 17, NASA TND-2146, Washington, D. C.

Yeager, P. R., 1966: The Problem of Ultra-High Vacuum Measurements, Research and Development, pg. 63.

## 4.3 CORONA DISCHARGE DENSITOMETER

If a gaseous electric discharge in the self-sustained, positive resistance, avalanche condition (corona or Townsend discharge) is maintained between an electrode pair with an inhomogeneous field distribution (high field gradient at one electrode), the current through and the potential across the discharge are a function of gas density, through its influence on ion mobility. The most stable geometry for this electric discharge is the concentric cylinder pair with the positive potential applied to the axial corona generating electrode. By applying a constant potential to the device, the corona current very nearly follows an equation of the form $\ln \rho = KI + \rho_o$, where $\rho$ is gas density, $\rho_o$ is gas density at corona starting, I is current, and K is a constant dependent on electrode dimensions and on gas composition. This relationship holds for air densities above $10^{-3}$ kg/m$^{-3}$. At densities of the order of $10^{-4}$ kg/m$^{-3}$ the discharge no longer can be maintained in its space charge controlled Townsend regime and it goes over directly into a constant potential general ionization glow discharge (Penning gauge region).

## 4.3.1 INSTRUMENT

### 4.3.1.1 NARRATIVE DESCRIPTION OF THE INSTRUMENT

The basic instrument consists of a cylinder-wire discharge pair which constitutes the actual sensor, and a regulated high voltage power supply with a series resistor feeding the coaxial discharge pair. For very wide density range operation, the series resistor in combination with the supply potential is chosen to provide a shallow load line and the output is taken across the discharge pair (potential output). For narrower density range, high resolution operation, a steeper load line is used in conjunction with current output measurement obtained with a small series dropping resistor. This latter approach is used in the stratospheric corona altimeter (Lilienfeld, 1965). This instrument includes a temperature compensating network for altitude measurements independent of temperature differences between the inside of the device and the free environment. Typical operating values for the above instrument are: supply voltage 1000V dc with a 20 megohm series resistor, output current range 0-25 microamperes, corresponding air density range $5 \times 10^{-2}$ to $6 \times 10^{-4}$ $kg/m^{-3}$ (air). The sensing cylinder is about 4 cm long and 2.5 cm in diameter with an axial nichrome wire 0.008 mm in diameter.

### 4.3.1.2 INTERPRETATION OF MEASUREMENT

Additional information needed to interpret measurement - Gas composition or electrical characteristics (mobility and ionization potentials) have to be know,.

Method of analysis and interpretation of data - The output of the instrument has to be interpreted through its calibration, which preferably should be performed in an atmosphere similar to that under which it is to operate. Obviously, the knowledge of air compostion may follow the actual measurement and thus a subsequent calibration of an earthbound model would suffice. Otherwise, the output is directly related to density as mentioned above.

### 4.3.1.3 INSTRUMENT CHARACTERISTICS

Total and dynamic ranges - The available device covers the range of $5 \times 10^{-4}$ to $5 \times 10^{-2}$ $kg/m^{-3}$ (air) but laboratory experiments of a slightly modified version using potentials of the order of 4 kV extended this range to sea level densitites (1.2 $kg/m^{-3}$). The upper density limit of the technique itself is limited only by the applied potential.

Accuracy - For air (known gas composition case), the repeatability or precision is better than 0.1% of the actual value over the entire range.

Signal to noise - >100dB

Frequency response - Time constant is less than one second and is potentially faster if the application requires it.

Environmental effects - High background ionization (>$10^6$ esu/$cm^3$) could affect accuracy. Local ionizing fields which could produce above concentration should be avoided.

4.3.1.4 INSTRUMENT OUTPUT

Output signal - The output is analog dc current or voltage, calibrated. Levels suitable for direct VCO conversion.

Bits per observation - 7 bits minimum.

4.3.1.5 PAYLOAD INTEGRATION

Values given below are for the stratospheric corona altimeter (Lilienfeld, 1965) which is the only presently operational instrument based on this principle. Numbers in parentheses represent estimates of state of the art miniaturization of above device for planetary applications.

Weight - 2 lbs (1.25 lbs)

Volume - 50 $in^3$ (15 $in^3$)

Power - 0.25 W (0.15 W)

Radio frequency interference - None

Magnetic moment - Not known

Erection, orientation - Not critical

Compatibility with sterilization at 145°C - High, if electronic circuitry (high voltage power supply) components are properly chosen.

Special requirements - Free access of ambient air.

4.3.1.6 STATE OF DEVELOPMENT

Operational for terrestrial stratospheric application.

## REFERENCES


Lilienfeld, P., 1965: Stratospheric Altimeter based on the Density Dependence of a Corona Discharge in Air, Rev. Sci. Instr., 36, 979-982.

Loeb, L. B., 1965: Electrical Coronas, University of California Press.

NYO-9677 Semi-Annual Progress Report of Stratospheric Monitoring Program July 1962-January 1963, Del Electronics Corp., Mt. Vernon, New York (AEC Contract No. AT (30-1-2363.

NYO-9678 Semi-Annual Progress Report of Stratospheric Monitoring Program February 1963-August 1963, Del Electronics Corp., Mt. Vernon, New York (AEC Contract No. AT(30-1)-2363.

Oertel, H., 1952: Knallwellenoszillographie mittels Koronasonde, Zeit. Angw. Phys., 4, 177-183.

## 4.4 VOLTAGE BREAKDOWN GAUGE (Paschen Effect Gauge)

The electronic breakdown potential between two electrodes is a function of the product of gas density and electrode separation. This dependence is called Paschen's Law. This property can also be expressed as the dependence of breakdown potential on the total number of gas molecules contained in the volume between the electrodes. This potential, as a function of the above product exhibits a minimum which usually lies between 300 and 400 volts, regardless of electrode geometry, at density-distance products between about $10^{-3}$ and $3 \times 10^{-3}$ kg $m^{-3}$ x cm (in air). The above dependence applies both to the breakdown starting potential as well as the extinction potential, and the difference between these two voltages is also a function of gas density (for a given interelectrode distance). Such an electric discharge can be incorporated as the nonlinear element in a relaxation type oscillator circuit whose frequency will depend on the difference between starting and extinction potential of the discharge and thus be related to gas density. Since the ionization characteristics of each gas are different, the above dependence has to be established for each gas composition.

### 4.4.1 INSTRUMENT

#### 4.4.1.1 NARRATIVE DESCRIPTION OF THE INSTRUMENT

Various versions of this type of instrument have been developed but no widespread utilization has been reported. The density element consists of a discharge electrode pair either of the coaxial or the Penning configuration, although other geometrics are applicable. The discharge gap is part of a relaxation oscillator of the same type as a glow lamp oscillator. Figure 4-1 illustrates the essential components of the circuit. The output is a pulse train whose frequency is a function of the gas density. This frequency is equal to

$$f = \left\{ (C + C') \left[ R \ell n \frac{1}{1 + \delta/(V - V_F)} + R_i \ell n \left( \frac{V_F}{V_F - \delta} \right) \right] \right\}^{-1}$$

where C is the external capacitance (5000 pF), $C'$ is the discharge capacitance, R is the external resistance (20 megaohms), $R_i$ is the discharge resistance, V is the applied potential (1000 volts), $V_F$ is the starting potential, and $\delta$ is the difference between the starting and the extinction potentials.

Typical circuit values are shown in parenthesis. The sampling resistor p, across which the output is generated, is small compared with R and has a negligible effect on the operation. By the use of a magnetic field (Penning configuration), the range of the instrument is about $2 \times 10^{-5}$ kg $m^{-3}$ (air) to about $10^{-2}$ to $10^{-1}$ kg $m^{-3}$ (depending on applied potential). Without magnetic field, the low end only extends to about $10^{-3}$ kg $m^{-3}$. Hirsch (1961) contains an extended description of this type of instrument.

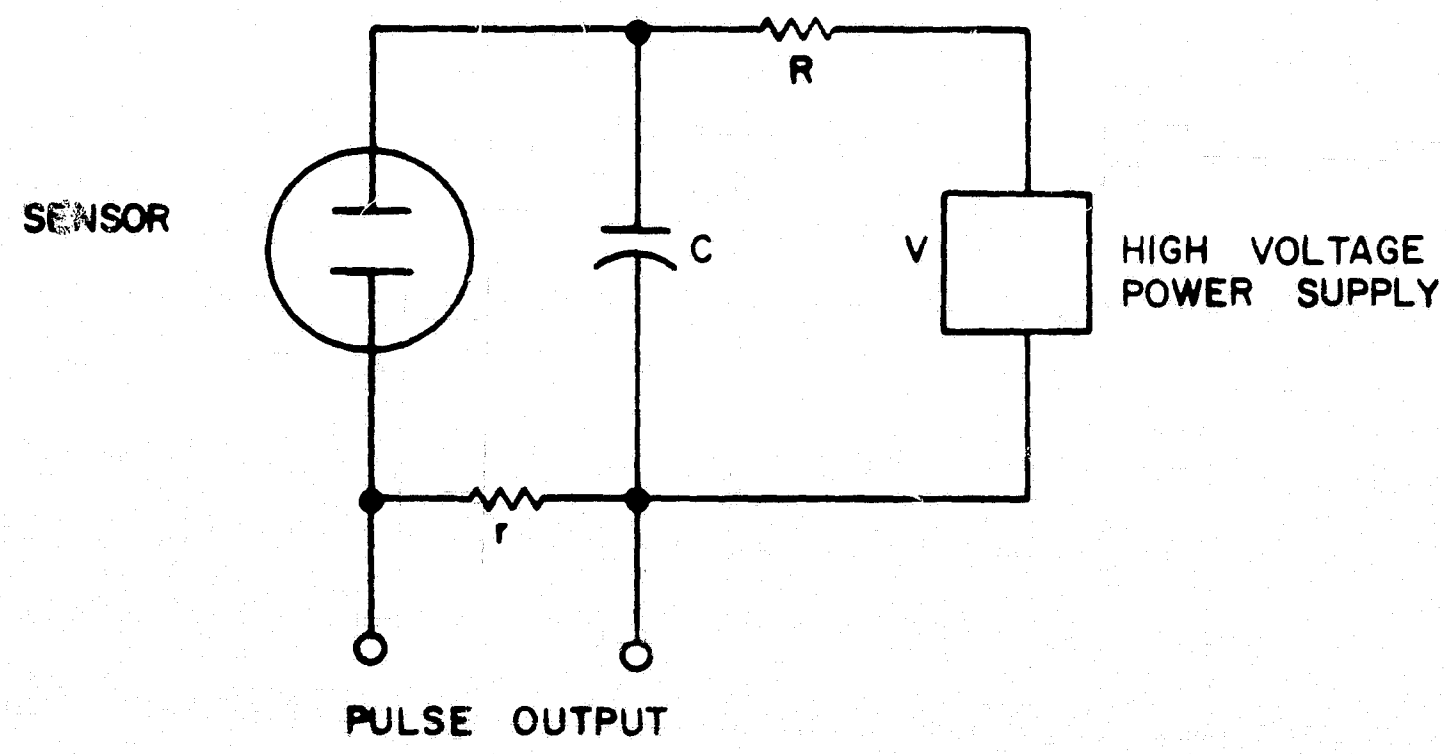


Figure 4-1. Voltage breakdown gauge.

#### 4.4.1.2 INTERPRETATION OF THE MEASUREMENT

Additional information needed to interpret measurement- The only parameter that has to be known is the gas composition. However, the influence of gas composition on the calibration of the instrument is not great. For the specific case of using it in a pure $CO_2$ environment with a calibration for air would introduce an error of only about 5 percent (Cobine, 1958) thus making it directly applicable for both Mars and Venus measurements.

Method of analysis and interpretation of data - The pulse frequency is related to gas density through a laboratory calibration.

#### 4.4.1.3 INSTRUMENT CHARACTERISTICS

Total and dynamic ranges - Typically $10^{-3}$ to $10^{-1}$ kg $m^{-3}$ without magnetic path elongation, $10^{-5}$ to $10^{-1}$ kg $m^{-3}$ with magnetic path elongation.

Accuracy - One percent of actual reading with respect to original calibration.

Signal to noise - Better then 40 dB.

Frequency response - Time constant of the order of 0.1 second of less.

Environmental effects - High background air ionization ($> 10^5$ $cm^{-3}$) would affect operation. Dust particles may precipitate on electrodes affecting operation. Filtering may be required. Susceptible to magnetic fields greater than about 100 G (actual limit dependent on field orientation with respect to discharge electrodes) at densities below $10^{-3}$ kg $m^{-3}$; no susceptibility above.

#### 4.4.1.4 INSTRUMENT OUTPUT

Output signal - Digital, pulse train, calibrated, frequency approximately inversely proportional to density.

Bits per observation - Ten bits.

#### 4.4.1.5 PAYLOAD INTEGRATION

Weight - 0.5 lb., approximately.

Volume - 10 $in.^3$, approximately.

Power - 0.05 watt, approximately.

Radio frequency interference - Probably low.

Magnetic moment - Fields of the order of 1000 G may be present.

Erection, orientation, or booms - Not critical.

Compatibility with sterilization at 145°C - High.

Special requirements - None.

4.4.1.6 STATE OF DEVELOPMENT

Experimental. Adaptable for use in Martian environment.

## REFERENCES - VOLTAGE BREAKDOWN GAUGE


Cobine, J.D., 1958: Gaseous Conductors, Dover, pg. 164.

Hirsch, E.H., 1961: Vacuum measurement by means of alternating gas discharges. Rev. Sci. Instr., 32, 1373.

## 4.5 ACOUSTIC TECHNIQUE

An acoustic technique that allows gas density to be obtained involves the measurement of sound speed and the specific acoustic impedance (z) of the gas. The specific impedance of acoustic waves in a gas is defined as the ratio of the instantaneous acoustic pressure to the instantaneous "particle" velocity. This type of impedance is a characteristic property of the gas and the types of waves that are being propagated through it. Its simplest form is $\rho_o c$ where $\rho_o$ is the density of the gaseous medium and c is sound velocity in the gas. If sound velocity and acoustic impedance can be measured then gas density can be derived.

In the literature on acoustics, two other forms of acoustic impedance are encountered. In general, the acoustic impedance (Z) of a fluid medium acting on or through a surface of given area S is the complex quotient of the acoustic pressure at the surface divided by the volume velocity at the surface. The acoustic impedance is related to the specific acoustic impedance at a surface by $Z = z/s$. The radiation acoustic impedance ($Z_r$) defined as the ratio of the force exerted by a piston on a medium to the velocity of a piston, is used to calculate the coupling force between acoustic waves and a driving source or driven load and is part of the mechanical impedance of a vibrating system associated with the radiation of sound. Radiation impedance is related to specific acoustic impedance at a surface by $Z_r = zS$ and the acoustic impedance by $Z_r = ZS^2$. Although it may seem redundant to have three definitions of acoustic impedances, the literature on the subject supports this practice because of its utility in different kinds of calculations relative to sound generation by transducers, sound transmissions by pipes, and sound reception by microphones.

A simple application of this technique for measuring gas density has been discussed in terms of planetary exploration by Hanel et al. (1963) and by Hanel (1964). Essentially it is as follows.

Admit atmospheric gas into a cylindrical tube (pressure equalization) in which the temperature of the gas is thermostatically controlled and therefore known. At one end of the tube is a transducer vibrating at a fixed frequency; the other end of the tube contains sound damping material to eliminate reflected waves. Two microphones are mounted flush with the interior wall of the cylinder and separated by distance large in comparison to the wavelength of sound waves (8 to 9 wavelengths).

Since the frequency of the sound wave is fixed the speed of the wave is directly related to wavelength, and phase comparison between the sound signals received by the two microphones will give sound speed. The specific acoustical impedance of the sound wave must be extracted from the pressure signal recorded by the microphone. Direct calibration of the instrument is one way to obtain the relationship between the signal amplitude generated by a microphone and the acoustic impedance of the transmitting

gaseous medium. In the application by Hanel (1963; 1964), he proposes to obtain this calibration of theinstrument in a $N_2$ atmosphere with pressures ranging from 20 to 150 mm Hg.

4.5.1 INSTRUMENT

4.5.1.1 NARRATIVE DESCRIPTION OF THE INSTRUMENT

The instrument consists of the following components.

(a) A test tube whose temperature is thermostatically controlled with oneend closed by sound absorbing material. The tube is about a meter lcng and 0.5 cm in diameter.

(b) A fixed frequency generator connected to a transducer at the opposite end of the tube.

(c) Two capacitor type microphones whose signals are amplified and brought out to

(1) a phase comparator and
(2) an amplitude comparator.

4.5.1.2 INTERPRETATION OF THE MEASUREMENT

Sound speed is determined directly from the phase comparator. Acoustic impedance is determined from the amplitude comparator, and the gas density within the tube is derived from the acoustic impedance measurement.

The ambient temperature ($T_a$) must be measured independently in order to obtain ambient density ($\rho_a$) from the chamber or tube density ($\rho_c$). Through the equation of state and the condition of pressure equalization the following relationship holds

$$\rho_a = \frac{\rho_c \ T_3}{T_a} .$$

In a planetary atmosphere whose composition is not known, the ratio of specific heats ($\gamma$) and the mean molecular mass ($\bar{M}$) are not known. By applying the equation of state for a perfect gas, the mean molecular mass can be determined from this experiment using the following formula

$$\bar{M} = \frac{\rho \ RT}{P} = \frac{z \ T_3 \ R}{cP}$$

where $T_3$ is the thermostatic regulated temperature of the tube, c is sound velocity (measured), z is the acoustic impedance (measured) and P is the ambient pressure (must be measured by an independent sensor).

4.5.1.3 INSTRUMENT CHARACTERISTICS

Total and dynamic range - The range of sound velocity that will be measured in these experiments will depend upon the composition

but not on the range of planetary temperatures since temperature will be fixed at the thermostatically regulated value. Hanel's instrument is designed for a sound velocity range of 290 to 365 m/s in a Venus probe and 347 to 365 m/s in a Mars probe.

Accuracy - If the phase velocity of the sound wave can be measured to ±1 percent, the speed of sound can be derived to ±0.05 percent.

Signal to noise - The signal to noise ratio will depend upon the choice of capacitor microphone and amplifier and is not known for Hanel's instrument.

#### 4.5.1.4 INSTRUMENT OUTPUT

The instrument output of direct concern is the signal voltage that is generated in response to a variable capacitance.

#### 4.5.1.5 PAYLOAD INTEGRATION

The weight and volume of an acoustical instrument of the type described is not known exactly but volume should not exceed 100 cubic inches and the weight should be less than 1 kg; how much less will depend upon the specific design.

#### 4.5.1.6 STATE OF DEVELOPMENT

A bread-board model of the instrument described by Hanel (1963; 1964) has already been constructed.

### REFERENCES - ACOUSTIC TECHNIQUE

Hanel, R.A., 1964: Exploration of the atmosphere of Venus by a simple capsule. NASA Tech. Note, TN-D-1909, July, 19pp.

Hanel, R.A., L.E. Richtanger, R.A. Stampfl, and W.G. Stroud, 1963: Experiments from a small probe which enters the atmosphere of Mars. NASA Tech. Note, TN-D-1899, December, 19pp.

Kinsler, L.E., and A.R. Frey, 1962: Fundamentals of Acoustics, John Wiley & Sons, New York, 500pp.

## 4.6 THERMAL CONDUCTIVITY GAUGES

This technique can be used for either the measurement of density or pressure and operates on the relation between the rate of heat transfer and the density or pressure.

A wire of diameter d cm is stretched along the axis of a tube of diameter D cm. If the gas molecules have on the average temperatures of $T'_g$ and $T'_w$ on arrival and departure respectively from the wire, the rate of energy transfer E from wire to gas and subsequently to the outer cylinder, is given by

$$E = Kn\,(T'_w - T'_g) \qquad w/cm^2$$

where K is a constant and n is the number of molecules striking the wire each second. Since n is directly proportional to the pressure at any given gas temperature, the expression can be rewritten

$$E = K'(T'_w - T'_g)\,P$$

where K′ is a new constant that includes the proportionality constant for the n to P relationship. Thus, the rate of heat transfer from wall to wall is proportional to the pressure if $T'_w - T'_g$ is a constant.

The temperature $T'_w$ depends upon 1) The temperature of the wire surface, 2) the type of surface, 3) the temperature of the incident molecules, and 4) the type of molecules. The increase in molecular temperature is directly proportional to the temperature difference between the surface and the incident molecules for a given gas and a particular surface. An accommodation coefficeint is defined by

$$\alpha = \frac{T_r - T_i}{T_s - T_i}$$

where $T_s$, $T_i$, and $T_r$ are the temperatures of the surfaces, the incident and the reflected moleucles respectively. Putting the coefficient into the basic equation, we have

$$E = \alpha\, K'P\,(T_w - T'_g)\ .$$

Renaming the constant K′ and considering that molecules possess both rotational and translational energy, the following final expression results

$$E = 1.47 \times 10^{-5}\ \frac{\gamma + 1}{\gamma + 1}\left(\frac{1}{M}\right)^{1/2}\left(\frac{273}{T_g}\right)^{1/2}\ \alpha(T_w - T'_g)P$$

where $T_g$ is the temperature of the gas outside the cylinder, M is the molecular weight, and $\gamma$ is the ratio of the specific heats. Using the equation of state for unit mass the expression can also be written as follows:

$$E = 1.47 \times 10^{-5} \frac{\gamma + 1}{\gamma - 1} \left( \frac{1}{M} \right)^{1/2} \left( \frac{273}{T_g} \right)^{1/2} \alpha R T'_g \rho$$

where R is the universal gas constant referred to unit mass of gas and $\rho$ is the density.

### 4.6.1 PIRANI GAUGE

#### 4.6.1.1 NARRATIVE DESCRIPTION OF THE INSTRUMENT

This instrument measures the heat loss from the wire electrically with a Wheatstone bridge network that both heats the wire and measures its resistance. A hot wire is included in a bridge with two other arms having equal resistance and the fourth arm being variable. At a very low pressure, a voltage is applied to the bridge and is set at some convenient value, and the variable resistor is adjusted to give balance. An increase of pressure, which increases the heat loss, lowers the wire temperature and hence unbalances the bridge. The wire temperature can be increased and, therefore, the bridge rebalanced, if the heat input is increased by increasing the bridge voltage. When the bridge has been rebalanced, the resistance of the hot wire, and, therefore, its temperature, must be at the original value.

Mathematically, the pressure can be expressed as follows:

$$p = \text{constant} \times (V^2 - V_o^2)$$

where $V_o$ is the voltage when the bridge is initially set and V is the voltage at a later time when the bridge is rebalanced. A similar expression can be derived for density by substituting for pressure with the equation of state.

#### 4.6.1.2 INTERPRETATION OF MEASUREMENT

The specific data given below are the characteristics of a Pirani Gauge manufactured by Edwards High Vacuum, Inc., Grand Island, New York.

Additional information needed to interpret measurement - Atmospheric composition

Method for analysis and interpretation of data - The output in volts has a linear relationship with density (pressure). This empirical relation is found by applying a known current or voltage and measuring the resultant temperature at various pressures.

#### 4.6.1.3 INSTRUMENT CHARACTERISTICS

Total and dynamic range - The overall range of this instrument is from 9 x $10^{-4}$ g/cm$^3$ to 3 x $10^{-9}$ g/cm$^3$.

Accuracy - The accuracy is $\pm$ 10% between 2 x $10^{-5}$ g/cm$^3$ and 3 x $10^{-8}$ g/cm$^3$ and is unspecified for the limits of the overall range.

Signal to noise - Not specified

Frequency response - Not specified

Environmental effects - Radiation losses limit the use of the Pirani Gauge to measurement of densities less than 2 x $10^{-7}$ g/cm$^3$ in the free atmosphere.

#### 4.6.1.4 INSTRUMENT OUTPUT

Output signal - The analog output for the Pirani Gauge is voltage, which is linearly related to density (pressure).

Bits per observation - The number of bits per observation is eight for the range of this instrument.

#### 4.6.1.5 PAYLOAD INTEGRATION

Weight - 5 lbs 12 oz.

Volume - 9-1/4 in. x 8-3/8 in. wide x 9-1/2 in. deep

Power - Not indicated

Radio Frequency interference - Not known

Magnetic moment - Not known

Erection, orientation, or booms - Not specified

Compatibility with sterilization at 145°C - The indicated maximum operating temperature is 40°C. It is not clear whether sterilization could be performed without damage to the instrument.

Special requirements - None

#### 4.6.1.6 STATE OF DEVELOPMENT

This is an instrument which is currently available from commercial sources for immediate operation.

### 4.6.2 HAVENS GAUGE

The Havens Gauge is simply a special configuration of the Pirani Gauge in which a Pirani Gauge is mounted inside a bellows that is alternately compressed and released by an electric motor. This operation yields a fluctuating output voltage, which can be amplified and rectified to determine atmospheric density (pressure). This instrument can be used to measure densities as low as $4 \times 10^{-12}$ g/cm$^3$.

## REFERENCES - THERMAL CONDUCTIVITY GAUGE

Leck, J. H., 1957: Pressure Measurement in Vacuum Systems, The Institute of Physics, London.

## 4.7 SCATTERING TECHNIQUES

The scattering technique operates on the principle that scattering is primarily a function of the density of the atmosphere. Four types of sensors measure beta particle forward scattering, X-ray, gamma-ray, and ultraviolet backscattering. The X-ray and gamma-ray devices are described below as examples of this technique.

### 4.7.1 X-RAY BACKSCATTERING

#### 4.7.1.1 NARRATIVE DESCRIPTION OF THE INSTRUMENT

In this type of scattering technique, an X-ray source emits X-rays at a constant rate over a given time increment (Johnson, 1964). The detector is away from the source such that only scattered X-ray photons can impinge upon the detector. The density is determined by counting the number of X-rays that reach the detector in a given time interval. This number is proportional to the amount of air molecules enclosed by the X-ray beam.

The relationship between the emitted X-ray photons ($I_o$) and the percent of the photons which are scattered and detected ($I_d$) is given by

$$I_o = \frac{I_d \ (4\pi)^2 \ r}{G \left( \frac{\sigma_s}{\rho_o} \right) \rho \ A_d}$$

where
- $r$ = the distance between the X-ray tube and the detector,
- $G$ = a function of collimation angle,
- $\rho$ = air density,
- $A_d$ = area of the detector,
- $\sigma s/\rho_o$ = Compton scattering cross-section.

From the above equation it can be seen that gas density varies linearly with the number of detected photons for a constant source.

The detector is a scintillator-photomultiplier combination which is a very sensitive radiation counting device. When the X-ray photons impinge upon the detector, the scintillator converts them to a shower of light photons, a percentage of which reach the photomultiplier. The light flashes are then converted to electrons by the photomultiplier, the number of electrons is multiplied by a factor of $10^5$ to $10^8$ and the number of electron bursts is counted.

#### 4.7.1.2 INTERPRETATION OF MEASUREMENT

Additional information needed - Atmospheric composition, since Compton scattering cross section depends on composition.

Method of analysis and interpretation of data - The output is in the form of 1 volt, microsecond pulses occurring at a rate of 1000 pps to 100,000 pps. This pulse rate is linearly related to the number of impinging photons and thus linearly related to density.

#### 4.7.1.3 INSTRUMENT CHARACTERISTICS

Total and dynamic ranges - The sensor was designed to measure densities between $1.2 \times 10^{-3}$ g/cm$^3$ and $1.7 \times 10^{-5}$ g/cm$^3$. On Earth, this is from about sea level to 30 km. It may be possible to extend the range to $10^{-7}$ g /cm$^3$.

Accuracy - Theoretical accuracies have been computed for both a test chamber and simulated aircraft flight conditions. The total r.m.s. error for the test chamber is between 2 and 3 percent for densities between $10^{-3}$ and $10^{-6}$ g/cm$^3$. At densities less than 10-6 g/cm$^3$, the error begins to rise, caused by backscatter from detector coincidence error. This error is due to overlap of individual light pulses in the scintillator. The theoretical errors for the aircraft flight are about percent for densities between $10^{-3}$ and $10^{-6}$ g/cm$^3$ and become larger as $10^{-7}$ g/cm$^3$ is approached. For the flight test, the error analysis included considerations of statistical variations in X-ray emission, rate of aircraft descent, shock layer effect, electronic drift and cosmic background.

Signal to noise - Noise is one of the factors limiting the range of the instrument. The noise comes from the photomultiplier tube and is caused by "dark current." This type of current is a result of electrons escaping from the photosensitive cathode due to thermal vibrations. The individual electrons emitted cause pulses in the output of substantially smaller amplitude that those resulting from the incoming X-rays. To combat this difficulty, a threshold discriminator can be used to distinguish between "dark current" and X-rays. This requires that the signal be above the threshold level before it is counted.

Frequency response - The time constant is extremely small. Only a short distance is travelled at the speed of light by a scattered photon that reaches the detector. The operations within the detector are also virtually instantaneous.

Environmental effects - This instrument is designed to withstand the rigors of a high altitude environment and shock forces. The effect of cosmic background at high levels is much greater than at sea level. By counting pulses only in a certain energy range (discrimination technique) this effect can be considerably reduced.

#### 4.7.1.4 INSTRUMENT OUTPUT

Output signal - The calibrated output is in pulse form, and the sampling period is 0.533 sec. A linear relation exists between the number of detected photons and gas density with a fixed X-ray source strength. When the count rate is relatively low (around 10,000 pps), the relationship begins to lose its linearity. By making adjustments in the circuitry, the pulse rate would be boosted for a given density, and linearity resumed. This newly established linear relation would then continue until the lower densities would again reduce the count rate.

Bits per observation - Pulse rates transmitted accurate to three places with exponent would require 10 bits per observation.

#### 4.7.1.5 PAYLOAD INTEGRATION

Weight - The X-ray detector and emitter probably weigh less than 20 lbs.

Volume - The above two components probably occupy less than 1 $ft^3$ of space.

Power - The suggested power requirements were voltage between 1500 and 2500V, a current of 0.2 mA, a load regulation of 0.1% no load to full load, and a ripple of 0.2%.

Radio frequency interference - None

Magnetic moment - Not known

Erection, orientation, or booms - See special requirements

Compatibility with sterilization at 145°C - The aircraft instrumentation can withstand temperatures at least as high as 71C.

Special requirements - The orientation of the emitter-detector system must be carefully determined and care must be taken that the detector receives only scattered photons.

#### 4.7.1.6 STATE OF DEVELOPMENT

The instrument is not ready for operational use. Giannini Controls reports that laboratory tests have been completed and the results are encouraging. Aircraft tests (aboard the X-15) have not yet been reported. However, the designed instrument is capable of withstanding the expected environment.

### 4.7.2 GAMMA-RAY BACKSCATTERING

#### 4.7.2.1 NARRATIVE DESCRIPTION OF THE INSTRUMENT

The general operation of the gamma-ray backscattering instrument is about the same as that for the X-ray backscattering device and the theory is only slightly different.

When gamma rays pass through matter, the beam is exponentially attenuated by one of three major processes: 1) photoelectric, 2) Compton scattering and 3) pair formation (Shepard and Dicks, 1963). Within a specified energy range, one usually predominates. In this case, it is Compton scattering where a fraction of the incident gamma-ray photons are knocked out of the beam by collisions with the electrons in the exposed matter. Each photon that is removed represents a collision with an electron, so that the number of photons knocked out of the beam is directly proportional to the electron or matter density.

The general equation for the counting rate of photons is given by

$$C_W = n\ V\ N_p\ d(\sigma)$$

where

$C_w$ = wanted counting rate, $C - C_b$, counts/min.,
$C$ = total counting rate,
$C_b$ = background counting rate,
$n$ = electron number density, electrons/$cm^3$,
$V$ = sensitive volume size, $cm^3$,
$N_p$ = beam intensity, photons/$cm^2$ min.,
$d(\sigma)$ = differential collision cross-section, $cm^2$/electrons.

Also,

$$n = \rho \frac{Z}{A} N_A$$

where

$\rho$ = measured density of gas,
$Z$ = atomic number, electrons/atom,
$A$ = atomic weight, gm/mole,
$N_A$ = Avogadro's number.

Thus, in a manner similar to X-ray determination of density, the gas density can be measured with a detector capable of counting individual photons coming from a radiation source and scattered from a particular volume. The composition of the gas must be known.

When a photon hits the scintillation crystal, the flash of light that is produced causes an electron cascade in the photomultiplier tube which enters the preamplifier as an electron pulse. The energy given up by the photon in the crystal determines the light intensity. This relates the pulse amplitude produced by the photomultiplier to the photon energy. The preamplifier sends the pulse along to the linear amplifier. The pulse amplitude is increased by several orders of magnitude by the linear amplifier and then it continues into the pulse height analyzer. Here only certain pulse heights are accepted by this discriminator. Only those heights between two preset levels are spaced through to the counter.

4.7.2.2 INTERPRETATION OF MEASUREMENT

Additional information needed - Composition of atmosphere.

Method for analysis and interpretation of data - A scaler counts within a present time interval the number of pulses caused by the impinging photons. The number of photons counted is linearly related to the gas density.

4.7.2.3 INSTRUMENT CHARACTERISTICS

The instrument characteristics, instrument output and payload integration data listed below are for an instrument which has been flight tested by Reichle (1965). A Nike Apache rocket was the test vechicle and lifted the package to over 90 km.

Total and dynamic ranges - The range of the instrument is dependent on source strength. A 24 Curie Cerium radioactive source gave measurements (where the counting rate was exponential with height) of density between $8.9 \times 10^{-5}$ g/cm$^3$ and $1.1 \times 10^{-6}$ g/cm$^3$. Very high source strengths are necessary to measure densities down to $10^{-9}$ g/cm$^3$. Reichle (1965) did not indicate if densities larger than $8.9 \times 10^{-5}$ g/cm$^3$ were measured (from 20 km to the surface). It is possible that the counting equipment could not handle the large counting rates that would occur.

Accuracy - After subtracting the background counting rate, the determined densities agreed rather closely with the 1962 U. S. Standard Atmosphere.

Signal to noise - The background scattering gives a certain counting rate. As the density and counting rates decrease, this background level is approached. When the background level is reached, this is the effective lower limit of the measurement.

Frequency response - The time constant is very small. The photons travel a short distance at the speed of light.

Environmental effects - The instrument had to be quite rugged to withstand the shocks of launch and the extremes of the high altitude environment.

4.7.2.4 INSTRUMENT OUTPUT

Output signal - The calibrated output is in pulse form. In the flight testing of this particular instrument, the pulses were stored on tape and the counting was done by a ground-based electronic counter.

Bits per observation - Ten bits per observation would be needed.

4.7.2.5 PAYLOAD INTEGRATION

Weight - The entire payload weighs 125 lbs. in version tested.

Volume - Probably less than 2 $ft^3$.

Power - Not indicated

Radio frequency interference - Not indicated

Magnetic moment - Not known

Erection, orientation, or booms - None

Compatibility with sterilization at 145°C - Could not be determined.

Special requirements - The detector and radiation source must be placed so that no direct gamma-ray emission falls upon the detector.

4.7.2.6 STATE OF DEVELOPMENT

The instrument package is still in the developmental stage. More flight tests are planned. Efforts are being made to reduce the background count rate.

REFERENCES - SCATTERING TECHNIQUES - X-Ray and Gamma

Hakewessel, D. B., 1966: Feasibility stude for a X-ray backscatter free air density sensor, Giannini Controls Corp., NASA Contract Rpt. No. 66148, NAS 1-4249, 123 p.

_____, 1966: Measurement of Atmospheric Density Using Gamma Backscatter Techniques, Giannini Controls Corp., 17 pp.

Johnson, D. L., 1964: X-ray Air Density Determination, Giannini Controls Corp., Final Rpt, AF 33(657)-11631, 81 p.

Reichle, H. G., Jr., 1965: Flight Test Results of Gamma-Ray Scattering as a Technique for Air Density Measurements, NASA, Langley Res. Center, NASA-TMX-56837, 11 pp.

## 4.8 EXCITATION TECHNIQUES

Excitation techniques depend on the relationship between the excitation radiation of gas molecules and gas density.

### 4.8.1 ULTRAVIOLET AIR DENSITY GAUGE

The ultraviolet air density gauge utilizes the rearrangement radiation from molecular nitrogen for the measurement of density. Air is excited to visible fluorescence by shining a beam of ultraviolet light through it.

The absorption length where the intensity has fallen to 1/e of its initial intensity is expressed by

$$L = \frac{A}{N_o \sigma}$$

where A is the molecular weight of the gas, $N_o$ is the Avogadro number, and $\sigma$ is the cross section for nitrogen. This absorption length is related to the physical path length $\ell$ and the density $\rho$ by

$$\ell = \frac{L}{\rho}$$

The change in the intensity of the fluorescence between two distances $x_1$ and $x_2$ from the source is given by

$$\Delta I = I_o [\exp (x_2/\ell) - \exp (x_1/\ell)]$$

$\Delta I/Io$ is the fraction of the initial energy between 500Å and 700Å that is absorbed between $x_1$ and $x_2$. Five percent of the energy absorbed between $x_1$ and $x_2$ is radiated in the visible, thus

$$E_v = 0.05 E_o \frac{\Delta I}{I_o}$$

where $E_o$ is the initial energy available between 500Å and 700Å.

A detector of area A located a distance R from the radiating element senses the fraction of the reradiated energy $E_v$ given by

$$f = \frac{A}{4\pi R^2}$$

Thus, the total energy received at the detector $E_r$ is expressed as follows:

$$E_R = 0.05f\ E_o \frac{\Delta I}{I_o} \text{ or}$$

$$E_R = 0.05f\ E_o \frac{x_2 - x_1}{\ell} \quad \text{if } x << \ell$$

This energy can be expressed in terms of the average number of photons incident on the detector area A.

#### 4.8.1.1 NARRATIVE DESCRIPTION OF THE INSTRUMENT

The instrument consists of a collimated, excitation ultraviolet source and a photomultiplier tube detector with focused optics. It can detect the fluorescence of molecular nitrogen in the visible when bombarded by 500Å to 700Å photons. A sequence of filters and source modulators is utilized to insure that only gas molecules contribute to the signal, and not reflections from dust or ice crystals. The intensity of the fluoresence as a function of the amount of energy fed into the ultraviolet source would be a measure of air density.

#### 4.8.1.2 INTERPRETATION OF MEASUREMENT

Additional information needed to interpret measurement - Relative concentration of $N_2$ in the atmosphere.

Method for analysis and interpretation of data - A photomultiplier tube detects the return signal of the radiated energy in the visible and very-near ultraviolet portion of the spectrum. The number of incident photons is proportional to the density.

#### 4.8.1.3 INSTRUMENT CHARACTERISTICS

Total and dynamic ranges - The instrument is capable of measuring atmosphere densities from $5 \times 10^{-8}$ gm/cm$^3$ (~80km) to $10^{-14}$ gm/cm$^3$ (~350km).

Accuracy - The accuracy is dependent on knowledge of the sky albedo, internal background and systematic errors in the determiations. Internal background errors are produced by extraneous electrical signals that might stimulate the phototube or from visible light from the source that is reflected or scattered into the phototube by dust particles, ice crystals, engine exhaust products or other condensed matter. Nonlineritiés in the detection system and variations in the source strength produce the systematic errors. An accuracy of 1.5-2.0% is expected.

Signal to noise - The chief contribution to instrument noise will be from sky background. By conservatively estimating the changes in albedo light with changing altitude the signal-to-noise ratio would be 20 to 1 at 300km.

Frequency response - Instantaneous

Environmental effects - No serious effects are expected.

4.8.1.4 INSTRUMENT OUTPUT

Output signal - The output is digital, calibrated, and linear. The number of incident photons in the detector is related to the density.

Bits per observations - Eleven per observation would be required for three place accuracy (7 bits) and for the exponent (4 bits).

4.8.1.5 PAYLOAD INTEGRATION

Weight - Not less than 10 lbs.

Volume - Not less than 1 cu. ft.

Power - 100 watts peak power needed to get 1 watt of visible radiation.

Radio frequency interference - None

Magnetic moment - Not known

Erection, orientation, or booms - Not critical

Compatibility with sterilization at 145°C - Unknown.

Special requirements - None.

4.8.1.6 STATE OF DEVELOPMENT

This instrument is still in the pre-flight test stage. Undoubtedly, further development will be necessary for instrument use on other planets.

### 4.8.2 ELECTRON BEAM DENSITY GAUGE

This instrument is geometrically similar to the ultraviolet density gauge with an electron gun as the source of the electron beam and a photomultiplier as the detector. The field of view from the photomultiplier intersects the fluorescence produced by the electron beam and the detector records the fluorescent energy.

The amount of light (in watts per centimeter) of electron path length that is isotropically emitted by the ionized air through which the electron beam passes is expressed by

$$I = KN(dE/dx)\ \frac{\rho}{1 + 5.49 \times 10^{4}\rho} \quad \text{watts/cm} \qquad (1)$$

where $\rho$ is the air density in $gm/cm^3$; $dE/dx$ is the energy lost per electron per centimeter in joules - $cm^2/gm$; N is the number of electrons per second; and K is the fraction of energy lost that goes into light.

The amount of light received by the photomultiplier that is emitted by the fluorescing air is given by the relation

$$I_r = fI \qquad (2)$$

where f is the fraction of the light emitted by the gas that is collected by the photocathode of the photomultiplier tube. Therefore the relation between the energy collected by the photocathode and density is given by

$$I_r = fKN\ \frac{dE}{dx}\ \frac{\rho}{1 + 5.49 \times 10^{4}\rho} \quad \text{watts/cm} \qquad (3)$$

#### 4.8.2.1 NARRATIVE DESCRIPTION OF THE INSTRUMENT

An electron gun shoots out a collimated electron beam. Some of the energy is transformed into fluorescence. This energy is sensed by a photocathode of a photomultiplier tube. The photomultiplier tube field of view is oriented such as to intersect a sizeable portion of the electron beam.

#### 4.8.2.2 INTERPRETATION OF MEASUREMENT

Additional information needed to interpret measurement- Atmospheric composition

Method for analysis and interpretation of data - The photomultiplier tube receives the fluourescent energy from the electron beam. The amount of energy is related to atmospheric density according to (3).

4.8.2.3 INSTRUMENT CHARACTERISTICS

Total and dynamic ranges - Density can be measured between 75 and 130 km with this technique. Below 75 km the scattering angle for the electrons become large and they diffuse rather than form a beam.

Accuracy - Could not be determined

Signal to noise - The background signal, which is light from the day sky, is about the order of magnitude of the signal received from a one-meter long column of ionized air (the usual size measured). Also, a 1P28 photomultiplier tube has an equivalent noise power of the signal at the photocathode, when measured through a 100 cps bandpass filter. Thus, the electron beam must be modulated to detect the signal.

Frequency response - Not known

Environmental effects - None expected to be serious.

4.8.2.4 INSTRUMENT OUTPUT

Output signal - The calibrated analog voltage is in pulse form. It is linearly related to the gas density.

Bits per observation - Eleven bits per observation are needed.

4.8.2.5 PAYLOAD INTEGRATION

The values below are approximate as no instrument for extraterrestrial observations is currently available.

Weight - Probably over 10 lbs.

Volume - Probably over 1 cu. ft.

Power - 50 watts (approx.)

Radio interference - None

Magnetic moment - Not known

Erection, orientation, or booms - The proper relative orientation of the electron beam gun and the photomultiplier tube is necessary.

Compatibility with sterilization at 145°C - Unknown.

Special requirements - None

4.8.2.6 STATE OF DEVELOPMENT

This instrument is in the early development stage. No flight or laboratory calculation of error has yet been made.

4.8.3 BREMSSTRAHLUNG

This method utilizes an electron beam to probe the density of a small volume of gas which is located a short distance from the measuring device. The measured parameter is the number of Bremsstrahlung X-rays generated within a selected segment of the volume irradiated by the electron beam. The generation process is the electron-gas atom interaction. The attractive aspect of the technique is that the response of this measurement system is dependent upon the average atomic number of the atoms constituting the irradiated volume but is independent of the chemical form, degree of ionization and temperature of the gas. Its main limitation is that it can only be utilized at altitudes above 100km (in the Earth's atmosphere). An existing rocket-bound system utilizing this technique has a potential error in density measurement of 39% at present with an ultimate capability suggested that can reduce this error to 10%. (Sellers and Ziegler, 1965).

The main components of this measurement system are an electron gun (with power supply and beam focusing and deflection controls) and a proportional counter X-ray detector (with power supply and amplifier for the detector pulse output).

The signals that must be recorded and interpreted are the voltage and current of the electron gun and the pulses resulting from the X-ray detector. The atmospheric density can be computed from these three output signals provided a theoretical evaluation is made of the cross-section for the production ofa Bremsstrahlung X-ray of energy between k and k + dk by the interaction of a nonrelativistic electron of rest energy $mc^2$ and kinetic energy (k) with a nucleus of charge $Z_1$. The evaluation of this cross-section is the principal contributors to the 10% ultimate error associated with this technique.

## REFERENCES - EXCITATION TECHNIQUES

Cato, G. A., 1964: "Ultra-high Altitude Measurement Systems for Pressure, Density, Temperature, and Winds," Electro-Optical Systems, Inc., Final Report Contract NAS8-5226, EOS Rept. 3780, 149p.

Sellers, B., and Ziegler, C. A., 1965: A Rocket Borne Air Density Measurement System Utilizing Electron-Bremsstrahlung- Design and Development, Parametric, Inc., Sci. Rep. No. 1 (July) AFCRL-65-507, (AD620682) 79 p.

## 4.9 VISCOSITY GAUGES

The rate of transfer of momentum B from a surface moving with velocity u in the plane of the surface, to a stationary surface parallel to it at distance d, is given, at low pressures, by the equation

$$B = \frac{\eta u}{d + 2\zeta} \qquad (1)$$

where $\eta$ is the coefficient of viscosity and $\zeta$ the coefficient of slip, which is proportional to the mean free path L, and therefore, is inversely proportional to the density. Thus (1) can be written as

$$B = \frac{\eta u}{d + 2\ bL} \qquad (2)$$

where b is a constant that varies with the nature of the gas and that of the surface. At very low pressures $L \gg d$ and (2) becomes

$$B = \frac{\eta u}{2\ bL} \qquad (3)$$

and, since

$$\eta = 0.5\ \rho\ v_a\ L$$

where $\rho$ is the density of the gas and $v_a$ is the average velocity of the molecules, (3) can be written as

$$B = K_1\ \rho\ v_a\ u$$

and

$$B = K_2\ P \sqrt{\frac{M}{R_o T}}\ u$$

where $K_1$ and $K_2$ are constants, M is the molecular weight, P is pressure, and $R_o$ is the universal gas constant.

Another similar expression can be derived from considerations similar to those used in deriving the laws of molecular flow. This expression is given by

$$B = K\ u\ P \sqrt{\frac{M}{T}}$$

where K is a constant. Density can be calculated by the equation of state.

Two different types of gauges are used. The first is the "decrement" types where a surface is set in oscillation and the rate of decrease of the amplitude of oscillation is taken as a measure of the density (pressure). Damping occurs due to the gradual equalization of energy between the moving surface and the molecules of gas striking it.

In the second method, the density is measured by setting a surface in continuous rotation and determining the amount of twist imparted to an adjacent surface. Molecules that strike the moving surface acquire a momentum in the direction of motion which they tend to impart to the other surface. Then if that surface is suspended and free to rotate about an axis which is normal to the direction of motion of the rotating surface, it will be twisted around until the force due to the incident molecules is balanced by the torsion of the suspension.

### 4.9.1 QUARTZ FIBER GAUGE

#### 4.9.1.1 NARRATIVE DESCRIPTION OF THE INSTRUMENT

This operation of this instrument is based on the "decrement" principle (Dushman, 1949). The gauge consists of a fine quartz fiber (diameter 0.005 to 0.01 cm) sealed into the top of a glass tube. Oscillations of the fiber are set in motion by tapping the glass bulb gently. The rate of decrease of the amplitude of the bulb is observed by means of a telescope and lamp. Density is determined from the relation

$$\rho = \frac{\sqrt{M}}{RT}\left(\frac{B}{t_{0.5}} - C\right)$$

where T is temperature, R is the gas constant, $t_{0.5}$ is the interval of time required for the maximum amplitude to decrease to half value, and B and C are constant characteristic of the fiber.

#### 4.9.1.2 INTERPRETATION OF MEASUREMENT

Additional information needed to interpret measurement - The temperature of the gas must be known.

Method for analysis and interpretation of data- The density varies linearly with $1/t_{0.5}$. Optical methods are used to determine $t_{0.5}$.

#### 4.9.1.3 INSTRUMENT CHARACTERISTICS

Total and dynamic ranges - The range of this sensor is determined by the constants B and C. For a fiber 3 to 8 cm long and 0.0045 cm in diameter measuring the density of air, the lowest density the sensor could measure would be $1.8 \times 10^{-10}$ g/cm$^3$ .

Accuracy - Not indicated.

Signal to noise - Not indicated.

Frequency response - The length of time for the amplitude of the oscillation to decrease to half value is actually the measured quantity that is inversely related to density.

Environmental effects - This is a delicate instrument and would have to be protected against the rigors of space travel.

#### 4.9.1.4 and 4.9.1.5 INSTRUMENT OUTPUT and PAYLOAD INTEGRATION

The specific output and payload integration parameters would have to be determined for space usage. Undoubtedly, some form of automatic optical device would have to be designed in order to monitor the oscillations of the quartz fiber.

#### 4.9.1.6 STATE OF DEVELOPMENT

This sensor was primarily developed for use in the laboratory to measure pressure (density) where near vacuum conditions are needed. No effort has been reported to adapt this device for any other purpose.

### 4.9.2 MOLECULAR GAUGE

#### 4.9.2.1 NARRATIVE DESCRIPTION OF THE INSTRUMENT

This gauge consists of a glass bulb in which are contained a rotating disk and, suspended above it, a second disk (Dushman, 1949). The disk, made of thin aluminum, is attached to a steel or tungsten shaft mounted on jewel bearings and carrying a magnetic needle. A small mirror, about 0.5-cm square, is attached to the second disk (usually made of mica) by a framework of thin aluminum. The first (lower) disk is rotated with a rotating magnetic field produced outside of the bulb. This field is produced by a Gramme ring supplied at six points with current from a commutating device rotated by a motor. The speed of the latter can vary between a few to over 10,000 revolutions per minute.

The angle of torque, $\alpha$, on the second disk is given by the equation

$$\alpha = \frac{K \gamma^2 r^4}{I} \; Pw \sqrt{\frac{M}{T}}$$

where K = constant, which depends upon the nature of the gas and the accommodation coefficients for transfer of momentum,
r = radius of rotating disk,
I = moment of inertia of disk,
$\gamma$ = period of oscillation,

w = angular velocity of rotation,
P = pressure,
T = temperature,
M = molecular weight.

Therefore, for a given gauge, the torque on the upper disk is proportional to the product of the speed of rotation of the aluminum disk and $P\sqrt{M/T}$ . The sensitivity of the gauge is increased by increasing the speed of rotation; also, by illuminating the mirror and using an arrangement similar to that used for galvanometers, it is possible to measure low pressures or small densities.

4.9.2.2 INTERPRETATION OF THE MEASUREMENT

Additional information needed to interpret measurement- Temperature must be determined simultaneously with the density (pressure) measurement.

Method for analysis and interpretation of data - For constant temperature the angle of torque on the upper disk is linearly re related to pressure. This angle is measured by the angular deflection of the mirror suspended from the top of the glass bulb.

4.9.2.3 INSTRUMENT CHARACTERISTICS

Total and dynamic ranges - Densities as small as $8.4 \times 10^{-14}$ g/cm$^3$ can be measured.

Accuracy - Not indicated.

Signal to noise - Not indicated.

Frequency response - The time constant could not be determined.

Environmental effects - Like the quartz fiber gauge, this instrument appears to be delicate and would require special protection from the conditions associated with space travel, rocket takeoffs and landings.

4.9.2.4 and 4.9.2.5 INSTRUMENT OUTPUT and PAYLOAD INTEGRATION

The specific details of instrument output and payload integration are not available. If the technique were thought to be usable, these details could be determined. Since the instrument uses a rotating magnetic field, any strong external magnetic field might alter the magnetic moment of the sensor.

4.9.2.6 STATE OF DEVELOPMENT

This sensor was designed for laboratory use. Considerable development and design would probably be necessary to use it as a sensing device for planetary atmospheres.

## REFERENCES - VISCOSITY GAUGES

Dushman, S., 1949: Scientific Foundations of Vacuum Technique, John Wiley and Sons, Inc., 882p.

## 4.10 ABSORPTION TECHNIQUES

Absorption techniques depend upon the fact that the absorption of electromagnetic radiation is a function of the denisty of the absorbing medium.

### 4.10.1 FILTER PHOTOMETER AIR DENSITY GAUGE

Optical absorption of the sun's radiation in various spectral regions can lead to the determination of atmospheric density in accordance with the equations

$$\ell n \frac{I_2}{I_1} = \alpha \rho (h_2 - h_1)$$

where $I$ = radiance
$\alpha$ = absorption coefficient
$h$ = altitude
$\rho$ = density

Subscript

1 = lower altitude
2 = higher altitude

The absorption coefficient, $\alpha$ depends on the molecular species responsible for the absorption; which in turn determines the choice of wavelength in the earth's atmosphere. Absorption of molecular oxygen provides the most accurate measurement between 1800Å (at 90 km) and 2000Å (at 40 km). Between 90 and 120 km the solar Lyman $\alpha$ emission line at 1215Å is a convenient radiation source. Above 120 km, where oxygen is dissociated, the absorption of soft X-rays can be used, which is proportional to the total mass and is independent of molecular aggregation. For the atmospheres of Mars and Venus, which contain very little oxygen, the near infrared bands of $CO_2$ could be used.

#### 4.10.1.1 NARRATIVE DESCRIPTION OF THE INSTRUMENT

The following discussion refers to the technique as it has been applied to the earth's upper atmosphere. The instrument consists of a fork-mounted detector and solar tracking sensor. Depending on the wavelength of the incident radiation, the ultraviolet radiation detector operates by means of photoionization and photoelectron production. The detector usually consists of a conducting cavity which can be filled with a gas. An electrode is introduced into the cavity thus making the detector a two-terminal device. The incident radiation comes through a window and interacts with the chamber walls and the gas. Between 1000Å and 1500Å the ultraviolet

photon has enough energy to ionize its gas. Presence of the photon is indicated by collection of the ion and electrons. Depending on the ionization potential of the gas, the response may be enhanced at certain wavelengths by the proper selection of gases. At wavelengths above 1500Å the response is almost all due to the photoelectron production, as in an ordinary phototube. Quenching gases, which recombine with the photoelectron before it can be collected, can be used to suppress the response. Also, the response can be lowered by proper tube geometry.

#### 4.10.1.2 INTERPRETATION OF MEASUREMENT

Additional information needed to interpret measurement - Relative atmospheric composition and ultraviolet absorbance.

Method for analysis and interpretation of data - The output of this instrument is a train of pulses that is proportional to the density.

#### 4.10.1.3 INSTRUMENT CHARACTERISTICS

Total and dynamic ranges - Optical absorption of the sun's radiation is made at selected wavelengths between 60Å and 2000Å. In the earth's atmosphere, the lower limit of the instrument's measuring capability is 40 km and the upper boundary is above 120 km.

Accuracy - Detector drift, absolute energy calibration, and atmospheric dust would be the three primary error sources for this instrument. The drift error is perhaps the most serious and can be held to less than 1% per day for the photomultiplier. The greatest drift is experienced by the X-ray detector; 10 percent over several hours. It is difficult to presently ascertain the dust error that might occur on other planets.

Signal to noise - The signal in the 1200-2000Å at unit optical depth with a photomultiplier tube is about $2\mu$ amp per square cm of collecting area. This level is at least 1000 times the dark current due to thermionic emission.

The Lyman-$\alpha$ detector produces about $10^{-8}$ amp of ion current for a flux of 1 erg/cm$^3$- sec. This current is in contrast to a noise of less than $10^{-16}$ amp.

The X-ray detector supplies pulses in excess of $10^{-8}$ amp for the X-ray solar intensity above 120 km. The number of counts per second will be around several thousand above background of $< 100$ counts/sec due to cosmic rays and hard X-rays.

Frequency response - The time constant of the instrument is small, probably less than 0.1 second.

Environmental effects - No serious problems are expected as a result of the environment.

4.10.1.4 INSTRUMENT OUTPUT

Output signal - The filter photometer gives calibrated logarithmic, analog output.

Bits per observation - 12 bits.

4.10.1.5 PAYLOAD INTEGRATION

Weight - Probably about 10 lbs.

Volume - Between 1/2 and 1 $ft^3$ (approx.)

Power - Probably at least 50 watts.

Radio frequency interference - None

Magnetic moment - Not known

Erection, orientation, or booms - The detector must be pointed directly at the sun during the observation period.

Compatibility with sterilization at 145°C - Unknown.

Special requirements - None

4.10.1.6 STATE OF DEVELOPMENT

Development would undoubtedly be needed for the atmospheres of Mars and Venus. Also, the composition of the atmosphere must be determined. The wavelengths selected for the observations on the other planets may have to be changed because of different atmospheric compositions.

4.10.2 ALPHA, BETA, AND GAMMA ABSORPTION

This technique is based on the measurement of radioactive emission by means of a detector directly exposed to it, and separated from the source by a volume of air whose density is to be determined. Radiation absorption and scattering by the intervening molecules reduce the detected radiation level which becomes a function of the gas density. For alpha and beta radiation, the useful range of densities depends on the width of the energy spectrum of the emission. In general, beta particles exhibit a wider spread of energies and thus are more suitable for this purpose. On the other hand, a narrow energy distribution implies a high sensitivity over

the reduced range. The attenuation of alpha and beta particles is mainly a result of inelastic collisions with bound electrons of air molecules, while gamma attenuation is caused by three processes; a) photoelectric absorption, b) Compton scattering, and c) position-electron pair generation.

The development of these techniques in general has been limited to theoretical studies and laboratory experiments with the purpose of applying radiation absorption methods for the measurement of low density air (corresponding to terrestial conditions above 150,000 feet), with the exception of one instrument, an alpha-densitometer which was developed for use on stratospheric balloons, at altitudes between about 80,000 and 150,000 feet. In general, the application of radiation to the measurement of atmospheric densities has been concentrated on scattering measurements which has been discussed in another section. The scattering approach, in general, offers the advantage of in situ measurement of ambient density since the volume to be sensed can be outside the source-detector geometry reducing or eliminating errors associated with temperature differences, outgassing, etc. which are characteristic of absorption schemes.

## REFERENCES - FILTER PHOTOMETER

Cato, G. A., 1964: "Ultra-High Altitude Measurement Systems for Pressure, Density, Temperature, and Winds," Electro-Optical Systems, Inc., Final Report, Contract NAS8-5226, EOS Rept. 3780, 149p.

## 4.11 MICROWAVE REFRACTOMETER

Refractive index of an atmosphere may be used to determine any one of several of its properites if all others are known. Density, pressure, temperature, and water vapor density as well as composition affect the refractive index. The instrument has been used experimentally as a method of measuring atmospheric properties and is discussed under water vapor sensor.

## 4.12 VIBRATING REED

The density of a gas is determined from two measurements of decay time of a vibrating reed, one for a reference and another for a test reed, and from a set of calibration curves. The loss in energy of a vibrating reed is accounted for by two distinct mechanisms, namely the internal friction of the reed material and damping by gas surrounding the reed.

In considering the energy dissipation due to gas drag, a constant Reynolds number is assumed, and the energy lost per cycle is

$$23\ C_D\ p_g\ LbV^3/200f$$

where $C_D$ is the drag coefficient, $p_g$ is the gas density, L is the length of the reed, b is the breadth of the reed, V is the peak velocity at the tip of the reed, and f is the natural frequency of the reed.

The reference reed is placed in a chamber filled with gas with a known density, while the test reed is open to the gas whose density is to be determined. A measurement of the time or the number of cycles for each of the reed's vibrations amplitude to decay to 20db of maximum value is taken. From this and a set of calculated calibration curves, the density of the gas in the sample chamber may be determined.

The useful range of the device is up to approximately 0.1 g $cm^{-3}$ where the sensitivity is the order of 900 m/s g $cm^{-3}$. At lower densities of the order of 0.02 g $cm^{-3}$, the sensitivity is 2050 m/s g $cm^{-3}$. For a more accurate system, a digital system should be used to count the number of cycles in the 20 dB folding time.

## REFERENCES

Ledwidge, T. J. and Hughes, G., Gas Density Measurement by the Natural Damping of a Vibrating Reed, J. Sci, Instr. 44, (1967).

## 5. PRESSURE

The average surface pressure on Mars can be expected to lie between 5 and 14 mb, with a nominal average value of about 7 mb (House, et al., 1967). An instrument for measurement of Martian surface pressure should be capable of measuring between 3 mb and 25 mb. This range should be sufficient to cover uncertainties in our present estimate of surface pressure, surface pressure variations due to uncertainties in landing site (elevation or depression), possible reductions in surface pressure due to condensation of atmospheric carbon dioxide, and meteorological variations of surface pressure. The pressure decreases with altitude by 1/e each scale height. The average scale height is about 10 km near the surface and decreases to about 8 km above 30 km altitude.

The surface pressure on Venus is 20 atm, according to the Venus IV observations. The scale height is about 12 km near the surface and decreases to about 6 km at a height of 30 km. (These estimates of scale height are based upon a predominantly $CO_2$ atmosphere, surface temperature of $600^{\circ}K$, and lapse rate of $10^{\circ}C/km$).

## 5.1 DIAPHRAGM GAUGES

Diaphragm gauges operate on the principle that the pressure exerted on a thin membrane causes a change in one of its mechanical characteristics (positional deplacement, vibrational damping, etc.).

### 5.1.1 ANEROID BAROMETER

#### 5.1.1.1 NARRATIVE DESCRIPTION OF THE INSTRUMENT

The aneroid barometer fundamentally consists of two parts - a closed box of thin metal, partly or fully evacuated, and a strong spring. The spring operates to keep the box from collapsing under pressure of the atmosphere, and at a given pressure there is an equilibrium between the forces of the spring and the atmosphere. The elastic properties of the spring determine the characteristics of the whole instrument. One side of the box or aneroid chamber is attached to a support, the opposite side of the aneroid is linked to drive an indicator or pen for recording. There are many variations of the aneroid construction and lever mechanisms.

The aneroid barometer must contain some device for temperature compensation. Hysteresis and creep are other factors which contribute to errors and are inherent in the aneroid barometer. The aneroid barometer offers sensitivities of about 0.2 mb. However, the absolute accuracy of the instrument is somewhat less than desirable; for this reason, it is not recommended for high precision absolute pressure measurements.

The modern aneroid barometer consists of a number of aneroid cells in series connected to a mechanical magnifier. The mechanical linkage is connected to, and drives a low torque position type transducer. There are many variations in the type of transducers including capacitors, reluctance and strain gauges all using the aneroid element as the basic movement.

A Paulin-type aneroid barometer manufactured by United Geophysical Company uses a capacitor transducer. The capacitor plates are located immediately above the aneroid chamber. The capacitor is connected in a Wheatstone bridge circuit. Current in the signal circuit is so adjusted that it is zero when the middle, movable condenser plate is in the null position. Measurement is provided for by the positioning of the movable plate relative to the null position. Typical specifications for aneroid barometers are presented below.

#### 5.1.1.2 INTERPRETATION OF THE MEASUREMENT

Additional information needed to interpret the measurement - None.

Method for analysis and interpretation of data - Depends upon the type of transducer selected — generally a dc voltage output which varies in a linear fashion with barometric pressure.

5.1.1.3 INSTRUMENT CHARACTERISTICS

Total and dynamic range - For the Earth's atmosphere, a dynamic range of between three to eight inches Hg, depending upon the design, centered at approximately 29 inches Hg. Wider ranges are available (10 mb to 1000 mb) for radiosonde applications.

Accuracy - Approximately 0.3 percent of full scale range without transducer.

Signal to noise - Dependent upon transducer and electronics.

Frequency response - Not known.

Environmental effects - Calibration is affected by temperature changes.

5.1.1.4 INSTRUMENT OUTPUT

Output signal - Dependent upon transducer and electronics.

Bits per observation - Using a range of six inches Hg a ten-bit word will yield a resolution of 0.0117 inches Hg.

5.1.1.5 PAYLOAD INTEGRATION

Weight - Approximately one pound.

Volume - Approximately 75-cubic inches.

Power - Dependent upon electronics.

Radio frequency interference - None.

Magnetic moment - Unknown.

Erection, orientation, or booms - None.

Compatibility with sterilization at 145° C - Yes.

Special requirements - None.

5.1.1.6 STATE OF DEVELOPMENT

The aneroid barometer has been used in the Earth's atmosphere for many years. No major problems anticipated for extraterrestrial use.

### 5.1.2 BELLOWS-TYPE BAROMETER

The bellows-type barometer is very similar to the aneroid barometer, the difference being in the construction of the pressure sensitive chamber. The aneroid makes use of a single small chamber whereas the bellows-type chamber is elongated with the walls manufactured in the shape of a bellows. The use of the bellows-type construction of the pressure chamber results in greater movement for a given pressure change. However, this may also be accomplished by stacking a number of aneroid chambers in one barometer.

### 5.1.3 VIBRATING DIAPHRAGM PRESSURE TRANSDUCER

#### 5.1.3.1 NARRATIVE DESCRIPTION OF THE INSTRUMENT

This type of transducer measures pressure by sensing the damping effect of the gas on the vibration of a thin metal diaphragm (King, 1966). The diaphragm is under radial tension and is in a continuous vibration that is maintained electrically at its mechanical resonant frequency. Two metal plates provide a means of electrically forcing and detecting the vibration of the diaphragm. A space between the plates and the diaphragm is filled with the gas whose pressure is to be measured. A loss of energy from the diaphragm is created by gas damping and this loss is sensed by its effect on the diaphragm damping factor. Therefore, the electrical power required for a given amplitude of vibration is a measure of gas pressure.

The forcing plate of the transducer is supplied with a dc potential and an ac voltage from an electronic oscillator set at the mechanical resonant frequency of the tensioned diaphragm. A generated electrostatic forcing function causes the diaphragm to vibrate synchronously with the ac driving voltage and at an amplitude which is a function of the driving signal and the diaphragm damping factor. The vibrator's amplitude may be indicated due to a periodic vibration in the capacitance between the diaphragm and the sensing plate caused by the diaphragm's vibration. Since the power needed for a given amplitude of vibration is a function of the damping on the diaphragm, the power can be maintained to indicate the pressure.

The total energy lost through diaphragm vibration is a sum of electrical energy losses, mechanical energy losses, and energy losses caused by the gas. It is the variations in the energy losses caused by the gas that are a reflection of the changes in pressure. The expression for the gas energy loss is given by

$$\frac{V_o V_1}{X_1} = \frac{\pi^{7/2} \, (2RT\,m)^{1/2} \, \gamma^2}{16\, A\, e\, \omega\, \bar{\alpha}_1} \, X_o^{\,2} P_o$$

where $V_o$ = initial voltage applied to the forcing plate,

$V_1$ = amplitude of the superimposed voltage applied to the forcing plate,

$R$ = gas constant,

$T$ = temperature,

$\gamma$ = ratio of specific heats,

$m$ = molecular weight of the gas,

$A$ = area of the diaphragm,

$e$ = dielectric constant,

$\omega$ = resonant frequency of the diaphragm in radians/sec.

$\bar{\alpha}_1$ = analogous shear stress coefficient,

$X_o$ = distance between the forcing plates and the diaphragm,

$X_1$ = peak displacement of the diaphragm averaged over the area of the fixed plate,

$P_o$ = equilibrium pressure being measured by the transducer.

In practice, $$\frac{V_o V_1}{X_1} = f\ (P_o \cdot \text{gas properties}) + P_m + P_r$$

where $P_m$ = mechanical losses,

$P_r$ = electrical losses.

Since the mechanical and electrical losses are independent of $P_o$, they can be calculated separately and applied as a correction to the measurements.

5.1.3.2 INTERPRETATION OF THE MEASUREMENT

Additional information needed to interpret measurement - A knowledge of temperature and gas composition is necessary to successfully maintain the calibration of the instrument. However, the effect of temperature and gas composition can be minimized by transducer design and selection of materials. If the instrument is to be used over a wide range of gas compositions and temperatures, these parameters should be known for proper interpretation of the signal.

Method for analysis and interpretation of data - The output is in $V^2/m$ and is linearly related to changes in pressure.

5.1.3.3 INSTRUMENT CHARACTERISTICS

Total and dynamic ranges - Pressures between $10^{-5}$ and $10^3$ mm Hg can be measured with the transducer. The dynamic range of the instrument varies between $10^4$ ($10^{-5}$ mm Hg) and $10^{12}$ ($10^3$ mm Hg) $V^2/m$.

Accuracy - The accuracy of the instrument is ±1 percent over most of the range of the instrument. At the ends of the total range, the errors are somewhat higher. Other errors would be introduced if the temperatures of the gas and the gas composition were not known.

Signal to noise - The signal is considerably stronger than any background noise.

Frequency response - The time constant is about 0.005 second at high pressures. For low pressures, special circuitry that maintains a constant amplitude of diaphragm vibration can allow the time constant to approach that at high pressures.

Environmental effects - None anticipated.

5.1.3.4 INSTRUMENT OUTPUT

Output signal - The calibrated output is in analog form ($V^2/m$). There is a linear relationship between $V^2/m$ and pressure.

Bits per observation - Eleven bits per observation will be needed. Seven bits for the numerical value of the voltage (accurate to two places) and four bits for the order of magnitude.

5.1.3.5 PAYLOAD INTEGRATION

Weight - Less than 2 lbs.

Volume - Less than 0.2 $ft^3$.

Power - Probably less than 50 watts.

Radio frequency interference - None.

Magnetic moment - Unknown.

Erection, orientation, or booms - No special orientation.

Compatibility with sterilization at 145°C - The instrument can probably withstand sterilization.

Special requirements - None.

5.1.3.6 STATE OF DEVELOPMENT

Two sensors were flown on a free-falling probe experiment in the Earth's atmosphere (Sommer and Boissevain, 1967). One of the units operated satisfactorily.

### 5.1.4 CAPACITANCE-TYPE BAROMETERS

#### 5.1.4.1 NARRATIVE DESCRIPTION OF THE INSTRUMENT

The capacitance barometer consists of a highly stressed metal diaphragm positioned between two fixed capacitor plates. The diaphragm forms the separation between two gas-tight enclosures. A difference in total pressure within the enclosures produces a force which deflects the diaphragm and varies the capacitance of the diaphragm and the fixed capacitor plates. A measuring circuit, usually an ac bridge, is used to determine the capacitance change, which is related to the total pressure change.

Capacitance barometers are manufactured to be essentially free from temperature effects and are useful over a wide range of pressures.

#### 5.1.4.2 INTERPRETATION OF THE MEASUREMENT

Additional information needed to interpret the measurement - None.

Method for analysis and interpretation of data - The output of the measuring circuit is a dc signal which is analog to the pressure over a given design range with the use of a calibration curve.

#### 5.1.4.3 INSTRUMENT CHARACTERISTICS

Total and dynamic range - The instruments cover a total range from 0.01 to 1000 mm Hg divided into nine dynamic ranges.

Accuracy - 0.1 to 0.25 percent of reading; linear to 0.05 percent.

Signal to noise - Unknown.

Frequency response - Time constant = 3 ms at 760 mm Hg.

Environmental effects - None.

#### 5.1.4.4 INSTRUMENT OUTPUT

Output signal - A 0 to 5 volts dc signal analog to the pressure for each range is produced by the measuring circuit.

Bits per observation - For a resolution of 1 percent of any given dynamic range, a seven-bit word is needed.

#### 5.1.4.5 PAYLOAD INTEGRATION

Weight - 1.75 lb.

Volume - 12 cubic inches (sensor).

Power - Approximately 25 watts.

Radio frequency interference - None.

Magnetic moment - Unknown.

Erection, orientation, or booms - None.

Compatibility with sterilization at 145°C - Yes.

Special requirements - None.

5.1.4.6 STATE OF DEVELOPMENT

Sensors are commercially available. Electronic measuring circuit must be developed for use in space probes.

## REFERENCES - DIAPHRAGM GAUGES


Datametrics Inc., Technical Specifications for Capacitance Manometers. Waltham, Mass.

Her Majesty's Stationery Office, 1956: Handbook of Meteorological Instruments, London.

King, J., 1966: A Vibrating Diaphragm Transducer, NASA SP-5020, August, 27pp.

Lion Research Corp., Pressure Meter Bulletin PM-100, Newton, Mass.

Sommer, S., and A. Boissevain, 1967: Astronautics and Aeronautics, Feb., 50-54.

Wallace and Tierman, Precision Aneroid Barometer. Specification Sheets, Belleville, New Jersey.

## 5.2 BOURDON TUBE GAUGE

To this group belong mechanical pressure-measuring instruments employing as their sensing elements a curved or twisted tube, flattened in cross section. One end of the tube is closed, and the fluid pressure to be measured is applied through the other end. As the inside pressure is increased, the tube becomes more nearly circular in cross section, and tends to straighten. The motion of the free (closed) end of the tube is a measure of the internal pressure. The fundamental principle that motion of a bourdon tube is proportional to applied pressure is credited to Eugene Bourdon, nineteenth century French inventor. The bourdon pressure element may be made in any one of a number of shapes. The most common forms are the C tube, the spiral and the helical element.

### 5.2.1 INSTRUMENT

#### 5.2.1.1 NARRATIVE DESCRIPTION OF THE INSTRUMENT

For electrical pressure transducers, the twisted tube bourdon type is often preferred but the choice of shape depends on the associated electrical transducer. Bourdon tube transducers are of various types, the most common is the bonded strain gauge.

In general these instruments, as well as those with mechanical linkage readout and the high precision optical-fused quartz tube gauges, are used for industrial and aerospace hardware pressure measurements and not for meteorological applications. Thus an instrument specifically designed for atmospheric studies and in particular for remote planetary operation has not been developed. The advantage of the bourdon technique is its ruggedness and dependability, qualities which would warrant such a development.

#### 5.2.1.2 INSTRUMENT CHARACTERISTICS

Only those characteristics will be given here which typify existing instruments and, in particular, the bourdon tube sensor; other characteristics relevant to planetary applications will be omitted for the above stated reason.

Additional information needed to interpret measurement- None

Method for analysis and interpretation of data - Dependent on deflection sensing system used. Usually analog voltage proportional to pressure for a strain gauge (variable resistance).

#### 5.2.1.3 INSTRUMENT CHARACTERISTICS

Total and dynamic range - Dependent on particular tube used. Lowest range 0-65 torr with 0.003 torr resolution. Highest

range 0-100,000 psi with 1.0% resolution.

Accuracy - About 0.1% for the sensor itself, and up to 0.1% of full scale for the strain gauge.

Frequency response - Basic transducer, 10-100 Hz, strain gauge up to 2000 Hz.

Environmental effects - None

5.2.1.4 INSTRUMENT OUTPUT

Output signal - Dependent on sensing transduction, can be made digital. Output is calibrated and linear, proportional to pressure.

Bits per observation - 10 for a two decade range of pressures.

5.2.1.5 PAYLOAD INTEGRATION

Values are for basic tube sensor

Weight - 1 - 2 lbs.

Volume - 20 $in^3$ approx.

Power - 0.1 to 1 W (electronic amplification)

Erection, orientation, or booms - Non critical

Compatibility with sterilization at 145°C - Very high

Special requirements - None

State of development - Industrial application, not suitable for planetary ise. Minor development appears to be required for such use.

REFERENCES

Bulletin 021, Texas Instruments, Inc., Houston, Texas

McGraw-Hill Book Co., 1960: Encyclopedia of Science and Technology, Vol. 2, p 311.

## 5.3 HYPSOMETERS

Physically a hypsometer consists of a chamber in which a liquid is maintained at its boiling point. The chamber is specially designed to minimize the presence of air diffusion and superheating of the liquid. The temperature at which the liquid boils is a function of the atmospheric pressure, according to the following relation

$$\frac{d(\ell n\ p)}{dT} = \frac{L}{R_g T^2}$$

where p is the pressure; T is the temperature; L is the latent heat of vaporization, a function of temperature alone; and $R_g$ is the universal gas constant.

At sea level pressure, where water boils at 100°C, it is easily seen from this relationship that the decrease of temperature per millibar decrease in pressure is about 0.027°C. To determine the pressure to 0.2 mb we must be prepared to measure the temperature to about 0.005°C. The sensitivity of the hypsometer increases with decreasing pressure. This inherent characteristic of the hypsometer makes it attractive for possible use in low pressure environments.

## 5.3.1 THERMISTOR HYPSOMETER

### 5.3.1.1 NARRATIVE DESCRIPTION OF THE INSTRUMENT

In order to obtain satisfactory operation over a wide range of atmospheric pressure or within a narrow range in the low pressure region, it is desirable that the pressure transducer used exhibit characteristics such that sensitivity increase with decreasing pressure. The thermistor type hypsometer presents a solution for such a requirement.

If the logarithm of the resistance of a thermistor is plotted as a function of the reciprocal of the temperature, the resulting curve approximates a straight line. The sensitivity of the thermistor hypsometer is given by

$$\frac{dR_T}{dp} = -\frac{\beta R_g}{L}\,\frac{R_T}{p}$$

where $R_T$ is the resistance of the thermistor and $\beta$ is the nominal constant of the thermistor. The negative sign indicates that a reduction in pressure results in an increase in thermistor resistance. From the equation, it is clear that the sensitivity of the thermistor type hypsometer increases rapidly with decreasing pressure.

The inherent accuracy of the hypsometer may be considered independent of the type of temperature transducer selected. Since the basic dependent variable in the hypsometer is the temperature of the boiling fluid, the effect of the limitations of the temperature transducer become apparent once the relationship between pressure and the temperature of the hypsometer fluid is established. The desired relationship may be obtained from the pressure vs. temperature curve, or the equation may be used to determine the accuracy of the selected temperature transducer. Another source of error introduced by the temperature transducer is the finite thermal lag exhibited by the transducer. This error may be kept negligibly small for most applications if a small bead type thermistor is used as the temperature transducer.

A major and obvious factor which affects the repeatability of the boiling point temperature characteristics of any hypsometer is the purity of the fluid. With this fact in mind, it is advantageous to use a hypsometer design in which the liquid vaporized may be condensed so that the purity of the fluid is not changed appreciably.

A thermistor hypsometer manufactured by Cambridge Systems of Newton, Massachusetts is based upon the highly stable boiling point of butyl benzene. An internal reservoir furnishes fluid to a heated glass wick assembly. The wick assembly vaporizes this fluid with the heat required for vaporization being controlled by a precision thermistor placed

in the saturated vapor stream in the wick. An independent proportionally controlled thermal servo system regulates the heat required for vaporization as a function of pressure. Another precision thermistor temperature sensor is utilized to sense and compensate for variations in ambient temperature. The vaporized fluid is internally condensed and returned to the reservoir, thereby permitting long operation. The readout of the hypsometer is via a precision thermistor thermometer.

5.3.1.2 INTERPRETATION OF THE MEASUREMENT

Additional information needed to interpret the measurement - None

Method of analysis and interpretation of data - Output of sensor is a change in resistance of the thermistor thermometer. The log pressure vs. log resistance relationship is approximately linear. From resistance, temperature of the boiling fluid may be found from which the pressure may be derived.

5.3.1.3 INSTRUMENT CHARACTERISTICS

Total and dynamic range - Total range 1200 to 2.0 mb.

Accuracy - 1% of measurement

Signal to noise - Dependent upon electronics

Frequency response - Not available

Environmental effects - Present design cannot be used in ambient temperatures above 40°C or below -40°C.

5.3.1.4 INSTRUMENT OUTPUT

Output signal - Output of instrument is a resistance change of a thermistor thermometer - specifications for resistance thermometers apply.

5.3.1.5 PAYLOAD INTEGRATION

Weight - .750 g $\pm$ 10%

Volume - Approximately 12 cubic inches

Power - 3 watts maximum

Radio frequency interference - None

Magnetic moment - Unknown

Erection, orientation, or booms - None

Compatability with sterilization at 145°C - Without liquid, yes.

Special requirements - None

5.3.1.6 STATE OF DEVELOPMENT

Commercially available, generally custom made to specifications.

## REFERENCES

Sapoff, M., "Theory of Thermistor Hypsometers," Victory Engineering Corp., Springfield, New Jersey.

Technical Specifications Bulletin 137B1, Cambridge Systems, Newton, Mass.

## 5.4 PIEZOELECTRIC CRYSTALS AND SEMICONDUCTORS

A variety of piezoelectric transducers has been developed making use of various properties of crystals and semiconductors by which their electrical behavior is affected by changes in pressure of the ambient gas. Only their principle of operation will be presented here since they have not been developed to the point of full operational availability especially in terms of establishing their reliability and accuracy under field conditions.

### 5.4.1 PIEZOELECTRIC CRYSTALS

If a quartz crystal, which is part of an oscillator circuit, is exposed to the environment, the acoustic impedance of this medium affects the electrical properties of the crystal. The damping effect of the gas modifies the amplitude of the oscillations of the crystal, and this change becomes a function of pressure. In practice, one experimental gauge of this type was operated with an amplitude stabilized amplifier. A feedback loop maintained the crystal oscillation amplitude at a constant level to prevent rupture, and the variable feedback bias was used as output of the circuit. Useful operation was obtained over the pressure range of 0.1 to 1000 torr with oscillation frequencies of the order of 50 to 200 kHz. Gas composition affects the calibration of the circuit, and thus, has to be known.

### 5.4.2 SEMICONDUCTORS

It has been found that if the junction of a tunnel diode or the emitter-base junction of a planar type transistor is exposed to varying gas pressure, its current-potential characteristics are altered as a function of the applied pressure. The tunnel diode is operated in the amplifier or oscillator mode. Its application to the measurement of planetary atmospheric pressures seems remote at this point since most of the laboratory evaluations have been made at pressures significantly above terrestrial sea level pressures.

The piezo-transistor appears to be a rather recent development, where the emitter-base junction of a silicon planar transistor is mechanically coupled to a small diaphragm. Sensitivities of the order of 10 volts/gr force, or about 1 volt/inch $H_2O$ differential pressure, and a high degree of linearity (1%) appear to be characteristics of this device.

Its compactness and compatibility with electronic circuit elements could make this pressure sensing transistor a valuable tool for the remote measurement of pressures. Other specifications for this device (Stow Labs. Pitran) are: temperature coeff. -0.5%/°C, hysteresis 1%, mechanical resonance frequency: 100 kHz, temperature range: -40 to + 60°C.

## 5.5 LIQUID BAROMETERS

An atmosphere, by virtue of its weight, exerts a pressure on a surface imersed within it. This atmospheric pressure is equal to the weight of a vertical column of the atmosphere, of unit area, and extending to the outer limit of the atmosphere. The most generally used method of measuring the pressure of the atmosphere involves balancing it against the weight of a column of liquid. The measurement is expressed as the height of the column of the particular liquid, such as inches of water.

### 5.5.1 NARRATIVE DESCRIPTION OF THE INSTRUMENT

The atmospheric pressure may be determined using any fluid in a liquid barometer provided the height of the column, the density of the fluid, and the value of the acceleration due to gravity is known. The most common type of liquid barometer is the mercury barometer. In this instrument, the pressure of the atmosphere is equated against a column of mercury, the height of this column being accurately measured. This instrument for use in an atmosphere similar to Earth's must, of necessity, be bulky, heavy, and rather delicate. The instrument consists of some form of U-tube with one limb hermetically sealed. The other limb is open to the atmosphere, and often takes the form of a cistern. The tube is filled with mercury and positioned in the vertical plane with the closed end of the tube becoming the uppermost point of the instrument. The mercury will stand in the closed tube at a certain distance above the level in the open tube or cistern. This height may be determined by various means and when reduced to standard conditions is often adopted as a measurement of the atmospheric pressure.

There are various means of attaching transducers to the mercury barometer for remote or automatic reading of the instrument. The instrument discussed here is manufactured by Exactel Instrument Company of Mountain View, California. The height of the column of mercury is determined by a servo-mechanism which is designed to seek a float that is placed in the tube on top of the column of mercury. A position transducer is attached to the servo-drive and indicates the height of the mercury column electrically.

### 5.5.2 INTERPRETATION OF THE MEASUREMENT

Additional information needed to interpret the measurement - The temperature of the mercury must be known precisely. The gravitational acceleration of the planet must also be known.

Method of analysis and interpretation of data - The output of the instrument is a binary representation of the height of the mercury column which is a direct measurement of atmospheric pressure.

### 5.5.3 INSTRUMENT CHARACTERISTICS

Total and dynamic range - For the Earth's atmosphere, a 32-inch mercury range is used; however, special instruments have been supplied with ranges up to 240 inches of mercury.

Accuracy - 0.002-inch mercury.

Signal to noise - Unknown.

Frequency response - Under 10 seconds.

Environmental effects - Subject to temperature and gravity changes.

### 5.5.4 INSTRUMENT OUTPUT

Output signal - Output options include both analog and digital position encoders. Digital encoders provide a direct representation of the atmospheric pressure in inches of mercury.

Bits per observation - Dependent upon encoder selected.

### 5.5.5 PAYLOAD INTEGRATION

Weight - Approximately 100 lbs.

Volume - Approximately 6 cubic feet.

Power - Unknown.

Radio frequency interference - None.

Magnetic moment - Unknown.

Erection, orientation or booms - Must be erected in a vertical position.

Compatibility with sterilization at 145°C - Unknown.

Special requirements - The instrument is extremely delicate. Extreme care must be used when installing instrument. For these reasons and because of its physical size and weight, it is assumed that this instrument could not be used for space exploration.

### 5.5.6 STATE OF DEVELOPMENT

The instrument is fully developed for use on Earth. For other or special users, the techniques are fully developed; however, the actual hardware is custom manufactured.

## REFERENCES - LIQUID BAROMETERS

Exactel Instrument Company, Exactel Servobarometer PMS500, Mountain View, California.

Middelton, W.E., and A.F. Spilhaus, 1958: Meteorological Instruments. University of Toronto Press.

## 5.6 KNUDSEN RADIOMETER GAUGE

This gauge is used for the measurement of very low pressures and is independent of gas composition (Leck, 1957). The radiometer force is pressure dependent from 0 to 10 mm Hg and is linearly dependent at the lower end of the range. Consider two parallel plates $A_1$ and $A_2$ at temperature $T_1$ and $T_2$, respectively, the separation (d cm) being small when compared with their linear dimensions and to the molecular mean free path. The assumption is made that the molecules travelling towards $A_2$ from $A_1$ have a mean velocity $C_1$ cm/s dependent on the temperature $T_1$, and a velocity $C_2$ cm/s exists for molecules travelling from $A_2$ to $A_1$ dependent on $T_2$. $G_1$ and $G_2$ represent the corresponding rms velocities. At any instant there are $N_1$ and $N_2$ molecules/cm$^3$ with the mean velocities $C_1$ and $C_2$ respectively. In the gas surrounding the plates the molecular mean velocity, molecular rms velocity, and molecular density are given by C, G, and N respectively.

The effective pressure $p_1$ (dyn/cm$^2$) in the space between $A_1$ and $A_2$ is given by

$$p_1 = 1/3\ m\ N_1 G_1^{\,2} + 1/3\ m\ N_2 G_2^{\,2} \qquad (1)$$

where m is the mass.

Since, in equilibrium, the rate of entry is equal to the rate of departure from the interspace

$$1/4\ NC = 1/4\ N_1 C_1 + 1/4\ N_2 C_2 \qquad (2)$$

and

$$N_1 C_1 = N_2 C_2 \ . \qquad (3)$$

Substituting (2) and (3) into (1) gives

$$p_1 = 1/3\ m \left[ 1/2\ N\ G_1^{\,2} C/C_1 + 1/2\ N\ G_2^{\,2} C/C_2 \right] \ .$$

The pressure at any point in the gas is given by

$$P = 1/3\ m\ N\ G^2 \ .$$

Assuming a Maxmellian velocity distribution where

$$G/C = G_1/C_1 = G_2/C_2$$

the expression for $p_1$ can become

$$p_1 = 1/2\ p\left(\frac{G_1 + G_2}{G}\right) . \qquad (4)$$

$G_1$ and $G_2$ depend on the temperatures of the two plates $T_1$ and $T_2$. If $\alpha$ represents the accommodation-coefficient of the inside surfaces of $A_1$ and $A_2$, then

$$G_2 - G_1 = \alpha(G_2' - G_1)$$

$$G_1 - G_2 = \alpha(G_1' - G_2)$$

so that after algebraic manipulation (4) can be written as

$$p_1 = 1/2\ p\left(\frac{G_1' + G_2'}{G'}\right) .$$

The radiation pressure trying to force the plates apart is given by

$$P = p_1 - p = P\left(\frac{1}{2}\ \frac{G_1' + G_2'}{G'} - 1\right) .$$

Since $G_1'/G' = \sqrt{T_1/T}$ and $G_2'/G' = \sqrt{T_2/T}$

$$P = 1/2\ p\left(\sqrt{T_1/T} + \sqrt{T_2/T} - 2\right) .$$

Particular cases of $T_2 = T$ and the temperature of $A_2$ equal to $T_1$ on the inside and T on the outside gives

$$P = p\left(\sqrt{T_1/T} - 1\right) .$$

The above development shows that for a constant temperature distribution and for the same accommodation coefficient at both plates the resultant radiation pressure depends only on the gas pressure outside the region between the plates. For three plates the expression for P is given by

$$P = 1/2\ p\left(\sqrt{T_1/T} - \sqrt{T_3/T}\right) \qquad (5)$$

Thus, the force on the central plate is independent of its temperature. The density can easily be calculated from the equation of state (with knowledge of gas composition).

The assumption of infinitely large surface areas and exactly equal accommodation coefficients cannot be realized in practice. Fredlund (1937) considered a circular vane $A_2$ of radius r between two larger plates $A_1$ and $A_3$ and a distance d from each. The final expression for P is modified from (5) as follows:

$$P = 1/2\ p\left(\sqrt{T_1/T} - \sqrt{T_3/T}\right)\frac{\alpha_1(2 - \alpha_2)}{\alpha_1 + \alpha_2 - \alpha_1\alpha_2} .$$

## 5.6.1 FREDLUND GAUGE

### 5.6.1.1 NARRATIVE DESCRIPTION OF THE INSTRUMENT

There are many different variations of the Knudsen gauge. The Fredlund gauge is described here due to the relatively wide range of pressures and densities that can be measured with a linear relation between p and P. The gauge consits of a moving vane between two large metal blocks. The thermal deflecting force is balanced electromagnetically; the electrical force required to keep the vane in its central position is used to measure the deflecting force. Water, supplied from two thermostats, was used to maintain the necessary temperature difference between the metal blocks.

### 5.6.1.2 INTERPRETATION OF MEASUREMENT

Additional information needed to interpret the measurement - None.

Method for analysis and interpretation of data - A current is passed through the coils of each of the magnets. This current is proportional to the force on the foil of the moving vane and leads to the calculated pressure.

### 5.6.1.3 INSTRUMENT CHARACTERISTICS

Total and dynamic ranges - With a d of 0.85 mm, the linear operating range (where the mean free path of the molecules must not exceed d) of this gauge is between ~0 and $3.2 \times 10^{-3}$ mm Hg. Pressures as high as ~ 6 mm Hg can be measured less precisely in the nonlinear operating region where the deflecting force is a complicated function of gas density.

Accuracy - Accurate determination of the accommodation coefficients and the reduction of "edge effects" from the practical limitation that the surface cannot be infinitely large are necessary for accurate measurements. The "edge effects" error source can be limited by proper design of the gauge.

Signal to noise - Unknown.

Frequency response - The general expression governing the deflection $\theta$ of the freely swinging vane is given by

$$J \frac{d^2\theta}{dt^2} + \beta \frac{d\theta}{dt} + S\theta = G$$

where J is the moment of inertia, $\beta$ is the frictional damping coefficient, S the stiffness of the suspension (i.e., the restoring torque per unit deflection) of the moving vane and G the deflecting torque. This expression represents a damped oscillatory motion with a natural period,

$$T = 2\pi \sqrt{J/S} \text{ second.}$$

The response time of these gauges is about the time of the period and is a few seconds.

Environmental effects - The calibration of the instrument is quite delicate. Thus, the instrument should be protected from any anticipated severe jolts.

5.6.1.4 INSTRUMENT OUTPUT

Output signal - The calibrated output would be analog. For pressures less than $3.2 \times 10^{-3}$ mm Hg, the relationship between the observed radiation pressure and surrounding gas pressure is linear. At higher pressures the radiation pressure-gas pressure relation is more complex.

5.6.1.5 PAYLOAD INTEGRATION

Weight - Probably less than 4 kg.

Volume - The instrument is about 20 cm x 10 cm x 5 cm in size.

Power - No power is needed to operate the instrument. Small current is generated by the instrument itself.

Radio frequency interference - None.

Magnetic moment - The instrument contains two magnetic coils.

Erection, orientation, or booms - None.

Compatibility with sterilization at 145°C - Cannot be determined.

Special requirements - None.

### 5.6.1.6 STATE OF DEVELOPMENT

This is an old instrument developed for measurements of pressure under near vacuum conditions in the laboratory. Considerable development would be needed for planetary pressure measurements. However, the capability of the instrument to measure extremely low pressures independent of gas composition makes it attractive where such environmental conditions are anticipated.

## REFERENCES - KNUDSEN RADIOMETER GAUGE


Fredlund, E., 1937: Ann. Phys., 30, p. 99.

Leck, J.H., 1957: Pressure Measurement in Vacuum System, The Institute of Physics, London.

## 6. TEMPERATURE

Average temperatures near the surface of Mars can be expected to vary from a high of about 250°K at high latitudes in summer to a low of about 145°K at high latitudes in winter (House, et al., 1967). Superimposed on these temperatures, except at high latitudes, is a diurnal variation of about 100°K. Temperatures can be expected to decrease with altitude at a rate of about 5°C/km to stratospheric values between 60 percent and 90 percent of the average surface values, depending upon season and latitude.

Average temperatures near the surface of Venus are about 600°K, according to the Earth-based and Mariner II passive microwave observations and the recent direct observations of the Russian Venus IV spacecraft. Surface temperatures can be expected to vary as follows (Pollack and Sagan, 1965): subsolar point, 1000°K; antisolar point, $\leq$ 660°K; poles, 470°K. Uncertainties in these estimates may be 100°K or more. The temperature lapse rate is about 10°C/km in the first 25 km, according to the observations of the Venus IV spacecraft. This lapse rate probably persists up to the Venusian stratosphere, which probably has a temperature of about 200°K.

## 6.1 RESISTANCE THERMOMETERS

These thermometers employ the variation, with temperature, of the electrical resistance of metals and metal oxides. The higher the temperature coefficient of resistance, the better the material is for thermometric purposes.

Resistance thermometers are made from platinum, copper, nickel, balco, tungsten and semi conductors. Platinum is usually the preferred metal when performance and cost both must be considered; semiconductor materials exhibit an inverse temperature-resistance relation, and sensors of this material, commonly called thermistors, may also be used for measurement in a manner similar to metalic sensors. The resistance of these sensors becomes the analog of the sensor's temperature. Measuring the temperature of an environment can be accomplished by allowing the sensor to come to thermal equilibrium with the environment and measuring the sensor's resistance.

For precision resistance measurements in thermometry, some form of potentiometer circuit is generally used. The Wheatstone bridge circuit is the most common and is accurate enough for meteorological purposes. There are many variations in the design and specifications for individual measuring and indicating circuits available to the user depending upon his requirements.

Resistance thermometers fall into several classes:

(1) Resistance bulbs
(2) Thin wires
(3) Thermo ribbons
(4) Thermistors
(5) Thin film
(6) Junction diodes

## 6.1.1 RESISTANCE BULBS

### 6.1.1.1 NARRATIVE DESCRIPTION OF THE INSTRUMENT

Resistance bulb thermometers generally employ platinum, copper, or nickel elements. The element is wound on a bobbin which is then installed in a housing. The actual physical and electrical properties are dependent upon the application for which the sensor is designed. Resistance bulb thermometers are the most commonly used type of resistance thermometers where accuracy and rugged construction are desired.

### 6.1.1.2 INTERPRETATION OF THE MEASUREMENT

Additional information needed to interpret the measurement - None.

Method for analysis and interpretation of data - The resistance of the thermometer is generally determined by placing the resistance bulb into one leg of a Wheatstone birdge or an ac bridge circuit. The output signal of the bridge circuit is directly related to the resistance of the thermometer.

### 6.1.1.3 INSTRUMENT CHARACTERISTICS

Total and dynamic range -

| | | |
|---|---|---|
| Total range: | Platinum | -260°C to +500°C |
| | Copper | -140°C to +120°C |
| | Nickel | -184°C to +316°C. |

The dynamic range is dependent upon the specifications and type of bridge or measuring circuit used. A dynamic range of 100°C is common for resistance bulb thermometer systems.

Accuracy - Platinum types are generally the most accurate sensors. However, errors can be introduced by the measuring circuit. Platinum sensors are accurate to 0.25°C.

Signal to noise - Dependent upon electronics.

Frequency response - The frequency response is dependent upon the physical size and shape of the sensor. Sensors are available with time constants of from approximately one second to several minutes.

Environmental effects - The sensor must be shielded from radiation to insure proper measurement of the ambient temperature.

### 6.1.1.4 INSTRUMENT OUTPUT

Output signal - The sensor output consists of a resistance change. This is measured by a bridge circuit which is most cases produces a

dc voltage analog to the resistance of the sensor. This voltage is a linear representation of the temperature.

Bits per observation - 8 or 9 bits per observation.

6.1.1.5 PAYLOAD INTEGRATION

Weight - Sensor 1 oz to several pounds,
Bridge approximately one pound.

Volume - Sensor approximately 1 to 10 inches$^3$.
Bridge approximately 20 inches$^3$.

Power - Approximately two watts.

Radio frequency interference - None.

Magnetic moment - Unknown.

Erection, orientation, or booms - Sensor must be shielded from radiation.

Compatibility with sterilization at 145°C - Yes.

Special requirements - Sensor should be aspirated.

6.1.1.6 STATE OF DEVELOPMENT

Resistance bulb thermometer systems are available as off-the-shelf items from commercial manufacturers and are in routine use in temperature measuring systems.

### 6.1.2 THERMO RIBBONS

Thermo ribbons provide a fast response conversion of surface temperatures to accurate electrical signals. They are available for direct application to any surface. The unit employs a nickel iron element which provides a relatively high impedance thermometer. Thermo ribbons have the same features as resistance bulbs with the exception of frequency response and space requirements. The response time of these sensors, when used to determine environmental temperatures, is a function of the time required for the surface on which they are mounted to reach thermal equilibrium. It is very important that, for measurements of environmental temperature, the sensor not be mounted on a surface whose temperature is determined by factors other than the ambient temperature of the atmosphere.

### 6.1.3 THIN-WIRE RESISTANCE THERMOMETERS

Thin wire resistance thermometers employ the same principles and most of the features of the resistance bulb thermometer. The main differences are in their physical design and response characteristics. The thin wire thermometers are used primarily as laboratory instruments. They are constructed of thin platinum wires, 0.001-inch diameter, mounted in an open frame and are extremely fragile as compared to the resistance bulb thermometer. The response time of thin wire thermometers is well under one second. Contamination of the actual resistance element with dust and other materials presents some problems in accuracy when used in an environment outside the laboratory. With the exception of response times and the need for protection, the thin-wire resistance thermometer performance and use are identical with the resistance bulb thermometer.

### 6.1.4 THERMISTORS

The thermistor is one member of the family of electrical thermometers. It operates on the simple principle that the electrical resistance of the material varies inversely with temperature. The equation for the change in resistance with temperature is somewhat different for each type of thermistor and depends on the characteristics of the material used for the sensor. Its sensitivity is of the order of -4 percent per °C.

There are two types of thermistors currently in use in the Earth's atmosphere. The rod thermistor is the standard temperature measuring device for radiosonde flights which take place below 30 km. Its time constant is rather slow when compared to the bead thermistor that is used for temperature measurements in the stratosphere. Many of the characteristics of the two thermistor types are similar. Since the bead thermistor has more potential for use in thin atmospheres, such as Mars', it will be described in full below.

#### 6.1.4.1 NARRATIVE DESCRIPTION OF THE INSTRUMENT

There are many materials that can be used as the sensing element. Also, the thermistor has been made in different sizes. The thermistor element described below is part of a rocketsonde and the description refers to the complete package. The instrument descends by parachute from an altitude of about 80 km. The thermistor is exposed to the incident air flow as the instrumented package descends. The parachute has a fall rate of about 100 m/s at 60 km. The fall rate drops to about 20 m/s in the lower stratosphere. A typical flight recording is time versus pulse frequency in a manner similar to that used for radiosonde flights. The pulse frequency is a function of resistance which is linearly related to temperature.

The variation of thermistor temperature T with height can be expressed as follows:

$$\frac{dT}{dz} = \frac{\sigma A}{cV} T^4 - \left( \frac{1}{\gamma V} + \frac{2\ K\beta}{xcV} \right) T + \frac{1}{V\gamma} \left( T_e + \frac{rV^2}{2c_p} + \frac{W}{S} \right) + \frac{JAa}{4\ cV}$$

$$+ \frac{\sigma A}{cV} \left( 0.5 T_{be}^{\ 4} + 0.06 T_{ai}^{\ 4} \right) + 0.44 T_{ae}^{\ 4} + \frac{2\ K\ \beta T_s}{xcV}$$

where $T_e$ = temperature of environment (K),
$T$ = temperature of bead (K),
$A$ = surface area of sensor ($cm^2$),
$J$ = solar radiation flux (cal $cm^{-2}$ $s^{-1}$),

$\sigma$ = Stefan-Boltzmann constant,
$T_{be}$ = effective blackbody temperature of environment below (K),
$T_{ae}$ = effective blackbody temperature of environment above (K),
$T_{ai}$ = effective blackbody temperature of instrument above (K),
W = current through sensor ($\mu$W),
S = power dissipation of sensor ($\mu W\ K^{-1}$),
r = thermal recovery factor,
V = fall velocity (km $s^{-1}$),
$T_s$ = temperature of support (K),
K = thermal conductivity of lead wires (cal $cm^{-1}\ s^{-1}\ K^{-1}$),
$\beta$ = cross-sectional area of wire ($cm^2$),
c = heat capacity of bead (cal $K^{-1}$),
x = length of lead wires (cm),
z = altitude (km),
$\gamma$ = time constant of sensor,
$c_p$ = specific heat capacity at constant pressure for air ($km^2 s^{-2} K^{-1}$).

The expression shows that the temperature variation is principally influenced by the air temperature, radiation effects from the environment and the instrumentation, the fall velocity, and the configuration of the bead itself.

6.1.4.2 INTERPRETATION OF THE MEASUREMENT

Additional information needed to interpret the measurement - None.

Method for analysis and interpretation of data - A continuous record of pulse frequency is obtained. The pulse frequency is related to the resistance and the resistance is a linear function of temperature. Thus, temperature is related to the pulse frequency.

6.1.4.3 INSTRUMENT CHARACTERISTICS

Total and dynamic ranges - The pulse frequency varies between 10 and 200 c/s. This would correspond to a temperature range of approximately 60°C to -80°C.

Accuracy - A set of corrections has been prepared for the thermistor data. The corrections consider forced convection, infrared and solar radiation,compressional heating, lead wire conduction, and internal heating effects. These corrections vary with altitude with the corrections increasing with altitude. After the corrections are applied, temperature measurements are accurate within ± 2 percent below 60 km and ±3.8 percent at 65 km.

Signal to noise - High.

Frequency response - The radio frequency range of the monitored signal is between 1660 to 1700 mc and the data pulse frequency varies between 10 and 200 p/s. Variation of the time constant with altitude has been found to be from 1 s at 40 km to 100 s at 80 km.

Environmental effects - This is a reasonably rugged instrument that has withstood the shock of rocket launching. Radiation effects have been estimated and the necessary corrections applied to the measurements.

6.1.4.4 INSTRUMENT OUTPUT

Output signal - The calibrated output can be either digital or analog and the relationship between the pulse frequency and resistance is nonlinear and has to be determined empirically.

Bits per observation - A total of 8 bits per observation is required.

6.1.4.5 PAYLOAD INTEGRATION

Weight - Less than 3 lbs for the entire package that contains the bead and related equipment.

Volume - Less than 1/2 cubic foot.

Power - Less than 10 W (transmitter).

Radio frequency interference - In Earth atmosphere applications, there is interference from radiosonde data retrieval which also occurs in the 1680 mc band.

Magnetic moment - Not applicable.

Erection, orientation, or booms - No important requirements.

Compatibility with sterilization at 145°C - The instrument is compatible with sterilization.

Special requirements - The bead should be shielded from direct solar radiation.

6.1.4.6 STATE OF DEVELOPMENT

The bead thermistor is the standard instrument for stratospheric measurement. It has already been thoroughly flight tested.

## REFERENCES - THERMISTORS


Armstrong, I W., 1965: Improvement of accuracy of the ML-419 radiosonde temperature element for heights above 50,000 feet and up to 150,000 feet. Army Electronics Command, Tech. Rpt. ECOM-2634, 55pp.

Badgley, F. J., 1957: Response of radiosonde thermistors, Rev. Sci. Instr., 28(12), 1079-1084.

Ballard, H.N., 1966: The measurement of temperature in the stratosphere. AMS/AIAA Paper 66-385 presented at Conf. on Aerospace Met., Los Angeles, Mon. 28-31.

Blackburn, C.P., and D.B. George, 1964: Air launched rocketsounding study. Bendix Corp., Final Report, AF-19(628)-3264, 144pp.

Clark, G.Q., and J.G. McCoy, 1965: Measurement of stratospheric temperature. J. of Appl. Meteor., 4(3), 365-370.

Coppola, A.A., 1963: Radiosonde set AN/DM 9-6. USAEROL Tech. Rpt. 2354, Ft. Monmouth, New Jersey, 35pp.

Finger, F.G., R.G. Mason, and S. Teweles, 1964: Diurnal variation in stratospheric temperatures and heights reported by the U.S. Weather Bureau Outrigger Radiosonde. Mon. Wea. Rev., 92(5), 243-350.

Hodge, M.W., and C Harmantas, 1965: Compatibility of U.S. radiosondes. Mon. Wea. Rev., 93(4), 253-266.

McCoy, J.G., and C.L. Tate, 1965: The Delta-T Meteorological Rocket Payload. Army Electronics Research and Devel. Activity, WSMR, Rpt. No. ERDA-319, 8p.

Shaw, J.H., 1959: Theoretical analysis of radiation errors of radiosonde temperature elements. Ohio State University Research Foundation, Tech. Rpt. No. 2, DA-36-039-SC-78153.

Thompson, D.C., and D.P. Keily, 1966: The accuracy of thermistors in the measurement of upper air temperature. AMS/AIAA Paper 66-386 presented at Conf. in Aerospace Met., Los Angeles, Mon. 28-31, 17pp.

Wagner, N.K., 1964: Theoretical accuracy of a meteorological rocketsonde thermistor. J. of Appl. Meteor., 3(4), 461-469.

### 6.1.5 THIN FILM SENSORS

The development of the thin film sensor evolved from problems encountered with the bead thermistor at altitudes above 55 km. These problems were caused by the small size of the bead in an atmosphere where the molecular mean free path is long with respect to the size of the sensor. Convective coupling with the air is not efficient and slower response times result.

Thin film sensors have been found superior to bead thermistors for the measurement of rarefied air because of their inherently enhanced convective coupling.

#### 6.1.5.1 NARRATIVE DESCRIPTION OF THE INSTRUMENT

There are two different types of thin film sensors currently in use. The first is simply a bead thermistor imbedded in a 1/2-inch mylar sheet with a 400 Å coating of aluminum (McKennedy, 1967). This arrangement has the effect of giving the bead a larger surface area. Thus the molecular mean free path is no longer large compared to the size of the sensor.

The second sensor is a germanium thin film with a 1-inch thickness mica (muscovite) substrate. The surface area of the sensor is 1/4 in. by 1/4 in. while the area of the substrate is 1/2 in. by 1 in.

Both types of sensors are part of a radionsonde package ejected from a rocket in the neighborhood of 75 to 85 km and use the same type of telemetry system. This instrument descends by parachute sending pulse signals back to be monitored. The calibrated pulse signals are then interpreted in terms of temperature.

#### 6.1.5.2 INTERPRETATION OF THE MEASUREMENT

Additional information needed to interpret the measurement - None.

Method for analysis and interpretation of data - The pulse output is in cycles per second. This output is related to the resistance of the instrument system logarithmically. The resistance is, in turn, related to temperature.

#### 6.1.5.3 INSTRUMENT CHARACTERISTICS

Total and dynamic ranges - The range of the instrument is from 0 to 200 c/s which corresponds to a temperature range between 30°C and -55°C. Resistance varies between 10 K and 10 M ohms for the beaded sensor and 100 K and 10 M ohms for the germanium sensor.

Accuracy - The same factors that affect the bead thermistor measurements also contribute to errors in these measurements. For the thermistor mounted in the film, the estimated (not scientifically determined) errors are ±2°C and ±1°C below 45 km. No accurate error estimate can be made for the germanium sensor.

Signal to noise - High.

Frequency response - The time constant of the bead sensor is less than 2 s at 65 km. No time constant has not yet been determined for the germanium sensor although theory indicates a time constant similar to the bead sensor.

Environmental effects - Both types of sensors are rugged and should be able to withstand considerable shock. The necessary corrections have been estimated for radiation effects.

6.1.5.4 INSTRUMENT OUTPUT

Output signal - The calibrated output is in pulse form (c/s). Resistance is related logarithmically the pulse output and temperature is related to the resistance.

Bits per observation - Eight bits per observation are required.

6.1.5.5 PAYLOAD INTEGRATION

Weight - Less than 5 lbs.

Volume - The instrument package is $3\frac{1}{2}$ inches in diameter and 10-inches high.

Power - The radiosonde input power approx. 3 W.

Radio frequency interference - On the present data recovery frequency of 1680 Mc, there is interference from radiosonde data recovery operating in the same frequency.

Magnetic moment - Not known.

Erection, orientation, or booms - No unusual orientation of the instrument must be made.

Compatibility with sterilization at 145°C - Unknown.

Special requirements - No special requirements are anticipated.

### 6.1.5.6 STATE OF DEVELOPMENT

The bead in mylar sensor is considered operational while more testing is required before the germanium sensor acquires the the same status.

## REFERENCES - THIN FILM SENSORS


Bogdan, L., 1964: High Temperature, Thin Film Resistance Thermometers for Heat Transfer Measurement. Cornell Aeronautical Lab., Inc., NAS 8-823, 24pp.

_____, 1964: Measurement of Radiative Heat Transfer with Thin-Film Resistance Thermometers. Cornell Aeronautical Lab., Inc., NAS 8-823, 39pp.

Hayo, F.J., S.A. Weld, and P.G. Simeth, 1966: Loki-Dart Transponder Rocketsonde, Advanced Temperature Sensors and Thermoconductivity High-Altitude Pressure Gauges. Paper presented at the 6th Nat. Conference on Appl. Met., AMS/AIAA, March 1966.

McKennedy, B., 1967: Personal Communication. White Sands Missle Range, (November).

Staffanson, F.L., 1965: Study of Thin-Film Sensors for High Altitude Temperature. Upper Air Res. Lab., Univ. of Utah, Final Report, N60921-7156, 77pp.

### 6.1.6 JUNCTION DIODES

The following relations for a junction diode come from elementary semiconductor theory:

$$i = i_s[\exp(ev/KT) - 1]$$

$$i_s = AT^n \exp(-aE_g/KT)$$

where v and i are the diode junction voltage and current, $i_s$ is the reverse saturation current, e is the electronic charge, K is the Boltzmann's constant, T is the temperature in °K, $E_g$ is the gap energy expressed in volts, A is a constant for a given diode, and n = 3 for simple diffusion theory.

The temperature sensitivity of a P-N junction volt-ampere characteristic is due principally to the variation of reverse saturation current. The temperature sensitivity depends dominantly on the energy gap of the material. A linear junction voltage versus temperature relation is produced from basically exponential dependencies of reverse current on temperature and of forward current on junction voltage.

#### 6.1.6.1 NARRATIVE DESCRIPTION OF THE INSTRUMENT

This instrument operates from a fairly simple electric circuit. The circuit consists of a series resistance, a source, and two diodes in a bridge. This instrument's basic circuit can be represented by the following expression

$$\frac{dv}{dT} = -\alpha^* \left[1+v^*/(E-v)\right]^{-1}$$

where $-\alpha^* = (\partial v/\partial T)i$ and $v^* = (\partial v/\partial \ln i)_T$. The term in brackets can be made essentially independent of T by making $E \gg v$ thus

$$\frac{dv}{dT} = -\alpha^*[1+v^*/E]^{-1} .$$

#### 6.1.6.2 INTERPRETATION OF THE MEASUREMENT

Additional information needed to interpret the measurement - None.

Method for analysis and interpretation of data - The output of this instrument is linear junction voltage, which is related to the temperature. This voltage can be directly metered from the circuit.

### 6.1.6.3 INSTRUMENT CHARACTERISITICS

Total and dynamic ranges - The absolute value of the junction voltage of the temperature compensation diode is typically 130 mV at 1 mA and 20°C, varying about 60 mV per current decade. The nearly linear voltage-temperature characteristic is $(\partial v/\partial T) = -2.3$ mV/C°. Temperature below 60°C can be measured.

Accuracy - The chief factor affecting the accuracy of the circuit is the uniformity of the diodes. A spread of 20 mV was observed in a sample of 20 diodes and the slope (sensitivities) were within a few percent. Usually, a pair of diodes selected that had junction voltages within a few mV had slopes within two percent.

Signal to noise - Information not available.

Frequency response - The time constant is about 80 seconds in still air, based on response to a temperature step of 10°C.

Environmental effects - This should be a reasonably rugged instrument and should not be affected by the environment.

### 6.1.6.4 INSTRUMENT OUTPUT

Output signal - The voltage-temperature relationship is nearly linear. Most likely, the calibrated instrument output would be in analog form. However, it could be digitized.

Bits per observation - The number of mV for a complete range of observations will most likely be between 1 and 1000. Therefore, 10 bits per observation are needed.

### 6.1.6.5 PAYLOAD INTEGRATION

Weight - Probably less the 10 lbs.

Volume - Probably less than 1/2 $ft^2$.

Power - Probably less the 10 W.

Radio frequency interference - None expected.

Magnetic moment - Not known.

Erection, orientation, or booms - None.

Compatibility with sterilization at 145°C - Unknown.

Special requirements - None.

### 6.1.6.6 STATE OF DEVELOPMENT

This instrument has been thoroughly tested and should be ready for immediate use.

## REFERENCES - JUNCTION DIODES


Barton, L.E., 1962: Measuring temperature with diodes and transistors. Electronics, 35, 38-40.

Dimrick, R.C., and G.J Trezek, 1963: Photodiode as a sensitive temperature probe. Rev. Sci. Instru., 34, 981-983.

McNamara, A.G., 1962: Semiconductor diodes and transistors and electrical thermometers. Rev. Sci. Instru., 33, 330-333.

Sargeant, D H., 1965: Note on the use of junction diodes as temperature sensors. J. of Appl. Meteor.,4,(5), 644-646.

## 6.2 THERMOCOUPLES

Thermocouples are devices used for the measurement of temperature differences. Their operation is based on the Seebeck effect, a phenomenon whereby an electric current will flow in a circuit formed by two dissimilar metallic conductors, joined at two points, when the temperature at these junctions is different. The magnitude of this current is a function of the temperature difference, for a given pair of metals. If the circuit is left open a thermoelectric potential is developed across the open leads which again is a function of the temperature difference between the two junctions. The polarity of this potential depends on which junction has the higher temperature. The thermoelectric potential E follows approximately the parabolic equation of the form: $E = a + bt + ct^2 + \ldots$ + where t is the temperature difference between the two junctions and a, b, c are constants characteristics of each metal pair. For absolute temperature measurements, one junction, called the reference junction, has to be at a known temperature, while the measuring junction will be exposed to the unknown environment. In general thermocouples are preferred for difference measurements unless a reliable and well controlled reference temperature can be established, or if the unknown temperature is much lower or much higher than the reference, in which case errors of temperature of the latter junction have a reduced effect on the measurement. For planetary surface measurements, thermocouples may be useful in the determination of vertical profiles which require the accurate measurement of small temperature differences. However, if a reliably controlled reference temperature can be maintained, thermocouples can be used for fast and accurate ambient temperature determinations.

### 6.2.1 THERMOCOUPLE GAUGES

#### 6.2.1.1 NARRATIVE DESCRIPTION OF THE INSTRUMENT

A large variety of thermocouple gauges has been developed and used in many different applications. Their main differences reside in the choice of metal pairs for the junctions, which is often based on the characteristics of the environment to be evaluated (stability at high temperatures, resistance to corrosion, etc.).

Typical thermocouple pairs are: iron/constantan, copper/constantan, platinum/platinum-rhodium, chromel/alumel, carbon/silicon carbide, etc. Typical thermoelectric potentials for a 100°C difference (reference junction at 0°C) are between 0.6 and 6 millivolts, for the above combinations of metals. Most of them can be used to temperatures above 1000°C and down to -200°C, thus covering the ranges of planetary interest.

In general, for absolute temperature measurements a thermocouple thermometer for remote planetary applications would consists of a measuring junction, exposed to the ambient air, with appropriate radiation shielding, a reference junction maintained at constant temperature or with automatic temperature compensation, a stable d-c amplifier

with a voltage gain of the order of $10^4$ to provide an output compatible with telemetry. The constant temperature environment for the reference junction may already be part of other associated equipment which may require a tight temperature control, and thus no separate provisions of this type may be needed.

6.2.1.2 INTERPRETATION OF MEASUREMENT

Additional information needed to interpret measurement - None

Method of analysis and interpretation of data - The amplified thermoelectric potential is directly related to temperature through known calibration curves established for the particular junction metals.

6.2.1.3 INSTRUMENT CHARACTERISTICS

Total and dynamic range - Dependent on reference junction temperature and on the choice of junction metals. In general any interval between about 10 and 1500°K.

Accuracy - With careful calibration and tight reference control accuracies, better than 0.1°C can be achieved. (For industrial applications the usual accuracy is of the order of 3°C).

Signal to noise - The signal to noise, in this case, depends on the thermoelectric potential generated, and on the inherent noise characteristics of the d-c amplifier.

Frequency response - Time constants as low as 1 second are feasible.

Environmental effects - Proper choice of metals is required in corrosive atmospheres, for cryogenic temperatures, etc. Very high magnetic fields (several thousand gauss) may affect the accuracy of a thermocouple thermometer.

6.2.1.4 INSTRUMENT OUTPUT

Output signal - Analog, calibrated, approximately linear with temperature.

Bits per observation - Typically 10 for better than 1°C resolution.

6.2.1.5 PAYLOAD INTEGRATION

These parameters will be estimated on the basis of state of the art, and assuming that the temperature control for the

reference can be obtained elsewhere in the system; a complete flyable instrument is not readily available but could easily be developed with existing hardware.

Weight - 0.5 lbs (including amplifier and probe, excluding shield).

Volume - 10 $in^3$ (including amplifier and probe, excluding shield).

Power - Typically 0.2 watts (d-c amplifier).

Radio frequency interference - None

Magnetic moment - None

Erection, orientation, or booms - Non-critical, should be mounted to expose it to free ambient air.

Compatibility with sterilization at 145°C - Very high.

Special requirements - None

6.2.1.6 STATE OF DEVELOPMENT

Industrial and laboratory instruments; minor development required for planetary measurements and package integration.

## REFERENCES

Herzfeld, C. M., 1962: Editor, Temperature, its Measurement and Control in Science and Industry, Vol. 3, Reinhold Publishing Corporation, New York.
(This book contains a long list of relevant references)

McGraw-Hill Encyclopedia of Science and Technology, Vol. 13, pp 562-577.

## 6.3 DEFORMATION THERMOMETERS

The deformation thermometer is a thermometer using transducing elements that deform with temperature. The two most used instruments of this group are the bimetallic and Bourdon tube thermometers.

### 6.3.1 BIMETALLIC THERMOMETER

#### 6.3.1.1 NARRATIVE DESCRIPTION OF THE INSTRUMENT

Bimetal thermometers have as their sensing element a compound strip of metal (usually invar and brass or invar and steel) formed by welding. This strip of metal bends as the temperature changes, because of the difference in expansion of the two metals.

Let us take a welded strip of unit length where the thicknesses of the two metals are $h_1$ and $h_2$; Youngs moduli $E_1$ and $E_2$, respectively; and $\alpha_1$ and $\alpha_2$, their linear coefficients of expansion. Also, let $I_1$ and $I_2$ be the moments of inertia of the two cross-sections, which are given by

$$I_1 = h_1^3/12 \qquad \text{and} \qquad I_2 = h_2^3/12 \ .$$

At temperature $\theta_o$ the curvature of the strips is $1/\rho_o$ and at some higher temperature $\theta$ the curvature changes from $1/\rho_o$ to $1/\rho$. It is assumed that $1/\rho - 1/\rho_o$ is large compared to $h_1 + h_2$ and that curavture across the width of the strip can be neglected.

The forces acting on a segment of unit length are two axial tensions $P_1$, $P_2$ and two bending moments $M_1$, $M_2$. Since there are no external forces we have

$$P_1 + P_2 = 0 \ , \quad \text{or} \quad P_1 = P, \qquad P_2 = -P$$

and

$$M_1 + M_2 + \frac{1}{2} P(h_1 + h_2) = 0 \ .$$

From elementary elastic theory

$$M_1 = E_1 I_1 \left( \frac{1}{\rho} - \frac{1}{\rho_o} \right) \ , \qquad M_2 = E_2 I_2 \left( \frac{1}{\rho} - \frac{1}{\rho_o} \right)$$

so that

$$(E_1 I_1 + E_2 I_2) \left( \frac{1}{\rho} - \frac{1}{\rho_o} \right) = - \frac{P}{2} (h_1 + h_2) \ .$$

After some substitution and algebraic manipulation

$$\frac{1}{\rho} - \frac{1}{\rho_o} = \frac{(\alpha_2 - \alpha_1)\ (\theta - \theta_o)}{\frac{h_1 + h_2}{2} + \frac{2(E_1 I_1 + E_2 I_2)}{h_1 + h_2}\ \left(\frac{1}{E_1 h_1} + \frac{1}{E_2 h_2}\right)} .$$

This can be simplified by substituting

$$\delta = h_1 + h_2 , \quad m = h_1/h_2 , \quad n = E_1/E_2 , \quad I_1 = h_1^3/12 , \quad \text{and} \quad I_2 = h_2^3/12$$

such that

$$\frac{1}{\rho} - \frac{1}{\rho_o} = \frac{6(\alpha_2 - \alpha_1)(\theta - \theta_o)(1 + m)^2}{\delta[3\ (1 + m)^2 + (1 + mn)(m^2 + 1)/mn]}$$

and the above expression may be written

$$\frac{1}{\rho} - \frac{1}{\rho_o} = (A/\delta)\ (\alpha_2 - \alpha_1)(\theta - \theta_o) .$$

where A is a constant. This equation shows the dependence of the change in curvature on the thickness of the two metal strips, the difference in their coefficients of expansion (linear), and the temperature change.

Now let dS represent the distance the movable end of a bimetal strip (which is rigidly held at the other end) would move with a small change in temperature (from $\theta$ to $\theta + d\theta$). The final expression for the geometrical problem, with appropriate substitution from the above developments, is given by

$$dS = L^2\ \frac{B(\psi)}{\psi}\ \ \frac{A}{2\ \delta}\ (\alpha_2 - \alpha_1)d\theta$$

where L is a linear function of $\rho$ and $\phi$, a central angle for the strip at curvature $\rho$; $\psi$ is the angle between the chord connecting the two ends of the bent strip and a line tangent to the bimetal at the damped end at curvature $\rho$; and $B(\psi)$ is a complicated function of the above angle and $\psi_o$, an angle similar to $\psi$ only at curvature $\rho_o$. Movement is greatest for a straight bimetal and varies inversely as the total thickenss of the strip.

#### 6.3.1.2 INTERPRETATION OF THE MEASUREMENT

Additional information needed to interpret the measurement - None.

Method for analysis and interpretation of data - Most data from this instrument are continuously recorded on a calibrated graph with temperature indicated. The only variable remaining is temperature once the specifications of a particular instrument are indicated. Can be adapted for remote operation with electrical output.

#### 6.3.1.3 INSTRUMENT CHARACTERISTICS

Total and dynamic ranges - The range of the bimetal covers the entire range of meteorological temperatures (both surface and upper-air) and the instrument is used to measure higher temperature for industrial purposes.

Accuracy - The bimetal exhibits elastic hysteresis. The zero of the bimetal is inclined to drift, especially after a rapid change in temperature or when the strip has been newly bent or formed. After subjecting the bimetal to several cycles of temperature the hysteresis is less of a problem. The measurement errors are within tolerable limits for meteorological measurements, probably within $\pm$ 3°C.

Signal to noise - Unknown for remote application.

Frequency response - 21 sec.

Environmental effects - The bimetal and its immediate surroundings would be affected by absorption of direct solar radiation.

#### 6.3.1.4 INSTRUMENT OUTPUT, PAYLOAD INTEGRATION, AND STATE OF DEVELOPMENT

No practical instrument has been developed for remote operation. Such a device could be designed if necessary. However, for such purposes resistance thermometers have monopolized the field.

### 6.3.2 BOURDON THERMOMETER

The Bourdon thermometer consists of a curve tube of elliptical cross section, completely filled with some organic liquid. As the temperature changes the shape of the metal changes in response to differences in the cubical expansion coefficients of the liquid ($\gamma_e$) and the metal ($\gamma_m$). The theory of the Bourdon thermometer is quite similar to that of the bimetallic thermometer and the basic equation is as follows:

$$dS \sim LB(\psi)(\gamma_e - \gamma_m)d\theta \ .$$

The notation other than the cubical expansion coefficients is the same as that for the bimetal thermometer.

Excess internal pressure caused by high temperatures can lead to inaccuracies in determining high temperatures. Low temperatures present no difficulties. The time constant is greater than the bimetal thermometer. Also, the Bourdon thermometer is less rugged than the bimetal. No overall greater difference in accuracy or range (except at high temperatures) exists between the Bourdon and bimetallic thermometers.

## REFERENCES - DEFORMATION THERMOMETERS

Middleton, W.E.K., and A.F. Spilhaus, 1953: Meteorological Instruments. Univ. of Toronto Press, 286pp.

Timoshenko, S., 1925: Analysis of Bi-metal Thermostats. J. of Opt. So., of Amer. and Rev. of Sci. Instru., 11, 233-255.

## 6.4 ACOUSTICAL TECHNIQUES

Acoustical techniques are based upon the principle that for sound propagation in an ideal gas, the sound velocity, C, is related to the Kelvin temperature, T, by

$$C^2 = \frac{\gamma R T}{m}$$

where $\gamma$ is the specific heat ratio, R the universal gas constant, and m the molecular weight of the gas. The relationship provides a means of determining temperature through sound velocity measurements.

### 6.4.1 SONIC THERMOMETER

The system considered here for measuring the sound velocity consists of two transducers, spaced at a known distance, the circuitry for continuously measuring the delay time of an ultrasonic wave generated by one, and received by the other. The delay time is measured by a phase comparison of the received signal with a reference. The radian phase shift is related to temperature by

$$T = \frac{4\pi^2 \, md^2 \, f^2}{\gamma R \phi^2}$$

where T is the temperature of the gas, m is the molecular weight of the gas, d is the spacing distance, f is the frequency, R is the universal gas constand, $\gamma$ is the specific heat ratio of the gas, and $\phi$ is the radian phase shift.

The principles of the sonic thermometer are employed in the sonic anemometer and the same specifications are valid. The temperature determined by use of the sonic thermometer is available as an output in many sonic anemometers.

### 6.4.2 ROCKET GRENADE

In a thermally stratified medium such as the Earth's atmosphere a series of discrete sounds can be generated in the vertical at known height intervals. The difference between the arrival times at a ground-level detector of the sound pulses from the upper and lower explosions which define an atmospheric layer of known thickness can then be used to compute average sound speed and therefore average temperature for the layer provided, or course, that $\gamma/m$ (i.e., composition) is known. This is essentially how grenade explosions are used to determine temperature profiles in the Earth's atmosphere. For a detailed discussion of the instrumentation used in the measurement of temperature in the Earth's atmosphere by the grenade technique, refer to the write-up of the grenade technique under wind velocity.

## 6.5 RADIATION THERMOMETRY

A. Bolometers

B. Interferometer

C. Spectrometer

D. Optical Pyrometer

E. Pyranometer

These instruments and techniques are generally used for the measurement of surface temperatures, incident radiation from heated sources, hot gaseous effluents and rocket exhaust and plume temperatures. Except for the infrared bolometer, which will be described in detail, the application of the above listed instruments to planetary aeronomy is restricted to remote measurements from satellites and fly-by craft.

The measurement of atmospheric temperatures by means of infrared radiation is based on the measurement of emission of radiation by certain characteristic constituents of the air, selecting a narrow spectral region defined by a strong absorbtivity of the selected gas. For this application $CO_2$ has been found to be a convenient gas since it has strong absorption bands at 15$\mu$ and 4.3$\mu$. For terrestrial applications, the 15$\mu$ band is preferred since it contains a much larger fraction of the total energy radiated than that associated with the 4.3$\mu$ band; this would be more so in the case of the lower temperature Martian atmosphere. However, it appears that the shorter wave emission would be far superior for surface temperature measurements on Venus, on the basis of the latest information (550$^{o}$K approx. for Venus IV readings). Furthermore, $CO_2$ appears to be the main constituent of the atmosphere of both planets, thus essentially assuring the operation of this type of infrared temperature measurement on their surfaces. The depth of penetration into the atmosphere is a function of $CO_2$ concentration and atmospheric pressure, at terrestrial surface conditions this length is of the order of hundreds of feet. On the Martian surface this penetration would be of the same order of magnitude. On Venus this depth would probably be reduced to less than 100 feet.

### 6.5.1 INFRARED BOLOMETER

#### 6.5.1.1 NARRATIVE DESCRIPTION OF THE INSTRUMENT

The instrument consists of a radiometer head whose interior is maintained at a constant reference temperature. The field of view is a rectangle of 10° by 40°. The optical complement includes focusing and folding mirrors, spectral filter (15 $\mu$ band pass) and a gold plate rotating chopper which alternatively allows the target radiation to fall on the detector, or to block it, exposing the detector to the reference radiation level associated with the controlled cavity

temperature. The detector is a germanium-immersed thermistor bolometer. These optical elements, for the particular instrument developed by Barnes Engr., are shown in Figure 6-1. Its cavity reference temperature is held at 50°C ± 1°C. Phase demodulation of the square wave signal from the detector is obtained by a separate light-detector pickup synchronized with the radiation chopping frequency. The electronic circuitry includes amplification, synchronous rectification and filtering.

6.5.1.2 INTERPRETATION OF THE MEASUREMENT

Additional information needed to interpret measurement - Pressure and $CO_2$ density for the determination of penetration depth. If depth of penetration is to be varied, this can be accomplished by wavelength selection.

Method for analysis and interpretation of data - The output of the instrument is a function of the difference of temperature with respect to the internal reference temperature; it is thus necessary to transmit both pieces of information for proper evaluation.

6.5.1.3 INSTRUMENT CHARACTERISTICS

Total and dynamic ranges - The available instrument covers the range of -60°C to +30°C but this can be extended either way depending on the application.

Accuracy - Resolution is of the order of ±0.25°C. The overall accuracy depends on how closely the instrument can be maintained at its original calibration, and on the accuracy of the reference temperature measurement.

Signal to noise - Better than 52 dB at -60°C and 63 dB at + 20°C.

Frequency response - Typical time constant is 0.5 sec.

Environmental effects - None in particular.

6.5.1.4 INSTRUMENT OUTPUT

Output signal - Analog, calibrated, approximately linear.

Bits per observation - 7 for reference and 7 to 10 for air temperature (reference signal may be eliminated).

6.5.1.5 PAYLOAD INTEGRATION

No instrument has been developed for planetary remote operation. The subsequent information will be given for the existing

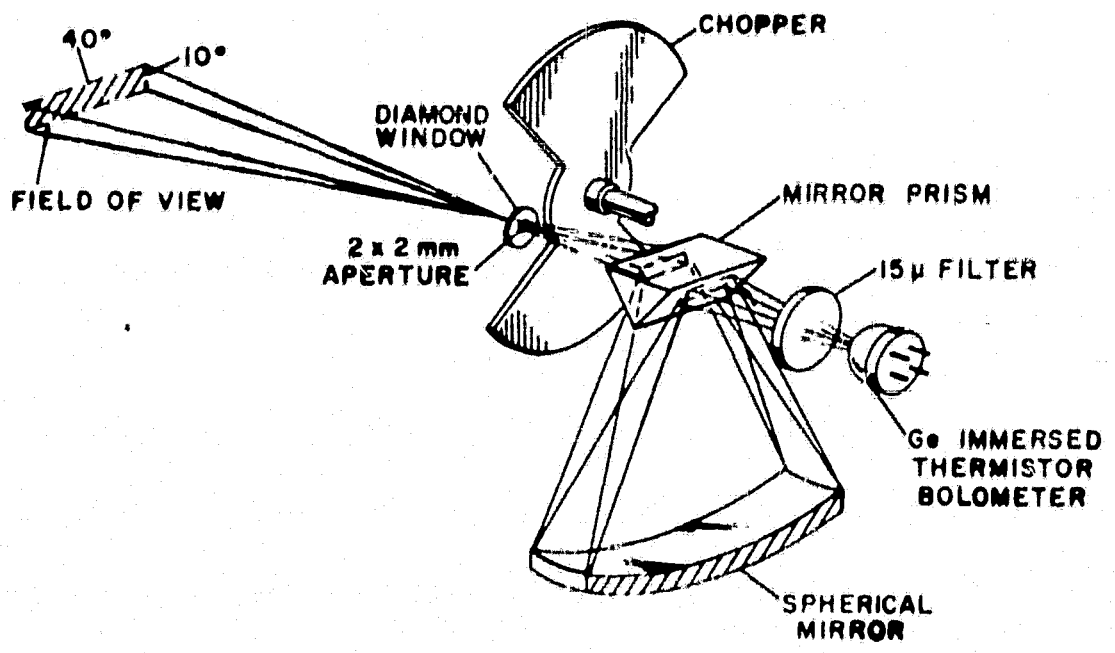


Figure 6-1. Optical system of infrared bolometer.

radiometer head but in combination with a miniaturized electronic complement whose characteristics are estimated.

Weight - 10 lbs (estimated).

Volume - 360 $in^3$.

Power - 10 W (estimated).

Radio frequency interference - None.

Magnetic moment - None.

Erection, orientation, or booms - Radiometer head should be pointed horizontally to measure ambient temperatures. If information on vertical profiles is desired, the head could be scanned in the vertical plane. Scanning in the horizontal plane may be desirable for averaging measurements.

Compatibility with sterilization at 145°C - Proper design of the system would be required.

Special requirements - Unobstructed field of view.

6.5.1.6 STATE OF DEVELOPMENT

Operational for field applications. Would require redesign for planetary applications.

## REFERENCES - RADIATION THERMOMETRY


Astheimer, A., R.W., 1963: An Infrared Radiation Air Thermometer. Proc. of 2nd Symposium on Remote Sensing of the Envir., Oct. 1962, Mich. Univ. Inst. of Sci. and Tech., Infrared Lab. Report No. 4864-3-X.

Barnes Engr. Co., 1963: Free Air Thermometer. Final Tech. Summary Report, DA36-039-SC-09771.

Combs, A.C., et al., Application of Infrared Radiometer to Meteorology. J. Appl. Meteor., 4, 253-262.

Fryberger, D., 1965: Experimental Feasibility Study of Remote Microwave Measurement of Atmospheric Temperature. IIT Research Inst., Final Report AF19-(628)-4022.

Kanzler, R.J., 1964: An Instrument for Air Temperature Measurement Using Infrared Emission of $CO_2$. Paper presented at the 5th Conf. on Appl. Meteor. of the Amer. Meteor. Soc., March 6, 1964, Atlantic City, N.J. (Barnes Engr. Co.).

Merrit, F , 1966: Satellite Sensing of the Lower Stratospheric Temperature Structure to Support SST Operations. AMS/AIAA Paper 66-372 presented at Conf. an Aerospace Meteor., Los Angeles.

Wark, D.Q., et al., 1966: Indirect measurements of atmospheric temperature profiles from satellites. Mon. Wea. Rev., 94, 351-362.

Westwater, G., et al., 1966: Ground Based Passive Probing in the Microwave Region. Nat. Bureau of Standards Report 9220.

## 6.6 LIQUID THERMOMETER

The great majority of all thermometers used to measure the near-surface temperature are of the type that depends on the expansion of a liquid in a glass envelope. The excess of the expansion of the liquid over that of the glass is measured by the changes in length of the liquid column in a narrow tube which is part of the container for the liquid.

### 6.6.1 MERCURY-IN-GLASS THERMOMETER

#### 6.6.1.1 NARRATIVE DESCRIPTION OF THE INSTRUMENT

The temperature is indicated by virtue of the differential expansion of mercury and glass. The volume coefficient of expansion of mercury is $182 \times 10^{-6}$ per °C while the coefficient of most glass is from $18 \times 10^{-6}$ to $27 \times 10^{-6}$. As the temperature rises, a greater portion of the glass tube above the bulb is filled, and the temperature is read directly from a calibrated scale on the instrument.

#### 6.6.1.2 INTERPRETATION OF THE MEASUREMENT

Additional information needed to interpret measurement - The ventilating speed should be known for computing the time constant.

Method for analysis and interpretation of data - The temperature is read directly from the scale posted on the instrument.

#### 6.6.1.3 INSTRUMENT CHARACTERISTICS

Total and dynamic ranges - Mercury freezes at -38.9°C and boils at 356.9°C. Therefore, these thermometers are restricted for temperatures between those two extremes.

Accuracy - There are three sources of error with this instrument. Two are of very minor importance (correction for emergence of stem and parallax reading) and the third (irreversible elastic errors) can be controlled by proper manufacture of the bulb. The accuracy of these instruments is quite good when they are shielded from direct solar radiation, generally within ± 2°C.

Signal to noise - Not determined.

Frequency response - For a ventilating speed of 4.6 m/sec and with a spherical bulb diameter of 1.12 cm, the time constant is 56 sec.

Environmental effects - The thermometer must be shielded from direct solar radiation or else the reading will be influenced by heat absorbed by the instrument and the measurement will be two high.

### 6.6.1.4 INSTRUMENT OUTPUT, PAYLOAD INTEGRATION, AND STATE OF DEVELOPMENT

No practical instrument has been developed for remote operation with an adequate electrical output. Such a device could be designed if necessary. However, for such purposes resistance thermometers have monopolized the field, and liquid thermometers remain the most useful direct reading temperature transducers.

## 6.6.2 SPIRIT-IN-GLASS THERMOMETER

The operation and general characteristics of this thermometer are the same as for the mercury thermometer except that the liquid is some organic substance. Ethyl alcohol ($C_2H_5OH$) is the most common substance; however, pentane ($C_5H_{12}$) and toluol ($C_6H_5CH_3$), among other compounds, are sometimes used. The freezing points of the above are below -100°C, and it is because of the low freezing points that they are used. These thermometers are not nearly as accurate as the mercury thermometer. The correction for the emergent stem is several times that for the mercury instrument. Unlike mercury, the spirit wets the glass; therefore, if the temperature falls rapidly a certain amount of the liquid remains on the walls causing the thermometer to read too low. Further, the organic substances polymerize somewhat when exposed to light and this leads to a diminution of the volume of the liquid, lowering the zero of the instrument.

Like the mercury thermometer, the spirit thermometer has been in use for many years and its characteristics are well understood.

## REFERENCES - LIQUID THERMOMETER

Middleton, W.E.K., and A.F. Spilhaus, 1953: Meteorological Instruments. Univ. of Toronto Press, 286pp.

## 6.7 CRYSTALS

Crystals are classified according to the way in which they are cut from the original crystal. Temperature has different effects upon the various types of cuts. The X-cut crystal has a negative temperature coefficient and the Y-cut crystal has a positive temperature coefficient. Both of these cuts are not used in the normal crystal controlled oscillator where temperature stability is desirable. In using the crystal to measure temperature, either the X or Y cut is selected for use in a crystal controlled oscillator. The material of the crystal is also selected to yield a large temperature coefficient such as that exhibited by rochelle salt. The frequency of the oscillator containing a crystal of this type is highly temperature dependent. Measurements of the frequency at various temperatures of the crystal are made to determine the sensor calibration. The instrument has been used with some experimental success; however, pressure also effects the resonant frequency of the crystal and development of usable systems has not been completed.

## 6.8 LASER PROBING

A polychromatic light detection system (PLIDAR) is theoretically capable of yielding temperature profiles in the troposphere (White, Nugent, and Carrier, 1965) Actually the PLIDAR technique is a combination of the LIDAR (light detecting and ranging) with the giant pulse Raman laser.

The LIDAR technique transmits into the atmosphere a large 30 n sec pulse from a ground-based ruby laser operating at 6943 Å . Various refractive index discontinuities scatter the pulse as it passes through the air. The backscattered part of the pulse is measured as a function of time by the photodetectors placed near the transmitter, and the distance of the scatterers from the transmitter can be calculated from the backscattered intensity versus time relationship. A pulse can be "tuned" to a desired atmosphere absorption band by the use of a Raman laser which shifts the frequency of the ruby laser pulse. The ruby radiation is shifted in energy by various multiples of the totally symmetric vibrational energies of the molecules of the Raman shifter by passing the optical radiation through a Raman shifter, either a liquid or high pressure gas, before being transmitted to the atmosphere. Further, the pulse may be passed in parallel through several Raman materials to produce one wavelength matching an atmospheric absorption line and another effectively in the clear of absorption.

The principle, the temperature structure, as well as pressure and density, can be determined by measuring the rate of change with height and the ratio of the intensities of backscattered radiation at the center of the absorption band and the backscattered radiation at the center of the adjacent window. One of the difficulties with the PLIDAR method is that the frequency of the giant pulsed laser be precisely matched with the spectral lines. In order to achieve the required frequency stabily the temperature of the ruby must be controlled with 0.1°C. Research is currently being conducted to see if this is possible. In addition, research is needed to select the materials for the Raman shifter that will not excessively broaden the frequency bandwidth of the output pulse.

### REFERENCES - LASER PROBING


Harris, E.D., L.J. Nugent, and G.A. Cato, 1965: Laser Meteorological Radar Study. Electro-Optical Systems, Inc., Final Report, Rpt. No. 5990, AF 19(628)-4309, AFCRL-65-177, 93pp.

White, G.R., L.J. Nugent, and L.W. Carrier, 1965: Laser Atmospheric Probes. Inst. Soc. A., Preprint No. 40.1-1-65, 20th Annual ISA Conference and Exhibit, Los Angeles, 11pp.

## 6.9 MICROWAVE REFRACTOMETER

Refractive index of an atmosphere may be used to determine any one of several of its properties if all others are known. Density, pressure, temperature, and water vapor density as well as composition affect the refractive index. The instrument has been used experimentally as a method of measuring atmospheric properties and is discussed under water vapor sensors.

## 6.10 MELTING-POINT THERMOMETER

The melting-point thermometer operates on the principle of closing an electric circuit when the melting temperature of a metallic compound is reached. Since the composition of the compound and thus its melting temperature are known, the temperature at the moment of the closing of the circuit is known. A given thermometer can be comprised of several compounds such that several temperatures can be measured. This device can measure a wide range of temperatures and is best suited for high temperature measurements. Once the compounds have melted, the instrument is no longer usable; therefore, only one set of measurements is possible. This instrument would be most applicable on Venus where high temperatures are expected. The output from the instrument is digital, the measurements occurring at discrete temperatures coincident with the melting of a particular compound. It is rugged and no additional parameters are necessary to interpret the measurement. Proper exposure of the compounds would be necessary to prevent solar radiation effects.

## 7. PARTICULATE SUSPENSIONS

Photometric and polarization studies suggest that the Martian yellow clouds are composed of particles whose diameters have been variously estimated to be between one and more than 20μ (see Ryan, 1964 for a review of available information on Martian yellow clouds). Presently available information does not allow reliable estimates of particle concentrations.

Deirmendjian (1966) has stated that the Cytherean atmosphere appears to contain large amounts of particulate matter which seems to be permanently in suspension. Quantitative data on particle sizes and concentrations are difficult to obtain. Polarimetric studies discussed by Dollfus (1966) suggest particles 2 to 3 microns in diameter. There is still a possibility that the clouds themselves may be composed of suspended particles rather than ice crystals or other condensates. And if the aeolosphere explanation of the high surface temperature is correct, there should be large amounts of dust in the lower atmosphere.

## 7.1 LIGHT TRANSMISSION MEASUREMENT

The extinction or attenuation of light transmitted through a volume of gas containing particles in suspension is related to particle concentration and size. The same is true of particles deposited on transparent substances. The phenomenon of light attenuation is due to the combined effects of total scattering and absorption of the incident radiation. For a homogeneously concentrated aerosol of small particles the light transmitted decreases exponentially as a function of pathlength and particle concentration.

For particle sizes above one micron extinction measurements yield information on particle-area concentration. Concentration and mean size can be determined for submicron spherical particles by attenuation measurements at various wavelengths. The simplicity of attenuation measurements makes it superior to scattering analysis; however, the latter is more sensitive, permitting measurement under lower concentration.

### 7.1.1 COLLECTED AEROSOL ANALYZER

#### 7.1.1.1 NARRATIVE DESCRIPTION OF THE INSTRUMENT

These instruments are based on the collection of aerosol particles on transparent or translucent substrates and the analysis is performed by measuring the increase in light attenuation through the substrate. Collection of particles is performed either by flow impaction, or by filtering, using a filter material as substrate. In both cases the substrate can be either fixed or indexed. Light transmission is measured by placing a light source on one side and a detector on the other, of the collection substrate.

#### 7.1.1.2 INTERPRETATION OF THE MEASUREMENT

Additional information needed to interpret measurement- For accurate aerosol evaluation, its composition should be known for the determination of its optical extinction.

Method for analysis and interpretation of data - Analog signal related to particle-area concentration.

#### 7.1.1.3 INSTRUMENT CHARACTERISTICS

Total and dynamic ranges - Range is flexible in terms of particle concentration depending on air sampling rate and duration. Particle size range depends on collection mechanisms (no specific information on size is obtained from this technique).

Accuracy - Dependent on type of aerosol.

Signal to noise - Dependent on type of aerosol.

Frequency response - Practically unlimited.

7.1.1.4 INSTRUMENT OUTPUT

Output signal - Analog, calibrated.

Bits per observation - About 10.

7.1.1.5 PAYLOAD INTEGRATION

The characteristics can only be estimated since an instrument for planetary missions has not been developed.

Weight - About 5 lbs.

Volume - About 1/2 $ft^3$.

Power - About 30 W.

Radio frequency interference - None.

Magnetic moment - Not known.

Erection, orientation, or booms - Not critical.

Compatibility with sterilization at 145°C - Instrument has to be designed to withstand it.

Special requirements - Proper enclosure to prevent substrate contamination before and during operation.

7.1.1.6 STATE OF DEVELOPMENT

Several commercially available instruments are available for terrestrial air pollution work. These instruments would have to be modified significantly for use on Mars or Venus.

### 7.1.2 ATMOSPHERIC ATTENUATION ANALYZER

Instruments of this type have been used on an experimental basis, especially for the evaluation of smokes emerging from stacks and other concentrated sources. For general measurements of air pollution the pathlengths required are substantial (of the order of 1 km), thus limiting the usefulness of this technique.

#### 7.1.2.1 NARRATIVE DESCRIPTION OF THE INSTRUMENT

The essential elements of a typical light extinction instrument are shown in Figure 7-1. Many variations have been considered in the literature, some of there are: (1) using the sun as light source and several reflecting spheres placed at various distances from a deflector, deviations from the inverse square law of radiation are detected and translated into light attenuation; (2) contrast measurements of natural or artificial black and white targets are made by photoelectric scanning. Instruments like the Slope-O-Meter will not be considered here since they are restricted to the measurement of dense smokes. Although this instrument uses a principle which could be applied over [illegible] pathlengths, namely the measurement of light attenuation as a function of wavelength.

Atmospheric turbidity instruments have been made where the solar radiation incident on a photo cell is measured and the reading is corrected for sun elevation.

#### 7.1.2.2 INTERPRETATION OF THE MEASUREMENT

Additional information needed to interpret measurement - It is necessary to know either the unattenuated light intensity or the absolute source intensity. For contrast measurements, unattenuated contrast has to be known for reference.

Method for analysis and interpretation of data - Dependent on particular measurement approach. In general the analog output would be related to particle-area concentration c by the equation of the form $I = I_o \exp(-kc)$. $I_o$ is the known unattenuated light intensity and I is the measured intensity.

#### 7.1.2.3 INSTRUMENT CHARACTERISTICS

Total and dynamic ranges - Particle diameters above one micron for single wavelength measurements and below one micron for multiple wavelength measurements. Lower concentration limit for a 100-m path is of the order of 100 particles of 1 micron diameter per cubic centimeter. High limit would be of the order of $10^4$ to $10^5$ $cm^{-3}$.

Accuracy - 10 to 30 percent depending on method and range.

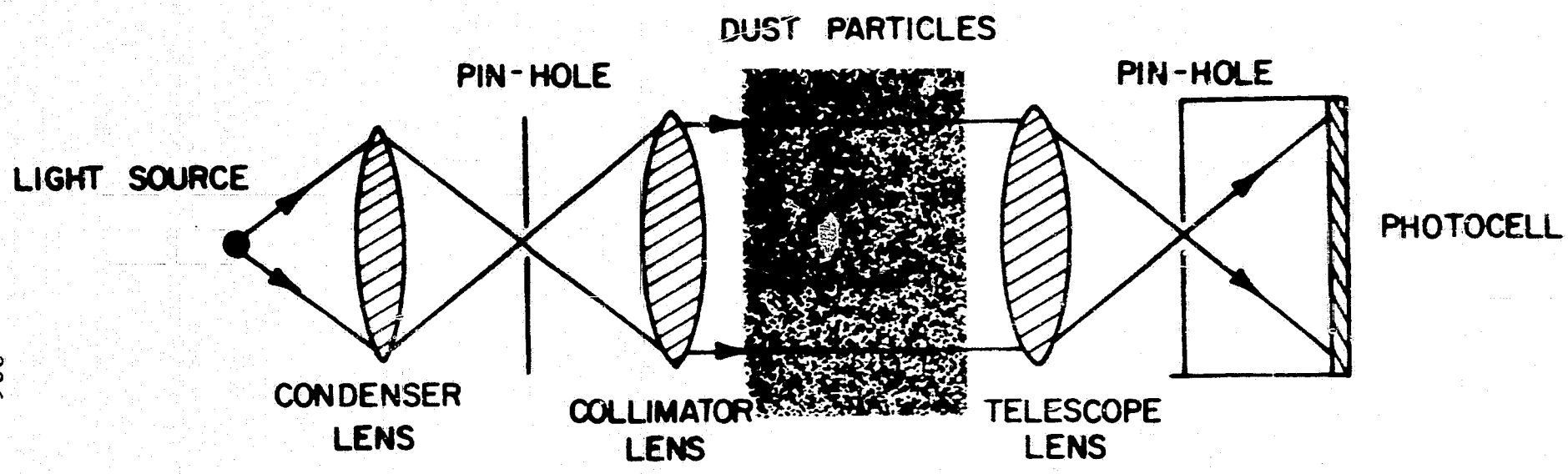


Figure 7-1. Essentials of light extinction instrument.

Signal to noise - Mainly dependent on intensity of light source, geometry of optics, and presence of spurious sources.

Frequency response - Practically unlimited.

Environmental effects - None in particular.

7.1.2.4 INSTRUMENT OUTPUT

Output signal - Analog.

Bits per observation - About 10.

7.1.2.5 PAYLOAD INTEGRATION

Since no practical instrument has been developed for this purpose no attempt will be made to estimate the relevant parameters.

Special requirements - Remote positioning of light source, mirror or contrast target. Sun could be used as source but would require continuous tracking.

7.1.2.6 STATE OF DEVELOPMENT

Experimental, far from operational for planetary missions.

## REFERENCES - LIGHT TRANSMISSION MEASUREMENT


Budgen, A.R., R.J. Hamilton, and G.H.S. Jones, 1960: J. Sci. Instru., 11, 371-377.

Conner, W.E., and J.R Hodkinson, A Study of the Optical Properties and Visual Effects of Smoke-Stack Plumes. U.S. Public Health Service Environmental Health Series, Govt. Printing Office, Washington, D.C.

Hodkinson, J.R., 1965: Aerosols. ed. K. Spuruy, Czechoslovak Academy of Sciences, Prague, 181-194.

McCormick, R.A., and D.M. Baulch, 1962: J Air Poll. Control Assoc., 12, 492-496.

Middleton, W.E.K., 1963: Vision Through the Atmosphere. Toronto Univ. Press.

Quinlan, R., and M.J. Corn, 1966: J. Amer. Ind. Hyd. Assoc.

Volz, F., 1959: Archiv. Met. Geophys. Bioklimat., 10, 100-131.

Walter, E., 1962: Staub 22, 162-165.

## 7.2 LIGHT SCATTERING ANALYSIS

In general the amount of light scattered by airborne particles is a function of particle size and thus a variety of instruments has been built based on this principle.

For particles with a diameter smaller than one-tenth the wavelength of the illuminating radiation, the scattering obeys Rayleigh's theory. As a consequence the angular distribution of the scattered light is symmetrical around the axis of illumination and independent of particle size and shape. The total intensity scattered for these small particles is proportional to the 6th power of their diameter.

Scattering by particles with a diameter larger than one-tenth of the incident radiation follows Mie's theory. In this size range, which covers most of the particles of interest suspended in the atmosphere as aerosol, the scattering law is more complicated. The total intensity for Mie scattering does not increase as fast with particle size as for Rayleigh scattering. For particle diameters greater than about twice the incident wavelength, the total scattered intensity is approximately proportional to the 2nd power of the diameter. The angular scattering characteristics also become increasingly complex with increasing particle size, and forward scattering becomes overwhelmingly predominant. In this range both particle refractive index and shape acquire an increasing role in the scattering characteristics. Polarization ratios also vary as a function of size.

The practical range of particle sizes covered by the light scattering technique lies between about 0.2 microns and 100 microns. The lower limit is defined by insufficient signal to noise ratio for the detection of rapidly decreasing scattering which follows the 6th power law mentioned above. The upper limit is given by increasing deviations from the Mie theory and increasing dependence on particle surface characteristics.

Light scattering instruments can be classified by a number of different criteria. An almost infinite number of variations of this technique can be found in the literature. The present study considered two main approaches: (a) measurement of bulk scattering of aerosols, and (b) measurement of single particle scattering.

### 7.2.1 DISCRETE PARTICLE COUNTER

#### 7.2.1.1 NARRATIVE DESCRIPTION OF THE INSTRUMENT

This instrument is based on the measurements of the light scattered by individual particles at a given angle or group of angles with respect to the axis of incident light flux. Forward scattering measurements are preferable because of decreased sensitivity to particle refractive index and significantly higher scattering flux levels.

The essential elements of a typical instrument of this type are depicted in Figure 7-2. The instrument operates as follows: The atmosphere is sampled by a flow system whereby the suspended aerosol particles are made to flow through a small (about one-cubic millimeter) volume illuminated by a light source with convergent beam optics. Detection of the forward scattering lobe is frequently accomplished by an annular reflecting or refracting area centered around the forward scattering axis, which concentrates the scattered light onto one or more photomultiplier tubes for single or multiple angle detection. The size of the optically sensitive volume defines the upper limit of particle number concentration which can be counted without excessive coincidence error produced when more than one particle is detected at a given time.

Individual particle counting provides information on particle size distribution and number concentration.

#### 7.2.1.2 INTERPRETATION OF THE MEASUREMENT

Additional information needed to interpret measurement - The only additional parameter required to derive the above information is the volumetric flow rate of the air sampled.

Method for analysis and interpretation of data - The output of the photomultiplier tube or tubes consists of a train of pulses of varying amplitude. The pulse amplitude is proportional to particle size as explained above. For multiple angle detection, particle size is obtained from the ratio of the intensities along each angle. Total particle number concentration is obtained by counting the number of pulses and relating this total count to the air volume sampled. Particle size distribution is obtained by subjecting the pulse train to pulse height analysis by means of amplitude discriminators (pulse ratio analysis for multiple angle detection). This pulse height discrimination can be accomplished either sequentially or simultaneously in time.

#### 7.2.1.3 INSTRUMENT CHARACTERISTICS

Total and dynamic ranges - Particle diameters: 0.2 or 0.3 microns to about 100 microns for single angle detection, and only 0.2 to 1.0 microns for multiple angle detection. Particle number concentration up to $10^3$ $cm^{-3}$ without flow dilution, up to $10^5$ $cm^{-3}$ with flow dilution. Low limit of concentation given by sampling duration (statistical confidence).

Accuracy - Depends primarily on aerosol to be measured. Significant deviations from sphericity and index of refraction will affect sizing accuracy. Overall accuracies better than ±20 percent of actual size are difficult to achieve over the entire size range for a "practical" aerosol. Errors are defined by the probability of coincidence detection at excessive concentrations.

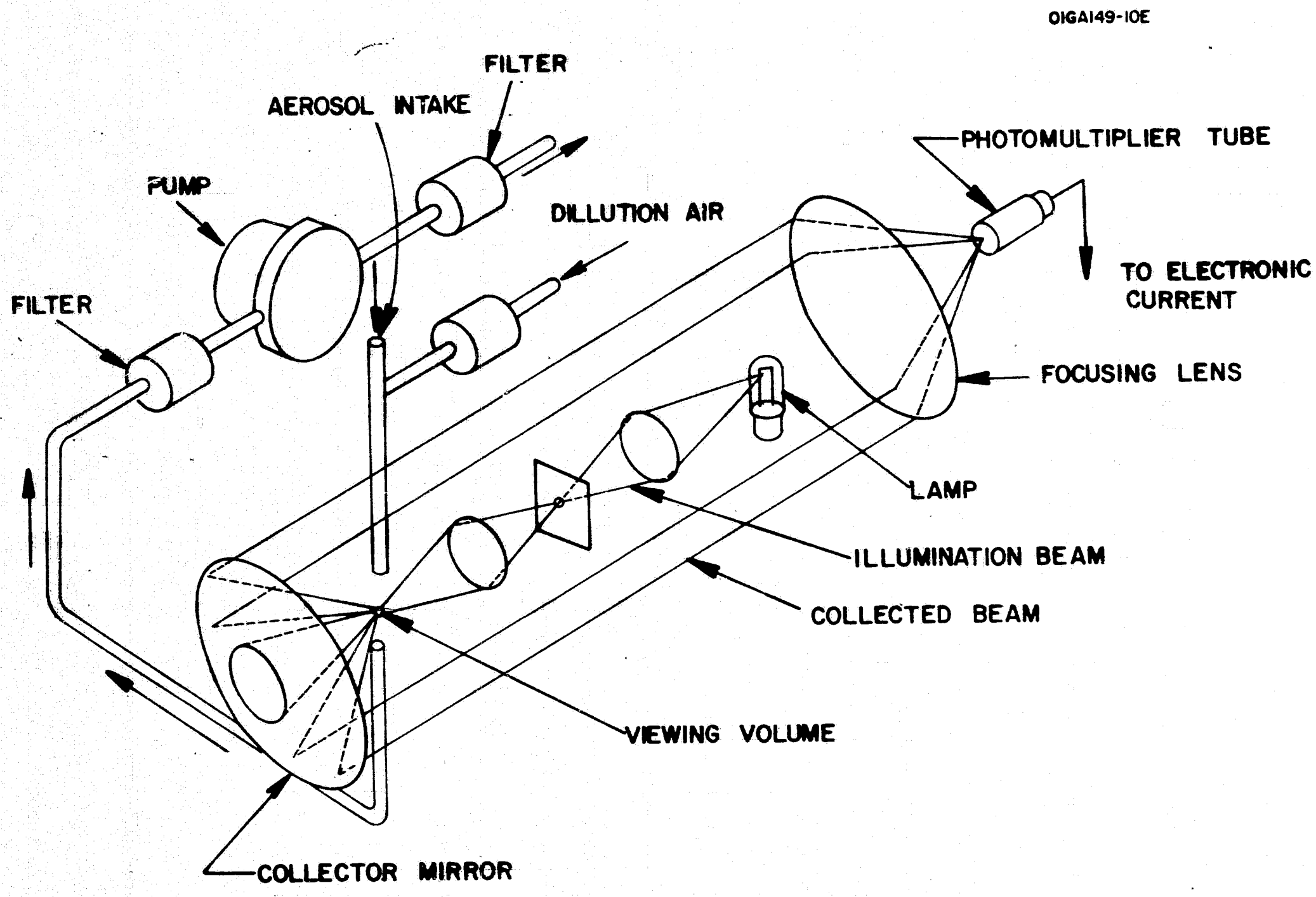


Figure 7-2. Essential elements of typical light scattering aerosol detection system.

Instrument calibration is performed initially by means of a known aerosol. Subsequent spot calibration can be effected by built-in secondary calibration schemes (optical fibers, etc.).

Signal to noise - This ratio defines the smallest detectable particle size, and it increases approximately as the square of the particle diameter above 1 micron for illumination with visible light. Typically s/n ratios are of the order of 20 for 1 micron diameter particle with photomultiplier at 25°C, and conventional incandescent lamp as source.

Frequency response - Response time essentially dependent on flow velocity and flow channel length between inlet and detection volume, typically one second.

Environmental effects - Large concentrations of particles below 0.1 micron can introduce counting errors.

#### 7.2.1.4 INSTRUMENT OUTPUT

Output signal - The output pulse frequency is related to number concentration. Telemetry channel defines particle size range. Flow rate could be predetermined and fixed. Otherwise, flow measurement would have either analog or digital output, depending on type of sensor.

Bits per observation - In addition to direct pulse counting, four to seven bits for particle size identification.

#### 7.2.1.5 PAYLOAD INTEGRATION

The characteristics for payload integration can only be estimated, at best, since a light scattering instrument for remote extraterrestrial operation is not currently available.

Weight - Not less than 10 lbs (approx.).

Volume - Not less than 1/2 $ft^3$ (approx.).

Power - About 50 watts.

Radio frequency interference - None.

Magnetic moment - Not known.

Erection, orientation, or booms - Not critical, free air access should be provided.

Compatibility with sterilization at 145°C - Instrument has to be designed using parts and components which can withstand this temperature under nonoperating conditions.

Special requirements - None.

7.2.1.6 STATE OF DEVELOPMENT

Several experimental as well as commercial instruments have been developed in the past decade and are used routinely in laboratories, industry and field research. None of these instruments is appropriate nor designed for use under extraterrestrial conditions, nor are they designed for remote operation including telemetry. Such an instrument would have to be developed.

7.2.2 BULK SCATTERING ANALYZER

This instrument is based on the measurement of light scattered at one or more angles with respect to the direction of incident light by a group or cloud of particles. Only characteristics differing from the discrete particle scattering instrument will now be mentioned. Single angle scattering measurements provide aerosol concentration information only if average particle size is known. Multiple angle detection results in average particle size information as well as concentration. This method is far less accurate than single particle counting, especially if the aerosol is significantly heterodispersed. The output signal consists of one or more analog signals (one or more angle detection), each a function of the light scattered at a particular angle. Time constants are of the order of microseconds or less. In terms of data handling this method is inferior to the discrete particle counting method in that it requires of the order of 10 bits per observation (single angle scattering) and more for the multiple angle system.

## REFERENCES - LIGHT SCATTERING ANALYSIS


Davies, C.N., ed. 1966: Aerosol Science, Academic Press, London, Chapter 10. (NOTE: This book, Chapter 10 by J.R. Hodkinson, contains a list of 182 pertinent references on this subject.)

Fenn, R.W., 1964: Aerosol-Verteilungen und atmosphärisches Streulicht. Beitr. Phys. Atm. 37, p. 69.

Harris, F.S., Jr., 1966: The laser in the study of atmospheric aerosols. Jour. Recherches Atm., p. 197.

Hodkinson, J.R., 1963: Light Scattering and Extinction by Irregular Particles Larger than Wavelength. I.C.E.S Pergammon Press, London.

Hodkinson, J.R., and J.R. Greenfield, 1965: Response calculations for light-scattering aerosol counters and photometers. Appl. Optics, 4, 11.

LaMer, V.K., and D. Sinclair, 1943: Measurement of Particle Size in Smokes, the Owl. OSRD 1668, Div. 10-601.2-MI.

Lowan, A.N., et al., Total Scattering Function for Complex Indices of Refraction. Math. Tables Project, National Bureau of Standards.

Martens, A.E., and J. D. Keller, 1967: A New Electro-Optical Instrument for Counting Airborne Particles. Bausch and Lomb, Inc., Rochester, New York, (to be published).

Mie, G., 1908: Ann. der Phys., 25, 377.

Lord Rayleigh, 1899: Scientific Papers. Cambridge Univ. Press, Vol. 1, 92-93.
Lord Rayleigh, Loc. Cit., 4, 1903, p. 400, Eq. 13.

Van DeHulst, H.C., 1957: Light Scattering by Small Particles. J. Wiley and Sons.

Zinky, W.R., 1962: A New Tool for Air Pollution Control: The Aerosol Particle Counter. Paper presented at 55th Annual Meeting of APCA, May 1962, Chicago, Illinois,

## 7.3 TELEVISION PARTICLE ANALYSIS

The direct visual analysis of aerosols has been the main tool in the investigation of particle characterisitics. Optical, ultra, and electro n microscopy are standard techniques used for the evaluation of collected or of suspended particles. The use of photography and television techniques has facilitated particle analysis, and more recently experiments have been performed using holographic techniques for the direct evaluation of airborne particles and fogs.

The television technique consists in essence of the remote transmission of visual information. This information can be either the field of observation of a microscope, or a hologram of a particle-laden air volume. The signal derived from the electro-optical scanning of the image can either be transmitted directly for remote interpretation or can be locally processed such that direct information on particle size distribution and number would be available for subsequent transmission.

If a microscope field of view is to be scanned by the television system, the particulate matter has to be collected by a suitable mechanism, i.e.; filter collector, impactor, electrostatic precipitator, etc. For holographic analysis, a hologram of the volume of air has to be made prior to its television analysis, which in this case, in addition to scanning, requires programmed variation of focus for three-dimensional cloud analysis. This technique will not be detailed here since it is judged to be too complex and undeveloped at this point.

### 7.3.1 MICROSCOPE-TV ANALYZER

#### 7.3.1.1 NARRATIVE DESCRIPTION OF THE INSTRUMENT

Analyzers of this type are available for laboratory use, and they include a television viewing monitor and a microscope for direct observation of a sample, in addition to the associated electronic circuitry and readout devices. The television tube, some of the elements of the microscope and the readout elements are irrelevant to this study. On the other hand, as expressed above, a particle collector would have to be integrated with this system. A block diagram of a possible instrument suitable for remote surface planetary particle analysis is shown in Figure 7-3. Remote processing of the video transmission appears preferable in terms of package complexity and telemetry. The received signal can be computer processed, furnishing direct information on particle size distribution and concentration if concurrent sampling flow rate information is transmitted.

#### 7.3.1.2 INTERPRETATION OF THE MEASUREMENT

Additional information needed to interpret measurement - The flow rate of the collection device, to determine aerosol concentration.

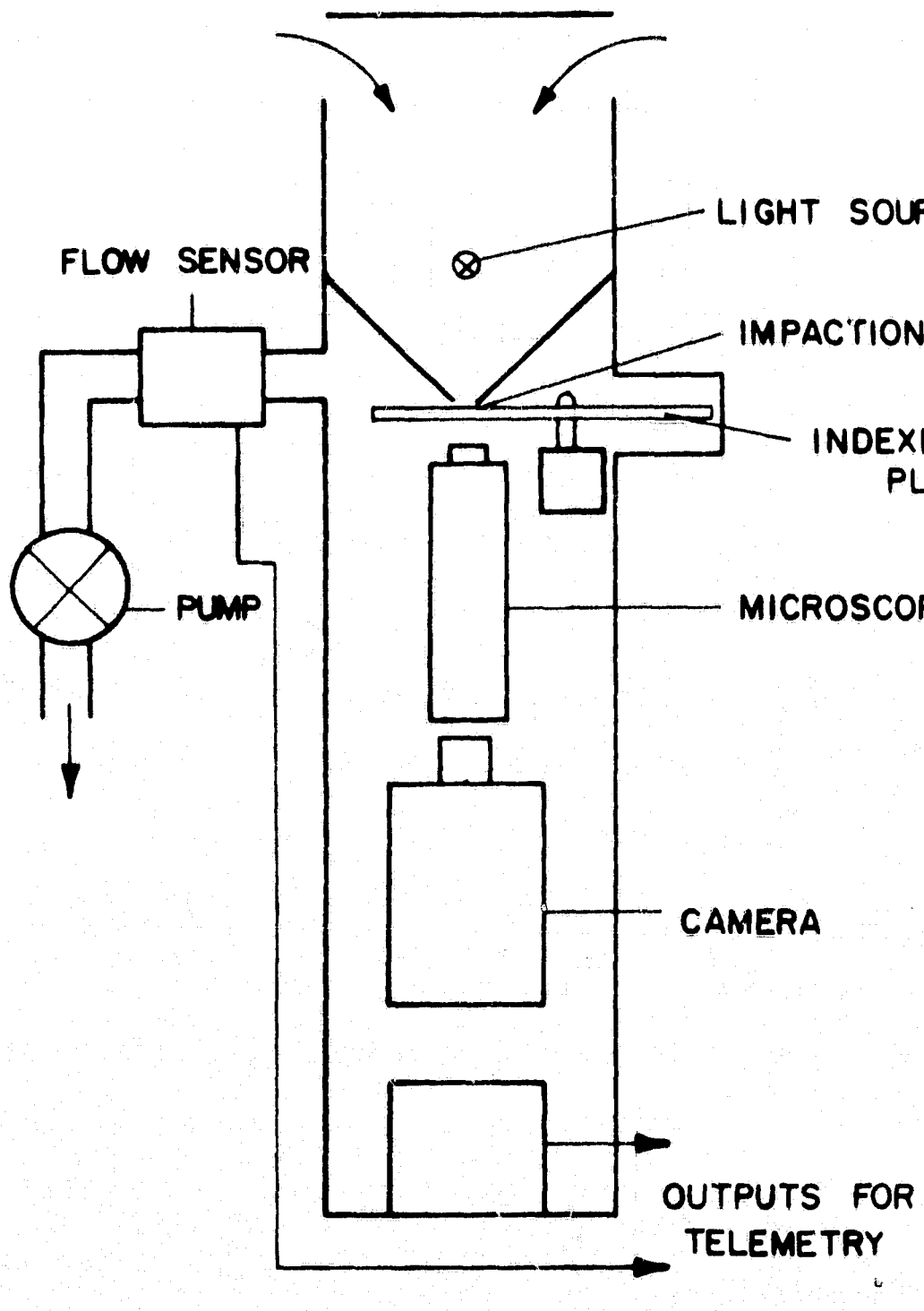


Figure 7-3. Microscope - TV analyzer.

Method for analysis and interpretation of data - The output of the video camera is to be transmitted, either in real time or through delayed recording as any other type of picture transmission. The received signal can either be displayed for visual monitoring or processed for automated analysis.

### 7.3.1.3 INSTRUMENT CHARACTERISTICS

Total and dynamic ranges - Particle diameters: about 0.5 microns and above (upper limit depending on microscope optics). Number concentration range only dependent on sampling periods.

Accuracy - Individual particle size and shape can be measured to essentially any degree of accuracy for solid particles, especially if calibration markers are included on the collection surface. Overall accuracy in terms of concentration and size distribution is in general limited to size discrimination of the collection mechanism.

Signal to noise - Dependent essentially on the optical contrast of the collected particles against the background.

Frequency response - Time constants are dependent on sampling flow rate and to a lesser extent on video scanning speed. Typical reaction times are less than one second.

### 7.3.1.4 INSTRUMENT OUTPUT

The output is a video signal containing the information on the particles scanned on a given field of view. Flow rate could be predetermined or transmitted; the sensor signal would define the type of conditioning required for telemetry.

Bits per observation - Typical video transmission.

### 7.3.1.5 PAYLOAD INTEGRATION and STATE OF DEVELOPMENT

No specifics can be stated at this point since no instrument of this type is available for remote operation. Existing instruments are for laboratory use.

### REFERENCES - TELEVISION PARTICLE ANALYSIS

Jarrell-Ash Bulletin No. 2.

Shuck, J., TV-Analyzing Computer Expands Scope of Microscopic Studies, Jarrell-Ash Reprint No. 18.

## 7.4 MICROPHONIC IMPACT DETECTION

Aerosol particles can be detected by impacting them on a pressure sensing detector. Particles striking such a detector transfer their momentum to the impacting surface. This transient pressure generates an electric pulse by means of the transducing action of the detector. These sensors in essence are piezoelectric, electromagnetic, capacitive, etc. microphones which have been used on various rockets, satellites and space probes for the detection of micrometeorite impacts. The magnitude of the pulse generated appears to be a function of the particle momentum (some disagreement exists on this point) and not its kinetic energy. Particle mass can be determined if the impact velocity is known. Wind blown particles can, in principle, be detected by utilizing their air flow imparted velocity. Aerosol particles, in general, can be accelerated artificially by means of forced air flow, electrostatic forces, etc. The limitation of this technique for aerosol measurements lies in the low signal to noise ratios which can be obtained. Noise is originated not only in the electric elements of the system, but also in the detection phase itself, due to wind or artificially induced air stream impingement flow past the detector. This air induced noise severely limits this technique to the detection of fast and large (massive) particles. Its use seems to be more adaptable to the Martian low air density environment than to the thick Venusian atmosphere, both in terms of noise and with respect to impaction size discrimination.

### 7.4.1 PIEZOELECTRIC PARTICLE IMPACT DETECTOR SYSTEM

#### 7.4.1.1 NARRATIVE DESCRIPTION OF THE INSTRUMENT

Instruments of this type have been developed for micrometeorite detection and also for experimental aerosol laboratory studies. No instrument exists at present which include an artificial impaction mechanism. Any system of this type consists of a detector or detector array, a pulse amplifier and pulse height discriminator for the determination of particle mass through an independent velocity measurement (anemometer, flow meter, etc.).

#### 7.4.1.2 INTERPRETATION OF THE MEASUREMENT

Additional information needed to interpret measurement - Wind speed for blown particles. Particle impact velocity for artificial acceleration.

Method for analysis and interpretation of data - Pulse count indicates number density and pulse height indicates particle mass.

#### 7.4.1.3 INSTRUMENT CHARACTERISTICS

Total and dynamic ranges - The minimum particle diameter (specific gravity = 1), dependent on impact velocity and noise, cannot be

specified at this point, probably not less than 10 microns under optimum conditions. The minimum detectable particle momentum is of the order of $10^{-5}$ dyn-sec, on the basis of recent laboratory experiments.

Accuracy - Mass value of the order of ±10 to ±15 percent for known particle velocities.

Signal to noise - Dependent on particle momentum and environmental noise. Minimum size would be noise limited.

Frequency response - Virtually zero time constant for wind blown particles, and of the order of 0.1 sec for artificial sampling

#### 7.4.1.4 INSTRUMENT OUTPUT

Output signal - The output for telemetry consists of a pulse train with telemetry channel mass identification. For wind blown particle detection, already available anemometer measurements would provide velocity information. For artificially induced impaction, flow velocity is measured and telemetered.

Bits per observation - In addition to direct pulse counting, 4 to 7 bits for particle mass information, and 7 bits for flow velocity information (not required for blown particles for which anemometry would already be available).

#### 7.4.1.5 PAYLOAD INTEGRATION and STATE OF DEVELOPMENT

This type of instrument has not yet been developed for airborne particle evaluation; however, micrometeorite detection instruments are available and could be adapted for this particular application, their design being suitable for space environments.

## REFERENCES - MICROPHONIC IMPACT DETECTION


Adams, H.E., 1961: Instrumentation for Use in the Study of Extra-Terrestrial Particles, AFCRL-1079, AF19-(604)-7352, Final Report, November.

Buck, R.F., Development of Apparatus for Micrometeorite Measurements, Research Foundation Report, Okla. State Univ., Contract AF19-(604)-7202, AFCRL, Bedford, Mass.

Neuman, F., 1963: A Micrometeoroid Velocity Detector, NASA TND-1977, Sept.

O'Neal, R.L., 1965: The Explorer XXIII Micrometeoroid Satellite. NASA TMX-1123, Aug.

Pollack, F.G., et al., 1964: Preliminary Experimental Investigation of a Double Capacitor Coincidence Discharge-Type Micrometeoroid Penetration-Sensor, NASA TMX-1037, Nov.

Reist, P.C., et al., 1967: Paper presented at AIHA Conf. 1967, Chicago.

Rogallo, V.L., and F. Neuman, 1965: A Wide-Range Piezoelectric Momentum Transducer for Measuring Micrometeoroid Impacts, NASA TND-2838, July.

## 7.5 ACOUSTIC ATTENUATION ANALYSIS

The description of this technique will be brief since it has not been carried beyond isolated laboratory experiments, and will be restricted to the physical principle and the possible applicability for remote planetary operation.

The attenuation of sound waves over a given air path is a function of the particulate concentration in the gas. Furthermore, the particle diameter defines the acoustic frequency of maximum attentuation, or in more general terms, a mean diameter of a polidispersed aerosol determines a characteristic frequency at which the attenuation is maximum. The discrepancy between various distribution functions has been found to be remarkably low (Tempkin and Dobbins, 1966). The attenuation equation for a polidispersed aerosol, which has been confirmed experimentally, is:

$$\bar{\alpha} = \frac{1}{\int_0^{R_\infty} N_r(R) R^3 dR} \int_0^{R_\infty} N_r(R) R^3 \left[ \frac{\omega\tau_d}{1+\omega^2\tau_d^2} + (\gamma+1)\left(\frac{C_p'}{C_p}\right) \frac{\omega\tau_t}{1+\omega^2\tau_t^2} \right] dR$$

where $\bar{\alpha}$ = attenuation per wavelength per unit mass fraction = $\frac{C \alpha \rho_o}{m\omega}$,

$C$ = speed of sound in gas,

$\alpha$ = coefficient of energy attenuation ($cm^{-1}$),

$\rho_o$ = mean gas density,

$m$ = mass concentration of aerosol,

$\omega$ = circular frequency,

$R$ = particle radius,

$N_r(R)$ = particle size distribution function,

$\tau_d$ = dynamic relaxation time of particles = $\frac{2\rho_p R^2}{9\mu}$,

$\rho_p$ = particle density,

$\mu$ = coefficient of gas viscosity,

$\gamma$ = ratio of specific heats of gas,

$C_p'$ = specific heat of particle,

$C_p$ = specific heat of gas at constant pressure,

$\tau_t$ = thermal relaxation time of particle = $\frac{3P\, C_p' \tau_d}{2C_p}$,

$P_r$ = Prandtl number of gas = $\frac{\mu C_p}{k}$,

$k$ = thermal conductivity of gas.

The particle diameter Do at which the maximum attenuation occurs is:

$$Do = (18\mu/\omega\rho_p)^{1/2} .$$

The sensitivity of this technique depends on numerous factors as can be seen from the above equations. A typical example will be given to illustrate the range of applicability. Assuming a path length of one meter, a frequency of 100 kHz ($\omega = 6.28 \times 10^5$ sec$^{-1}$), a relative attenuation of 1 percent, the minimum detectable aerosol concentration on the surface of Mars would be of the order of 1 mgr/m$^3$, while on Venus the sensitivity would be degraded to about 1 gr/m$^3$ due to the high Venusian surface air density. The level of the minimum detectable aerosol concentration can be reduced by increasing the path length and the sound frequency.

## REFERENCES - ACOUSTIC ATTENUATION ANALYSIS


Dobbins, R.A., and S. Temkin, 1964: Measurements of particulate acoustic attenuation. J. AIAA, 2, 1106.

Temkin, S., and R.A. Dobbins, 1966: Attenuation and dispersion of sound by particulate relaxation processes. J. Acous. Soc. Am., 40, 317.

_____, 1966: Measurement of attenuation and dispersion of sound by an aerosol. J. Acous. Soc. Am., 40, 1016.


Additional references are provided at the end of the above papers.

## 7.6 · BETA RADIATION ABSORPTION

A mass evaluation of aerosols can be obtained by measuring the attenuation of β radiation as it traverses a layer of collected particles. The collection substrate can either be a filter medium or a thin impaction film. The attenuation of the β radiation is only a function of the mass density and is independent of the chemical composition of the collected particles, their shape, density, optical properties, physical phase, etc. Thus this technique provides direct information on mass concentration of airborne material.

### 7.6.1 β ABSORPTION IMPACTOR MASS MONITOR

#### 7.6.1.1 NARRATIVE DESCRIPTION OF THE INSTRUMENT

This instrument is being developed for air pollution studies and a schematic of a prototype is shown in Figure 7-4. A 60 1/min pump provides the flow for the device which samples at 30 1/min ambient air. The 2 to 1 pressure ratio establishes sonic flow at the impaction nozzle thus providing a constant flow control. Lower flow rates can be accommodated by using a smaller diameter nozzle (present size is 1.5 mm diameter). The impaction substrate is a 6.3 micron thick mylar film resting on a $C^{14}$ beta source with an activity of 2 microcurie (higher activities will be used in subsequent models). The detector is an end window Geiger Miller tube which operates at about 600 V, with unlimited lifetime and 75 μsec dead time.

The collection-detection geometry is such that essentially all the particulate collection is concentrated in a very small area (about the size of the impaction nozzle orifice) and all the detected β radiation is constrained to pass through the mass collected. The G-M tube requires a regulated 600 V supply at negligible current. For prolonged, unattended operation an indexing mechanism for periodic advancement of the mylar film would be required.

#### 7.6.1.2 INTERPRETATION OF THE MEASUREMENT

Additional information needed to interpret measurement- Flow rate, if not predetermined and constant. Air density to determine cut-off particle size.

Method for analysis and interpretation of data - The output of the G-M tube consists of a train of pulses of constant amplitude. The pulse rate is related to the total mass collected in a given sampling period, which, related to volumetric sampling rate, indicates the mass concentration of aerosol.

#### 7.6.1.3 INSTRUMENT CHARACTERISTICS

Total and dynamic ranges - Particle diameters from about 0.1 microns up (dependent on air density). Minimum particle mass

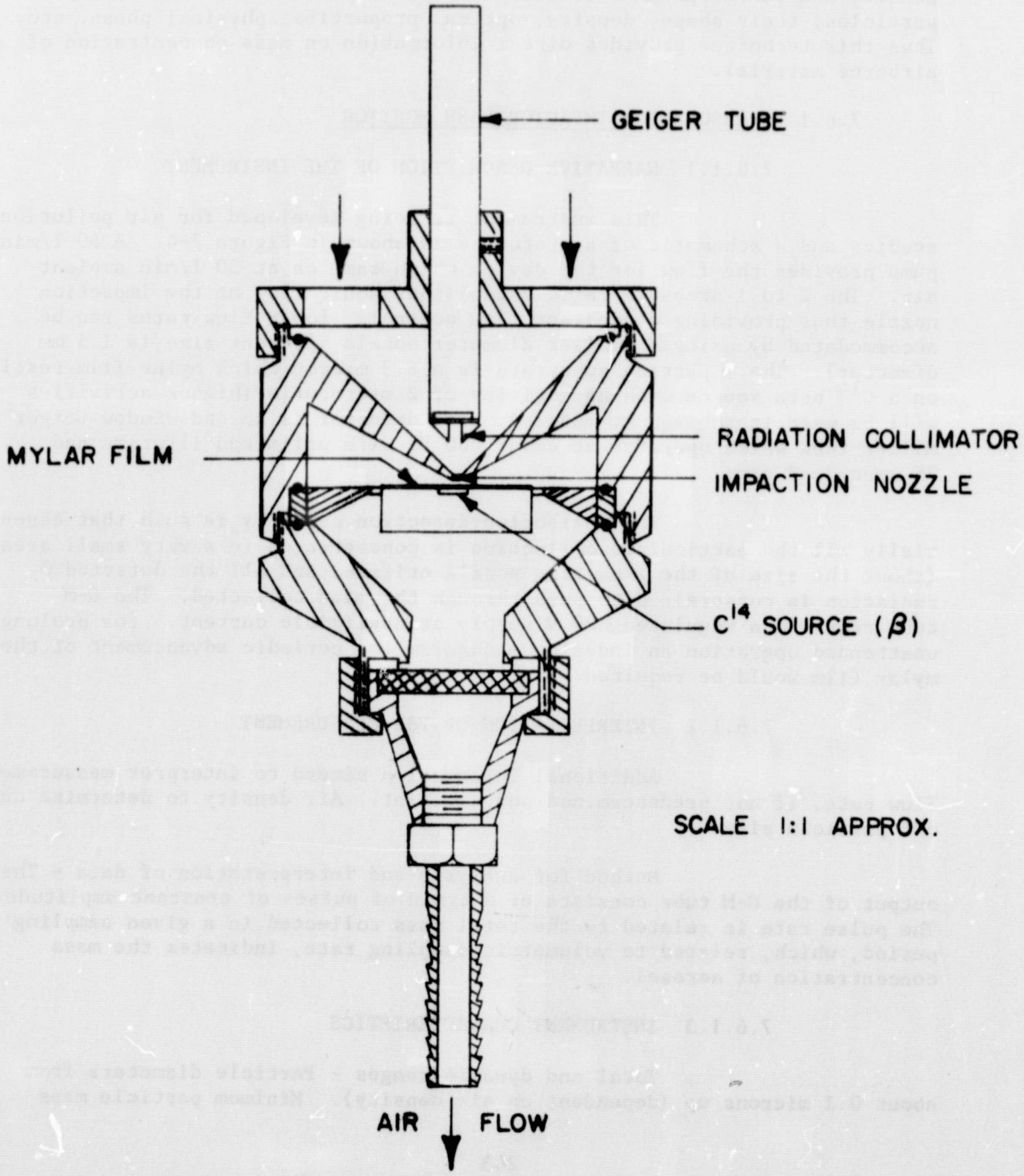


Figure 7-4. Beta absorption-impactor combination.

concentration dependent on sampling period. Minimum detectable mass of the order of 1 μg.

Accuracy - Better than 10 percent for particles above 0.5 microns and for integrated collections of less than about 10 μg. Accuracy is also dependent on number of pulses counted per data point, the counting error being equal to the square root of the number counted.

Signal to noise - Dependent on shielding against, and intensity of extraneous ionizing radiation sources. This aspect may be more serious on Mars.

Frequency response - The response time of this device is a function of count rate (typically of the order of a few counts per second per microcurie) and aerosol concentration.

Environmental effects - Accuracy and actual operation can seriously be affected by ambient ionizing radiation levels if improperly shielded.

7.6.1.4 INSTRUMENT OUTPUT

Output signal - Pulse train of the order of 1-V amplitude.

Bits per observation - Not applicable for direct pulse transmission; for analog rate output, 10 bits.

7.6.1.5 PAYLOAD INTEGRATION

Instrument would have to be designed specifically for planetary surface operation. Power would depend on sampling rate since pump is the major consumer.

Special requirements - Sensor shielding against unwanted radiation.

7.6.1.6 STATE OF DEVELOPMENT

Experimental, see above.

## REFERENCES - BETA RADIATION ABSORPTION


Bulba, E., and W.P. McShane, Automatic Stack Monitoring of a Basic Oxygen Furnace. Paper presented at 60th Annual Meeting of the APCA.

Bulba, E., and L. Silverman, A Mass Recording Stack Monitoring System for Particulates. Paper presented at 58th Annual Meeting of the APCA.

GCA Corporation, Ninth Quarterly Report, Contract DA-18-035-AMC-376(A), GCA-TR-67-25-G, Bedford, Mass.

Izmailov, G.A., 1961: Measuring the Gravimetric Concentration of Dust in the Air Using Beta-Radiation. Industrial Laboratory (USSR), 27, 1, 40-43.

## 7.7 CHARGED-PARTICLE MOBILITY ANALYZER

By imparting a known electric charge to aerosol particles, as a function of particle size, it is possible to infer this size by the measurement of total charge. The degree of electric charging which a particle acquires when exposed to an ionized gas environment, in the absence of an externally applied electric field, is a function of the particle residence time and the gaseous ion concentration. By controlling these two charging parameters, the mobility of a particle of a given size can be predicted. These charged particles can then be sized by means of an electric field. The aerosol concentration or the size distribution can be determined by selective current measurement.

### 7.7.1 WHITBY AEROSOL ANALYZER

#### 7.7.1.1 NARRATIVE DESCRIPTION OF THE INSTRUMENT

A schematic of this instrument is shown in Figure 7-5. This instrument has been designed for air pollution studies, aerosol analysis, etc. and some of its features could be omitted or simplified for remote operation. Particles are charged in the aerosol charging chamber by means of a sonic ionizer. The charged aerosol is injected into the mobility analyzer, which in essence consists of a concentric electrode pair across which a variable controlled potential is applied. Particles with a mobility below a minimum value, defined by the applied potential, are merely deflected by the field and escape the analyzer and are collected at the current collecting filter, their charge being transferred to ground through a current sensing electrometer. Particle size distribution and concentration are obtained by programmed step adjustment of the analyzer potential to govern the threshold of particle mobility required for collection on the axial analyzer rod. The variation of applied potential results in a corresponding variation of electrometer current.

#### 7.7.1.2 INTERPRETATION OF THE MEASUREMENT

Additional information needed to interpret measurement - Charged aerosol flow rate. Ionizer current can be internally regulated, and analyzer potential can be internally programmed and regulated.

Method for analysis and interpretation of data - Particle size distribution is inferred from the relationship between applied potential and detected current, and concentration is derived from the magnitude of the detected current.

#### 7.7.1.3 INSTRUMENT CHARACTERISTICS

Total and dynamic range - Particle diameters: 0.015 to 1.2 microns for a typical product of charger ion concentration times particle residence period of about $10^7$ sec $cm^{-3}$. Minimum particle rates of the order

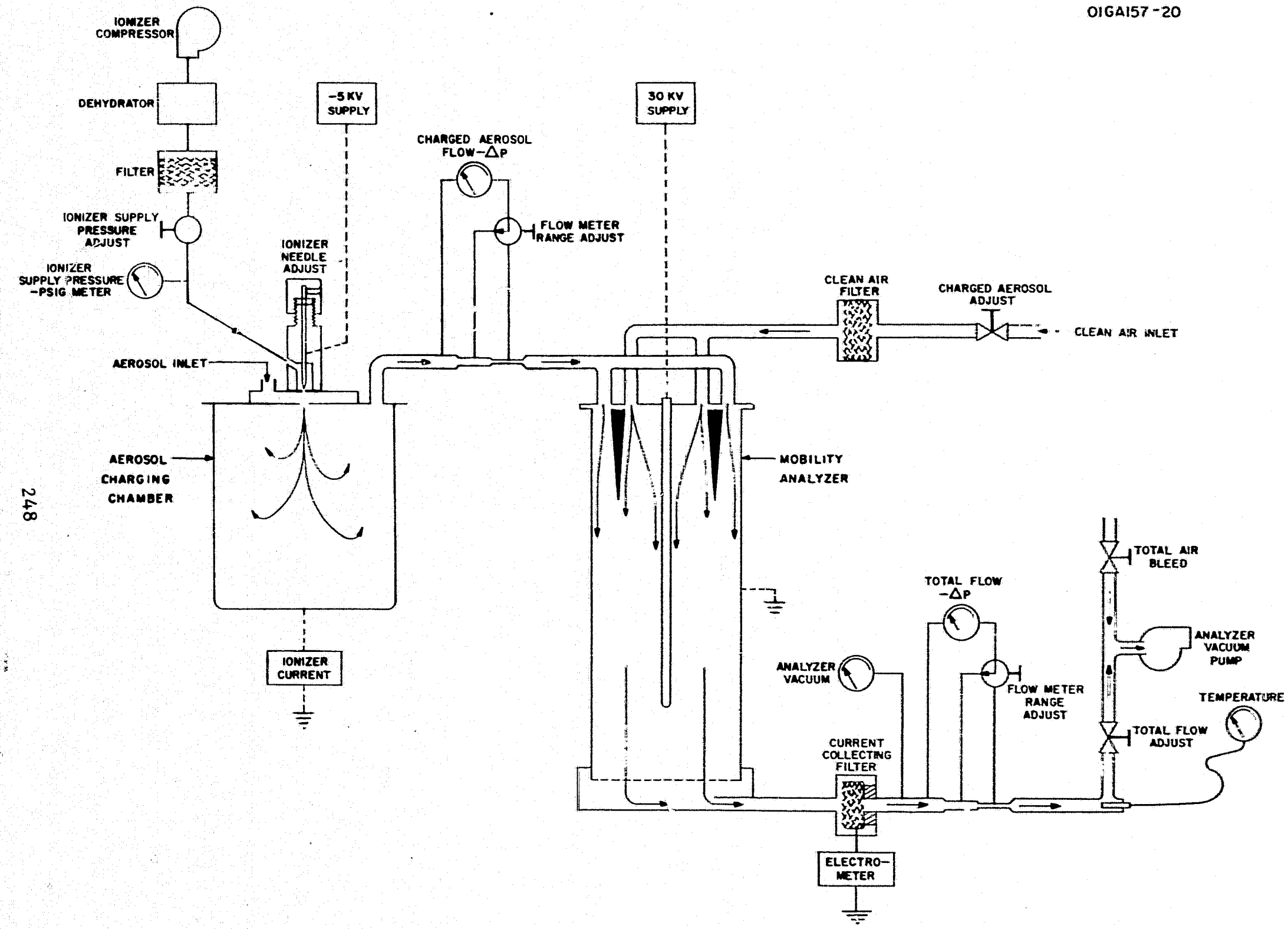


OIGA157-20

Figure 7-5. Whitby aerosol analyzer.

of $10^3$ $sec^{-1}$, which at a sampling flow rate of 10 l/min corresponds to $6 \times 10^3$ particles per liter.

Accuracy - Sizing accuracy approximately 10 percent.

Signal to noise - Increases linearly with particle rate (S/N $\simeq$ 1 for minimum detectable rate).

Frequency response - Response time is of the order of tens of seconds.

Environmental effects - Natural ionization of particles would affect the measurements. However, this background condition can itself be measured by alternately operating and shutting off the jet ionizer. Natural charge on particles could thus be measured.

7.7.1.4 INSTRUMENT OUTPUT

Output signal - Analog signal following changes produced by programmed analyzer potential changes. Logarithmic amplification would be required before telemetry.

Bits per observation - Total of about 11(7 for log of signal and 4 for voltage step identification) Four bits for flow rate, if required (the two mentioned flow rate measurements could be required).

7.7.1.5 PAYLOAD INTEGRATION

This type of instrument would have to be designed and developed for a planetary surface application. The existing device in its present design is totally unsuitable for such purpose.

Special requirements - Absence of strong ionizing sources.

7.7.1.6 STATE OF DEVELOPMENT

See above.

REFERENCES - CHARGED-PARTICLE MOBILITY ANALYZER

Whitby, K.T., 1961: Generator for producing high concentrations of small ions. Rev. of Sci. Instru., 32, 351-355.

Whitby, K.T., and W.E. Clark, 1966: Electric aerosol particle counting and size distribution measuring system for the 0.015 to 1μ size range. Tellus XVIII, 2, 573-586.

Whitby, K.T., B.Y. Liu, and C.M. Peterson, 1965: Charging and decay of Monodispersed aerosols in the presence of unipolar ion sources. J Coll. Sci., 20, p. 585.

## 7.8 HEATED FILAMENT DETECTOR

The description of this technique will be restricted to its fundamentals and no instrument details will be furnished since this approach has received only limited experimental laboratory use. Furthermore, its application is limited to liquid particles which precludes its use on most natural aerosols with the notable exception of fogs (liquid droplet suspensions). In this context the heated wire detector can serve to discriminate between solid and liquid aerosols. Furthermore, its use may be extended to the detection of liquid precipitation. Particle detection by this technique is based on the cooling effect of the impinging droplet on a heated wire, filament or wire grid. The basic principle of operation is identical to that of a constant current hot wire anemometer, where each particle generates a voltage pulse due to the transient decrease in wire resistance as the temperature decreases at the point of impact. Discrimination against wind induced signal is accomplished through frequency selective filtering. Particle mass (for a given specific heat) determines the voltage pulse height for a given filament current; thus, information on particle size can be inferred through pulse height discrimination. The instantaneous output voltage e is equal to:

$$e = \frac{dm}{dt} \frac{C_p' \phi^{3/2} R_w^{1/2}}{\alpha(A + B\sqrt{\bar{U}})^{1/2}}$$

where
- $R_w$ = mean value of wire resistance,
- $m$ = particle mass,
- $e$ = induced signal,
- $C_p'$ = particle specific heat,
- $\phi$ = $(R_w - R_o)/R_o$,
- $R_o$ = resistance of wire at ambient temperature,
- $\alpha$ = wire temperature coefficient of electric resistivity,
- $A$ = constant proportional to wire length and inversely proportional to $\alpha$,
- $B$ = constant proportional to the square root of the wire diameter, and inversely proportional to $\alpha$,
- $\bar{U}$ = mean air stream velocity,
- $t$ = time,

The signal to noise ratio is

$$\frac{S}{N} = \frac{2C_p'\sqrt{\bar{U}}}{\alpha B} .$$

Particles with diameters as low as 1 micron have been detected by this method. The low limit of detection is determined by the signal to noise ratio, which depends on the specific heat of the particle as well as on the turbulence of the medium.

## REFERENCES - HEATED FILAMENT DETECTOR


Goldschmidt, V.W., 1965: Measurement of Aerosol Concentrations with a Hot Wire Anemometer, Tr. Col. Science, 20, 617-634.

Reist, P.C., and W.A. Burgess, 1967: A Comparative Evaluation of Three Aerosol Sensing Methods. Paper presented at Amer. Industrial Hygn. Conference, Chicago.

Vonnegut, B., 1955: Means of Measuring Individual Aerosol Particles. U.S. Patent No. 2,702,471.

## 7.9 COULTER COUNTER

The Coulter counter bases its operation on the measurement of changes of electrical conductivity of a liquid electrolyte, flowing through a small orifice, due to the presence of suspended particles. Each particle, as it passes through the orifice increases the resistance of the path between two electrodes submerged in the electrolyte, one at each side of the orifice.

For aerosol measurements this instrument is combined with a means of suspending the airborne particles in the liquid electrolyte. This operation can be accomplished by an impinger or bubbler associated with the Coulter counter. This method will not be dicussed in detail because it has a very limited application to aerosol evaluations. Its particle size range is of the order of 20 to 1, the actual range given by the orifice size. Particles down to one micron in diameter have been detected. Sizing is accomplished by the measurement of the magnitude of the change of resistance as each particle traverses the sensing orifice.

## REFERENCES

The manufacturer, Coulter Counter Industrial Division, Franklin Park, Illinois, supplies a complete reference list on request.

# 8. REMOTE SENSING FROM ORBITERS OR FLYBYS

The inclusion of remote observation techniques in the present study throws open a wide range of possible experiments for both orbiters and flybys. Successful remote observations depend not only upon an accurate instrumental observation, but also on the validity of the inference technique used to deduce the particular meteorological or thermodynamic parameter one is attempting to measure. Thus, as opposed to in-situ observations, where, having made the observation, one can usually interpret it without great difficulty, remote observations must be processed with some sort of inversion technique, which depends upon the radiative transfer characteristics of the atmosphere, to derive the atmospheric parameter one is after. Hence, to analyze possible remote experiments that can be used for the measurement of meteorological and thermodynamic properties of Mars and Venus, one must first know something of the radiative transfer characteristics of these atmospheres. It is only then that a logical list of candidate experiments can be suggested. In the following pages are indicated some of the possible techniques that, based on our current knowledge of the radiative transfer characteristics of the atmospheres of Mars and Venus, seem appropriate. Since the major thrust of the present study was on in-situ observations, the discussions of the remote sensing techniques and instruments are not as detailed as those for the in-situ observations. The emphasis in these discussions is on the technique, and instrumentation details are kept to a minimum.

## 8.1 WATER VAPOR

### 8.1.1 ABSORPTION AND EMISSION RADIOMETRY

Water vapor has absorption bands in the near-infrared, infrared, and microwave regions of the spectrum. Observations of the intensities of reflected or transmitted solar radiation in these bands can be used to determine the amount of water vapor in the absorbing path. The vertical profile of water vapor could be determined from slant path observations of the absorption of solar radiation as the planet occults the sun. The absorption bands are pressure sensitive and a knowledge of the pressure distribution would be required for water vapor inferences to be made.

The basic equation is of the form

$$I = I_o \exp\left(-\int k \rho \, ds\right)$$

where I is the observed intensity of radiation, $I_o$ is the intensity of radiation outside the atmosphere, k is the absorption coefficient, $\rho$ is the water vapor density, and ds is an incremental length of path.

The water vapor absorption bands in the infrared and microwave regions can be used to determine the amount of water vapor in a planetary atmosphere from thermal emission observations. The observed intensity of radiation from the planet-atmosphere system in a water vapor band depends upon the amount of water vapor, the temperature distribution, and the pressure distribution. Thus, to determine the water vapor content with this technique, a knowledge of temperature and pressure profiles is required. In addition, if a microwave band is used, the emissivity of the surface would have to be known since microwave emissivities depart from unity for many naturally occurring surfaces.

The basic equation is of the form

$$I = \epsilon B_s \tau_s + \int_1^{\tau_s} B \, d\tau$$

where I is the observed intensity, $\epsilon$ is the surface emissivity, B is blackbody intensity, a function of temperature, and $\tau$ is transmissivity, a function of water vapor content and pressure. The subscript s refers to the surface.

A radiometer similar to that flown on Mariner II (Schwarz and Ziolkowski, 1964) could be used (Barrington et al., 1967) for the

infrared observations. The instrument would observe the radiation in the 6.3μ band and would have a spectral range of 5.5 to 6.5μ. Other candidate bands lie in the near-infrared region of the spectrum. The characteristics of a proposed radiometer system are discussed in Barrington et al. (1967). A single-channel superheterodyne Dicke radiometer operating near 1.35-cm wavelength would be suitable for the microwave experiment.

## REFERENCES

Barrington, A., A Caruso, and G. Manella, 1967: NASA TN D 4115, 13pp.

Schwarz, F., and A. Ziolkowski, 1964: Infrared Physics, 4, 113-126.

## 8.2 WIND VELOCITY

### 8.2.1 PHOTOGRAPHS OF CLOUDS AND TRACERS

Unfortunately, there is no satisfactory technique for remote determination of wind velocity. Sequential television photographs of cloud systems or cloud details from an orbiter would furnish information on cloud displacement, from which winds could be inferred. For Mars, pictures in the visible portion of the spectrum could be utilized for this purpose. For Venus, where no cloud structure is apparent in the visible region, analysis of UV photographs using techniques similar to the ground-based techniques employed by Smith (1967) is a possibility. There is also the possibility of releasing a tracer into the atmosphere from a descending capsule. Sequential photographs of the tracer cloud could then be analyzed to infer wind velocities. Possible tracers include the alkali metal vapors, which are discussed in the section on in-situ observations of wind velocities.

## REFERENCES

Smith, B.A., 1967: Science, 158, 114-116.

## 8.3 PRESSURE AND DENSITY

### 8.3.1 NEAR-INFRARED SPECTROSCOPY

Surface pressure on Mars may be determined with the use of techniques similar to the Earth-based spectroscopic techniques (see, for example, Belton and Hunten, 1966). For very weak carbon dioxide absorption bands (such as 0.87μ and 1.05μ), the amount of absorption of solar radiation by the Martian atmosphere depends upon the $CO_2$ amount and is essentially independent of atmospheric pressure. For the stronger $CO_2$ bands (such as at 1.6μ and 2.0μ), the absorption is a function of both the $CO_2$ amount and the pressure. Thus, by spectrometric observations of both weak and strong bands, the surface pressure as well as the $CO_2$ amount can be inferred. The experiment can be performed in two possible modes - looking down at Mars from an orbiter and measuring reflected radiation or looking at the sun through the atmosphere of Mars as Mars occults the source. The second mode allows the vertical distribution of pressure to be inferred. The required instrument is a near-infrared spectrometer.

An experiment similar in concept to the second mode of the experiment discussed above has been described by Coogan (1967). Rather than using the sun as a source of radiation, Coogan suggests a split trajectory dual planetary fly-by mode. If one of the fly-bys carries a suitable light source, such as a solar mirror, and the other a spectrophotometer, absorption versus altitude profiles can be obtained as the line of sight between the two fly-bys sweeps through the planetary atmosphere.

### 8.3.2 RADIO OCCULTATION

Radio occultation experiments for an orbiter or fly-by similar to the ones conducted by Mariner IV and Mariner V, can be used to infer atmospheric density and pressure. Such experiments require observations of perturbations to the amplitude and frequency of radio signals transmitted through the planetary atmosphere to the Earth by a spacecraft. The observed phase and amplitude changes depend upon the density distribution and composition of the planetary atmosphere, and are used to infer the refractivity versus altitude profile of the planetary atmosphere. From the refractivity profile, scale height, surface density and pressure can be deduced. This type of experiment can be conducted for both Mars and Venus. However, since the surface pressure on Venus is very high, the radius of curvature of the propagation path is smaller than the planet's radius. Under such conditions, the radio link between the spacecraft and the Earth never becomes tangential to the planet. Thus, the observed refractivity profile does not extend to the surface but to a level of critical refraction. This level depends not only on the surface pressure but also on the atmospheric composition. A possible way of extending the occultation technique to probe the atmosphere below the level of critical refraction is a bistatic radar experiment of the type discussed by Fjeldbo (1967). In such an experiment, scattering by the surface of the planet provides the radio link between the spacecraft and the Earth.

A beam of electromagnetic radiation is affected in two ways when passing through a neutral atmosphere having a higher index of refraction: the signal is retarded and the path of the radiant energy deviates from a straight line if the index of refraction is nonuniform. The total change in the observed Doppler velocity of the spacecraft is given by:

$$\delta\dot{L} = \frac{d}{dt} (\Delta\ell + \Delta R)$$

where $\Delta\ell$ and $\Delta R$ are the differential phase path lengths due to bending and retardation of the ray. The path length due to ray bending is related to the angle of refractive bending, $\epsilon(h)$, where h is height, by the expression

$$\Delta\ell = R_A \frac{\epsilon(h)^2}{2}$$

where $R_A$ is the distance of the spacecraft from the planet and

$$\epsilon(h) = 2\times10^{-6} N_s \int_R^\infty \frac{f(h) \exp\left[-\int_o^h f(h)\, dh\right]}{\left[1 - (R/r)^2\right]^{1/2}} dr$$

where $N_s$ is the refractivity near the surface of the planet, R is the distance from the center of the planet to the closest approach point of the ray, $r = r_o + h - R_A\epsilon$, where $r_o$ is the radius of the planet and

$$f(h) = -\frac{1}{\rho} \frac{d\rho}{dh}$$

where $\rho$ is atmospheric density. The expression for the differential phase path length, $\Delta R(h)$, is similar to that for $\epsilon(h)$ except that $f(h)$, where it appears before the exponential function, is absent. By matching the signals that would be produced by atmospheres of different compositions, surface pressures, and density profiles, with the observed Doppler velocity changes, it is possible to deduce these parameters for a planetary atmosphere.

The Mariner IV - Mars and Mariner V - Venus occultation experiments used S-band telemetry frequencies. Information on instrumental details may be found in Kliore et al. (1965) and Fjeldbo (1967).

### 8.3.3 GAMMA RAY SPECTROSCOPY

From measurements of gamma rays emerging from a planet-atmosphere system, it should be possible to deduce variations in surface pressure and, possibly, the magnitude of the surface pressure itself (Asaf and Kruger, 1966). The sources of gamma radiation are: (1) natural radioactivity produced by radioactive substances ($K^{40}$, $Th^{32}$, $U^{238}$ and $U^{235}$ and their daughters) at the surface of the planet and (2) cosmic rays. which upon striking an atmosphere, initiate reactions that result in the production of gamma rays. The natural radiation received by a detector on a spacecraft orbiting Mars can be written as (Asaf and Kruger, 1965)

$$R = fS \Delta A \exp [- \mu \bar{x}]$$

where f is a geometrical factor approximately equal to 1/2, S is the concentration of natural radioactivity in the surface in dpm per $cm^2$, $\Delta A$ is the detector area, $\mu$ is the atmospheric absorption coefficient in this energy range in $cm^2\ g^{-1}$, $\bar{x}$ is the average distance the radiation passes through the atmosphere in g $cm^{-2}$. In the energy range of interest (0.5 to 3.0 MeV), the absorption coefficients are nearly independent of atmospheric composition. Since $\bar{x}$ is related to the total pressure, changes in the observed signal can be used to obtain surface pressure variations. Asaf and Kruger (1965) indicate that surface pressure variations of about 0.3 mb could be detected on Mars. In theory, total pressure can be measured by comparing the intensities of spectral lines of different energies whose percentage yields are known. One must also be able to substract out the cosmic ray background in order to deduce the magnitude of the total pressure.

The instrument would be a $C_sI(T_l)$ crystal surrounded by a plastic scintillator and anticoincidence circuitry to discriminate against charged particles. Ebeogly (1966) presents detailed information on instrument characterisitics for this type of observation.

### 8.3.4 LASER BACKSCATTER

Because the amount of Rayleigh scattering is a function of atmospheric density and composition, laser observations of the light scattered back by a planetary atmosphere can be used to infer the atmospheric density profile if the composition is known. From the atmospheric density profile, a pressure profile could be constructed with the use of the hydrostatic equation. Instrumentation details for some ground-based laser systems intended for remote atmospheric sensing are given in the discussions of laser techniques for in-situ observations.

### 8.3.5 STELLAR REFRACTION

The stellar refraction technique relates the refraction angle of a star whose light has passed through some of a planet's atmosphere to atmospheric density. Refraction measurements are made from a satellite platform in orbit. The satellite provides the measurement of refraction angle of a known star as a function of time and the satellite ephemeris gives position as a function of time. This information gives the radius to the satellite, $r_s$, as measured from the center of the planet. With the knowledge of the true zenith of the star and the refraction angle, the zenith angle of the refracted ray is known. Snell's law yields an important constant: anywhere on the ray the product of refractive index, radius, and sine of zenith angle is constant. This constant is called the impact parameter. The refractive index is unity at the satellite, and $r_s \sin Z = \mu_o r_o$, where the subscript o indicates the point where the ray is tangent to the planet's atmosphere. Therefore, the basic measurement is refraction angle as a function of the impact parameter $\mu_o r_o$, as the ray path changes.

Integrating Snell's law along the ray path gives the following expression:

$$R = 2\, r_o \mu_o \int_1^{\mu_o} \frac{d\mu}{\mu[\mu^2 r^2 - \mu_o^2\, r_o^2]^{1/2}} .$$

This expression gives the refraction angle as a function of the impact parameter. An inversion of this equation gives the index of refraction $\mu$, as a function of height r. The inversion of the last equation is given by

$$\mu = \exp\left\{ -\frac{1}{\pi} \int_{\mu_r}^{\infty} \frac{R(\mu_o r_o)\, d(\mu_o r_o)}{\sqrt{\mu_o^2 r_o^2 - \mu^2 r^2}} \right\} .$$

The effects of this equation are as follows:

(1) It proves the existence of a unique inversion from refraction angles to densities.

(2) It permits a precise evaluation of the function including the ability to computerize the reduction of refraction data to density, temperature, and pressure.

(3) It permits a complete, definitive error analysis.

Since $\mu$ is proportional to density, it is a simple matter to determine density as a function of height if the composition of the atmosphere is known.

The basic observing equipment is a star-tracking telescope. A complete system for Earth-atmosphere application is described by Fischbach (1965).

## REFERENCES - PRESSURE AND DENSITY


Asaf, G., and Kruger, 1966: Measurements of Surface and Atmospheric Parameters by Gamma-Spectroscopy from a Martian Orbiter. Botsheva Seminar on Planetary Physics, ed U. Shafrir, Tel Aviv Univ., 40-45.

Belton, M., and D. Hunter, 1966: Astrophys. J., 145, 454-467.

Coogan, J.M., 1967: A Method for Studying Planetary Atmospheres Employing the Dual Flyby Mode. Paper No. 67-121, AIAA 5th Aerospace Sci. Meeting, 10 pp.

Ebeogly, D., 1966: IEEE Transactions on Nuclear Science, v. NS-12, 562.

Fischbach, F.F., 1965: A Satellite Method for Pressure and Temperature below 24 km. Bull. of the Amer. Meteor. Soc., 46(9), 528-532 (Sept.).

Fjeldbo, G., 1967: Radio Occultation Measurements of Planetary Atmospheres and Planetary Surface Topography. Paper No. 67-119, AIAA 5th Aerospace Sci. Meeting, 10 pp.

Kliore, A., D.Cain, G. Levy, V. Eshleman, G. Fjeldbo, and F. Drake, 1965: Science, 149, 1243-1248.

## 8.4 TEMPERATURE

### 8.4.1 INFRARED AND MICROWAVE RADIOMETRY

Surface temperature on Mars can be conveniently mapped from an orbiter with the use of an infrared radiometer observing in the 8-12μ water vapor window. The basic principle upon which such an experiment depends is that the intensity of radiation emitted by the surface is proportional to some power of the surface temperature. In an atmospheric window, there is negligible absorption of this radiation by the atmosphere. Thus, the measured intensity can be converted to a surface temperature. The proportionality factor depends upon the emissivity of the surface. For most common surface materials, infrared emissivities are close to unity. Clouds would hamper such an experiment; however, clouds on Mars are rare. A similar experiment has been flown on the TIROS weather satellites, and the radiometer characteristics are well described in the literature (see, for example, Bandeen et al., 1961).

Because of the cloud cover, surface temperature mapping of Venus presents a problem. Infrared radiation from the surface will be absorbed by the cloud layer. Microwave radiation, however, can penetrate the cloud layer, and surface temperature mapping of Venus could be accomplished from an orbiter with a microwave radiometer operating at cm wavelengths. A Dicke type radiometer, similar to the one flown on Mariner II (Jones, 1966), is indicative of the type of instrumentation required. Temperatures near the cloud level on Venus could be determined from infrared 8 to 12μ window observations.

If the carbon dioxide mixing ratio is known, the vertical temperature profile of Mars or Venus could be determined from horizon radiance observations in the 15μ $CO_2$ band. Measurements of the horizon radiance as a function of tangent height obtained from a zenith angle scan of the planet and its atmosphere can be inverted to obtain temperatures. The relevant instrumentation is a 15μ band radiometer with a narrow field of view and instrumentation to determine the pointing angle of the radiometer with respect to the nadir.

### 8.4.2 INFRARED SPECTROSCOPY

The vertical distribution of temperature above the surface of Mars and above the clouds of Venus could be inferred from intensity versus wavelength scans of the infrared thermal emission in a carbon dioxide absorption band, such as the 15μ band or 4.3μ band. A successful inversion of the observations depends upon a knowledge of the carbon dioxide amount. The techniques make use of the variation of absorption coefficient with wavelength in the band. At the center of the band, where the absorption coefficient is high, the measured radiation intensities originate in the upper layers of the atmosphere. At the edges of the band, where the absorption coefficient is low, the measured radiation intensisites originate

in the lower part of the atmosphere. Thus, a wavelength scan of the intensities essentially allows one to probe different levels of the atmosphere. And since the radiation intensities depend upon atmospheric temperature, it is possible to deduce the temperature structure.

Several spectrometers for performing similar observations in the Earth's atmosphere are under development. These include the satellite infrared spectrometer (SIRS) of ESSA (Hilleary et al., 1966) and the infrared interferometer spectrometer (IRIS) of the Goddard Space Flight Center (Chaney et al., 1967).

## REFERENCES - TEMPERATURE


Bandeen, W.R., R. Hanel, J. Licht, R. Stampfl, and W. Stroud, 1961: J. Geophys. Res., 66.

Chaney, L.W., L. Loh, M. Surh, 1967: A Fourier Transform Spectrometer for the Measurement of Atmospheric Thermal Radiation. Tech. Report, University of Michigan, Contract NASr-54(03), 106 pp.

Hilleary, D., et al., 1966: Mon. Wea. Rev., 94, 367-377.

Jones, D.E., 1966: JPL Technical Report 32-722, 57 pp.

## 8.5 PARTICULATE SUSPENSIONS

### 8.5.1 POLARIZATION AND SCATTERING OBSERVATIONS

Observations of the polarization of the radiation emerging from the top of a planetary atmosphere can be used to infer aerosol content, aerosol sizes, and possible, vertical distribution of aerosols. The inference of these parameters from such observations requires an understanding of the relevant scattering (Rayleigh and Mie)and absorption processes. Atmospheric aerosols affect the ambient radiation field. Kano (1964) has theoretically investigated the situation in which a concentrated aerosol layer is situated either at the top or bottom of a planetary atmosphere. It is found that the polarization features are very sensitively dependent upon the physical location of the aerosol layer. Polarization and scattering observations during twilight can yield aerosol information with good altitude resolution; such observations have been conducted for many years from ground-based sites on Earth to obtain information on stratospheric aerosols.

The observations should include the degree of linear polarization, the orientation of the plane of polarization in a predetermined coordinate system, and relative intensity variations of the emergent radiation in several spectral intervals (band width ~ 100 Å) in the visible region. The required instrumentation is a photopolarimeter of the type described in Ohring (1966).

A scattering experiment in the near infrared spectral region has been suggested for the detection of particulate matter in the atmosphere of Mars (Barrington, et al., 1967). At near-infrared wavelengths, Rayleigh scattering is negligible and, thus, aerosol scattering would be easy to detect. Barrington, et al. (1967) suggest a wavelength of 3.5μ, an atmospheric window, for the observations. The measurements of the scattering of the solar beam by the atmosphere would be made during periods immediately prior to or following occultation of the sun by the planet. A filter radiometer sensitive to the spectral region 3.4 to 3.6μ is the required instrument and is discussed by Barrington et al. (1967).

### 8.5.2 LASER OBSERVATIONS

Measurements of the intensities of light scattered back by a planetary atmosphere yield information on the atmospheric constituents causing the scattering. Atmospheric particulates participate in a Mie scattering process, which is sufficiently different from the Rayleigh scattering process due to atmospheric gases to permit deductions about the presence of the particulates. Height discrimination is obtained by the time delay of the laser pulse. Such a technique has been used to observe upper atmosphere particulates in the Earth's atmosphere from ground-based observations (see, for example, Fiocco, and Smullin, 1963). A high power, short pulse type of laser radar system is required. The operating characteristics of laser systems for atmospheric observations are discussed in the sections on in-situ observations.

## REFERENCES


Barrington, A., Caruso, A., and Mannella, G., 1967: NASA Tech. Note, TN D-4115, 13pp.

Fiocco, G., and Smullin, L. D., 1963: Nature, 199, 1275-1276.

Kano, M., 1964: Effect of a turbid layer on radiation emerging from a planetary atmosphere. Ph.D. Dissertation, Dept. of Meteorology, U. C.L.A.

Ohring, G., 1966: Meteorological experiments for manned earth orbiting missions, GCA Technical Report 66-10-N, Contract NASW 1292, 369pp.

# 9. SUMMARY LISTS OF TECHNIQUES AND INSTRUMENTS

This section contains summary lists of all the techniques and instrument types that have been discussed in the preceding pages of the report. The numbering scheme follows that used in the previous sections of the report.

## 2. LIST OF WATER VAPOR MEASUREMENT TECHNIQUES AND ASSOCIATED INSTRUMENT TYPES

2.1 CONDUCTIVITY HYGROMETERS

- 2.1.1 Phosphorous Pentoxide
- 2.1.2 Aluminum Oxide
- 2.1.3 Barium Fluoride
- 2.1.4 Lithium Chloride
- 2.1.5 Lithium Bromide
- 2.1.6 Lead Iodide
- 2.1.7 Carbon Strip
- 2.1.8 Ceramic Sensors

2.2 DEW/FROST POINT HYGROMETERS

- 2.2.1 Peltier
- 2.2.2 Gaseous Coolant

2.3 CAPACITIVE HYGROMETER

2.4 SPECTROSCOPIC HYGROMETRY

- 2.4.1 UV/Lyman Alpha
- 2.4.2 Infrared
- 2.4.3 Laser Scattering

2.5 PSYCHROMETER

2.6 THERMAL HYGROMETER

2.7 COOLED VAPOR TRAP

2.8 HAIR HYGROMETER

2.9 MICROWAVE REFRACTOMETER

2.10 COATED CRYSTALS

# 3. LIST OF WIND VELOCITY MEASUREMENT TECHNIQUES AND ASSOCIATED INSTRUMENT TYPES

# 4. LIST OF DENSITY MEASUREMENT TECHNIQUES AND ASSOCIATED INSTRUMENT TYPES

4.1 DECELERATION OF FALLING BODIES

4.2 LOW DENSITY IONIZATION GAUGES

4.3 CORONA DISCHARGE DENSITOMETER

4.4 VOLTAGE BREAKDOWN GAUGE

4.5 ACOUSTIC TECHNIQUE

4.6 THERMAL CONDUCTIVITY GAUGES

- 4.6.1 Pirani
- 4.6.2 Havens

4.7 SCATTERING TECHNIQUES

- 4.7.1 X-Ray
- 4.7.2 $\gamma$-Ray

4.8 EXCITATION TECHNIQUES

- 4.8.1 UV
- 4.8.2 Electron Beam
- 4.8.3 Bremsstrahlung

4.9 VISCOSITY GAUGES

- 4.9.1 Quartz Fiber Gauge
- 4.9.2 Molecular Gauge

4.10 ABSORPTION TECHNIQUES

- 4.10.1 Filter Photometer
- 4.10.2 Beta and Alpha Particle Absorption

4.11 MICROWAVE REFRACTOMETER

4.12 VIBRATING REED

# 5. LIST OF PRESSURE MEASUREMENT TECHNIQUES AND ASSOCIATED INSTRUMENT TYPES

5.1 DIAPHRAGM GAUGES

5.1.1 Aneroid

5.1.2 Bellows Type

5.1.3 Vibrating Diaphragm

5.1.4 Capacitance Type

5.2 BOURDON TUBE GAUGE

5.3 HYPSOMETERS

5.4 PIEZOELECTRIC CRYSTALS AND SEMI-CONDUCTORS

5.5 LIQUID BAROMETERS

5.6 KNUDSEN RADIOMETER GAUGE

# 6. LIST OF TEMPERATURE MEASUREMENT TECHNIQUES AND ASSOCIATED INSTRUMENT TYPES

# 7. LIST OF PARTICULATE SUSPENSIONS MEASUREMENT TECHNIQUES AND ASSOCIATED INSTRUMENT TYPES

# 8. LIST OF REMOTE SENSING TECHNIQUES

8.1 WATER VAPOR

8.1.1 Absorption and Emission Radiometry

8.2 WIND VELOCITY

8.2.1 Photographs of Clouds and Tracers

8.3 PRESSURE AND DENSITY

8.3.1 Near Infrared Spectroscopy

8.3.2 Radio Occultation

8.3.3 Gamma Ray Spectroscopy

8.3.4 Laser Backscatter

8.3.5 Stellar Refraction

8.4 TEMPERATURE

8.4.1 Infrared and Microwave Radiometry

8.4.2 Infrared Spectroscopy

8.5 PARTICULATE SUSPENSIONS

8.5.1 Polarization and Scattering Observations

8.5.2 Laser Observations

## REFERENCES TO METEOROLOGICAL CONDITIONS ON MARS AND VENUS


Belton, M., and D. Hunter, 1966: Ap. J., 145, 454-467.

Bottema, M., et al., 1965: Ann. Astrophy., 28, 225-228.

Dollfus, A., 1963: Compt. Rend., 256, 3250-3253.

Gifford, F., 1964: Mon. Wea. Rev., 92, 435-440.

Goody, R., and A. Robinson, 1966: Ap. J., 146, 339-355.

Hess, S., 1967: The lower atmospheres of Mars and Venus: Dynamics. Paper presented at 1967 Tucson Meeting on the Atmospheres of Mars and Venus.

House, F., G. Ohring, C. Sherman, and W. Tang, 1967: Study of the Martian atmospheric environmental requirements for spacecraft and entry vehicles. GCA-TR-67-12-G, Contract No. 951767, 160pp.

Kaplan, L.D., et al., 1964: Ap. J., 139, 1-15.

Leovy, C., and Y. Mintz, 1966: A numerical general circulation experiment for the atmosphere of Mars. Rand Memo. RM-5110-NASA, under contract NASr-21.

Ohring, G., W.Tang, and J. Mariano, 1965: Planetary Meteorology, NASA Contract Report NASA-CR-280.

Pollack, J.B., and C. Sagan, 1965: Icarus, 4, 62-103.

Ryan, J.A., 1964: J. Geophys. Res., 69,3759-3770

Schorn, R.H., et al., 1967: Ap. J., 147, 743-752.

Smith, B.A., 1967: Rotation of Venus: Continuing contraditions, Science, 158, 114-116.

Spinrad, H., and S. Shawl, 1966: Ap. J., 146, 328-329.

Tang, W., 1966: The general circulation of the Martian atmosphere. In Planetary Meteorology, GCA-TR-67-5-N, Final Rpt. under Contract NASW-1227, GCA Corp., Bedford, Mass.

# APPENDIX A

# SURVEY OF SIGNIFICANT METEOROLOGICAL INSTRUMENT DEVELOPMENTS SINCE 1956

## ABSTRACT

This report summarizes some of the recent (post 1956) innovations in meteorological instrument development. Included are discussions of instruments and techniques for the measurement of pressure, density, temperature, humidity, and wind speed and direction of the atmosphere. Extensive bibliographies of papers on meteorological instrumentation, arranged according to atmospheric parameter, comprise a major portion of the report.

## A.1. INTRODUCTION

As part of the effort on JPL Contract No. 951954, Aerometry Instrumentation Study, a concise survey of recent developments in meteorological observations of the Earth's atmosphere was performed. Recent developments have included new innovations as well as the refinement of standard techniques. Both types of developments are summarized in this report, which covers the post 1956 period.

Descriptive information is presented on the operating principle of each instrument category, the altitude range of operation, sources and magnitudes of instrument errors, response times, and other details pertinent to particular instrument types or techniques. Following the discussion of recent instrumentation developments for each atmospheric parameter, a pertinent and comprehensive bibliography on post 1956 instrumentation development is presented.

Three survey-type publications on recent instrument development proved to be extremely useful in the preparation of this report. These publications were by C.W. Thornthwaite Associates (Mather, et al., 1965 and 1967) and were concerned primarily with upper-air meteorological sensors to an altitude of 50 km, although some discussion was included of instruments designed to measure above this level. The bibliographies in the present report were compiled from the above publications, the Meteorological and Geoastrophysical Abstracts, and "A Bibliography of Meso- and Micro-Environmental Instrumentation" (Griffiths and Griffiths, 1966).

---

Mather, John R. et al, Recent Developments in Meteorological Sensors and Measuring Techniques to 150,000 Feet, Pt. 1, Analysis. C.W. Thornthwaite Associates, Laboratory of Climatology, Centerton, N.J., Contract No. DA-28-043-AMC-00001(E) Final Report April 20, 1965; Recent Developments in Meteorological Sensors and Measuring Techniques to 150,000 Feet, Pt. 2, Bibliography. C. W. Thornthwaite Associates, Laboratory of Climatology, Elmer, N.J., Publications in Climatology, 18(1), Pt. 2, 1965, 296 p., Contract DA-28-043-AMC-00001(E).

Mather, John R. et al, Developments in Meteorological Sensors and Measuring Techniques to 150,000 Feet, 1966. C. W. Thornthwaite Associates, Elmer, N.J., Climatology Lab, Final Report, 1 March 66-28 February 1967, June 1967, 183 p., Contract DA-28-043-AMC-00001(E).

Griffiths, John F. and Griffiths, M. Joan, A Bibliography of Meso- and Micro-Environmental Instrumentation. U. S. Weather Bureau, Technical Note 43-EDS, 2 July 1966, 352 p.

## A.2 TEMPERATURE

Most of the recent development in temperature measuring instruments has been directed toward upper air measurements. The sensitivity range and response times for these devices generally exceed those required for surface temperature measurements. Soundings have been performed using a variety of sensor techniques including: grenade rockets, sonic thermometers, thermocouples, bimetal units, electrical resistance elements, and indirect methods. Of these, only the electrical resistance thermometers or thermistors are employed routinely as sounding devices.

### A.2.1 THERMISTORS

Rod and bead thermistors represent the standard temperature sensing elements used aboard the radiosonde and rocketsonde, respectively. Rod thermistors measure temperature with an accuracy of ±1 C° up to 25 km. Above this altitude, radiation errors contaminate the observations (Armstrong, 19[illegible]. The bead thermistor is employed on rocketsondes to 60 km. Wagner (1964) examined possible errors in the measurements in the 30-60 km layer. His analysis included initial temperature of the sonde after nose-cone ejection, altitude at ejection, fall velocity and forced convection, viscous dissipation and aerodynamic heating, radiant heating, self-heating, and heat conduction along the lead from the instrument package. He found that the error increased from 4.5C° at 45 km to 19.0C° at 60 km.

### A.2.2 THIN FILM SENSORS

Thin film sensors are valuable where the molecular mean free path is long compared to the size of the sensor. Convective coupling of the air and the bead thermistor is less efficient above 55 km. It was felt that this difficulty might be resolved with a larger sensor which is transparent to solar and infrared radiation. For this purpose, thin film sensors have been developed. Films of the desired material are deposited on a transparent substrate. However, temperatures derived from a thin film sensor and a bead thermistor showed many discrepancies on a series of flights in 1965 conducted by Scallenger Research Institute. Efforts were continuing at that time to ascertain the causes.

### A.2.3 ROCKET GRENADE TECHNIQUE

The rocket grenade technique involves the explosion of a series of charges along a known rocket trajectory for determining the temperature profile between 30 and 90 km. Knowing the position and time of each explosion from optical or radar tracking and the times of arrival of the acoustic wave at an array of microphones on the ground, it is possible to determine the high-level

wind and temperature profile between adjacent bursts. From the known coordinates of the grenade explosions and the measured incidence angles of the sonic wave at the ground, one can determine the wind drift between consecutive explosions. Subtracting the wind effect from the total propagation velocity leaves the local sonic velocity, which is related to the local average temperature in the layer between the grenade explosions.

The greatest source of error is due to the uncertainty in determining the arrival time of the acoustic burst at the ground (Nordberg and Smith, 1964). Maximum temperature errors ranged between about 3°C at the first layer (between 30 and 40 km) to about 14°C at the highest layer, around 80 to 90 km.

### A.2.4 SONIC THERMOMETERS

The principle of acoustic measurement of temperature relies on the relation between the local speed of sound in the atmosphere and the ambient temperature. With the sonic thermometer it is not necessary to make assumptions that the thermometer is in thermal equilibrium with the environment since the measured temperature is determined by the measured speed of sound in air. As such the response times are high. In addition, radiation errors are not encountered since the intrinsic temperature of the transducer does not affect the measured speed of sound (except that the heat from the transducer influences the temperature of the air along the acoustical path).

There are two primary sources of error that are difficult to deal with. The first occurs when there is a wind component normal to the acoustical path. As a result, the acoustic wave follows a distorted pathway, thereby increasing the path by an unknown amount. The other major source of error is variability in atmospheric water vapor. This is a serious problem for sonic thermometry at the surface or low atmospheric levels where the error may be as large as 7°C.

### A.2.5 RADIATION THERMOMETERS

This instrument operates on the fact that in certain electromagnetic wave bands where atmospheric gases are strongly absorbent, the radiant emission of the gas is essentially equivalent to the emission in that wave band of a blackbody having the same temperature as the gas.

An infrared thermometer operating at 15 microns has been developed by Asthermier (1963). This instrument, for use in subsonic aircraft, passes the incoming radiation through a narrow pass-band filter and chops it to produce an ac signal proportional to the difference between the temperature of the atmospheric $CO_2$ and the regulared 50°C reference temperature of the optical cavity. The measured temperature represents a spatial average over the solid angle of the field-of-view and along a depth-of-view which depends on the absorptivity of the atmosphere in the wave band of operation. The best accuracy claimed for the system is 0.25°C achieved at 30°C.

Kanzler (1964) has developed a frequency scanning device between 13 and 15 microns that can detect temperatures up to 20 miles from the instrument. This device is being tested for possible detection of clear air turbulence.

A pyronometer measures the combined intensity of incoming direct solar radiation and diffuse sky radiation. The instrument consists of a recorder and a radiation sensing element which is mounted so that it views the entire sky. A specific design (called ARDONOX) for measuring low temperatures has been developed by Lorenz(1960). It consists of a cylindrical case in which a thermocouple of nickel construction senses the received radiation. For meteorological purposes, the instrument is provided with a filter which reflects short-wave radiation and is transparent to long wave radiation.

High altitude measurements (at the nightglow and aurora levels) have been performed by Hilliard and Shepherd (1966) with a modified (wider angle) Michelson interferometer viewing the Doppler width of atomic oxygen lines. The wide angle instrument has a 5-degrees field-of-view as compared to 0.2 degree for a Fabry-Perot spectrometer which made measurements with ±50°K accuracy for moderately bright auroras. The luminosity of this instrument may be of the order of a thousand times greater than the spectrometer at the same effective resolution. Hilliard and Shepherd found that a systematic relationship between the auroral brightness and observed temperature is often obtained over periods of a few hours. Brightness and temperature are inversely related. This inverse relation is crudely interpreted as following the atmospheric density curve: that is, that a uniform excitation per atom exists down to some cutoff line determined by the particle energy. Auroral brightness (and temperature) changes result primarily from changes in the particle energy spectrum.

Temperature errors for nightglow were estimated at ±50°K when the time for each measurement was 15 to 20 sec. However, since nightglow is a fairly stable phenomenon, averages over a large number of temperature points can be made and this error reduced significantly. The aurora errors are estimated at ±15°K at 200°K to ±30°K at 700°K.

### A.2.6 LASER PROBING

The Raman laser measurement technique involves shifting the frequency of the ruby laser pulse thereby "tuning" the optical pulse to a desired atmospheric absorption band. The optical radiation is passed through a Raman shifter, either a liquid or high pressure gas, before being transmitted through the atmosphere. Thus, the radiation is shifted in energy by different multiples of the totally symmetric vibrational energies of the molecules of the Raman shifter. The measurement of the rate of change with height of the ratio of the intensities of backscattered radiation at the center of the absorption band and the backscattered radiation at the center of the adjacent window will, in principle, permit the determination of the temperature structure, as well as that of density and pressure. White, Nugent, and Cornier (1965) state that

> ".... this method for the determination of temperature, density, and pressure could be very dependent on the absorption line strength, the line half-width, the number and extent of overlapping lines, the laser frequency stability and control, and the accuracy and precision with which the intensity and frequency measurements can be made."

It is necessary that the frequency of the giant pulsed laser be matched precisely with the spectral line before PLIDAR (polychromatic light detection and ranging) temperature soundings can be considered feasible. The required frequency stability is achieved by controlling the temperature of the ruby to within 0.1°C. Effort is also needed to select materials for the Raman shifter that will not excessively broaden the frequency bandwidth of the output pulse.

### A.2.7 INDEX OF REFRACTION

Fischbach (1965) devised a method for determining the atmospheric density below 40 km by measuring the stellar refraction from an orbiting satellite. The fundamental mathematics for the method is an inversion of the integration of Snell's law along the ray path. This is an inversion from refraction angles to densities. The initial pressure can be estimated and the densities integrated downward to yield pressure and temperature. A temperature accuracy of 5 percent at high altitudes would improve to about 0.1 percent near the surface.

### A.2.8 POTASSIUM AND SODIUM CLOUDS

Blamont (1961) studied the variations of the width of the resonance line of potassium with temperature at twilight. Earlier, he had conducted a similar study with sodium clouds above 100 km. The potassium study led to an experimental model of the temperature structure between 100 and 200 km.

### A.2.9 JUNCTION DIODES

Temperature sensitivity of a P-N junction volt-ampere characteristic is due principally to the variation of reverse saturation current (Sargeant, 1965). The basically exponential dependencies of reverse current on temperature and forward current on junction voltage interact to yield a linear junction voltage versus temperature relation. Also, the temperature sensitivity depends primarily on the energy gap of the material, and excellent uniformity of the diodes is possible with present manufacturing processes. The time constant for still air is 80 seconds based on a temperature step of 10°C. The most useful range of the instrument is from -30°C to 60°C.

## BIBLIOGRAPHY - TEMPERATURE


Ainsworth, J.E., Fox, D.F. and La Gow, H.E., "Upper-Atmospheric Structure Measurement made With the Pitot-Static Tube," J. Geophys. Res., 66:10, 3191-3213, (Oct. 1961).

Aizenshatat, B.A., "Radiation Method of Measuring the Active Surface Temperature," Glavnaia Geofizicheskaia Observatoriia, Trudy, No. 107: 76-79, (1961).

Aleksandrov, N.N., "The Plan for a New National Soviet Standard Mercury Meteorological Thermometer," Glavnaia Geofizicheskaia Observatoriia, Trudy, 103:57-67, (1960).

AMS Bulletin, "Automatic Weather Station for Canadian Artic," 42(11):796, (Nov. 1961).

Armstrong, R.W., "Improvement in Accuracy of the ML-419 Radiosonde Temperature Element for Heights above 50,000 Feet and up to 150,000 Feet," U.S. Army Elec. Command, Ft. Monmouth, N.J., Tech. Rpt. ECOM-2634, 55 p., (Oct. 1965).

Asthermier, A.R.W., "An Infrared Radiation Air Thermometer," Proc. of 2nd Symposium on Remote Sensing of the Envir., Oct. 1962, Mich. Univ. Inst. of Sci. and Tech., Infrared Lab. Report No. 4864-3-X, (1963).

Babdzhanov, P.B., "Determination of Temperature, Pressure and Density of the Atmosphere by Photographic Observations of Meteors," Geomagnetizm i Aeronomiia, Moscow, 6(1): 153-156, (Jan/Feb. 1966).

Ballard, H.N., "Rocketsonde Techniques for the Measurement of Temperature and Wind in the Stratosphere," U.S. Army Elec. Res. and Develop. Act., White Sands, N.M., ERDA-269, 106 p.

Ballard, H.N., "Measurement of Temperature in the Stratosphere," AMS/AIAA Conf. on Aerospace Meteorology, L.A., Calif., March 28-31, 1966, AMS/AIAA Papers, 66-385, 20 p., (March 1966).

Barber, C.R., "A Platinum Resistance Thermometer for Use at Low Temperature," J. Sci. Instr. 32(11):416-417 (Nov. 1955).

Benke, J., "Development of a Miniature Vortex Free-Air Thermometer," Cornell Aeronautical Lab., Inc., Buffalo, New York, Final Report, Contract No. a(s)-54-156 C, 69p., (Nov. 1, 1956).

Billings, R.G., "Means for Improving the Accuracy and Extending the Maximum Altitude of Mesospheric Temperature Measurements," AMS/AIAA Conf. on Aerosphace Meteorology, L.A., Calif., March 28-31, 1966, AMS/AIAA Papers, 66-388, 14 p., (March 1966).

Blamont, J.E., Donahue, T., and Lory, M., "Measurement of the Temperature in the Upper Atmosphere to 150 km in a Rocket Experiment," Phys. Rev. Letters 6, 403-404, (1961).

Blamont, J.E., and Lory, M.L., "Temperature Measurements in the Atmosphere from 100 to 200 km by Means of Potassium Clouds Emitted by Rockets," Academie des Sciences, Paris, Comptes Rendus 257(5):1135-1138 (July 29, 1963).

Bogorodskii, M.M., "Marine Gradient Apparatus for Studying Fields of Atmospheric Temperature and Humidity," Akademiia Nauk SSSR, Morskoi Gidrofizicheskii Institut, Trudy, 25:57-64, (1962).

Bollermann, B., and Walker, R.L., "New Low Cost Meteorological Rocket System for Temperature and Wind Measurement in the 75,000 to 200,000 Feet Altitude Region," AMS/AIAA Conf. on Aerospace Meteorology, L.A., Calif., March 28-31, 1966, AMS/AIAA Papers, 66-383, 23 p, (March 1966).

Champion, K.S., and Faire, A.C., "Falling Sphere Measurements of Atmospheric Density, Temperature, and Pressure, up to 115 km," AFCRL, Hanscom Field, Mass., Envir. Res. Papers No. 34, 27 p., (July 1964).

Clark, D.D., "Meteorological Rocket Sonde," J. Sci. Instr., 42(10): 733-736, (Oct. 1965).

Clark, G.Q, and McCoy, J.G., "Rocketsonde Measurement of Stratospheric Temperature," U.S. Army Elec. Res. and Develop., Act., White Sands, N.M., ERDA-242, 20 p., (Dec. 1964).

Clark, G.Q., and McCoy, J.G., "Measurement of Stratospheric Temperature," J. Appl. Met., 4(3): 365-370, (June 1965).

Cramer, H.E., Gill, G.C., and Record, F.A., "Fast Response Thermocouples," Mass. Inst. of Tech. In: Lettau, H.H., and Davidson, Ben, eds., Exploring the Atmosphere's First Mile, N.Y., Pergamon Press, Vol. 1: 216-219, (1957).

Dauvillier, A., and Schwob, Y., "A Multiple Meteorograph Recorder," J. Scientifique de la Meteorologie, Paris, 10(40): 149-155, (Oct/Dec. 1958).

Engler, N.A., "Development of Methods to Determine Winds, Density, Pressure, and Temperature from the ROBIN Falling Balloon," Univ. Res. Inst., Contract AF 19(604)-7450, Final Rpt., Nov. 1960-April 1965, AFCRL-65-448, 141 p., (May 1965).

Fink, C., "Radiosonde for Measuring the Fine Structure of Atmospheric Temperature," Meteorologische Rundschau, Berlin, 18(4): 110-114, (July/Aug. 1965).

Fischbach, F.F., "Satellite Method for Pressure and Temperature Below 24 km," Bull. Amer. Met. Soc., 46(9):528-532, (Sept. 1965).

Fryberger, D., "Experimental Feasibility Study of Remote Microwave Measurement of Atmospheric Temperature," IIT Research Inst., Chicago, Ill., Contract AF 19(628)-4022, Final Report, AFCRL-66-93, 35 p, (Dec. 31, 1965).

Glagolev, Iu.A., "Possibilities of Measuring Temperature in the Free Atmosphere by Means of Thin Resistance Thermometers Carried by Balloons up to Altitudes of 30-35 km," Tsentral'naia Aerologicheskaia Observatoriia, Trudy, No. 37: 62-74, (1960).

Glagolev, Iu.A., "Some Considerations Concerning the Possibility of Measuring Air Temperature in the Presence of Solar Radiation with Several Thermometers," Tsentral'naia Aerologischeskaia Observatoriia, Trudy, No. 37: 75-79, (1960).

Glagolev, Iu, "Rotating Aerological Thermometer," Meteorologiia i Gidrologiia, Moscow, No. 8:46-50, (July, 1962).

Godin, M.C., "A Modified Thermistor Thermometer," J. Sci. Instr., London, 40(10): 500-501, (Oct. 1963).

Groves, G.V., "Theory of the Rocket-Grenade Method of Measuring Temperature, Pressure, Density, and Wind Velocity in the Upper Atmosphere," Royal Soc. of London, Proceedings, Ser. A, 290(1420):44-73, (Feb. 8, 1966).

Hanson, D.W., "Instrumentation Requirements for the Remote Microwave Probing of the Atmosphere," U.S. National Bureau of Standards, NBS Report No. 8273, 41 p., (March 1964).

Hilliard, R.L., and Shepherd, G.G., "Upper Atmospheric Temperature from Doppler Line Widths, Pt. 4, a Detailed Study using the OI 5577Å Auroral and Nightglow Emission," Planetary and Space Sci., Oxford, 14(5): 383-406, (May 1966).

Hohne, W., "The Temperature Sensitivity Coefficients of Thermopiles of Galvanic Origin," Archiv fur Meteorologie, Geophysic und Bioklimatologie, Ser. B., 11(1): 126-134, (1961).

Hohne, W., "Technique for Producing Fast-Response Temperature Sensors and Resistance Thermometers," Germany (Democratic Republic), Meteorologischer und Hydrologischer Dienst, Veroffentlichungen, No. 18, 20 p, (1963).

Houghton, J.T., "Stratospheric Temperature Measurements from Satellites," Brit. Interplanetary Soc., London, Journal, 19(9):382-385, (May/June 1964).

Huovila, S., "On the Measurement of Temperature, Humidity, and Wind Velocity Very Near the Ground," (Inst. of Met., Univ. of Helsinki), Geophysica Helsinki, 6(3/4): 243-274, (1958).

Jacchia, L.G., and Slowey, J., "Densities and Temperatures from the Atmospheric Drag on Six Artificial Satellites," Smithsonian Inst., Wash., D.C., Astrophys. Obs., Special Rpt., No. 171, 111p. (March 26, 1965).

Jacchia, L.G., and Verniani, F., "Atmospheric Densities and Temperatures from the Drag Analysis of the San Marco Satellite," Smithsonian Inst. Wash., D.C., Astrophys. Obs., Special Rpt., 193, 10 p. (Nov. 12, 1965).

Jackson, R., "Newer Methods of Gas Temperature Measurement," British Coal Utilisation Research Assoc. Monthly Bull., 15(7): 245-256, (July 1951).

Johnson, N.R., Weinstein, A.S., and Osterle, F., "Influence of Gradient Temperature Fields on Thermocouple Measurements," Carnegie Inst. of Tech., Contract AF 18(600)-969, Final Report, Pt. 3, 30 p., (Sept. 1957).

Kaimal, J.C., and Businger, J.A., "Continuous Wave Sonic Anemometer-Thermometer," J. Appl. Met., 2(1): 156-164, (Feb. 1963).

Kamamoto, H., and Kimura, S., "On the Nickel Resistance Thermometer for Meteorological Use," J. of Met. Res., Tokyo, 5(1):31-36 (March 1953).

Kanzler, R.J., "An Instrument for Air Temperature Measurement Using Infrared Emission of $CO_2$," Paper presented at the 5th Conf. on Appl. Meteor. of the Amer. Meteor. Soc., March 6, 1964, Atlantic City, N.J. (Barnes Engr. Co.) (1964).

Kaplan, L.D., "Inference of Atmospheric Structure from Remote Radiation Measurements," (M.I.T. Cambridge), J. Opt. Soc. Am., 49(10):1004-1007 (Oct. 1959).

Konstantinov, A.R., "Errors of Inertial Devices Measuring Air Temperature and Humidity in an Atmosphere with Heterogeneous Temperatures," Nauchno-Issledovatel skii Gidrometeorologicheskii Institut, 26:145-156, (1961).

Kovacs, A., and Mesler, R.B., "Making and Testing Small Surface Thermocouples for Fast Response," Rev. Sci. Instr., N.Y., 35(4):485-488, (April 1964).

Kraus, H., "Temperature Measurement with Thermistors," Idojaras, Budapest, 69(1):1-8 (Jan/Feb. 1965).

Krechmer, S.I., "Field Radiant Meter for Measuring Air Temperature Gradients," Tsentral'naia Aerologicheskaia Observatoriia, Trudy, No. 22:96-97, (1957).

Latham, J., and Stow, C.D., " A Hygrometer for Use at Low Temperatures," J. Sci. Instr., London, 41(5):324-326 (May 1964).

Leleu, J., "Temperature Measurement by Resistance Probes," Electronique Industrielle, No. 59: 415-418 (1962).

Lenschow, D.H., "Technique and Results of Surface-Temperature Determinations with an Airborne Bolometer, (In: Lettau, H.H. ed., Studies of the Three-Dimensional Structure of the Planetary Boundary Layer, Wisconsin, Dept. of Met., Contract DA-36-039-SC-80282, Final Report, (Oct. 1962).

Lorenz, D., "Investigations with the ARDONOX, A New Instrument for Measuring Surface Temperatures," Meteorologische Rundschau, Berlin, 13(2): 54-57, (March/April 1960).

Malinovski, A. and Iordanov, D., "Electrical Remote Thermometers with a Thermistor Receiver," Khidrologiia i Meteorologii, Sofia, No. 1:3-11, (1960).

Mason, J.B.,"Study of the Feasibility of using Radar Chaff for Stratospheric Temperature Measurements," U.S. Army Elec. Command, Ft. Monmouth, N.J. ECOM 05012, 23 p, (Nov. 1965).

Meszaros, Erno, "General Remarks on the Improvement of the Pressure and Temperature Elements of Radiosondes," Idojaras, Budapest, 62(3):176-177, (May/June 1958).

Miller, P.H., "Modified Radiosonde for Obtaining Lower-Level Atmospheric Data," U.S. Naval Ordnanee Test Station, China Lake, Calif., NAVORD Report 6600: NOTS TP 2334, 16 p,(Oct. 1959).

Mitsuta, Y., "Sonic Anemometer-Thermometer for General Use," Meteor. Soc. Japan, Tokyo, Journal, Ser. 2, 44(1):12-24, (Feb. 1966).

Newman, J.B., "An Infrared Radiosonde," Johns Hopkins Univ. Lab. of Astrophys. and Phys. Met., Contract AF 19(604)949, Sci. Report No. 1, 28 p., (Aug. 15, 1956).

Nordberg, W., and W. Smith, "The Rocket Grenade Experiment," NASA TN D-2107, 32 pp, (1964).

Oleson, S., "Improved Sonic Anemometer-Thermometer," Standford Res. Inst. Menlo Park, Calif., Contract DA 36-039 AMC-03713(E), Final Report (Aug. 1965).

Paul, F.W., "Temperature Measurements with an Optical Pyrometer under Adverse Conditions," Appl. Optics, 3(2): 297-301,(Feb. 1964).

Pearson, P.H.O., "Investigation into the Response and Corrections to a Thermistor and a Platinum Wire Resistance Thermometer for Temperature Measurements in the Upper Atmosphere," Salisbury, Australia, Weapons Res. Estab., Tech. Note PAD 83, 15 p, (March 1964).

Pemberton, L.H., "Further Consideration of Emergent Column Correction in Mercury Thermometry," J. Sci. Instr., London, 41(4):234-236, (April 1964).

Petit, M., "Notes on the Vibrating Thread Thermometers for Stratospheric Soundings," Journal de Mecanique et de Physique de l'Atmosphere, Paris, Ser. 2, 1(4):179-190, (Oct/Dec. 1959).

Pirart, M., "Airborne Radiation Thermometer (FRB-1)," Fisheries Research Board,, Manuscript Report Series (Oceanographic and Limnological) No. 102,(Nov. 1961)

Raff, S.J., Parker, M.J., Snavely, B.L., et al., "Report on Phase I of the Feasibility Committee for 200,000 foot Altitude Instrumented HASP," U.S. Naval Ordnance Lab., White Oak, Md., NAVORD Report, 6763, 89 p.,(Dec. 15, 1959).

Ramanadham, R. and Murty, A.V.S., "A Thermistor Thermometer for Field Studies," J. of Sci. and Industrial Res., Sec. D, 21(12): 429-431 (Dec. 1962).

Reinhardt, M., and Franz, O., "Airplane Measurements of Horizontal Temperature Structure with a Special Temperature Measurement Element," Schweizer Aero-Revue, Bern, 37(1): 33-37, (Jan. 1962).

Rossi, V., "A New Finnish Radiosonde, a Radiosonde Provided with Thermostat," Ilmatieteellinen Keskuslaitos, Toimituksia, Finland, No. 43, 22 p., (1957).

Rudomanski, A.C., "Experimental Study for A Free Air Thermometer," Barnes Engr. Co., Stamford, Conn., Contract No. a(s) 57-636-c, Final Report April 1, 1957-March 31, 1958.

Ruskin, R.E., Schecter, R.M., Dinger, J.E., and Merrill, R.D., "Development of the NRL Axial-Flow Vortex Thermometer," U.S. Naval Res. Lab. Rpt. 4008, 32 p., (Sept. 4, 1952).

Sargeant, D.H., "Note on the Use of Junction Diodes as Temperature Sensors," J. Appl. Meteor., 4(5):644-646, (Oct. 1965).

Schelokov, V.V., "Airplane Thermometer," Geophys. Inst. Acad. Sci., USSR, Akademiia Nauk SSSR, Izvestiia, Sek. Geofizich, No. 5:569-576, (May 1956).

Shestopalov, L.A., "Results of the Development and Testing of the Bimetallic AM-15 Thermometer Probe," Nauchno-Issledovatel'skii Institut Gidrometeorologicheskogo Priborostroeniaa, Trudy, No. 12, 123-139 (1964).

Shestopalov, L.A., "Bimetallic Thermometer Elements with Increased Sensitivity," Nauchno-Issledovatel'skii Institut Gidrometeorologicheskago Priborostroeniia, Trudy, No. 13:99-109, (1965).

Sing, C.Y. and Chin, C.L.D., "Research for the Development of Airborne Atmospheric and Meteorological Instrumentation," Singco, Inc., Burlington, Mass, Contract AF19(628)-3244, Final Report, AFCRL-66-42, 59 p., (Nov. 1965).

Singh, M., "Lag Coefficient of Bimetal Thermometer of Chronometric Type Radiosonde (Model 2)," Indian J. of Met. and Geophys., 12(4):637-642, (Oct. 1961).

Skatskii, V.I., and Shchelokov, V.V., "Airplane Device for Complete Measurement of Meteorological and Dynamic Characteristics of the Atmosphere Including Clouds," Akademiia Nauk SSR, Izvestiia, Ser Geofiz. No. 8: 1270-1277, (Aug. 1963).

Stewart, R.M., Jr., and Kassander, A.R., Jr., "Fast Response Thermistors," Iowa State College, (In: Lettau, H.H. and Davidson, B., eds., Exploring the Atmosphere's First Mile, N.Y. Pergamon Press, Vol. 1:206-215)(1957).

Struzer, L.R., and Istomin, A.P., "Thermoelectric Method for Measuring Air Temperature Gradient in the Atmospheric Layer Near the Ground," Glavnaia Geofizicheshaia Observatoriia, Trudy, No. 129:66-87, (1962).

Tebo, A.R., "Precise Measurement of Atmospheric Temperatures," U.S. Army Elec. Res.and Devel. Labs., Ft. Monmouth, N.J., Tech. Rpt. 2405, 7 p. (Dec. 1963).

Thompson, D.C., and Keily, D.P., "Accuracy of Thermistors in the Measurement of Upper Air Temperature," AMS/AIAA Conf. on Aerospace Meteor., L.A., Calif., March 28-31, 1966, AMS/AIAA Papers, 66-386, 16 p., (March 1966).

U.S. Army Electronics Research and Development Activity, White Sands, "Performance Characteristics or Meteorological Rocket Wind and Temperature Sensors," Tech. Rpt. SELWS-M-4, 31 p., (Oct. 1962).

Usol'tsev, V.A., and Manuilov, K.N., "Basic Characteristics of the A-22-III Radiosonde," Nauchno-Issledovatel'skii Institut Gidrometeorologichesago Priborostroeniaa, Trudy, No. 5:3-16, (1957).

Vaisala, V., "Observations Concerning the Daily Variation of the Temperature and the Balloon Effect on the Temperature Measurement at High Altitude," Vaisala News, Helsinki, No. 28: 4-12, (1965).

Wagner, N.K., "Theoretical Time Constant and Radiation Error of a Rocketsonde Thermistor," J. of Met., 18(5):606-614, (Oct. 1961).

Wagner, N.K., "Theoretical Accuracy of the Meteorological Rocketsonde Thermistor," Freie Universitat, Institut fur Meteorologie und Geophisik, Meteorologische Abhandlungen, 36:527-535, (1963).

Wagner, N.K., "Theoretical Accuracy of a Meteorological Rocketsonde Thermistor," J. Appl. Met., Boston, 3(4):461-469, (Aug. 1964).

White, G.R., Nugent, L.J., and Cornier, L.W., "Laser Atmospheric Probes," Inst. Soc. A., Preprint No. 40.1-1-65, 20th Annual ISA Conf. and Exhibit, Los Angeles, 11 pp. (1965).

Woelfe, "Sonde for Accurate Temperature Measurements in the Free Atmosphere," Meteorologische Rundschau, Berlin, 17(5): 145-148, (Sept/Oct. 1964).

Wright Instruments, Inc., "Survey for NOL (Naval Ordnance Lab.) of High Altitude Atmospheric Temperature Sensors and Associated Problems," Vestal, N.Y., Contract N-60921-6136, Final Rpt., 295 p., (1961)

## A.3 PRESSURE

No really new pressure measuring techniques have been developed in the past several years. The research efforts have been directed toward improving existing instruments.

Atmospheric pressure measurements at high altitudes have been obtained in the following three ways: 1) calculation with the equation of state and the hydrostatic equation, 2) by an instrument on board a vehicle moving slowly with respected to the air, and 3) by measurement of the aerodynamic pressures exerted at selected points on the surface of a high speed vehicle, such as a high performance aircraft or rocket.

### A.3.1 HYPSOMETERS

The hypsometer measures pressure by determining the boiling point of a liquid. The pressure is computed from the temperature-pressure relationship (Clapeyron-Clausius equation) for the particular liquid. Increasing sensitivity of the instrument occurs with decreasing pressure, so that its optimum utility is at high altitudes. Different designs are necessary for descending and ascending hypsometers as descending hypsometers require a heating unit to maintain boiling.

Hypsometers have been tested to 70-75 km with plans to extend their capability to 90 km. The Weather Bureau and Bendix Corporation have developed instruments for use above 20 km while full atmospheric range hypsometers have been built by Victory-Engineering Corporation and Cambridge Systems.

The Bendix instrument (Wolber, 1964) avoids many of the difficulties regarding the location of the thermometer to measure the boiling liquid (safrole) by: ".... moving the liquid vapor equilibrium interface completely out of the liquid. This is accomplished by 'pumping' the superheated liquid up onto a thermometer suspended in the vapor. In this manner a liquid-vapor interface is formed on the thermometer itself. The superheated liquid effectively 'boils off' the thermometer into the surrounding vapor."

The following repeatability characteristics were found with a group of 25 test model hypsometers:

± 1 percent of pressure from 35 mm to 15 mm Hg
± 2 percent of pressure from 15 mm to 1.5 mm Hg
± 2 percent of pressure from 1.5 mm Hg to
± 15 percent of pressure at 0.075 mm Hg.

The Weather Bureau hypsometer employes Freon 11 and operates below 60 mb. A small bead thermistor on a straight glass rod serves as the temperature sensor, fitted with a tight wick which is immersed in foam polyethylene that fills a dewar flask.

It is hoped that the full-range hypsometer may replace the baroswitch for low altitude pressure measurements. An interesting feature of the Cambridge Systems instrument is the capability to operate for long periods at fairly high altitudes (minimum of 7 days at 2 mb). Measurements with this instrument are possible down to 0.5 mb.

### A.3.2 DIAPHRAGM GAUGES

This group of pressure sensors consists of the aneroid barometer, bellows-type gauge, the baroswitch, and capacitance-type diaphragm.

The aneroid barometer consists of two thin membranes usually of metal, forming the walls of a closed, evacuated chamber. One of the membranes is fixed at its center while the second membrane is free to move as the thickness of the chamber varies due to atmospheric pressure changes. The chamber wall is maintained at a given pressure by a spring element. A system of levers senses the small movement of the membrane. Constant level balloonsonde measurements have indicated errors of ±3 mb up to 16 km.

The bellows-type pressure gauge (Wenzel, 1964) consists of several aneroid barometer chambers stacked on top of each other. This instrument was designed to measure pressure below the region where early hypsometers were sensitive on rocketsonde flights. As the chamber contracts during descent, this contraction adjusts a potentiometer connected to the radiosonde circuit.

The baroswitch is similar to the aneroid barometer with a lever system connected to a switch. The switch is set to trip at a preset pressure or several pressures.

The capacitance-type diaphragm gauge has one membrane which seals a closed chamber. This membrane acts as one plate of a capacitor and as the pressure changes, the diaphragm deforms changing the capacitance of the system. The sensor has been employed for measurement purposes up to 120 km.

### A.3.3 IONIZATION GAUGES

Ionization gauges operate on the principle that when a sample of air is ionized, the ionization current, or the relation between the voltage at which the sample begins to conduct and the voltage at which ionization ceases, is proportional to the density or pressure of the sample.

The most common ionization gauge is the Alphatron that contains a radioactive source which emits particles which ionize the gas. These ions are collected at an electrode and, in conjunction with a voltage source, produce a small current. The pressure range of the gauge is such that it can be used up to 120 km with errors of 2 to 5 percent.

A high voltage gauge (Philips-Penning) applies 1000 volts or more between two electrically connected electrode plates mounted on both sides of a ring electrode. A magnetic field of 300-8000 oersteds is passed through the electrodes. The gas pressure is related to the current output.

The lower limit of application is determined by a decrease in the ion discharge current to a value comparable with the background current of electrons emitted from the cathode under the effect of a strong electric field. The minimum measurable pressure is $10^{-7}$ to $10^{-6}$ mm Hg (220-340 km). Generally, the maximum pressures measured are between $10^{-1}$ and 1 mm Hg (68-80 km).

The errors of measurement of gas discharge gauges are mainly due to instability of the discharge. At pressures of $10^{-4}$ to $10^{-5}$ Hg they reach ±10 percent,which is somewhat higher than for other ionization gauges.

The thermionic ionization gauge is similar to a glass triode radio tube containing a heated cathode,a grid, and a plate. On the plate, a positive potential of 100 to 250 volts is maintained. Ionization is caused by the heated cathode emitting electrons which are accelerated by the grid and collide with the gas molecules in the gauge chamber. The grid collects the electrons and negative ions while the positive ions are collected by the negative plate. Gas pressure is related to the ratio of plate to grid current. The range of pressures for best use of this device is between $10^{-3}$ to $10^{-8}$ mb. At pressures above $10^{-3}$ mb cathode disintegration occurs. The electron impact on the grid causes a soft X-ray radiation which liberates electrons from the plate at pressures below $10^{-8}$ mb. When the plate is in the form of a small wire suspended in a helical grid element, the range of the gauge is extended to $10^{-10}$ mb (Bayard-Alpert ionization gauge).

### A.3.4 THERMAL CONDUCTIVITY GAUGES

These gauges measure density and pressure by determining the heat transfer coefficient from a heated element to the atmosphere. At pressures below 13 mb, the heat transfer coefficient is a sensitive, virtually linear function of density, and hence pressure. In order to derive the heat transfer coefficient, it is only necessary to know the heat input to the thermal element and its temperature. These instruments are accurate but delicate. Also, the measurement is dependent on the atmospheric constituents.

The Pirani gauge is a thermal conductivity gauge where a fine wire element is heated to between 75 and 400°C and can be used for pressure between $10^{-3}$ and $10^{-8}$ mb. The temperature of the wire is measured by thermistors or by determining the resistance of a heated element in a bridge circuit. A Havens gauge is essentially a Pirani gauge mounted inside a bellows which is alternately compressed and released by a geared electric motor. This results in fluctuations of the output voltage which can be amplified and rectified to determine the ambient pressure. This modification of the Pirani gauge can be used up to 135 km ($\sim 10^{-5}$ mb).

### A.3.5 PITOT-STATIC TUBE

This is a device for measuring pressures in a moving fluid to determine the velocity. In this case, the velocity of the research vehicle is measured and it is density and temperature that are derived from the tube pressure measurements. The pitot-static tube consists of a concentric pipe arrangement in which the inner pipe is open at one end (pointing upstream) and the outer pipe is perforated along a circumference and closed at both ends. Each pipe is connected to a pressure measuring device. The inner pipe measures the total pressure and the outer pipe measures the static pressure. The difference in these two pressures is proportional to the density of the fluid and the square of the velocity. When the velocity of the vehicle is known, the density can be determined from the Rayleigh pitot-static tube equation.

Errors in the angle of attack, aerodynamic effects at supersonic speeds, and the particular configuration of the openings lead to corrections to the measured pressures. Deviations from the proper alignment of the pressure ports can introduce serious uncertainties in interpretation of the data. The possibility of losing the proper alignment is greatest at high speeds. Density errors of 5 to 15 percent are estimated on flights between 20 and 60 km of the X-15 aircraft. A rocket experiment using a pitot-static tube with diaphragm capacitance sensors had density errors of 5 to 10 percent between 45-90 km.

### A.3.6 LASER PROBES

Pressure could be calculated from laser-determined temperature and density profiles (White, Nugent, and Cornier, 1965). Remote measurements of pressure appear to be feasible but are beyond the present state-of-the-art (Harris, Nugent and Cato, 1965).

# BIBLIOGRAPHY - PRESSURE


Ainsworth, J.E., Fox, D.F., and LaGow, H.E., "Upper-Atmosphere Structure Measurement Made with the Pitot-Static Tube," J. Geophys. Res., Wash., D.C., 66(10): 3191-3213, (Oct. 1961).

AMS Bulletin, "Automatic Weather Station for Canadian Artic," 42(11):796, (Nov. 1961).

Babadzhanov, P.B., "Determination of Temperature, Pressure and Density of the Atmosphere by Photographic Observations of Meteors," Geomagnetizm i Aeronomiia, Moscow, &(1): 153-156, (Jan/Feb. 1966).

Bendix Corp., Research Labs. Div., "Development of a Hypsometer for Atmospheric Sounding," Southfield, Mich., Contract DA-36-039 SC 84992, Final Engineering Report, 38 p., (April 1964).

Blackmore, W.R., "A Thermistor Hypsometer," Can. J. Phys., Ottawa, 37(12): 1331-1338, (Dec. 1959).

Browne, J.A., "Atmospheric Pressure Measurement with Fused Quartz Pressure Gage," Trans World Airlines, Inc., Meteorology Dept. Technical Bulletin 65-2, 13 p., (Aug. 1965).

Bundke, W., "A New Technical Apparatus for Measurement of Low Pressure," Umschau, 53(24): 742-743, (Dec. 15, 1953).

Cambou, F., Cotin, F. and Reme, H., "New Device for Measuring Atmospheric Pressure, Using an Impulse Type Ionization Gage," Annales de Geophysique, Paris, 20(3): 346-347, (July/Sept. 1964).

Cena, G., "The New Mercury Barometer Used at Stations of the Servizio Meteorologico dell'Aeronautica," Rivista di Meteorologia Aeronautica, Rome, 19(3): 43-46, (July/Sept. 1959).

Champion, K.S.W., and Faire, A.C., "Falling Sphere Measurements of Atmospheric Density, Temperature, and Pressure, Up to 115 km," AFCRL, Hanscom Field, Mass., Environ. Res. Papers, No. 34, 27 p.,(July 1964).

Dauvillier, A., and Schwob, Y., "A Multiple Meteorograph Recorder," Journal Scientifique de la Meteorologie, Paris, 10(40): 149-155, (Oct/Dec. 1958).

Dmitriev, M.T., "Electrical Methods of Measurement of Atmospheric Pressure and the Radioactive Ionizing Manometers," Nauchno-Issledovatel'skii Institut Gidrometeorologicheskogo Priborostroeniia, Trudy, No. 14: 28-59,(1965).

Dowski, E.R., "High-Altitude Hypsometer Radiosonde Tests," U.S. Signal Research and Development Lab., Ft. Monmouth, N. J., Tech. Rpt. 2242, 15 p., (Dec. 1961).

Engler, N.A., "Development of Methods to Determine Winds, Density, Pressure, and Temperature from the ROBIN Falling Balloon," Univ. Res. Instit., Contract AF19(604)-7450, Final Rpt., Nov. 1960-April 1965, AFCRL-65-448, 141 p., (May 1965).

Fischbach, F.F., "Satellite Method for Pressure and Temperature Below 24 km," Bull. Am. Meteor. Soc., 46(9): 528-532, (Sept. 1965).

Groves, G.V., "Theory of the Rocket-Grenade Method of Measuring Temperature, Pressure, Density and Wind Velocity in the Upper Atmosphere," Royal Soc. of London, Proceedings, Ser. A., 290(1420): 44-73, (Feb. 8, 1966).

Harris, E.D., Nugent, L.J., and Cato, G.A., "Laser Meteorological Radar Study," Electro-Optical Systems, Inc., Final Report, Rpt. No. 5990, AF19(628)- 4309, AFCRL-65-177, 93 pp. (1965).

Hinkel, C., "A New Precision Aneroid Barometer," Meteorological Magazine, London, 91(1079): 154-157, (June 1962).

Israel, G., "Use of a Heat Conductivity Manometer to Measure Pressure Between Zero and 90 km," International Space Science Symposium 2nd, Florence, April 1961, Space Research, 2: Proceedings of the 2nd Symposium, p. 1013-1017, (1961).

Israel, G., "Heat Manometer Utilizable Aboard Rockets from the Surface to 90 Kilometers, Pt. 1," Journal de Macanique et de Physique de l'Atmosphere, Paris, Ser. 2, 3(10):73-99, (April/June 1961).

Liu, V-C, "On a Pitot Tube Method of Upper Atmosphere Measurements," J. Geophys. Tes., Wash., D.C., 61(2, Pt. 1): 171-178, (June 1956).

Meszaros, E., "General Remarks on the Improvement of the Pressure and Temperature Elements of Radiosondes," Idojaras, Budapest, 62(3): 176-177, (May/June 1958).

Niemann, H.B. and Kennedy, B.C., "Omegatron Mass Spectrometer for Partial Pressure Measurements in Upper Atmosphere," Rev. Sci. Instr., N.Y., 37(6): 722-728, (June 1966).

Pellisari, L., "New Barometric Altimeter," Rivisti di Meteorologia Aeronautica, Rome, 17(2): 66-67, (April/June 1957).

Raff, S.J., Parker, M.J., Snavely, B.L., et al., "Report on Phase I of the Feasibility Committee for 200,000 Foot Altitude Instrumented HASP," U.S. Naval Ordnanace Lab., White Oak, Md., NAVORD Report, 6763, 89 p. (Dec. 15, 1959).

Rossger, E. and Ranike, G., "Barometric Altimeter with Sliding (Movable) as Well as Compressible and Extensible Calibration Curves," Archiv fur Meteorologie, Geophysik und Bioklimatologie, Ser. A, Vienna, 12(4): 482-501, (Jan. 1962).

Rossi, V., "A New Finnish Radiosonde, A Radiosonde Provided with Thermostat," Ilmatieteellinen Keskuslaitos, Toimituksia, Finland, No. 43, 22 p., (1957).

Sing, C.Y. and Chin, C.L.D., "Research for the Development of Airborne Atmospheric and Meteorological Instrumentation," Singco, Inc., Burlington, Mass., Contract AF19(628)-3244, Final Report, AFCRL-66-42, 59 p., (Nov. 1965).

Svec, H.J. and Gibbs, D.S, "A Recording Mercurial Manometer for the Pressure Range 0.760 mm of Mercury," Rev. Sci. Instr., 24(3): 202-204, (March 1953).

Usol'tsev, V.A., and Manuilov, K.N., "Basic Characteristics of the A-22-III Radiosonde," Nauchno-Issledovatel'skii Institut Gidrometeorologicheskogo Priborostroeniaa, Trudy, No. 5:3-16, (1957)

Wenzel, "Air-Launched Rocketsonde Study," Final Report, General Dynamics, AF19(625)-3265, AFCEL-64-59, (1964).

Wolber, W., "Development of a Hypsometer for Atmospheric Sounding," Bendix Corp., Final Engineering Report., (1964).

## A.4 DENSITY

Until this past decade, nearly all density profiles were calculated from readily available pressure and temperature profiles through the ideal gas law and the hydrostatic equation. Missile and satellite programs have required information on the densities of the upper atmosphere. Therefore, greater development of direct density measurements has resulted.

### A.4.1 FALLING SPHERE METHOD

This method is based on the measurement of the decleration of a sphere due to aerodynamic drag. The drag force depends on several factors including: the shape of the object, drag area, mass, fall velocity relative to the air and the density of air. At present, the difficulty of accurately determining the drag coefficient represents the weakest link in finding density by this method. For spheres, the drag coefficient is a function of the Reynolds and Mach numbers. The drag coefficient varies slowly with Mach number except in the transonic zone (M ~ 1). In this region the drag coefficient changes very rapidly with Mach number and has not been well defined empirically.

#### A.4.1.1 The Inflatable Sphere

A standard density measuring system is the ROBIN (ROcket Balloon INstrument) inflatable sphere with a corner reflector. Upon rocket ejection at altitude, the 100 gram, 0.5-mil mylar plastic balloon is inflated to a superpressure of 12 mb. Assuming proper inflation, the balloon yields useful data between 30 and 70 km with errors of 2 to 3 percent between 30 and 60 km. At 70 km the balloon is passing through the transonic region so that an error assessment is difficult within this immediate region. With a new metallized sphere (Carten, 1966) the altitude range is extended to 100 km.

Another inflatable sphere was developed by the University of Michigan (Peterson, et al., 1965). This 50-g instrument was used for measurements in the region from 32 to 120 km.

#### A.4.1.2 The Rigid Sphere

The University of Michigan has performed density measurements with a 7-inch, 5-kg aluminum shell sphere with the accelerometer in a fixed position at the center surrounded by telemetry equipment. With this large mass-to-area ratio, the fall velocity remains supersonic, and the above transonic drag coefficient difficulties are not encountered.

#### A.4.1.3 The Active Sphere

The drag acceleration data are acquired by telemetering the output from the accelerometer to a ground tracking station. The first of the two types of accelerometers that have been employed is called the

transit-time accelerometer. The time required for a freely falling mass to drop a fixed distance is measured and the drag acceleration is equal to the distance divided by the square of the time elapsed. This method is not satisfactory when there are rotations or abrupt changes in the wind (which often occur below 50 km) thus producing spurious accelerations.

The second acceleration device involves a system of three mutually perpendicular linear accelerometers which comprise a seismic system and associated position-error detector, a restoring mechanism, and a servo error-signal amplifier. This arrangement allows the transmission of continuous data along three orthogonal axes. Any rotational or wind accelerations can be separated and corrected for in the data.

### A.4.2 PRESSURE-DENSITY GAUGES

The diaphragm gauge, the ionization gauge, and the thermal conductivity gauges used in the pitot-static tube configuration measure pressure, although the density can be calculated. These instruments were described in the previous section on pressure measurements. Diaphragm gauges can measure the density directly from balloonsondes. With rocket probes, all three instruments can be used in pitot-static tubes to measure pressure. Then, the density can be calculated from the Rayleigh pitot formula for a diatomic gas when the ambient pressure, the impact pressure, and the velocity of the rocket are known. A modified form of the Rayleigh equation is used at high supersonic speeds. In this case, the ambient pressure is estimated. A correction must be made for the rocket acceleration when diaphragm gauges are used.

The accuracy of the diaphragm gauges ranged betwen 2 to 10 percent from 20 to 100 km for data obtained by Ainsworth. The accuracy of the Spencer radioactive ionization gauge was 5 percent from 30 to 100 km. A 5-to 10-percent error is expected for the DENPRO (Density Probe Program) for altitudes between 40 and 90 km (Masterson, 1964; and Nordberg, et al., 1964).

### A.4.3 REMOTE SENSING TECHNIQUES

From high velocity rockets and boosters, the ambient density must be measured beyond the region of thermal shock, and boundary layer effects. As a result, remote sensing devices have been developed, all of which are suitable for rocket probes.

#### A.4.3.1 Forward Scattering Technique

The forward scattering of beta rays for density measurements was developed by Parametric, Inc. The main sources of errors, which are estimated to be about 15 percent, are the short penetration distances of the beta

rays at low altitudes, cosmic ray interference at high altitudes, and the interaction of the beta rays with the Earth's magnetic and electric fields. Mounted in a rocket probe on the wing of the X 15, this method can be used between 30 and 75 km.

A.4.3.2 Backscattering Technique

This technique is based on the same principle as forward scattering. The only difference is that the particles are reflected back in a direction that will return them to the detector located near the source. The number of backscattered particles is related to the density of the air as long as the source strength is strong enough to penetrate the region where the scattered particles will be deflected into the detector.

A.4.3.2.1 Beta Particle

This type of backscatter is caused by Rutherford scattering in which the beta particles interact with the electric field of the nucleus and the orbital electrons. A proposed method (Cato, 1964) indicates that densities up to 30 km can be measured by averaging the counting rate over a 2-sec period. Statistical stability is achieved at 30 km by a backscatter pulse count of 1600.

A.4.3.2.2 X-ray Backscatttering

Ideally, this method has an accuracy of 3 to 5 percent at 60 km according to laboratory tests conducted by NASA-Langley. The instrument is intended for operational use in a re-entry space vehicle.

A.4.3.3 Filter Photometer Air Density Gauge

This is a proposed system for density measurements above 75 km that would measure the absorption of the sun's ultraviolet energy at selected wavelengths to derive a vertical profile on an ascending rocket. Changes in density are sensed as a filter photometer measures the changes in the absorption between two levels based on a known air composition. Shock waves of the ascending rocket have no effect on the system and rocket contaminants constitute only a very small portion of the total air column. It is estimated that densities can be calculated between 40 and 200 km with 10-percent accuracy. Complex electronics are needed to telemeter the data and it is required that measurements be made in four wavelengths in order to cover the altitude range.

A.4.3.4 Electron Beam Density Gauge

An electron beam with an energy of 10 kev or higher is "shot" into space and causes fluorescence. This is a method for density measurements above 75 km.

### A.4.3.5 Ultraviolet Air Density Gauge

This is another fluorescence method that is feasible above 75 km. Molecular nitrogen will glow in the visible if the emitted wavelengths are between 500Å and 700Å. The density of the nitrogen molecules is a function of the intensity of the fluorescence. When the proportion of nitrogen in the air is known at a given height, the density of the air can be calculated. The estimated error for the initial tests ranged between 10 and 20 percent; errors of 1 to 2 percent are anticipated for a final operational system.

## A.4.4 INDEX OF REFRACTION

This stellar refraction method for measuring the density profiles below 40 km has been described under temperature sensors.

## A.4.5 LASER TECHNIQUES

Using lasers the density profile can be inferred from the measurement of oxygen concentration using a pulsed device. The density is proportional to the oxygen concentration since the percentage of the oxygen in the atmosphere is essentially constant at lower levels.

## A.4.6 OTHER METHODS

Two other methods for measuring density are the tracking of ionized trails of meteors (above 50 km) and satellite drag perturbations (above 120 km).

The meteor trail technique basically involves the serial photography of meteor trails and the theoretical relation between density and the acceleration and luminescence of the trails (Kramer, 1962; Babadzhanov, 1966).

Atmospheric drag is one of several perturbing forces acting on a satellite in motion. Other forces include the irregular shape of the Earth, the pressure of solar radiation, and the attraction of the nearest celestial bodies. The drag force is related to density and is mathematically separated from the other forces.

## BIBLIOGRAPHY - DENSITY


Ainsworth, J.E., Fox, D.F., and LaGow, H.E., "Upper-Atmosphere Structure Measurement Made With the Pitot-Static Tube," J. Geophys. Res., Wash., D.C., 66(10): 3191-3213, (Oct. 1961).

Babadzhanov, P.B., "Determination of Temperature, Pressure and Density of the Atmosphere by Photographic Observations of Meteors," Geomagnetizm i Aeronomiiz, Moscow, 6(1):153-156, (Jan./Feb. 1966).

Carten, A.S., "Meteorological Measurement Accuracies for Use in the Design and Operation of Aerospace Vehicles,"AMS/AIAA Paper 66-349 presented at Conf. on Aerospace Met., L.A., March 28-31, 1966, (1966).

Cato, G.A., "Ultra-high Altitude Measurement Systems for Pressure, Density, Temperature, and Winds," Electro-Optical Systems, Inc., Final Report, Contract NAS8-5226, EOS Rpt. 3780, 149 p., (1964).

Champion, K.S.W., and Faire, A.C., "Falling Sphere Measurements of Atmospheric Density, Temperature, and Pressure, Up to 115 km," AFCRL Hanscom Field, Mass., Environmental Research Papers, No. 34, 27 p., (July 1964).

Engler, N.A., "Development of Methods to Determine Winds, Density, Pressure, and Temperature from the ROBIN Falling Balloon," Univ. Res. Inst., Contract AF19(604)-7450, Final Rpt., Nov. 1960-Apr. 1965, AFCRL-65-448, 141 p.,(May 1965).

Groves, G.V., "Theory of the Rocket-Grenade Method of Measuring Temperature, Pressure, Density and Wind Velocity in the Upper Atmosphere," Royal Soc. of London, Proceedings, Ser. A, 290(1420): 44-73, (Feb. 8, 1966).

Haycock, O.C., et al., "Investigation and Development of Circuitry on the Falling Sphere Experiment," Utah Univ., Salt Lake City, Upper Air Res. Lab., Contract AF19(604): 6658, Final Report, 112 p, (Oct. 1964).

Jacchia, L.G. and Slowey, J., "Densities and Temperatures from the Atmospheric Drag on Six Artificial Satellites," Smithsonian Inst., Wash., D.C., Astrophys. Obs., Special Rpt., No. 171, 111p. (Mar. 26, 1965).

Jacchia, L.G., and Verniani, F., "Atmospheric Densities and Temperatures from the Drag Analysis of the San Marco Satellites," Smithsonian Inst., Wash., D.C. Astrophys. Obs., Special Rpt., 193, 10 p., (Nov. 12, 1965).

Kramer, E.N., "Determining Atmospheric Density from Meteor Data," Geomagnetizm i Aeronomiia, Moscow, 2(1): 134-139, (1962).

Landini, M., Russo, D. and Tagliaferri, G.L., "Atmospheric Density in the 120-190 km Region Derived from X-ray Extinction Measured by the U.S. Naval Res. Lab Satellite 1964-01-D," Nature, London, 206(4980): 173-174, (Apr. 10, 1963).

Masterson, J.E., "Status of the Direct Probe Sounding Technique for Density," Bull. Am. Meteor. Soc., 45(3):175, (Mar. 1964).

Nordberg, W., and W. Smith, "The Rocket-Grenade Experiment," NASA TN D-2107, 32 pp., (1964).

Peterson, W.J., and Hansen, H., K. McWatters, and F. Bonfanti, "Falling Sphere Measurements over Kwajalein," J. of Geophys. Res., 70(18): 4477-4489 (1965).

## A.5 HUMIDITY

Attempts to accurately determine the moisture profile above 7 km have motivated nearly all of the research on moisture sensing devices during the past decade. Cold temperatures and low water vapor contents cause failure of the standard radiosonde electric hygrometer above this level. Most of the recently developed instruments could be applied for surface measurements in situations where extreme conditions are encountered. Of the recently developed instruments, the frost-point hygrometer is the only device available for measuring the small amounts of moisture found in the stratosphere. Other techniques require further development. Of these, several types of electric hygrometers have shown the most promise for the immediate future.

### A.5.1 DEW/FROST POINT HYGROMETERS

In the dew point technique, an air stream impinges against a small thermostated mirrored surface and the mirror is cooled until dew or frost forms. Stable dew formation is maintained by controlling the mirror temperature through the use of a sensing and control circuit. The dew point is the temperature of the mirrored surface. Dew/frost formation is sensed by an optical system. This optical system plus the mirror refrigeration system lead to relatively large instruments. Recent models have been compacted by taking advantage of improved thermoelectric techniques to regulate the mirror temperature. Since careful shielding of the optics is necessary, air samples must be aspirated. As a result, moisture contamination of the samples might occur. At low humidities, any moisture carried from lower levels presents major difficulties in obtaining representative samples. Honeywell has developed a technique to determine frost layer thickness using alpha particle absorption by the moisture film. This device has the advantage of not requiring optical shielding, and it is claimed to be free of errors due to uncertainty in film thickness. This instrument will measure frost points as low as -100°C.

Generally, these hygrometers have an accuracy of ±0.5°C under sea level conditions and ±2°C at frost points below -60°C under laboratory conditions. The response speed is approximately 2°C $sec^{-1}$ although it is directly proportional to relative humidity. The instruments have the capability of detecting dewpoint-temperature spreads up to 70°C for dewpoints higher than -80°C.

Below temperatures of -90°C water molecules tend to lose their mobility and frost formation is slow. Thus, it is difficult for the dew/frost point hygrometer to accurately determine frost points below this level.

An instrument which can measure dewpoints below -86°C with a slow response time is a temperature controlled gaseous coolant (nitrogen) technique that has been described by Fraser and Weart (1961). This instrument

is capable of measuring dewpoints as low as -190°C. The gauge itself consists of a "cold finger" of gaseous coolant projecting into a chamber. The gas whose dewpoint is to be measured is directed onto a cold surface whose temperature has been lowered by the coolant. The surface of the cold finger is highly polished stainless steel to facilitate the observation of the frost formation. A 30-minute response time is required for dewpoints at -160°C.

### A.5.2 ELECTRIC HYGROMETERS

An electric hygrometer works on the principle of a change in the conductivity of an electrolytic strip in response to changes in relative humidity. The standard U.S. radiosonde contains a strip with a hygroscopic lithium chloride coating. An increase in the resistance indicates a decrease in relative humidity. Moisture absorbed by the soluble hygroscopic salt changes the ionic mobility.

The lithium chloride element has a high lag coefficient at low temperatures so that it is relatively inefficient at the higher levels reached by the radiosonde balloon. In addition, if the element picks up water droplets it suffers from a washout effect. Also, in a direct current circuit, caution must be exercized to protect the element from polarization effects. The instrument has an operating range of 11 to 100 percent relative humidity. Substitution of lithium bromide extends the operating range down to a relative humidity of 5 percent (Asheson, 1965).

The carbon strip sensor is the standard element in the Army-Navy sounding systems. In the carbon humidity element, absorption of moisture alters the dimensions of the insoluble matrix containing dispersed carbon particles which constitute the conductor. Changing separation of the particles varies the resistance. Some improvement in response time is noted. Also the carbon film does not seem to be damaged by passage through rain clouds.

A barium fluoride sensor was developed as a result of a continuing investigation of materials for use in evaporated-film electric hygrometer elements. Absorption of moisture affects the surface electrical conductivity of several materials. Thin films of these materials have a short diffusion path for water molecules which yields a rapid response to changes in ambient humidity. Barium fluoride and lead iodide films produced by evaporation under vacuum have resistance changes of 3 or 4 decades for a relative humidity change from 100 to 10 percent. The time constant for 90 percent response at -20°C for the barium fluoride sensor is around 2 seconds, as compared with more than 100 seconds for lithium chloride. The median value of hysteresis for the film was about 1.5 percent RH with a maximum of 4 percent. Recently, considerable improvement in storage stability has been achieved thus offering a partial solution to a serious calibration drift problem with age.

An equivalent resistance-capacitance circuit constitutes the basics of operation of the aluminum oxide sensor. Moisture absorbed by the sensor leads to changes in both resistance and capacitance. Changes in circuit resistance occur as moisture is absorbed along the side walls of the pores in the oxide layer. Moisture absorbed by the base of the pores changes the capacitance. Hysteresis appears to be negligible for both resistance and capacitance. These instruments measure down to the -80 to -90°C range. The response is about one second for a 10-percent change in relative humidity.

The electrolytic hygrometer with the application of phosphorous pentoxide is described by MacCready and Lake (1965):
" The phosphorous pentoxide moisture sensor is, in theory, a chemical moisture trap and electrolytic cell. The trapping agent, $P_2O_5$, maintains a very low water vapor pressure and equilibrates quite rapidly. The electrolytic cell has two platinum electrodes wound as a very tight double helix on the inside of a small glass tube. The electrolyte, the $P_2O_5 \cdot H_2O$, is introduced as a 10-percent solution in acetone. When the acetone has evaporated, a potential is applied across the two electrodes to drive off the moisture which is present in the hydrate. The sensor is then prepared to pick up moisture from the atmosphere, electrolyze it, and pass the current necessary to read."

Response times are on the order of 1 to 10 seconds, depending on the cell. The cell will operate at temperatures down to -20°C but it is not certain whether low temperatures affect the response time. The operating range is from 0.01 to 30 g/kg mixing ratio. Accuracte sensing of the mass flow rate is critical to the mixing ratio determination. The mass flow sensor can detect changes of less than 0.05 cc/min.

### A.5.3 SPECTROSCOPIC HYGROMETRY

These instruments are more experimental than those discussed above. Basically the technique is to sense radiation in a water-vapor absorption band to determine the water-vapor concentration in the atmosphere. Experiments have been performed at Lyman-alpha (1215.6Å), and water-vapor absorption bands in the infrared. Moisture determinations for layers can be made by incremental changes in the absorption by the atmosphere as a rocket or balloon passes through the atmosphere. Other experiments have scanned the infrared spectrum to deduce a water-vapor profile.

One instrument (which senses in the water-vapor band at 1.3425μ) has a sensitivity of 1 to 2 ppm at low humidities and several ppm at very high humidities. Stability of the calibration is good up to one week and varies somewhat between instruments a month after calibration.

### A.5.4 CAPACITIVE HYGROMETER

This device employs the change in capacitance following changes in the absorbed moisture in a thin hygroscopic liquid layer. The hygroscopic liquid is thinly coated on granules of Fluorapak, an inert fluoracarbon prepared for chromatographic columns. If the equilibrium between the layer of hygroscopic fluid and water vapor in the ambient air is ideal, then it is possible to apply Raoult's law. This law states that the partial pressure of water vapor over the hygroscopic fluid is proportional to the fractional molecular weight of water absorbed in the film. Also, the dielectric constant is a function of the quantity of water in the liquid phase. Thus, changes in capacitance are related to changes in the relative humidity.

Laboratory tests have shown that this instrument can measure partial pressures of water vapor of 1 mb with 10-percent accuracy. The instrument appears to have a lower limit of 0.1 mb which corresponds to a frost point of $-40^{\circ}C$.

### A.5.5 LASER TECHNIQUE

The PLIDAR technique has been proposed to determine the molecular number density of water vapor up to 10 km by Harris, Nugent, and Cato (1965), and White, Nugent, and Carrier (1965). This technique employs two pulsed ruby lasers (or a single laser providing two simultaneous pulses at different frequencies by Raman shifting). One of the pulses would be tuned to 6933.8Å, the wavelength of a strong water vapor absorption band while the other would be tuned to an adjacent atmospheric "window".

The molecular number density of the water vapor can be determined from measurements of the height derivative of the ratio of the intensities of light backscattered from the two pulses provided that the water-vapor absorption is known. This coefficient is related to temperature and pressure. Therefore, the temperature profile must be known. It has been suggested that the temperature profile be determined from the relation between absorption line structure and temperature, but the functional relation is not well known.

Another approach involves the time history of the spectral distribution of the backscattered energy. This energy is interpreted in terms of the spatial distribution of water vapor.

### A.5.6 MICROWAVE REFRACTOMETER RADIOMETER

Microwave hygrometers work on the principle that the resonance frequency of a cavity at microwave frequencies depends upon the refractive index of air, which is a function of water vapor content. Also, it has been proposed that microwave radiometers could be used to determine the total

precipitable liquid water in clouds and precipitation, since the absorption of microwave radiation depends upon the amount of $H_2O$.

### A.5.7 ICE SPHERE

Measurement of the rate of mass change of a ventilated ice sphere enables the relative humidity in its environment to be determined. The sphere is suspended from a sensitive quartz spring and the vertical movements accompanying the mass changes are indicated, by means of an optical device, by pulses recorded on an electromagnetic counter. Measured relative humidities are accurate to ±5 percent over the temperature range 0 to $-60^{\circ}C$.

### A.5.8 COBALT METHOD

Benzina (1966) describes a colorimetric method for determining the relative humidity of the atmosphere based upon variations in the color of a cobalt salt solution with absorption of moisture and on the fact that water solutions of $H_2SO_4$ are characterized by a definite amount of water vapor above their surfaces depending upon their concentration. Using filter paper moistened by a 16-percent solution of $COCl_2$ a color scale was established for relative humidities between 15 and 100 percent. Correspondence was established between relative humidities measured colorimetrically and psychometrically.

### A.5.9 COOLED-VAPOR TRAP

This method freezes out the water vapor and carbon dioxide from the air directly, by drawing the air through a vapor trap cooled in liquid nitrogen (Barclay, et al., 1960). The amount of carbon dioxide collected is then used as a measure of the total amount of air sampled, assuming the ratio of carbon dioxide to air to be constant. This apparatus was flown once at a mean altitude of 27 km.

### A.5.10 THERMAL(ULTRA-DRY BULB) HYGROMETER

A flow of air is passed through a hygroscopic porous bed. In transit, the temperature of the air rises (temperature of adiabatic drying). The temperature rise of the air is a measure of absolute humidity. This method seems primarily designed for measuring humidity over a fairly wide range as the instrument retains its sensitivity at low humidity values.

# BIBLIOGRAPHY - HUMIDITY


Appleman, H.S., "Relative Humidity Errors Resulting from Ambiguous Dew-Point Hygrometer Readings," J. Appl. Meteor., 3(1):113-115, (Feb. 1964).

Asheson, D.T., "Some Limitations and Errors Inherent in the Use of the Dew Cell for Measurement of Atmospheric Dew Points," Monthly Weather Review, 91(5): 183-190, (May 1963).

Asheson, D.T., "Lithium Bromide Dew Cell," J. Appl. Meteor., 4(5): 646-648, (Oct. 1965).

Badinov, I.Ia, Andreev, S.D., and Lipatov, V.B., "Measurement of Humidity in the Upper Atmosphere," Akad. Nauk SSSR. Mexhdovedomstvennyi Geofizicheskii Komitet, Meteorologicheskie Issledovaniia: Sbornik Statei (II Razdel Programmy MGG), No. 12: 66-79, (1966).

Ballinger, J.G., Koehler, L.E., and Murphy, R.D., "Contamination Effects in Stratospheric Humidity Measurements," Honeywell Inc. Systems and Res. Div., Contract AF19(628)-3857, Final Report, July 1964 to July 1965, 95p. (Aug. 1965).

Ballinger, J.G., et al., "Toward Improved Measurements of Stratospheric Humidity with Balloon-borne Frost-point Hygrometers," U.S. Air Force, Cambridge Research Center, Air Force Surveys in Geophysics, No. 167: 231-259, (July 1965).

Barclay, F.R., Elliott, M.J.W., Goldsmith, P., and Jelley, J.V., "A Direct Measurement of the Humidity in the Stratosphere Using a Cooled-Vapour Trap," Royal Meteor. Soc., Quart. Journal, 86(328): 259-264, (Apr. 1960).

Barzhenevskii, N.S., and Belkina, M.M., "A Carbon Humidity Sensor," Leningrad, Nauchno-Issledovatel'skii Institut Gidrometeorologicheskogo Priborostroeniia, Trudy, No. 14: 60-74, (1965).

Barzhenevskii, N.S., and Mel'ster, R.A., "Study of Electrolytic Humidity Sensors," Leningrad, Nauchno-Issledovatel'skii Institut Gidrometeorologicheskogo Priborostroeniia, Trudy, No. 12: 89-96, (1964).

Beaubien, D.J., and Francisco, C.C., "Design, and Construction and Evaluation of an Electronic Dew Point Indicator," Cambridge Systems, Inc., Newton, Mass., Contract AF19(604)-8812, Final Report, 42 p., (Jan. 1962).

Benzina, G.I., "Determination of the Relative Humidity of the Air by Means of the Cobalt Method," Gigiena i Sanitariia, Moscow, No. 1: 60-61, (Jan. 1966).

Bogorodskii, M.M., "Marine Gradient Apparatus for Studying Fields of Atmospheric Temperature and Humidity," Akademiia Nauk SSSR. Morskoi Gidrofizicheskii Institut, Trudy, 25:57-64,(1962).

Boyuoucos, G.J. and Cook, R.L., "Humidity Sensor: Permanent Electric Hygrometer for Continuous Measurement of the Relative Humidity of the Air," Soil Science, Baltimore, 100(1):63-67, (July 1965).

Charlson, R.J., "Liquid Film Hygrometer," Science, Wash., D.C., 143(3610): 1031-1032, (March 1964).

Charlson, R.J., and Buettner, K.J.K., "Investigations of Some Techniques for Measurement of Humidity at High Altitudes," Wash. Univ., Seattle, Dept. of Atmos. Sci. Contract AF19(628)-303, Sci. Rpt. No. 1, 11p., (Mar. 1963).

Charlson, R.J., and Buettner, K.J.K., "Liquid Film Hygrometry," Wash., Univ. Dept. of Atmos. Sci., Contract AF19(628)-303, Sci. Rpt. No.2, 74 p, (May 1964).

Charlson, R.J., Buettner, K.J.K., and Maykut, G.A., "Liquid Film Hygrometry," Wash. Univ., Seattle, Dept. of Atmos. Sci., Contract AF19(628)-303, Final Report, Feb. 1, 1964 - July 31, 1965, 12 p., (March 1966).

Cook Research Labs., Skokie, Ill., "Improved Infrared Absorption Hygrometer for Aircraft Observations of Atmospheric Moisture," Contract AF33(038)-2324, Interim Report PR 17-24, 7 p.,(May 1965).

Cunningham, R.M., "Microwave Refractometer Used as a Humidity Sensor in Cloud Physics," International Symposium on Humidity and Moisture,Wash., D.C., May 1963, Humidity and Moisture, Vol. 2, p. 615-627, (1965).

Dauvillier, A. and Schwob, Y., "A Multiple Meteorograph Recorder," Journal Scientifique de la Meteorologie, Paris, 10(40): 149-155, (Oct./Dec.1958).

Downes, J.G., and Nordon, P., "The Thermal or Ultra-Dry Bulb Hygrometer," J. Sci. Instr., London, 40(12): 596-598, (Dec. 1963).

Dulk, G.A., "Development and Flight Test of a Dew-Point Hygrometer Utilizing Thermoelectric (Peltier)Cooling," U.S. Proving Ground, Aberdeen, Md., Ballistic Res. Labs. Memorandum Report, No. 1308, 29 p., (Nov. 1960).

Elagina, L.G., "Optical Device for Measuring Turbulent Humidity Pulsations," Akad. Nauk SSSR, Izvestiia, Ser. Geofiz, No. 8: 1100-1107 (Aug. 1962).

Fateev, N.P., "New Automatic Condensation Hygrometer," Glavnaia Geofiz. Observatoriia, Trudy, No. 83: 3-19, (1958).

Foster, N.B., Volz, D.T., and Foskett, L.W., "A Spectral Hygrometer for Measuring Total Precipitable Water," Wash., D.C., U.S. Weather Bureau, 26 p.,(June 1963).

Fraser, M.J., and Weart, H.W., "Apparatus for Measuring Dewpoints Below -86°C," Rev. Sci. Instr., 32(2): 221-222, (Feb. 1961).

Gerthsen, P., Gilsing, J.A., and van Tol, M., "Automatic Dew-Point Hygrometer Using Peltier Cooling," Philips Tech. Rev., Eindhoven, Netherlands, 21(7): 196-200, (1959/60).

Glazova, E.F., "Measurement of Air Humidity by Resistance Thermometers," Glavnaia Geofiz. Observatoriia, Trudy, 103: 90-92, (1960).

Gokhale, N.R. and Gatha, K.M., "A New Dew-Point Hygrometer," Indian Journal of Meteorology and Geophysics, Delhi, 10(3): 337-340, (July 1959).

Gralenski, F., "Design Modification and Laboratory Testing of the ML-592/TMQ-11 Electronic Dew Point Sensor," Cambridge Systems, Inc., Newton Mass., Contract AF19(628)-4216, Final Report, Nov. 1964-June 1965, 39 p., (June 1965).

Grantham, D., Sissenwine, N., and Salmela, H., "AFCRL Stratospheric Humidity Progra ," U.S. Air Force, Cambridge Research Center, Air Force Surveys in Geophysics, No. 167: 261-272, (July 1965).

Greinacher, H., "A Diffusion Hygrometer with Direct Reading," Schweizer Archiv fur Angewandte Wissenschaft und Technik, Zurich, 20(6):198-200, (June 1954).

Griffin, O.G., and Strinfield, C.M., "Dew Point Meter Based on Thermoelectric Cooling," J. Sci. Instr., London, 41(4): 241, (Apr. 1964).

Gruber, A., "A Modification of the American Radiosonde AMT-4 to Eliminate Errors Due to Condensation of Moisture," Archiv fur Meteorologie, Geophysik und Bioklimatologie, Ser. A., Vienna, 12(4): 474-481, (Jan. 1962).

Hanson, D.W., "Instrumentation Requirements for the Remote Microwave Probing of the Atmosphere," U.S. National Bureau of Standards, NBS Report No. 8273, 41 p., (Mar. 1964).

Harris, E.D., Nugent, L.J., and Cato, G.A., "Laser Meteorological Radar Study," Electro-Optical Systems, Inc., Final Report, Rpt. No. 5990, AF19(628)-4309, AFCRL-65-177, 93 -, (1965).

Hohne, W., "Resetting of the LiCl Dew Point Hygrometer," Idojaras, Budapest, 67(4): 213-225, (July/Aug, 1963).

Houghton, J.T., "Effect of Contamination on Spectroscopic Determinations of Stratospheric Water Vapour," Royal Met. Soc., Quart. J., 92(392): 281-283, (Apr. 1966).

International Symposium on Humidity and Moisture, Wash., D.C., May 1963, Humidity and Moisture, Vol. 1-4, (1965).

Johansson, G., "Moisture Analysis by Use of Microwaves," Internat. Symp. on Humidity and Moisture, Wash., D.C., May 1963, Humidity and Moisture, Vol. 2, p. 609-610, (1965).

Jones, F.E., "Performance of the Barium Fluoride Film Hygrometer Element on Radiosonde Flights," J. Geophys. Res., Wash., D.C., 68(9): 2735-2751, (May 1, 1963).

Kaplan, L.D., "Inference of Atmospheric Structure from Remote Radiation Measurements," (M.I.T. Cambridge), J. Opt. Soc. Am., 49(10):1004-1007, (Oct. 1959).

King, R.L., and Parry, H.D., "Field Tests and Calibration of the Total Atmospheric Water Vapor Hygrometer," Internat. Symp. on Humidity and Moisture, Wash., D.C., May 1963, Humidity and Moisture, Vol. 2, 450-457, (1965).

Kolomets, N.V., Starnzas, M.S., Stil'bans, N.S., and Fateev, N.P., "The Measurement of Atmospheric Humidity with Semiconductor Thermocouples," Zhurnal Teknicheskoi Fiziki, Moscow, 26(3): 686-692, (1956).

Konstantinov, A.R., "Errors of Inertial Devices Measuring Air Temperature and Humidity in an Atmosphere With Heterogeneous Temperatures," Nauchno-Issledovatel'skii Gidrometeorologicheskii Institut, 26:145-156, (1961).

Mastenbrook, H.J., "Frost-Point Hygrometer Measurements in the Stratosphere and the Problem of Moisture Contamination," Internat. Symp. on Humidity and Moisture, Wash., D.C., May 1963, Humidity and Moisture, Vol. 2, 480-485, (1965).

MacCready, P., and Lake, J., "Mixing Ratio Indicator," In Humidity and Moisture, Vol. 1, ed. A. Wexler, Reinhold, N.Y., 512-521 (1965).

Rohrbough, S., "Study of High Altitude Water Vapor Detectors," General Mills, Inc., Electronics Division, St. Paul, Minnesota, Contract AF19(628)-483, Sci. and Final Rpt., 27 p.,(Mar. 31, 1963).

Rossi, V., "A New Finnish Radiosonde, a Radiosonde Provided With Thermostat," Ilmatieteellinen Keskuslaitos, Toimituksia, Finland, No.43, 22p. (1957).

Sargent, J., "Recording Microwave Hygrometer," Rev. Sci. Instr., 30(5): 348-355, (May 1959).

Skatskii, V.I., and Shchelokov, V.V., "Airplane Device for Complete Measurement of Meteorological and Dynamic Characteristics of the Atmosphere Including Clouds," Akad. Nauk SSR, Izvestiia, Ser. Geofiz., No. 8: 1270-1277,(Aug. 1963).

Usol'tsev, V.A. and Manuilov, K.N., "Basic Characteristics of the A-22-III Radiosonde," Nauchno-Issledovatel'skii Institut Gidrometeorologicheskogo Priborostroeniaa, Trudy, No. 5:3-16, (1957).

Waters, J.L., "Adaptation of an Electrolytic Water Vapor Detector for Balloon Measurement of Water Content of the Atmosphere," Waters Associates, Framingham, Mass., Contract AF19(604)-5464, Final Report on Phase 2, 10 p., (Apr. 1960).

Wexler, A. and Hyland, R.W., "NBS Standard Hygrometer," U.S. National Bureau of Standards, Monograph No. 73, 35 p., (May 1, 1964).

White, G.R., Nugent, L.J., and Carrier, L.W., "Laser Atmospheric Probes," Inst. Soc. A., Preprint No. 40.1-1-65, 20th Annual ISA Conf. and Exhibit, Los Angeles, 11 pp, (1965).

Wildhack, W.A., "Hygrometer, Type 26-301, Moisture Monitor," (manufactured by the Consolidated Electrodynamics Corporation, 300 North Sierra Madre Villa, Pasadena, California), Rev. Sci. Instr., 28(1): 63-64, (Jan. 1957).

Wood, R.C., "The Infrared Hygrometer as a Potential Meteorological Aid," Bull. Am. Meteor. Soc., 40(6): 280-284, (June 1959).

## A.6 WIND DIRECTION AND SPEED

Three general techniques for upper air wind measurement have been developed or refined during the past decade. These are 1) passive tracking of a target, 2) acoustic (grenade) technique, and 3) measurement of the wind sensitive aspect of a rocket. The passive tracking technique is the most widely used and extensively developed. Tracking is accomplished with both optical and radar techniques with rising and falling spheres, balloons, parachutes, and chaff as well as vapor and meteor trails. These techniques have provided some wind information up to 300 km.

Developments in surface wind instrumentation have focussed on measuring very light and very strong winds (primarily with hot wire anemometers). In addition, increased interest in atmospheric turbulence and diffusion studies has resulted in the development of more responsive anemometers and wind vanes. Further, these micrometeorological efforts have brought about instruments for measuring the vertical component of the wind.

### A.6.1 PASSIVE TRACKING OF A TARGET

In this technique a ground-based instrument is utilized to view the movements of a sensor passing through the atmosphere. The assumption is made that the sensor is responding in a known fashion to the ambient winds. It is obvious that this assumption is not completely valid and that the degree of responsiveness is dependent on the characteristics of the individual sensors.

Passive tracking of the radiosonde balloon was first performed by theodolite but in the past decade sophisticated radar has permitted tracking of the sensor over long distances. The development of radar has coincided with an increasing need to learn about the fine scale structure of the upper altitude wind field.

#### A.6.1.1 Balloons

Most of the balloon effort has concentrated on the development of sensors that are independent of Reynolds number. Operation of a balloon at a Reynolds number which is supercritical gives random lateral balloon motions which obscure all but the gross features of the sounding. Also, flight in the subcritical regime gives satisfactory balloon-wind measurements because the self-induced spiral or zigzag movements tend to be regular and average out over a vertical distance commonly used for wind calculations (MacCready, 1965).

Balloons that are currently used for detailed wind sounding purposes include 1) ROSE (a metalized superpressure rising balloon), 2) ROBIN (a small mylar descending balloon with integral radar target), 3) Jimsphere (a superpressure ROSE balloon roughened with the addition of a number of

conical cups pointed outward from the surface of the balloon). Scoggins (1965) has reported that the drag coefficient for the Jimsphere is essentially independent of Reynolds number. The roughness elements satisfactorily reduce the induced motion of smoother spheres. The Jimsphere and ROSE balloons are generally used from the surface to 30 km while the ROBIN is employed from 30 to 70 km.

The rms errors for the ROBIN balloon sphere are as follows (Lenhard and Wright, 1963): 1) 4.4 kts between 60 and 70 km, 2) 1.8 kts between 50 and 60 km, 3) 1.1 kts between 40 and 50 km.

### A.6.1.2 Other Passive Sensors

Radar-reflective parachutes and dipole chaff are two frequently used sensors. The parachute is ejected from a rocket at about 65 to 70 km and is useful down to about 30 km. Chaff is effective from 15 to 90 km. Light chaff gives the best results above 40 km due to the slower descent rate.

The total wind error for the 15-foot parachute used with the ARCAS launch vehicle is about 3 m/sec for 1-minute average winds.

Errors for the chaff depend on the altitude and the type of material. Estimates differ widely, ranging from ±4 kts (Aufm Kampe and Lowenthal 1963) to a 30-kt difference for simultaneous chaff and parachute observations at 65 km (Jenkins, 1962). In the 30-to 40-km range, Bruch and Morgan (1961) estimated the error to be between 12 and 14 kts.

## A.6.2 ACOUSTIC-GRENADE SOUNDING

Shock waves from rocket-grenade explosions have been used to determine the wind structure of the upper atmosphere from measurements of the travel time to microphones at ground level. The wind for the layer between grenade explosions (usually 1.5 to 3 km) can be determined by analysis of the generated acoustic waves reaching the ground-based recorder. These wind profiles lack the detail that is available from other methods. Most of the recent work on the acoustical technique has primarily involved improvements in the acoustic recording system, especially the microphone. The acoustic technique requires careful calibration and handling of sizeable amounts of equipment and is not practical for experiments where size is a factor.

## A.6.3 RESISTANCE FILM

This is an aircraft-borne heated device for detecting the jet stream. The system was designed to detect wind velocity differences of 0.01 miles per hour with a time averaging ability such that the period of averaging of the instantaneous wind is only long enough to allow the jet stream velocity gradients along the wing of an airplane to become clear.

Temperature differences are measured between thermal probes (heated platinum films) mounted on each wing-tip of an aircraft. Each sensor operates as an arm of half of a four-arm resistance bridge. Sensitivity is increased by heating the film to high temperatures.

### A.6.4 LASER TECHNIQUES

The wind is sensed by the application of optical Doppler techniques to PLIDAR signals from atmospheric aerosols moving with the wind.

For successful measurement of winds by PLIDAR, the Doppler frequency shift must be greater than the output pulse frequency bandwidth. The Doppler-velocity measurements are satisfactory for particle velocities to about 500 m/sec. At higher velocities, the laser beam must be subcarrier modulated. White, Nugent, and Carrier (1965) state: "... it is readily apparent that transmitter characteristics are critical factors in any laser system designed to measure wind velocity by Doppler techniques. Direct optical Doppler will require excessive receiver bandwidth; however, it will allow better range resolution. Subcarrier Doppler, on the other hand, while requiring receiver bandwidths of only tens of kilocycles, will require absolute transmitter frequency stability on the order of kilocycles, and range resolution can be seriously degraded."

### A.6.5 PRESSURE DIFFERENCE TRANSDUCER

There are two techniques that are described by Morrissey (1965) of AFCRL for wind measurements from sensors released from aircraft: (1) The first instrument is a transducer which is able to determine pressure differences on opposite sides of the rotating sensor. Gyroscopic action is used to rigidly orient the sonde in the vertical direction and the angle of attack is sensed. The sensor is rotated at one revolution per second which provides sampling in all directions every 100 feet of altitude for fall rates as high as 350 ft/sec. (2) The sonde is sensitive to the angle of attack and its inclination to the vertical is sensed. Further, the sonde is designed to seek a zero angle of attack. A rotating accelerometer is the sensor whose sensitive "plane" (plane instead of axis due to rotation) is normal to the aerodynamic axis of the sonde. The angle between the plane and the vertical is the output of the sonde which is related to the wind at any level.

### A.6.6 DISPLACEMENT OF THE OZONOSPHERE

Wurtz and Neiswander (1963) have developed a technique for the measurement of upper level winds by using the ozonosphere as a target. If structure could be observed, the pattern could be followed as it moves by a fixed-field ozonosphere radiometer. This gas target is more responsive to wind movement than any introduced sensor (balloons, chaff, etc.) and

continuous observations would be possible. This technique would be most fruitful in the 15-to 22-km layer. Early studies have been generally inconclusive.

### A.6.7 IONOSPHERIC DRIFT

Fraser (1965) describes a method where the horizontal wind is measured by ground-based radio equipment by the Mitra (spaced receiver) technique. This technique measures ionospheric drift velocities. The motion of the electron density fluctuations in the upper atmosphere is detected by a radio wave diffraction technique. The elctron cloud velocity thus determined can be interpreted as movement of the neutral air if the collision frequency between the electrons and the neutral air molecules is high enough so that the anisotropy introduced by the Earth's magnetic field can be neglected. This assumption seems valid to 120 km. Solar control of the ionization processes does not allow continuous measurements all day (with a single radio frequency). Observations can be made down to 75 km in the summer and 65 km in the winter.

Approximations introduced in the technique can cause the calculated velocity to be 50-percent higher than the true velocity and vector direction errors of $20^{o}$ to $30^{o}$ are possible. The height of observation is accurate to about 3 km below 100 km, and between 5 and 8 km at heights of 120 km.

### A.6.8 LIFTING SENSORS

The vertical wind profile can be measured from the surface to 30 km in 10 to 15 minutes by a missile-like body with a large cruciform or annular wing (Stengel, 1966). Using the linearized equations of motion to determine the wind response transfer, a sample configuration is shown to have a maximum resolution more than an order of magnitude better than a drag wind sensor (balloon, chaff, etc.) with the same fall velocity. By employing an iterative technique, the accuracy of the wind-profile estimate can be increased by at least an order of magnitude.

### A.6.9 CHEMICAL RELEASE

There are two types of chemical clouds that have been used for wind measurement. One is composed of trimethyl aluminum (TMA) and the other of alkali metals. The combination of both techniques has permitted wind determinations through the night from twilight to twilight in the high atmosphere.

#### A.6.9.1 Trimethyl Aluminum (TMA) Clouds

The liquid is ejected from a rocket and subsequently vaporized at the low pressures. It then chemically combines with one or the other of

the oxygen allotropes and emits visible radiation. Spectra of the radiation have been analyzed to show both line and continuum emissions (Rosenberg, et al., 1963a). The lower end of the usable light range is about 100 km due to the failure of the compound to produce an excited state because of a diminished percentage of the TMA-oxygen reaction at lower heights (Rosenberg, et al., 1963b).

The cloud is visible against the sky background both at twilight and at night. Triangulation photographs of the visible cloud allow a determination of the wind. Identified slopes on the cloud photographs permit height determinations to within 100 meters and wind velocities within 3 m/sec (Rosenberg, el al., 1966).

### A.6.9.2 Alkali Metal Clouds

The vaporization of metallic sodium, cesium, and lithium and their subsequent release from a rocket have been used to form photographable trails from about 85 km up to 200 km. The radiation from these clouds is a resonance scattering phenomena. Therefore, they are limited to twilight situations when the solar-illuminated clouds can be photographed against reduced sky background intensities. Typical sodium vapor trail photographs have been analyzed to give wind velocities every kilometer.

## BIBLIOGRAPHY - WIND DIRECTION AND SPEED


AMS Bulletin, "Automatic Weather Station for Canadian Artic," 42(11):796, (Nov. 1961).

Angell, J.K., "Use of Tetroons for Mesometeorological Investigations," Mon. Wea. Rev., 88(8): 277, (Aug. 1960).

Atlas, D., "Radar Wind-Velocity-Measurement Technique," U.S. Air Force, Office of Aerospace Res, Res. Rev. 4(1): 3, (Mar. 1965).

Aufm Kampl, H., and M. Lowenthal, First Internat. Symp., Rocket and Satellite Meteor., Wash., 1962, (1963).

Baliles, M.D., and Kohler, J.P., "History of Weather Bureau Wind Measurements," U.S. Weather Bureau, Key to Meteorological Records Documentation No. 3, 151, 68 p. (1963).

Ballard, H.N., "Rocketsonde Techniques for the Measurements of Temperature and Wind in the Stratosphere," U.S. Army Elec. Res. and Develop. Act., White Sands, N.M., ERDA-269, 106 p.

Bardeau, H. and Saporte, R., "Direct Reading Anemometer Using a Hot Thermistor," Journal de Recherches Atmospheriques, Clermont-Ferrand, No. 1: 56-64, (Jan./Mar. 1964).

Beling, T.E., Benders, D.R. and Plante, R.L. "Measurement of Wind Shear," United Res., Inc., Cambridge, Mass., Contract DA 36-039 SC-84850, Final Report, 40 p. (1961).

Berger-Landefeldt, U., "Long-Range Measurements of the Vertical Component of the Wind," United Nations Educ., Scientific and Cultural Organ., Arid Zone Res., No. 25, p. 71-75, (1965).

Bhattacharyya, J.C. and Prakash, S., "A Mean Windspeed Indicator," Indian J. Meteor. and Geophys., Delhi, 15(2): 277-280, (Apr. 1964).

Bollermann, B and Walker R.L., "New Low Cost Meteorological Rocket System for Temperature and Wind Measurement in the 75,000 to 200,000 feet Altitude Region," AMS/AIAA Conf. on Aerospace Meteor., L.A. Calif., Mar. 28-31, 1966, AMS/AIAA Papers, 66-383, 23 p.,(Mar 1966)

Bruch, A., and Morgan, G.M., New York Univ., College of Engineering, Final Report Contract AF19(604)06193, (May 1961).

Champagne, F.H., and Lundberg, J.L., "Linearizer for Constant Temperature Hot Wire Anemometer," Rev. Sci. Instr., N.Y., 37(7): 838-843, (July 1966).

Champion, K.S.W., and Zimmerman, S.P., "Winds and Turbulence at 200,000 to 400,000 Feet from Chemical Release," U.S. Air Force, Cambridge Res. Labs., Air Force Surveys in Geophysics, No. 140, Vol. 2: 225-235, (Mar. 1962).

Cooke, T.H.,"A Smoke Trail Technique for Measuring Wind," Royal Meteor. Soc., Quart. J., 88(375): 83-88, (Jan. 1962).

Crouser, H.H., "Wind Speed Measuring System, Frequency Type," Mon. Wea. Rev., Wash., D.C., 90(1): 23-25, (Jan. 1962).

Doe, L.A.E, "A Three Component Thrust Anemometer for Studies of Vertical Transports above the Sea Surface," Canada, Bedford Inst. of Oceanography, Darmouth, N.S., Report B.I.O., 63-1, 87 p., (Apr. 1963).

Eckstrom, C.V., "Theoretical Study and Engineering Development of Jimsphere Wind Sensor," Schjeldahl, C.T., Co., Northfield, Minn., Contract NAS8-11158, Final Report, 81 p.,(July 1965).

Eddy, A., et al., "Determination of Winds from Meteorological Rocket Sondes," Texas Univ., Austin, College of Engineering, Atmos. Sci. Group, Contract DA-23-072-AMC-1564, Report No. 2, 29 p., (Nov. 1965).

Engler, N.A., "Development of Methods to Determine Winds, Density, Pressure, and Temperature from the ROBIN Falling Balloon," Univ. Res. Inst., Contract AF19(604)-7450, Final Report, Nov. 1960-Apr. 1965, AFCRL-65-448, 141 p., (May 1965).

Engler, N.A., and Wright, J.B., "Wind Sensing Capability of the ROBIN," AFCRL No. 140, Vol. 2: 237-247, (Mar. 1962).

Ervet, P., and Robuchon, A., "High Precision Measurement of Upper Winds by Mean of Two Automatic Tracking Radars," La Meteorologie, Paris, Ser. 4, No. 54, 121-128, (Apr./June 1959).

Fraser, G.J., "Measurement of Atmospheric Winds at Altitudes of 64-120 km Using Ground-Based Radio Equipment," J. Atmos. Sci., 22(2):217-218, (Mar. 1965).

Fujita, T., Black, P.G., and Loesch, A.G., "Use of Wet-Beam Doppler Winds in the Determination of the Vertical Velocity of Raindrops Inside Hurricane Rainbands," Chicago, Univ. Dept. of the Geophys. Sci., Satellite and Mesometeor. Res. Proj. Paper No. 59, 32 p., (Apr. 1966).

Glass, R.I., Jr., "Improved System for Measuring Wind Components," U.S. Army Elec. Res. and Devel. Act., White Sands, N.M., ERDA-267, (Feb. 1965).

Gorelik, A.G., Kostarev, V.V. and Chernikov, A.A., "Coordinate-Doppler Method of Wind Observation," U.S. Air Force, Cambridge Res. Labs., Res. Translation T-R-512, 7 p., (Dec. 1965).

Groves, G.V., "Meteorological and Atmospheric Structure Studies with Grenades," International Space Science Symposium, 4th, Warsaw, 1963, Space Research, 4, 155-170 (1964).

Groves, G.V., "Theory of the Rocket-Grenade Method of Measuring Temperature, Pressure, Density and Wind Velocity in the Upper Atmosphere," Royal Soc. of London, Proceedings, Ser. A, 290(1420): 44-73, (Feb. 8, 1966).

Heinrich, H.G., et al., "Modification of the ROBIN Meteorological Balloon, Vol.2, Drag Evaluations," Litton Systems, Inc., Appl.Sci. Div., St. Paul, Minn., Contract AF19(628)-2945, Final Report (Part 2), April 15, 1963-April 30, 1965, (Sept. 1965).

Hohne, W., "Wind Measuring Equipment for Ship Weather Stations," Zeit. fur Meteorologie, Berlin, 14(10): 225-233, (Oct. 1961).

Holmes, R.M., Gill G.C. and Carson, H.W., "Propellor-Type Vertical Anemometer," J. Appl. Meteor., 3(6): 802-804,(Dec. 1964).

Hussenot, C., and Ricou, F., "Improvements Effected in the Constant Temperature Hot Wire Anemometer by the Use of a 'Chain of Diodes' as Linearization Circuit," Acad. des Sci., Paris, Comptes Rendus, 253(23): 2629-2631 (Dec. 4, 1961).

Jenkins, K.R., "Empirical Comparisons of Meteorological Rockets Wind Sensors," J. Appl. Meteor., 1(2), 196-202 (1962).

Jenkins, K.R. and Webb, W.L., "High Altitude Wind Measurements," J. Meteor. 16(5): 511-515, (Oct. 1959).

Kaimal, J.C., and Businger, J.A., "Continuous Wave Sonic Anemometer-Thermometer," J. Appl. Meteor., 2(1): 156-164 (Feb. 1963).

Kaplan, L.D., "Inference of Atmospheric Structure From Remote Radiaion Measurements," (MIT Cambridge), J. Opt. Soc. Am., 49(10): 1004-1007 (Oct. 1959).

Karmin, I., "The Resolving Anemometer," Am. Meteor. Soc. Bull., 40(9): 473-476,(Sept. 1965)

Karpusha, V.E., Protopopov, N.G., Sternzat, M.S. et al., "M-45 Self-Recorder for Recording the Mean Velocity and Direction of Wind," Glavnaia Geofiz. Observatoriiz, Trudy, 103:93-102, (1960).

Kaulin, N. Ia., "Measurement of Wind Velocity," Glavnaia Geofiz. Observatoriia, Trudy, No. 108: 48-58,(1960)

Kempo, J.F., "Stable Hot- Wire Anemometer for Low Speeds," Amer. Soc. of Heating and Air Cond. Engineers, Transactions, 64:163-174 (1958).

Kolbig, J, "Determining Wind Profiles up to 300 m Above the Ground by Stereophotogrammetric Measurement of Smoke Tracers," Aeit. fur Meteor. Berlin, 17, Supplement: 149-153, (1965).

Kondo, S., "Stratospheric Wind Measurement Using Passive Reflector," Tateno, Japan, Aerological Observatory, Journal 7(4): 295-302, (Mar. 1964).

Konstantinov, A.R., "Critical Evaluation of the Methods and Devices for Experimental Investigation of Wind Structure," Kiev. Ukraine, Nauchno-Issledovatel'skii Gidrometeorologiceskii Institut, Trudy, 26: 111-136, (1961).

Lenhard, R., and Wright, J.B.,"Mesospheric Winds from 23 Successive Hourly Soundings," AFCRL Report, 63-836, 17 p., (1963).

MacCready, P.B., Jr., and Jex, H.R., "Response Characteristics and Meteorological Utilization of Propeller and Vane Wind Sensors," J. Appl. Meteor., 3(2): 182-193, (Apr. 1964).

MacCready, P.B., Jr., "Comparison of Some Balloon Techniques," J. of Appl. Meteor., 4(4): 504-508, (1965).

McGregor, R.R., "Transistor Cup Anemometer," J. Sci. Instr., London, 37(6): 189-190, (June 1960).

Meszaros, E., "General Remarks on the Improvement of the Pressure and Temperature Elements of Radiosondes," Idojaras, Budapest, 62(3): 176-177, (May/June 1958).

Mitsuta, Y., "Sonic Anemometer-Thermometer for General Use," Meteor. Soc. of Japan, Tokyo, Journal, Ser. 2, 44(1):12-24, (Feb. 1966).

Morrissey, J.F., "System for the Determination of the Vertical Wind Profile from an Aircraft," U.S. Air Force Cambridge Research Labs., Hanscom Field, Mass., Instr. Papers No. 79, (Sept. 1965).

Murphy, C.H., Bull, G.V, and Edwards, H.D., "Upper Atmospheric Winds Measured by Gun Launched Projectiles," Issued as AMS/AIAA Conf. on Aerospace Meteor., L.A., Calif., Mar. 28-31, 1966, 66-403, 10 p., (Mar. 1966).

Nami, L., and Paracchini, S., "Electric Anemograph Adapted for Remote Recording of Winds Exceeding 100 km/hr," Rivista di Meteor. Aeronautica Rome, 14(2): 23-27, (Apr./June 1954).

Nordberg, W. and Smith, W., "The Rocket-Grenade Experiment," U.S. Nat. Aeronaut. and Space Admin., Tech. Note, D-2107, 32 p., (Mar. 1964).

Oleson, S., "Improved Sonic Anemometer-Thermometer," Standford Res. Inst. Menlo Park, Calif., Contract DA36-039 AMC-03713(E), Final Rpt., (Aug. 1965).

Pilie, R.J., Jiusto, J.E., and Rogers, R.R., "Wind Velocity Measurement with Doppler Radar," Weather Radar Conf., 10th, Wash., D.C., April 1963, Proc., p. 329a-329L.

Reiche, L.P., and Ludwig, F.L., "A High-Precision Vectorial Integration System for Anemometers," Bul. Am. Meteor. Soc., 42(5): 314-316, (May 1961).

Reid, D.G. and Sumner, C.J., "A Simple Wind Direction Recorder and an Example of its Field Use," Weather, London, 14(6): 198-203, (June 1959).

Rink, J., "Hot Wire Anemometer with a Wide Range of Measurements," Zeit. fur Meteor., Berlin, 17(5/6): 159-169 (1964).

Rosenberg,N.W., "Chemical Releases at High Altitudes," Science, Wash.,D.C. 152(3725): 1017-1027, (May 20, 1966).

Rosenberg, N. W., Golomb, D., and Allen, E.F., Jr., "Chemiluminescence of Trimethyl Aluminum Released into the Upper Atmospher," J. Geophys. Res., 68(20), 5895-5898, (Oct. 1963).

Rosenberg, N.W., Golomb, D., and Allen, E.F., Jr., "Chemiluminescent Techniques for Studying Nighttime Winds in the Upper Atmosphere," J. Geophys. Res., 68(10):3328-3330, (May 1963).

Rosenberg, N.W., "Space and Time Correlations of Ionospheric Winds," Space Science, 1(2): 149-155, (Feb. 1966).

Sanuki, M., Kimura, S., and Hayashi, H., "Proposed Wind Vane with Practically No Overshoot," Papers in Meteor. and Geophys., Tokyo, 16(2): 84-89, (Sept. 1965).

Scoggins, J.R., "An Evaluation of Detail Wind Data as Measured by the FPS-16 Radar/Spherical Balloon Technique," U.S. National Aeronautics and Space Administation, Tech. Note, D-1572,(May 1963)

Scoggins, J.R., "Status of Jimsphere Development," Bull. Amer. Meteor. Soc., 46(1): 21, (Jan. 1965).

Shinohara, T., "On the Results of Experiment for Practical Use of Three-Cup Anemometer," J. Meteor. Res., Tokyo, 10(7): 587-590, (July 1958).

Sing, C.Y. and Chin, C.L.D., "Research for the Development of Airborne Atmospheric and Meteorological Instrumentation," Singco, Inc., Burlington, Mass., Contract AF19(628)-3244, Final Report, AFCRL-66-42, 59 p., (Nov. 1965).

Smalley, J.H. and Flink, L.R., "Modification of the ROBIN Meteorological Balloon, Vol. 1, Design and Test," Litton Systems, Inc., Appl. Sci. Div., St. Paul, Minn, Contract AF19(628)-2945, Final Report (Part 1), Apr. 15, 1963-April 30, 1965 (Sept. 1965).

Stengel, R.F, "Wind Profile Measurement Using Lifting Sensors," J. of Spacecraft and Rockets, N.Y., 3(3):365-373, (Mar. 1966).

Subramanian, D.V., "Note of Wind-Finding with Weather Radar," Indian J. of Meteor. and Geophys., Delhi, 16(3): 453-458, (July 1965).

Sumbal, J., "Simple Modification of the MEZ Hot-Wire Anemometer for Measurement of Directional Velocities in Two-Dimensional Air Flow," Vodohospodarsky Casopis, Bratislava, 12(2): 220-224, (1964).

Surazhskii, D.Ia., "New M-38 Anemorhumbometer," Meteor. i Gidrologiia, Leningrad, No. 4: 45-47, (Apr. 1957).

Surazhskii, D.Ia., "Anemograph M-27," Nauchno-Issledovatel'skii Institut Gidrometeor. Priborstroeniia, Trudy, No. 5: 98-106, (1957).

Svarchevskii, V.N., "Instrument for Recording Great Wind Velocities and Gustiness," Glavnaia Geofiz. Observatoriia, Trudy, No. 83: 43-49, (1958).

Tritton, D.J., "The Use of a Fibre Anemometer in Turbulent Flows," J. Fluid Mech., 16(2): 269-281, (June 1963).

U.S. Army Electronic Research and Development Activity, White Sands, "Performance Characteristics of Meteorological Rocket Wind and Temperature Sensors," Tech. Rpt. SELWS-M-4, 31 p., (Oct. 1962).

White, G.R., Nugent, L.J., and Carrier, L.W., "Laser Atmospheric Probes," Inst. Soc. A., Preprint No. 40.1-1-65, 20th Annual ISA Conf. and Exhibit, Los Angeles, 11 pp. (1965).

Wurtz, and Neiswander, R.S., "Ground-Based Mapping of Upper Air Winds," Final Report, Te Company, Contract DA-36-039 SC-90685, (1963).

Yajima, Y., "On the Robinson's Factor of Anemometer FC-1," J. Meteor. Res., Tokyo, 14(8): 560-562, (Aug. 1962).